Thomas Rauschenbach *Editor*

Modeling, Control and Optimization of Water Systems

Systems Engineering Methods for Control and Decision Making Tasks

Springer

Modeling, Control and Optimization
of Water Systems

Thomas Rauschenbach
Editor

Modeling, Control and Optimization of Water Systems

Systems Engineering Methods
for Control and Decision Making Tasks

Contributed by
Thomas Bernard, Albrecht Gnauck, Marco Jacobi,
Divas Karimanzira, Oliver Krol, Torsten Pfützenreuter,
Buren Scharaw, Thomas Westerhoff

Editor
Thomas Rauschenbach
Fraunhofer IOSB-AST
Ilmenau
Germany

Preface

This book approaches the topic of "water systems" from the perspective of systems engineering and automation technology. Why is it worthwhile to devote an entire book to this approach?

Currently, the efficient use of water resources is rapidly gaining importance in all parts of the world. The drivers of this development are diverse. Here it is worth mentioning the rapid economic growth in some parts of the world, e.g. in Asia and the increasing trend towards urbanization, which is most apparent in the growth of existing and in the emergence of new megacities. The contributions of the climatic changes with the intensification of extremes, such as floods and droughts are also important. These challenges require undoubtedly interdisciplinary efforts of politicians, scientists, and technicians.

A contribution can therefore be made by technologies that support people in making decisions relating to the operation of water systems and in dealing with special situations or automatically control the water systems. Due to the often very high complexity of the considered systems—resulting not least from the necessary holistic approach—optimal solutions can only be found on the basis of simulation models.

The focus of this book is on the introduction of approaches to the modeling of the different parts of the water cycle. These approaches are designed for use in decision-making systems and automatic control and are characterized by low complexity and simulation times, so that they can be used in real-time applications for computing optimal actions or control strategies.

Thus, these models differ from the detailed physical model approaches commonly used in hydrology or hydraulic. The approaches presented in this book are based on simplifications, which are justified by their applications in decision-making or for automatic control and offer several benefits for these purposes.

In addition to the models, their integration and usage in decision support systems are shown and several application examples are given.

As an editor I would like to thank the authors who made this book possible. On their behalf, I would like to thank the publishers for their excellent support and advice in the creation of the book.

Ilmenau   Thomas Rauschenbach
June 2015

Contents

Chapter 1
Introduction

Thomas Rauschenbach

Models in Systems Engineering and Automation

For water systems, many models exist for example in the fields of hydrology and hydraulics, which describe the phenomena in these systems in detail. Such detailed models are absolutely necessary for solving tasks of these scientific areas and have reached a very high level of development. Should, however, decision support systems or control strategies for water systems be designed, then other type of models are required. In the area of system engineering and automation, the goal of modeling is not to provide a highest possible detailed model of the real process. Rather, the key is to describe the task behavior with a model of low complexity and ease of handling. Usually models are classified in 'white-box', 'gray box' and 'black-box' [201]. 'White-box' models are based on the consistent application of the physical description of the relationship between inputs, outputs and internal states (state variables) of a system, in general through difference equations or differential equations. With these models, the behavior of systems can be described precisely. But at the same time, it means a very high cost for the identification of the model structure and the determination of model parameters. Extensive knowledge of the system being modeled is necessary, which can be obtained only with time and/or cost-intensive investigations. The 'gray-box' introduces simplifications in the models. This type of model is developed for defined tasks. Therefore, only essential physical interrelationships for the specific application are to be considered, but by no means describes all the phenomena of reality. Unknown parameters, which can only be determined with great effort, are, for example, determined by an estimation procedure from measured data. Also the linearization around an operating point of nonlinear relations can be assigned to the 'gray-box' models.

T. Rauschenbach (✉)
Fraunhofer IOSB-AST, Ilmenau, Germany
e-mail: thomas.rauschenbach@iosb-ast.fraunhofer.de

The 'black-box' models represent the highest form of abstraction; they describe the input-output behavior of a system based on measured data (time series). The main task is to find a linear or non-linear relationship between the input and output variables which best reflects the underlying dependencies. The parameters of this function are determined by parameter estimation method based on the available data. There is no knowledge about the structure of the modeled system. But that should in no way lead to worry about the limits of validity of the model generated.

Based on the example of a one-dimensional modeling of flow behavior in a channel, the different model structures will be explained in brief. For this the Saint-Venant equations designate the 'white-box' model. They are a system of two partial differential equations. The first differential equation is called the continuity equation and is based on the mass balance. The second equation is called the equation of motion and is based on the energy balance of the system. Level and flow hydrographs can be simulated very well through the description of physical phenomena with this system of differential equations. The solution of the differential equation system can be done only numerically and requires a high computational cost. Also, the parameterization is not to be underestimated, because the hydrological and geometric data must be determined for a large number of transverse profiles.

This book presents for the simulation of one-dimensional flow a 'gray box' model. It is based on the Saint-Venant equations. These are converted into difference equation models. That is, this is done by a discretization in time and space. To succeed in simplification of the mathematical description, not all phenomena of the flow behavior can be represented as described by the Saint-Venant equations. For the control at greatly changed flow rates of unsteady flow component cannot be neglected. Therefore, a term is introduced, which for this purpose a mathematical description provides accurate and thus an enhanced simulation model is created, which meets the requirements on the controller. This is a typical example of a 'gray box' model.

'Black-box' models for the one-dimensional flow often consider only the continuity equation. This allows the lead times between water level measuring stations to be calculated and by the inclusion of a first order differential equation, the effects that are caused by the inertia of the water masses, also. Transient flow behavior as in the 'gray box' model cannot be simulated. This kind of models is however sufficient only and only if a stationary behavior is assumed.

The main objective of this book is to introduce models that are appropriate for decision-making and optimal control of water systems. The demarcation to the well-known hydrologic models that exist in various forms is done by this objective at the same time. Users of the models presented in this book, are those who develop simulation-based systems for optimum operation and management. The decision horizons can range from short-term (minutes, hours) to long-term (months, years).

The model approaches presented in this book offer in their particular field of application the following benefits:

- The accuracy is sufficient for decision making and control.
- There is a limitation to the physical, chemical or biological variables required for decision making and control.

- The computational effort for the simulation is low.
- Simulation-based optimization strategies can be implemented with the models and used in real-time.
- The effort of parameterization is relatively low.
- Missing parameters can be determined from measured data.
- The models can be quickly adapted to new situations or changes in behavior, such as by automatic adaptation of the parameters based on measurement data.
- Through coupling of component models, complex water systems can be modeled, which can also exhibit strong nonlinear behavior, such as by overbank flooding, by the integration of retention areas, by backwater effects, etc.

The structure of the book is clarified by Fig. 1.1. It shows the water cycle in a simplified form with the three main parts, water resources, transportation, and water use. For each of these parts modeling approaches are presented in the book and it is shown how they can be applied in model-based systems for decision-making and/or control. Chapter 2 deals with the water resources, which consists of the surface water and groundwater models. First, the catchment area models are presented that describe the quantitative formation of the water resources from precipitation. For the use of water resources, their quality is crucial. For this reason, a sub chapter is dedicated to the modeling of water quality of freshwater ecosystems. Groundwater is an important water resource. Its modeling in terms of water quantity and water quality is therefore described in detail. Since surface water and groundwater interact, they cannot be viewed in isolation from each other. Therefore, Chap. 2 concludes with the description of simulation approaches for the coupling of the two resources.

Chapter 3 focuses on the models for water transport. Here, the natural water ways, which include rivers, retention areas and reservoirs are described. Man-made waterways, especially piping systems and channels, are also taken into account. In Chap. 4 aspects of water use are considered. It begins with models for water demand with respect to different types of use. Especially, the expected water demand is an essential information for deriving decisions for the optimal operation of water systems.
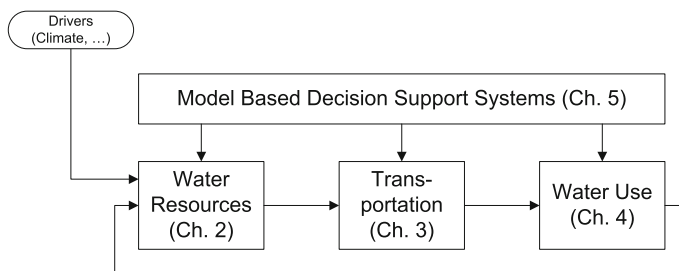
Fig. 1.1 In the book addressed parts of the water cycle

After description of the models in the previous chapters, methods of model-based optimal decision making are presented in Chap. 5. It is shown how the simulation models can be integrated into the decision support systems and how practically applicable entire systems can be set up.

The application of the methods presented in the book is shown in Chap. 6 with five practical examples. Here, the experience on how user requirements can be taken into account to achieve a high level of acceptance among users is also given.

Chapter 2
Water Resources

Thomas Rauschenbach, Albrecht Gnauck, Oliver Krol,
Thomas Bernard and Torsten Pfützenreuter

2.1 Catchment Area Modeling

Thomas Rauschenbach

2.1.1 Introduction

Water resources as sources for the utilization of water are an essential element of the water cycle. One of these elements is the surface water found open-lying and uncombined on the Earth's surface. Lakes and rivers are fed by precipitation in the appertaining catchment area. Thus, the mathematical description of the behavior of those areas is an important prerequisite for the modeling, control and optimization of water systems. This is the only way to allow statements about the amount of the available water resources (balance) and their dynamic behavior. In the model area, it is not the point precipitation which is relevant but the area precipitation instead.

T. Rauschenbach (✉) · T. Pfützenreuter
Fraunhofer IOSB-AST, Ilmenau, Germany
e-mail: thomas.rauschenbach@iosb-ast.fraunhofer.de

T. Pfützenreuter
e-mail: torsten.pfuetzenreuter@iosb-ast.fraunhofer.de

A. Gnauck
Environmental Informatics, Brandenburgische TU Cottbus Inst.-Senftenberg, Cottbus, Germany
e-mail: ah-gnauck@t-online.de

O. Krol
Neustadt a.d. Weinstrasse, Germany
e-mail: ohaesner@gmail.com

T. Bernard
Fraunhofer IOSB, Karlsruhe, Germany
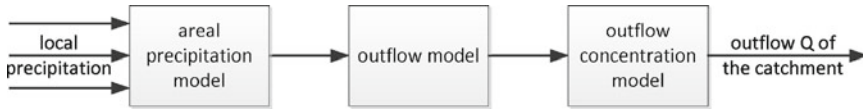e-mail: thomas.bernhard@iosb.fraunhofer.de

Fig. 2.1 Basic elements of a catchment area according to [150]

Here, "area precipitation" denotes the distribution of the precipitation amount over the whole surface of the catchment area and over the whole period under consideration. According to [150], the discharge resulting from the area precipitations in the catchment area occurs in two phases, as shown in Fig. 2.1. The discharge formation describes the transformation of the precipitation into the discharge by taking the evapotranspiration and the area retention into account. It determines the portion of the precipitation which becomes effective for the discharge. The discharge formation occurs over the whole surface in each point of the catchment area. The discharge concentration denotes the concentration of the discharge formed over the whole surface over the discharge cross section of the catchment area. Here, the distribution over the time of the discharge formed over the discharge cross section of the catchment area is modeled. In this book, a number of conceptual catchment area models are presented. These models describe the whole catchment area by applying only few, concentrated parameters. The advantage of such an approach is that—due to the low number of parameters and the simple model structure—the parameter determination can be carried out by applying methods of process analysis using available measuring values. Furthermore, it is no longer necessary to determine the parameters for soil structures, land use etc. in the case of geomorphologically based models. However, transferring the parameter vector of the conceptual models to some physical properties of the model area turns out to be more difficult. Thus, only some assumptions for the parameters of the single basins can be made semi-analytically. Furthermore, it is difficult to use conceptual models for extrapolation as the real physical behavior is not exactly simulated but in a simplified form only. Especially the modification in the land use and, thus, the modification in the precipitation-discharge behavior can only be realized indirectly by adapting the model parameters by means of the measuring values. The structure of the models, however, allows very well statements about the condition of the soil water store in the catchment area and, thus, also forecasts concerning the effect of precipitation events. In the following, three conceptual models are presented. By applying the Lorent–Gevers model, the authors set up many simulation models successfully. The HBV model is widely used in Scandinavia, and the Tank model first applied in Japan has been used for catchment area modeling elsewhere.

2.1.2   Model According to Lorent and Gevers

2.1.2.1   Basic Structure

The basic structure as seen in Fig. 2.2 consists of three partial models [202]. Partial model 1 describes the non-linearity contained in the overall model—the soil moisture storage. The measured gross rainfall PB and the estimated potential evapotranspiration ETP serve as input. The second partial model calculates the surface discharge R from the net rainfall PN. The third partial model is used to calculate the basic discharge B from percolation D. These two partial discharges are summarized to form the discharge from the catchment area Q.

2.1.2.2   The Partial Models

As described above, partial model 1 contains a non-linear storage. Here, the stored water S on the surface, which is composed of the amount of water contained in the plants and in the soil, is calculated at time k. Mathematically, this can be represented in the following form:

$$S(0) = S_{start} \tag{2.1}$$
$$S(k) = S(k-1) + SI(k) - E2(k) - D(k) \tag{2.2}$$

As any surface can store only a limited amount of water, a maximum value S_{max} is defined. By means of this value, the storage deficit DEF can be calculated as difference between maximum and current soil moisture. The following relation holds:

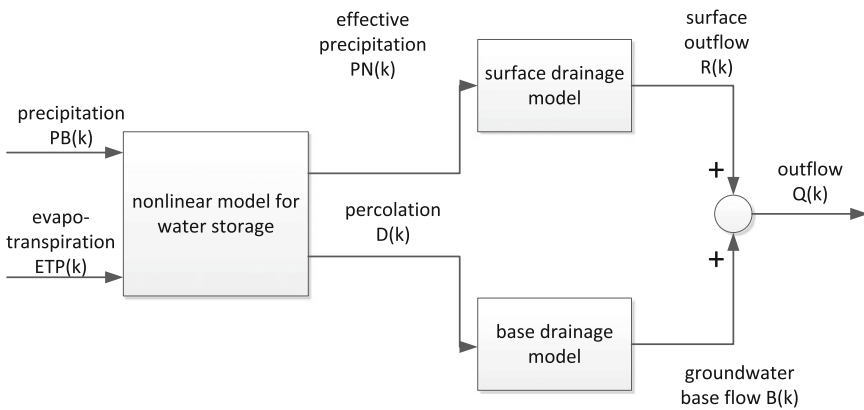$$DEF(k) = S_{max} - S(k) \tag{2.3}$$

Fig. 2.2   Basic structure of the catchment area model according to Lorent and Gevers

The net rain can be calculated by making the following assumption. Here, two cases must be told apart. In the first case, evapotranspiration is greater than precipitation. In the second case, precipitation is greater than evapotranspiration. Therefore, first that portion of the precipitation is calculated which gets lost directly through evapotranspiration. This portion is called $E1$ and is calculated in the following way:

$$E1(k) = \begin{cases} PB(k) & \text{if } PB(k) < ETP(k) \\ ETP(k) & \text{if } PB(k) \geq ETP(k) \end{cases} \tag{2.4}$$

Now, the effective precipitation PE is calculated. This is the portion of the precipitation which does not get back to the atmosphere through evapotranspiration. Thus, the following relation results:

$$PE(k) = PB(k) - E1(k) \tag{2.5}$$

From the storage deficit and the effective precipitation, the auxiliary quantity SI results. It describes how much water has been stored by the soil or the plants. Later, this amount of water will either infiltrate or evaporate. The following relation holds:

$$SI(k) = DEF(k-1)\left(1 - e^{-\frac{PE(k)}{b \cdot DEF(k-1)}}\right) \tag{2.6}$$

Here, b is a free parameter. Based on the equations set up above, the net rain can be calculated as follows:

$$PN(k) = PB(k) - E1(k) - SI(k) \tag{2.7}$$

The net rain denotes the portion of precipitation which becomes effective directly as surface discharge. Using the relations for SI and $E1$ the following two cases can be told apart for the calculation:

$$PN(k) = \begin{cases} 0 & \text{if } PB(k) < ETP(k) \\ PB(k) - ETP(k) - (S_{max} - S(k-1))\left(1 - e^{-\frac{PB(k)-ETP(k)}{b \cdot (S_{max}-S(k-1))}}\right) & \text{if } PB(k) \geq ETP(k) \end{cases} \tag{2.8}$$

Now, as the net rain PN and the gross rain PB are known, the discharge coefficient C_R can be calculated from these two quantities as follows:

$$C_R(k) = \frac{PN(k)}{PB(k)} \tag{2.9}$$

Due to the physical facts, the discharge coefficient $C_R(k)$ can assume values ranging between zero and one only. The Lorent–Gevers model says that this discharge coefficient increases with the soil moisture, with precipitation being constant. If the soil moisture is constant, the discharge coefficient increases with precipitation.

In order to be able to calculate the evapotranspiration auxiliary quantity $E2$, a case-by-case analysis must be made again. $E2$ describes that portion of the stored water which either evaporates or transpires. It is defined as follows:

$$E2(k) = \begin{cases} ETP(k) - E1(k) & \text{if } SI(k-1) + SI(k) \geq ETP(k) - E1(k) \\ S(k-1) + SI(k) & \text{if } SI(k-1) + SI(k) < ETP(k) - E1(k) \end{cases} \quad (2.10)$$

By means of this quantity, the overall evapotranspiration can now be calculated. It results from the sum of $E1$ and $E2$:

$$E(k) = E1(k) + E2(k) \quad (2.11)$$

The percolation can be determined by means of the maximum percolation D_{max} and the following relation:

$$D(k) = \begin{cases} \frac{D_{max}}{S_{max}}(S(k-1) - (ETP(k) - PB(k))) & \text{if } SI(k-1) + SI(k) \\ & \geq ETP(k) - E1(k) \\ & and\, PB(k) < ETP(k) \\[2ex] \frac{D_{max}}{S_{max}}(S(k-1) + (S_{max} - S(k-1))\left(1 - e^{-\frac{PB(k) - ETP(k)}{b \cdot (S_{max} - S(k-1))}}\right) & \text{if } SI(k-1) + SI(k) \\ & \geq ETP(k) - E1(k) \\ & and\, PB(k) \geq ETP(k) \\[2ex] 0 & \text{if } SI(k-1) + SI(k) \\ & < ETP(k) - E1(k) \end{cases} \quad (2.12)$$

From this equation, it can be seen that the percolation increases with the amount of stored water. If a substantial amount of water is stored in the soil, more water will drain away. Now, the amount of stored water results analogously as it is calculated from the amount of stored water in the preceding calculation step and the amount of water which has not drained away:

$$S(0) = S_{start} \quad (2.13)$$

$$S(k) = \begin{cases} \left(1 - \frac{D_{max}}{S_{max}}\right)(S(k-1) - (ETP(k) - PB(k))) & \text{if } SI(k-1) + SI(k) \\ & \geq ETP(k) - E1(k) \\ & and\, PB(k) < ETP(k) \\[2ex] \left(1 - \frac{D_{max}}{S_{max}}\right) \cdot \\ (S(k-1) + (S_{max} - S(k-1))\left(1 - e^{-\frac{PB(k) - ETP(k)}{b \cdot (S_{max} - S(k-1))}}\right) & \text{if } SI(k-1) + SI(k) \\ & \geq ETP(k) - E1(k) \\ & and\, PB(k) \geq ETP(k) \\[2ex] 0 & \text{if } SI(k-1) + SI(k) \\ & < ETP(k) - E1(k) \end{cases} \quad (2.14)$$

The parameters b, S_{max} and D_{max} should now be chosen such that the mean square deviation of the discharge forecast becomes minimum so as to correspond best to the physical properties of the area.

In the following, the partial models 2 and 3 are presented. They describe the flow behavior of the surface discharge and the basic discharge.

The surface discharge $R(k)$ is linearly dependent on the net rainfall and can be determined by applying the following equation:

$$R(k) = \sum_{j=1}^{N} a_j R(k-j) + \sum_{j=1}^{M} b_j PN(k-j), \tag{2.15}$$

Here, N is the order of the autoregressive portion, and M is the order of the exogenous influence. Thus, an ARX model set-up (autoregressive model set-up with exogenous influence parameter) is available. According to the theory of the modeling of stochastic processes, it is also possible to choose an ARMAX model set-up. Such a set-up allows the model errors to be taken into account as white noise ε of order P. Then, the following relation holds:

$$R(k) = \sum_{j=1}^{N} a_j R(k-j) + \sum_{j=1}^{M} b_j PN(k-j) + \sum_{j=1}^{P} c_j \varepsilon(k-j) + c_0 \tag{2.16}$$

The parameters a, b and c can be estimated using the least square method. By analyzing the ground water draining curve, the following approximation has turned out to be practical. Thus, the ground water basic flow B can be approximated by means of the following equation:

$$B(k) - B_0 = (B(k_0) - B_0)e^{-\frac{k-k_0}{\tau_h}} \tag{2.17}$$

The start time of the ebbing of the ground water is k_0. B_0 is the restricted discharge flow rate characteristic of the period under consideration. Therefore, the basic flow can also be split up into a fast-flowing and a slow-flowing portion:

$$B(k) = BR(k) + BL(k) \tag{2.18}$$

BL is the nearly constant portion of the basic discharge. At the beginning, it corresponds to B_0, and varies only very slowly. On the other hand, BR varies more quickly. This can be clearly seen particularly during dry periods as in such cases BL varies only slowly. Because BR and BL are assumed to originate from two different ground water reservoirs, the following equations can be obtained:

$$BR(k) = \alpha BR(k-1) + (1-\alpha)D(k-dr) \tag{2.19}$$
$$BL(k) = \beta BL(k-1) + (1-\beta)D(k-ds) \tag{2.20}$$

Here, D is the percolation term with the different dead times dr and ds for the two portions of the basic discharge. In the case of a longer dry period, this term is accordingly almost 0 or also negligible. From the ground water draining curve, it is possible to determine α with $(\alpha = e^{(-1/t_h)})$ by estimating the time constant t_h. The parameters for the slow ground water basic flow can be calculated from times during which no surface discharge takes place and no rainfall has been recorded since long.

For the model according to Lorent and Gevers, two expansions can be reasonable. The first expansion proposed is an interception storage. The precipitation flows first through the interception storage until it has reached its maximum storage capacity SZ_{max}. The precipitation stored in this storage SZ cannot drain off and, thus, can only decrease through evaporation. The maximum storage capacity SZ_{max} depends on the vegetation density and must be determined separately. For calculation, the following cases must be told apart:

$$SZ_{max} - SZ(k - 1) \geq PB(k) \tag{2.21}$$
$$SZ_{max} - SZ(k - 1) < PB(k). \tag{2.22}$$

This case-by-case analysis is necessary in order to determine which portion of the precipitation can be contained in the interception storage $(AZ(k))$ and how much of it seeps in $(PE(k))$. In the first case, the whole precipitation can be absorbed by the interception storage. Hence, $AZ(k)$ corresponds to $PB(k)$. Accordingly, $PE(k)$, $PN(k)$ and $SI(k)$ are equal to zero. The second case occurs when the amount of rainfall is bigger than the storage capacity of the interception storage. Then, the following mathematical relations result:

$$AZ(k) = SZ_{max} - SZ(k - 1) \tag{2.23}$$
$$PE(k) = PB(k) - AZ(k) \tag{2.24}$$
$$PN(k) = PB(k) - AZ(k) - SI(k). \tag{2.25}$$

In the first case, the evaporation portion $E1$ can be determined in the following way:

$$E1(k) = \begin{cases} ETP(k) & \text{if } SZ(k - 1) + AZ(k) \geq ETP(k) \\ SZ(k - 1) + AZ(k) & \text{if } SZ(k - 1) + AZ(k) < ETP(k) \end{cases} \tag{2.26}$$

Now, the amount of water stored in the interception storage $SZ(k)$ can be calculated. The following relations hold:

$$SZ(0) = SZ_{start} \tag{2.27}$$

$$SZ(k) = \begin{cases} SZ(k - 1) + AZ(k) - E1(k) & \text{if } SZ(k - 1) + AZ(k) \geq ETP(k) \\ 0 & \text{if } SZ(k - 1) + AZ(k) < ETP(k) \end{cases} \tag{2.28}$$

Another expansion of the model according to Lorent and Gevers consists in adding a so-called residual soil moisture or also a limit value *WBC*. If the residual soil moisture *SC* is lower than this limit value, then the surface storage can be depleted only through evaporation but no longer through percolation. It is assumed that this effect is connected with the capacity of the capillary water storage of the plants, which ensures that the soil moisture remains greater than zero even in the case of longer dry periods. From this results the following equation for the amount of percolating water *D*:

$$D(k) = \begin{cases} 0 & \text{if } D(k) < SC - S(k) \\ D(k) - SC + S(k) & \text{if } D(k) \geq SC - S(k) \end{cases} \tag{2.29}$$

Accordingly, the storage content *S* results to:

$$S(k) = \begin{cases} S(k) + D(k) & \text{if } D(k) < SC - S(k) \\ SC & \text{if } D(k) \geq SC - S(k) \end{cases} \tag{2.30}$$

2.1.3 The Tank Model

2.1.3.1 Basic Structure

The Tank Model was developed by M. Sugawara. Its main form is based on four water tanks arranged vertically in series. The rainfall just as the potential or also real evapotranspiration have an effect on the upper tank. This one generates a water flow which produces an immediate discharge through the two outlets, and also a water flow which does not entail an immediate discharge through the soil outlet. The water flow which is not directly discharge-effective goes into the water storage arranged underneath. This tank presents the same behavior until the last tank—the ground water reservoir—is finally reached. In general, the groundwater reservoir allows the water to flow out only via a lateral outlet instead of the outlet in the ground. Therefore, two discharges are obtained from the first tank because this one has two lateral outlets whereas the other water tanks are provided with only one lateral outlet each. At the end of these lateral outlets, a smoothing filter is mounted to each of them. Because of the four water tanks, which are arranged in series, the system is very complex, as any changes made to one of the upper water tanks will inevitably have an effect on the low-lying tanks. In practice, often modified tank models are employed [156, 193, 290]. There are very many variants for a great number of different applications. Here, a slightly modified tank model shall be presented. The number of tanks has been reduced to three, as it was also the case in [193]. By doing so, a structure is created which is more similar to the other two models presented here. Just as it is the case with the model according to Lorent and Gevers, this version of the tank model has one outlet—which can be seen as surface outflow—one outlet—which can be seen as intermediate outflow—and one outlet, which can be regarded as basic outflow (Fig. 2.3).
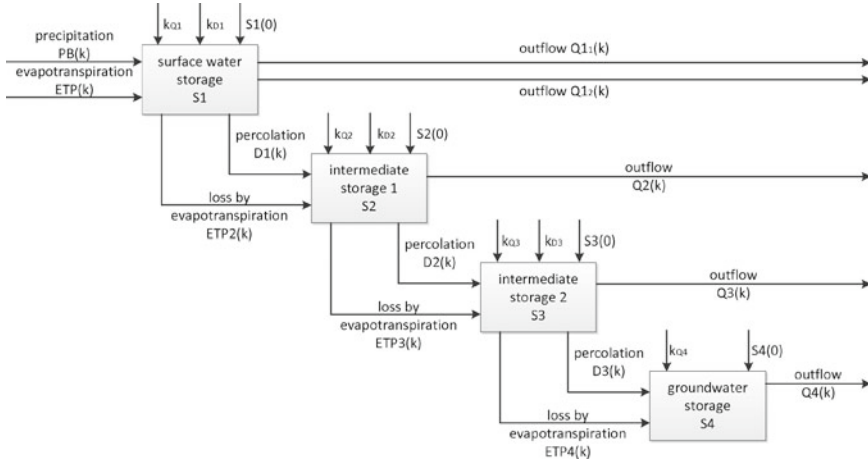
Fig. 2.3 Basic structure of the Tank model

2.1.3.2   Mathematical Description

The mathematical bases of the tank model are simple. The model takes on its complexity through the fact that the behavior of the preceding tanks exerts an influence on the subsequent tanks. For the storage content S of the upper tank, the following mathematical relation results:

$$S(0) = S_{start} \tag{2.31}$$

$$S(k) = S(k-1) + PB(k) - ETP(k) - Q_1(k) - Q_2(k) - Q_G(k). \tag{2.32}$$

The lateral outflow of a tank $Q_{outflow1}$ depends on the following parameters:

- type of outflow (soil or lateral outflow),
- type of function *funcidx*,
- current water level $S(k)$,
- height of outflow (height inside the tank at which outflow starts)h_{level}, and
- minimum storage content S_{min}.

By means of *funcidx*, one of the following functions for calculating the discharge can be chosen:

$$Q_{outflow1} = c_{amount} \begin{cases} \sqrt{S(k) - h_{level}} & funcidx = 1 \\ S(k) - h_{level} & funcidx = 2 \\ 1 & funcidx = 3 \\ \arctan(S(k) - h_{level}) & funcidx = 4 \\ \left(\dfrac{\arctan \frac{S(k) - h_{level}}{c_1}}{\pi} + \dfrac{1}{2} \right)(S(k) - h_{level}) & funcidx = 5 \\ \dfrac{\tanh\left((S(k) - h_{level} + 1)^{10} - 5\right)}{2} \left(\sqrt{S(k) - h_{level}} + 0.1 \right) & funcidx = 6 \end{cases} \tag{2.33}$$

Here, c_{amount} is a parameter which weighs the discharge, and which can thus be regarded as equivalent to the size of the opening of the tank. The parameters c_{amount} and c_1 must be determined by means of real data. For *funcidx* 1, 2 and 3, the discharge is zero if $S(k) < h_{level}$. In practice, some good experience was made with the calculation according to *funcidx* 6.

For the soil outlet, some simplifications result as the water level—by definition— is always greater than/equal to the height of the soil outflow. In the case of the lateral outlets, the water level can be below the height of the outlet. Equation (2.34) is only valid for $S(k) > S_{min}$. For $S(k) = S_{min}$, no outflow will take place. Some own investigations have shown that this way of calculating the outflow yields better quality values than in the case of the variant where there is always a ground water discharge whenever there is water in the tank. The soil outflow $Q_{outflow2}$ can be mathematically described as follows:

$$
Q_{outflow2} = c_{amount}
\begin{cases}
\sqrt{S(k) - h_{level}} & funcidx = 1 \\
S(k) - h_{level} & funcidx = 2 \\
1 & funcidx = 3 \\
S(k) - h_{level} & funcidx = 4 \\
S(k) - h_{level} & funcidx = 5 \\
\sqrt{S(k) - h_{level}} & funcidx = 6
\end{cases}
, \tag{2.34}
$$

Starting from this relation, Eq. (2.32) can be executed sequentially for calculating the contents and, thus, the outflows of the individual tanks. If the delay times and the dead times remain out of consideration, these outflows result in the total discharge Q_{total} of the catchment area:

$$
Q_{total}(k) = Q1_{tank1}(k) + Q2_{tank1}(k) + Q1_{tank2}(k) + Q1_{tank3}(k) \tag{2.35}
$$

2.1.4 The HBV Model

2.1.4.1 The Basic Structure

The HBV model was developed by S. Bergstrøm and is being employed in many different countries under a big number of various climatic conditions [290]. It is a partially distributed conceptual model and is subdivided into basins distributed over the model area, and a ground storage which globally collects the water from the individual basins of the entire model area.

Figure 2.4 shows the schematic representation of the variant of the HBV model described here. The two regions can clearly be recognized: the basin area and the ground storage area. In this case, the model has three basins, with each of them being provided with an own snow storage. Basins are composed of two water reservoirs. The first one stores the water bound in snow or ice whereas the second one contains the amount of water which is found in the form of soil moisture in the model area.
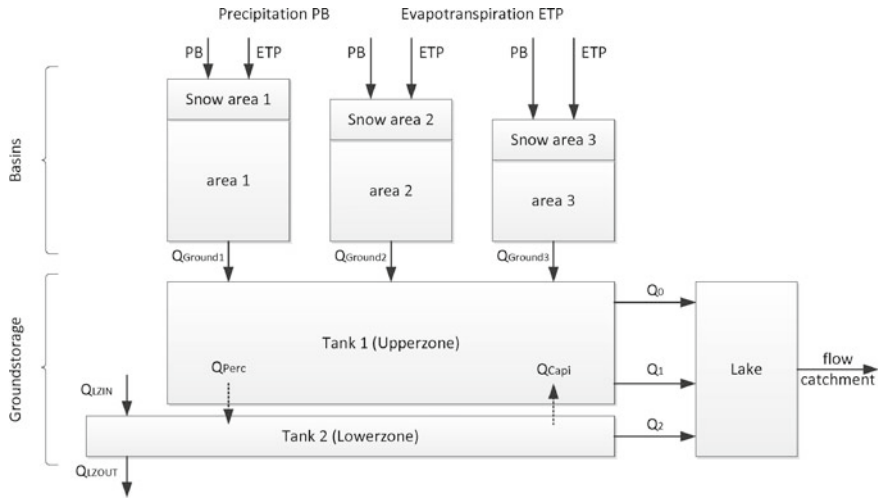
Fig. 2.4 Principle structure of the HBV model

As the main purpose of the basins is to subdivide the entire model area into height classes, it is important to calculate different temperatures for the single basins. Basins lying at a greater height are cooler than basins lying at a lower height. For the local temperature of the basin, the following equation results:

$$T_{local}(k) = -0.6\frac{h}{100m} + T_{reference}(k). \tag{2.36}$$

$T_{reference}$ is the reference temperature in the model area. Normally, it should be measured in the region of the lowest height classes to serve as input data record for all basins later. Furthermore, the potential evapotranspiration $ETP(k)$ is converted into the real evapotranspiration $ETR(k)$ in the HBV model, which is done by using the following relation:

$$ETR(k) = \begin{cases} ETP(k) \cdot ETR_{max}\frac{S_{soil}(k)}{LP} & \text{if } S_{soil}(k) < LP \\ ETP(k) \cdot ETR_{max} & \text{otherwise} \end{cases} \tag{2.37}$$

Here, S_{soil} is the content of the ground moisture storage, and LP is the limit value of the soil moisture, which still allows the maximum possible amount of evaporation. If the local temperature T_{local} is lower than the temperature for the snow accumulation T_{Tacc}, the precipitation will be led to the snow storage. Before that, however, a correction factor $c_{snowfall}$ is applied to eliminate the linear measurement error from the precipitation. The snow accumulation is calculated as follows:

$$S_{snow}(0) = S_{snow,start} \tag{2.38}$$

$$S_{snow}(k) = S_{snow}(k-1) + c_{snowfall} \cdot PB(k) - ETR(k) \qquad (2.39)$$

However, if the local temperature of the basin T_{local} is higher than the temperature for the snow melt T_{Tmelt}, water from the snow storage can get into the soil moisture storage. Via the factor c_{melt} it is possible to check how much snow can melt. $melt(k)$ defines the potential condensation water, with the following relation holding true:

$$melt(k) = c_{melt} \cdot (T_{local}(k) - T_{Tmelt}) \qquad (2.40)$$

From the potential condensation water $melt(k)$ and from the content of the snow storage $S_{snow}(k)$, the real amount of molten snow just as the newly resulting content of the snow storage can be determined. Thus, the following relations result:

$$S_{snow}(0) = S_{snow,start} \qquad (2.41)$$

$$S_{snow}(k) = \begin{cases} S_{snow}(k-1) - melt(k) & \text{if } S_{snow}(k-1) > melt(k) \\ 0 & \text{otherwise} \end{cases} \qquad (2.42)$$

$$Q_{soil}(k) = \begin{cases} melt(k) & \text{if } S_{snow}(k-1) > melt(k) \\ S_{snow}(k-1) & \text{otherwise} \end{cases} . \qquad (2.43)$$

If the temperature is greater than or equal to the temperature for the snow accumulation, the precipitation will be modeled only as liquid rather than as snow. Then, the precipitation can have a direct effect on the soil water storage. The inflow of water $Q_{soil}(k)$ into the soil moisture storage is calculated as follows:

$$Q_{soil}(k) = \begin{cases} PB(k) - ETP(k) & \text{if } T_{local}(k) \leq T_{Tmelt} \\ PB(k) - ETP(k) + melt(k) & \text{if } S_{snow}(k-1) > melt(k) \\ & \text{and } T_{local}(k) > T_{Tmelt} \\ PB(k) - ETP(k) + S_{snow}(k-1) & \text{if } S_{snow}(k-1) \leq melt(k) \\ & \text{and } T_{local}(k) > T_{Tmelt} \end{cases} . \qquad (2.44)$$

As the amount of water contained in the soil moisture storage is known in this calculation step, it is possible to calculate how much water will stay in this soil moisture storage $S_{soil}(k)$ and which portion of water will flow into the groundwater storage area $Q_{ground}(k)$. The followings relations hold true:

$$Q_{soil}(k) = Q_{soil}(k-1) \cdot \left(\frac{S_{soil}(k-1)}{S_{max}} \right)^{\beta} \qquad (2.45)$$

$$Q_{ground}(k) = Q_{soil}(k-1) \cdot \left(1 - \left(\frac{S_{soil}(k-1)}{S_{max}} \right)^{\beta} \right) \qquad (2.46)$$

Here, S_{max} is the maximum storage capacity of the soil moisture storage, and β is a free parameter. Thus, the new content of the soil moisture storage can be determined in the following way:

$$S_{soil}(0) = S_{soil,start} \tag{2.47}$$

$$S_{soil}(k) = S_{soil}(k-1) + Q_{soil}(k). \tag{2.48}$$

In the groundwater storage too, two water reservoirs are contained. These reservoirs are vertically arranged in series just as in the basins. There are two sorts of tanks: an Upperzone Tank UZ and a Lowerzone Tank LZ. The Upperzone Tank is provided with the two outflows Q_0 and Q_1. There are also two sorts of inflows. One inflow results from the basins, the other is the constant inflow into the Lowerzone Tank. These inflows bring about the new water levels in the two water reservoirs. In addition, there are also two water flows occurring between the two water reservoirs. The flow from the upper into the lower water reservoir (the percolation) is called Q_{perc}. The flow of water occurring in the opposite direction (the capillary water flow) is called Q_{capi}. In addition to the inflows and water flows between the water reservoirs, there are also water outflows. The upper tank is provided with two outlets. Outlet Q_0 is arranged at the height of L_{UZ}, whereas outlet Q_1 is attached to the ground of the tank. The Lowerzone Tank as well has two outlets. Outlet Q_2 is arranged at a relative height of zero. Here, attention has to be paid to the fact that the ground of the Lowerzone Tank can be shifted further downwards by the term LZ_{offset}. In addition, there is a constant outflow Q_{LZout} for the Lowerzone Tank. For the storage content of the upper water reservoir S_{UZ} of the groundwater storage and of the lower water reservoir S_{LZ}, the following relations hold true:

$$S_{UZ}(0) = S_{UZ,start} \tag{2.49}$$

$$S_{UZ}(k) = S_{UZ}(k-1) + Q_{in}(k) - Q_{perc}(k) + Q_{capi}(k) - Q_0(k) - Q_1(k) \tag{2.50}$$

$$S_{LZ}(0) = S_{LZ,start} \tag{2.51}$$

$$S_{LZ}(k) = S_{LZ}(k-1) + Q_{LZ,in}(k) \tag{2.52}$$
$$+ Q_{perc}(k) - Q_{capi}(k) - Q_2(k) - Q_{LZ,out}(k)$$

Here, $Q_{LZ,in}$ is the constant inflow, and $Q_{LZ,out}$ is the constant outflow of the lower water reservoir. When the new water levels are available, the outflow from the outlets can be calculated. For the potential outflow $Q_{0,pot}$ of Q_0, the following relation results:

$$Q_{0,pot}(k) = \begin{cases} c_{0,amount} \cdot (S_{UZ}(k-1) - L_{UZ}) & \text{if } S_{UZ}(k-1) > L_{UZ} \\ 0 & otherwise \end{cases} \tag{2.53}$$

with the parameter $c_{0,amount}$. If there is enough water available, the total potential outflow can flow out of the water reservoir. If not, however, only a fraction of the potential outflow can become effective. The following ansatz can be applied:

$$Q_0(k) = \begin{cases} 0 & \text{if } S_{UZ}(k-1) \leq L_{UZ} \\ Q_{0,\,pot}(k) & \text{if } S_{UZ}(k-1) > L_{UZ} \\ & \text{and } (S_{UZ}(k-1) - L_{UZ}) > Q_{0,\,pot}(k) \\ S_{UZ}(k-1) - L_{UZ} & \text{if } S_{UZ}(k-1) > L_{UZ} \\ & \text{and } (S_{UZ}(k-1) - L_{UZ}) \leq Q_{0,\,pot}(k) \end{cases} \quad (2.54)$$

For the outlet Q_1, the following equations result by analogy:

$$Q_{1,\,pot}(k) = \begin{cases} c_{1,\,amount} \cdot S_{UZ}(k-1) & \text{if } S_{UZ}(k-1) > 0 \\ 0 & \text{otherwise} \end{cases} \quad (2.55)$$

with $c_{1,\,amount}$ being the parameter, and

$$Q_1(k) = \begin{cases} 0 & \text{if } S_{UZ}(k-1) \leq 0 \\ Q_{1,\,pot}(k) & \text{if } S_{UZ}(k-1) > 0 \\ & \text{and } S_{UZ}(k-1) > Q_{1,\,pot}(k) \\ S_{UZ}(k-1) & \text{if } S_{UZ}(k-1) > 0 \\ & \text{and } (S_{UZ}(k-1) - L_{UZ}) \leq Q_{1,\,pot}(k) \end{cases} \quad . \quad (2.56)$$

The potential outlet Q_2 can be calculated as follows:

$$Q_{2,\,pot}(k) = \begin{cases} c_{2,\,amount} \cdot (S_{LZ}(k-1) - LZ_{offset}) & \text{if } S_{LZ}(k-1) > LZ_{offset} \\ 0 & \text{otherwise} \end{cases} \quad (2.57)$$

Here again, $c_{2,\,amount}$ is the parameter. If there is a sufficient amount of water available, the total potential outflow can leave the water reservoir. It holds:

$$Q_2(k) = \begin{cases} 0 & \text{if } S_{LZ}(k-1) \leq LZ_{offset} \\ Q_{2,\,pot}(k) & \text{if } S_{LZ}(k-1) > LZ_{offset} \\ & \text{and } (S_{UZ}(k-1) - LZ_{offset}) > Q_{2,\,pot}(k) \\ S_{LZ}(k-1) - LZ_{offset} & \text{if } S_{LZ}(k-1) > LZ_{offset} \\ & \text{and } (S_{LZ}(k-1) - LZ_{offset}) \leq Q_{2,\,pot}(k) \end{cases} \quad . \quad (2.58)$$

The total model outflow Q_{total} is calculated as follows, with any delay and dead times being ignored:

$$Q_{total} = Q_0(k) + Q_1(k) + Q_2(k). \quad (2.59)$$

Percolation and capillary rise are calculated in the way described below. These values can only be determined if in the respective water reservoirs the water level is above the ground of the water reservoir. The equations are defined only for $k_{perc} = [0, 1]$ and $k_{capi} = [0, 1]$. Thus, it holds:

$$Q_{perc} = k_{perc} S_{UZ}(k-1) \quad (2.60)$$
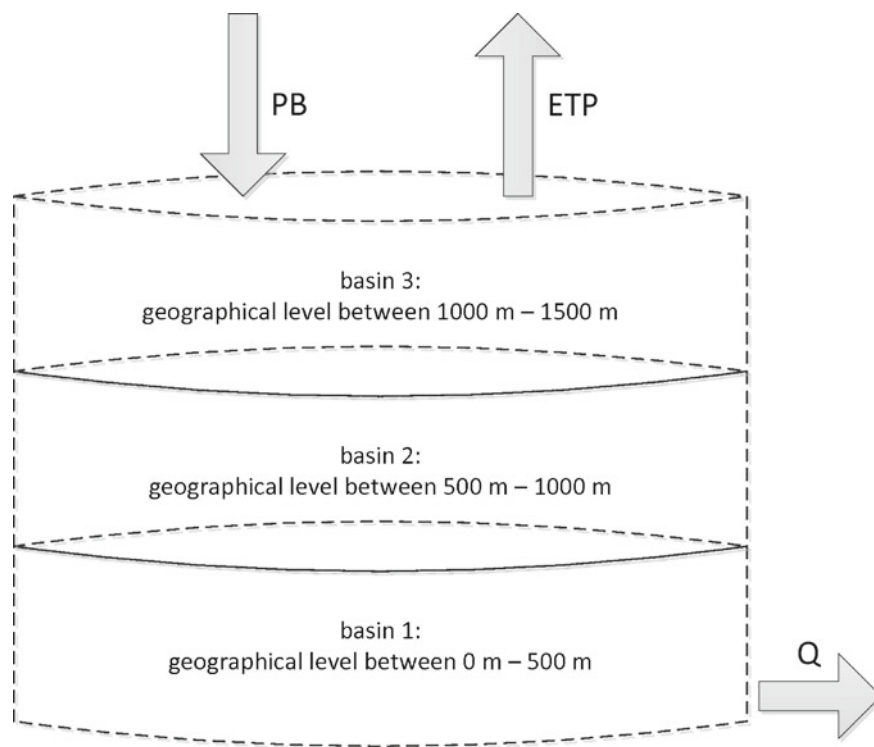$$Q_{capi} = k_{capi}(S_{LZ}(k-1) - LZ_{offset}). \quad (2.61)$$

Fig. 2.5 Subdivision of a model area into three altitude classes

There are different ways of subdividing the basins for the HBV model. An optimum variant would be the classification into altitude classes and land use classes. As such an optimum classification is often not possible due to a lack of relevant data, the model areas are often subdivided into altitude classes only. Figure 2.5 shows the schematic subdivision of a model area into those altitude classes.

2.2 Water Quality Modeling for Freshwater Ecosystems

Albrecht Gnauck

2.2.1 Introduction

Freshwater ecosystems as rivers, ponds, lakes and reservoirs are complex nonlinear open systems and dynamic elements of a system of higher order (a landscape or a biome). Water bodies and biomes are interrelated by inputs into the water and outputs from the water to the surrounding area [291, 340]. Urbanisation and land use transformations, industrial, economic and technological developments as well as

global climate changes have been increasing environmental impacts on freshwater ecosystems. Chemicals and other pollutants released to freshwater ecosystems alter their biological structure, and cause changes of matter concentrations. The term "water quality" reflects the biological, chemical and biochemical composition of dissolved and/or suspended water ingredients as affected by natural and artificial or man-made activities [229]. Then, in the simplest case, the water quality of a freshwater ecosystem can be predicted by means of a biological or mathematical model with linear structure.

Mathematical modeling of water quality processes within freshwater ecosystems has passed the periods of passionately discussed fashion trends of water management options [31, 264, 265, 287] and also the phase in which methods of systems theory have been applied to the problem [168, 171, 172, 174, 249–252, 272]. Since about 1960 water quality models became important consideration for water resources management [304]. The aim of water quality modeling and simulation is an information mining process of actual freshwater ecosystem states and their temporal and spatial developments [295]. Direct measurements and indirect observations of concentrations of chemical, physical and biological water quality indicators serve as information bases of changes of pollution loads and freshwater ecosystem states [55, 126].

Mathematical models are useful instruments in the survey of complex systems. The application of models for water management is almost obligatory for understanding the interrelationships between the structure and the functioning of complex systems as freshwater ecosystems. It is not possible to survey the many components and their reactions in a freshwater ecosystem without the use of a mathematical model as synthesis tool [170]. At present, a choice can be made between at least five lines of water quality modeling procedures:

1. Stochastic or black-box modeling procedure [126, 304]: The deterministic nature of relationships within freshwater ecosystems is assumed to be widely superimposed by stochastic effects. Therefore, applications of classical probability theory and statistical procedures on water quality data are widely used. Evaluations of the water quality state of a freshwater ecosystem by experimentally obtained water quality data by means of regression type statistical models are important tools for water quality management.
2. Deterministic or analytic modeling procedure [170, 319]: The dynamics of each of the water quality processes involved is described by means of ordinary or partial differential equations studied by experiments and coupled within one overall system model. Different management assumptions, exogenous effects by driving variables and endogenous changes of matter concentrations are simulated by means of simulation software packages with different spatial-temporal resolutions.
3. Structural dynamics or thermodynamic optimisation modeling procedure [169]: Methods developed and tested in systems theory and process engineering branches are modified for applications to water quality processes and management options. They are coupled with another.

4. Management or decision making modeling procedure [220, 322]: Simulation models developed in the context of freshwater ecosystem management are coupled with multi-criteria optimisation procedures to get optimised decisions for eco-technological and socio-economic impacts on water quality. Model-based decision support systems including GIS applications are applied to manage river basins and single freshwater bodies [97, 223, 283, 363].
5. Water quality indicators and freshwater ecosystem services modeling procedure [37, 134, 135, 207, 271, 362]: Consideration of socio-economic and ecosystem health aspects in dynamic water quality models combined with different categories of freshwater ecosystem services.

Several attempts have been made to unify the trends of mathematical modeling of water quality with theoretical knowledge [86, 115] and experimental modeling findings [298]. The modeling approaches are represented by dynamic modeling and simulation procedures [173, 219], by methods of artificial intelligence [58, 266], by using genetic algorithms [139], or by other information theory based approaches [111, 117, 228]. As a result, one gets dynamic water quality models with different mathematical structures which are used to describe the time-varying behavior of biological and chemical water quality constituents, to simulate the influence of changing natural and man-made environmental conditions on water quality processes, to forecast spatial and temporal developments of water quality levels, as well as to spread objectified fundamentals for optimal water quality management and decision making. On the other hand, mathematical water quality models may be distinguished by the type of the water quality process or by the type of freshwater ecosystem or landscape under consideration. Therefore, classifications of water quality models are often represented by state space characteristics (discrete or continuous), by the type of models used (linear or nonlinear), by the type of time behavior of models (stationary or non-stationary), or by the type of parameters (lumped or distributed). Nonlinear feedbacks within an ecosystem cause changes of characteristics of signals and systems states during signal transfer processes by modulation of amplitudes, frequencies and phases, and/or by quantification (discrimination of time domain of amplitudes or sampling frequencies of signals) [119, 170]. Another classification is given by the type of systems adaptability and stability [311].

2.2.2   General Aspects of Water Quality Modeling

Mathematical models of water quality are always simplified and abstract pictures of reality which results in a formal representation. A mathematical water quality model provides for a reduction of redundancy and acts as a link between theoretical and empirical cognition. A model is never identical with reality but rather constitutes the fiction of the modeller. Relations between major state variables of a given model will usually not be in full congruence with the relations between state variables of a real freshwater ecosystem. The reality must be distorted (error of relations).

A real system-model comparison can be made for error assessment which is continued until the model is in sufficient agreement with the real system. Such a model testing procedure leads to an improvement of the verbal and/or mathematical model or to an accumulation of wider knowledge on the water quality of a freshwater ecosystem under consideration and can be repeated several times. Once a mathematical model has been tested it may be applied also to other states of the same system or even to systems which have not directly been subjects of the study at hand. This approach is defined as prediction.

The systems approach to water quality modeling, the understanding of freshwater ecosystem processes and their mathematical representation are connected with the amount of available data of water quality processes and freshwater ecosystem compartments. Data sets (or time series) of water quality constituents serve as information base for parameter estimations, for evaluation of mathematical models by verification and validation, and to check water quality management options. Following [131] four cases of water quality modeling lines may be distinguished:

1. Many data and little process/system understanding: For water quality modeling black-box models with different structures (single input–single output, single input–multiple output, multiple input–single output, multiple input–multiple output) are helpful tools for water quality modeling [286, 304].
2. Many data and good process/system understanding: Deterministic water quality models should be applied [170, 294].
3. Few data and little process/system understanding: Univariate and multivariate statistical procedures should be used for water quality modeling [126, 246].
4. Few data and good process/system understanding: Systems analysis methods and process engineering models should be used for water quality modeling [272, 315, 358].

Mathematical water quality models can be used to reveal dynamic freshwater ecosystem properties. They reveal gaps in the knowledge on river basins including lakes and reservoirs and their management regulations, and can therefore be used to set up management and research priorities.

All water quality modeling approaches have common roots but their applicability is quite different [236]. Mathematical models of water quality processes represent the functioning of freshwater ecosystems. They are characterised by algorithmic representations and their interpretations of relationships combining water quality states and matter transfers. Water quality processes within freshwater ecosystems may be considered as stochastic transfer systems (Fig. 2.6). They are characterised by measurable inputs, immeasurable inputs or (stochastic) disturbances, state variables as well as by measurable outputs and measurement errors [131, 170, 242].

Generally, the inputs $x(t)$ are transformed into outputs $y(t)$ by a nonlinear random transfer operator $\mathbf{G}$ which is formed by the water quality processes which are characterised by state variables of interest. The operator $\mathbf{G}$ describes the transient behavior of the water quality processes $y(t) = \mathbf{G} \cdot x(t)$. Between input variables and output variables exists some time dependent redundancy depending from concentration levels of water quality state variables and their kinetic transfer rates. During
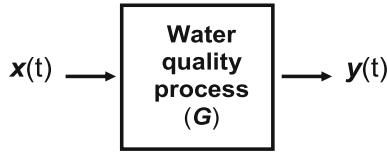
Fig. 2.6 General representation of a stochastic water quality transfer system
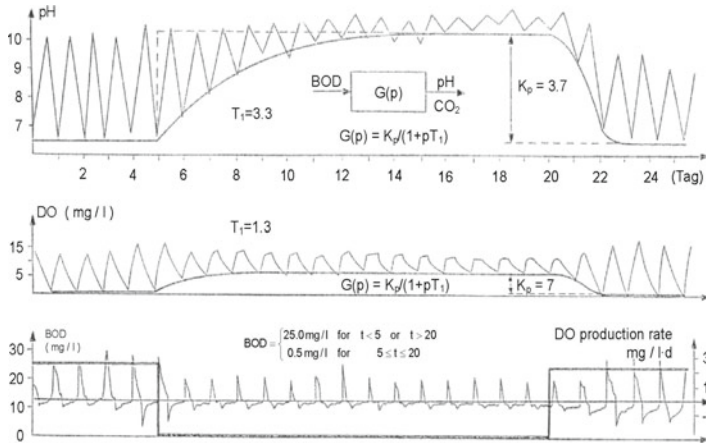

Fig. 2.7 Adaptation of water quality indicators due to management operations (modified from [119])

transition processes all inputs will be smoothed and damped while output variables will be damped, equalised or amplified [328]. Because of random changes of state variables and of fluctuations of environmental driving forces switching processes take place at different time strokes within intervals $(a_i(t), a_i(t))$ and with probability densities $w_i(t)$ of time delays of water quality variables and probabilities $p_i(t)$ for each realisation of a state transfer: $p_i(t) = \int_{a_i(t)}^{b_i(t)} w_i(t) \, dt$. State transitions will be observed after certain time delays [115]. Then, a state transfer is characterised by a quadrupel $\Theta_i(t) = \{a_i(t), b_i(t), w_i(t), p_i(t)\}$. A state transfer takes place absolutely (positive transfer) if $p_i(t) = 1$. If $0 < p_i(t) < 1$ (uncertain transfer), then exists a probability $q_i(t) = 1 - p_i(t)$ that a transfer does not take place.

Nonlinear dynamic water quality processes within freshwater ecosystems are often initiated by switching processes of input variables due to external or internal driving forces and management operations as well [119]. They are overlaid by stochastic disturbances and produce freshwater ecosystem responses or changes of water quality levels respectively with different transfer time constants. Figure 2.7 shows the results of a water quality process adaptation to new systems conditions caused by management operation. Water quality changes depend not only from the reaction kinetics of chemical or biochemical processes, but also from the adaptation time to new chemical/biochemical equilibriums. The water body is polluted by an organic load of 25 mg/l BOD (down). Uniform variations of pH (top) and DO

(middle) express the initial equilibrium state of the water quality system. Disturbing the water quality state by setting the organic load (BOD) nearly to zero (management operation) new equilibriums of the state variables pH and DO will be reached after some time. The adaptations to new equilibrium states are different for pH and DO. For both variables the variations are smaller than before. The adaptation of DO to a new equilibrium runs much faster than for pH. For both variables adaptation and recovery times are different. The freshwater ecosystem responses return to former variations with nearly the same amplitudes after switching off the management operation.

Generally, a mathematical water quality model should contain all the characteristic features which are essential in the context of the problem to be solved or described. In the case of river basin management, a water quality model must contain the features which are of interest for water management of the entire river basin. The model has to cover hydrological, economic and ecological aspects where natural and man induced reactions of such a complex system might be not necessarily the sum of all individual reactions.

Three sub-models have to be established for water quality modeling:

1. The hydrodynamic sub-model which describes the fluid dynamics of the water body under consideration,
2. The thermodynamic sub-model which describes the energy distribution within the water body and the related dependencies of physical, chemical and biological processes from water temperature,
3. The biochemical sub-model which describes the changes of chemical and biological substances within the water body.

Classical dynamic water quality models are based on stationary or instationary mass balances of the state variables C_i of interest (C—concentration of ith substance) which are simply expressed by the following equation:

$$Accumulation = input - output \pm reactions.$$

The term "accumulation" means the accumulation of an ingredient within a water body. It depends from the mass import into the control volume and the mass export out of the control volume, and from chemical and biological reactions within the control volume. The term "reactions" may be positive if the reaction contributes to the mass of an ingredient. Otherwise it will be negative. In the case of conservative substances the reaction term will be zero. If steady state processes are considered where $dC/dt = 0$, then no accumulation will take place within the water body. The output results from input and reactions:

$$Output = input \pm reactions.$$

Without consideration of variable "time" one gets static linear and nonlinear regression type models of water quality. The difficulties in establishing mass balance models are in most cases attributable to problems in formulating the source and

loss terms. Many of the processes involved cannot be measured or only indirectly determined.

Mass balances of water quality variables are based on the hydrological balance of the water body of interest. Hydrological inputs are closely coupled with meteorological ones. Water mass may be considered as an inert substance with different inputs and outputs from the water body itself. Therefore, the term "accumulation" can be understood as "change in storage" [284]. The distribution of flow rates may be described in the following way as difference between positive and negative balance terms:

$$\Delta Q(t) = PV(t) + DV(t) + Q_{in}(t) - EV(t) - Q_{out}(t), \qquad (2.62)$$

where the terms on the right side of the equation represent precipitation $PV(t)$, condensation on surface $DV(t)$ (usually negligible), horizontal inflow (surface water and groundwater) $Q_{in}(t)$, evaporation or evapotranspiration $EV(t)$ (in plant growth environments), and horizontal run-off $Q_{out}(t)$ respectively. The storage capacity of ground, which has bearings also upon the chemical composition of water, plays an important role in the context of horizontal inflow and run-off. Irregular heating of the earth's surface is a cause for geographical differences in precipitation and evaporation, which may entail positive to strongly negative hydrological balances in different regions. Direct hydrological data of run-off quantities are usually available as daily mean values from level gauging [30]. If gauges are not available, values may be derived alternatively by means of correlation or estimation form several stations in the vicinity or by means of annual mean values of specific run-off characteristic of the region under review. Determination becomes difficult for impounded rivers where sizable displacements in flow distribution may be caused by storage capacities of reservoirs and weirs. Distinct diurnal run-off patterns are generally produced by peak power generation.

For input into water quality models, run-off data are used in tabulated form or the annual pattern may be approximated by periodic regression functions or by polynomials. Characteristic patterns are available for various places, but stochastic variations in consecutive years are so large that long series of observations are required. An annual pattern, generally, depends also on mean flow rates even for one and the same site. In the absence of real data, run-off series may be set up by means of Markov chains or Monte-Carlo simulations [60, 62, 175, 281]. The log-normal distribution of flows is one of their characteristic properties. This is partly related to with the flood waves which are transported in the river in a characteristic mode.

Water management of complex river basins requires mathematical simulation models of water mass and water quality for different time and space horizons allowing a process control according distinct management goals. Besides of long-term goals like realisations of political water management strategies or ecological landscape ideals, medium-term goals like sanitation and/or restoration activities in river catchments and short-term operations like remediation of damages after floods or pollution catastrophes [21, 70]. Since the fundamental contribution of Streeter and [306] to water quality modeling especially DO-BOD models were developed up to 1975 (Table 2.1). The consideration of morphometry and complex hydrodynamic

processes within water bodies as well as the coupling of models with optimisation procedures led to powerful simulation models for water management during the period 1975–1985 [319]. With growing complexity of management tasks in river basins further theoretical and practical demands have been arisen for extensions of such models since 1985. Model-based environmental planning and decision making characterise this phase up to 1995 [181]. Based on modern developments of hydrological engineering procedures and new software technologies decision support models including GIS were developed for water management of river basins [148]. About 2005 more scientific impetus was added to water management models by the use of environmental variables to indicate global climatic changes and environmental pollution levels [297, 321, 332]. Additionally, the inclusion of socio-economic relationships and the evaluation of ecosystem services came now in the focus of environmental informatics and management [69, 135]. Since the beginning of the new millennium, aspects of long-term ecological research [219] and ecosystem health [362] as well as new methodological developments in water management modeling including water quality like game theory [350] or Petri Net modeling [105] offer further perspectives in engineering and water quality management. They require new software tools for their applications and management supporting functions. Table 2.1 gives a short overview on essential steps of development of water quality models.

2.2.3 Water Quality Models for Rivers

Rivers represent horizontally structured freshwater ecosystems with water flow as the dominant ecological influence variable. Realistic water quality models describe matter transport due to physical phenomena like diffusion, advection (convection) and dispersion as well as temperature dependent degradation of organic matter by chemical and biochemical reactions within the water body. Water quality in rivers is often characterised by its content of dissolved oxygen over a fixed distance or at a fixed point of the water body which is one of the main indicators to model river water quality. Other measures of water quality are the dissolved oxygen deficit compared with temperature dependent saturation concentration at equilibrium, or by BOD which represents the amount of biodegradable matter. Generally, the DO concentration of a water body is a common measure of non-toxic organic pollution, but there are many other variables by which it can be directly or indirectly affected. The DO content describes the so-called ecological self-purification power of the water body. In the case of sufficient ecological conditions the following relationship between oxygen production P and respiration R is valid:

$$P/R > 1.$$

In the case of river water pollution by non-toxic organic substances the bacterial decay of these substances leads to an increase of respiration and a decrease of oxygen production. The maximum self-purification capacity will be reached if $P = R$. If

Table 2.1 Essential steps of water quality modeling

Time	Model development	Reference
1925	DO–BOD model	[306]
1935–1950	Modifications of DO–BOD model for different waste water impurities	[94, 320]
1950–1965	Critical review of DO–BOD processes, consideration of hydrodynamic processes	[52, 81, 235]
1965–1975	Consideration of additional variables in the DO balance equations of water bodies, consideration of eutrophication processes in models	[234, 315, 317]
1975—1980	Extensions of DO–BOD models, application of new parameter estimation methods	[56, 272, 356]
1980–1985	Coupling of DO–BOD balance models with optimisation procedures, balance models for lakes and reservoirs	[21, 140, 185, 294]
1985–1995	Consideration of water quality models in environmental planning models including GIS, developments of decision support models for river basins	[97, 176, 163, 319]
1995–2000	Consideration of eutrophication and socio-economic processes in planning models for river basins, considerations of water quality changes due to global climate change, environmental risk models	[51, 136, 166, 181, 188]
2000–today	Consideration of ecological indicators, aspects of ecosystem services and ecosystem health in water quality models, application of game theoretic and discrete modeling procedures for water management, consideration of long-term research aspects in water quality modeling	[68, 95, 104, 119, 349, 363]

$R > P$, than the water quality conditions will be changed from oxic to anoxic ones. The self-purification capacity has been passed over. In consequence, in the following river stretches an oxygen deficit will be observed. This phenomenon is known in the literature as the so-called oxygen sag curve [81]. With ongoing decay of organic biomass and additionally oxygen input by photosynthesis and re-aeration the ratio P/R will be greater 1.

Dynamic river water quality models are based on mass balances which are derived from the continuity equation and which describe the longitudinal and transversal distributions of conservative and non-conservative substances in the water body concerned [229, 272, 284]:

$$
\begin{aligned}
\partial C/\partial t = {} & \partial/\partial x (D_x \cdot \partial C/\partial x) \\
& + \partial/\partial y (D_y \cdot \partial C/\partial y) - v_x \cdot \partial C/\partial x \\
& - v_y \cdot \partial C/\partial y + sources - sinks.
\end{aligned} \tag{2.63}
$$

In water quality management, stochastic models are suitable for short-term forecasting, provided that the processes involved are of stationary nature. In opposite of that, deterministic models can be used also in long-term control of water quality and

in parallel with instationary processes. Key elements of the mass balance modeling approach are [170, 204, 238, 284]:

1. A defined control volume (the water body under consideration),
2. Inputs and outputs that cross the boundary of the control volume,
3. Transport phenomena within the control volume and across the boundaries,
4. Reaction kinetics of state variables within the control volume.

The applicability of a dynamic water quality model is delimited by the choice its structure. Therefore, major influence variables should be clearly verified by measured data before computation of simulation runs is actually started [116]. Parameter estimations and simulations should be made by means of independent data. Analogous demands must be met when a river model is to provide forecasts of water quality for a given river stretch. Signal analyses of measured data (correlation coefficient, ACF, CCF, power spectra, digital filter analysis, and wavelet analysis) provide starting information for modeling and enable a general description of causal relationships.

2.2.3.1 Static Experimental Models

The simplest static water quality models consist of multiple linear regression functions (first-order polynomials) of the observed variables. They are mathematically described as follows:

$$y = a_0 + \sum a_i x_i, \quad i = 1, \ldots, n. \tag{2.64}$$

It characterises the stochastic dependency of one goal variable y from n ($n \geq 2$) input variables $x_1, x_2, \ldots, x_n$. The parameters (coefficients) b_n are called (partial) regression coefficients where a is called regression constant. Major influence variables are selected by means of partial correlation coefficients of the data set. An example of such a model is given by a simple multiple input–single output model with the DO concentration as goal function to express the variations of dissolved oxygen content in a river cf. [306]:

$$DO = a + b_1 T + b_2 Q + b_3 BOD.$$

Such static linear multiple regression models are often used to calculate expectations of chemical and biological water quality indicators [265]. The estimation results depend on the available river data base as well as from stationary chemical and hydrodynamic river conditions.

Additionally, autoregressive models of the form $y(t) = a_0 + \sum a_i(t - i)$ may be considered as multiple linear models. For the lower part of the River Spree an autoregressive model was successfully applied to forecast the DO changes over a week:

$$DO(t) = a_0 + \sum a_i DO(t - i). \tag{2.65}$$

The effectiveness of a linear approach will differ by the hydrodynamic characteristics of rivers. For rivers with a flow velocity $v = 0.5\,\text{m/s}$ sufficient accuracy is obtainable even from ordinary regression models and no substantive improvement in model quality would be get from applications of recursive regression procedure [125]. Differentiated exponential weighting of recursive regression models would not yield any additional benefit. For their simplicity and sufficient accuracy for most practical purposes, multiple linear models can be used in establishing management strategies, provided that the most important variables of the process are taken into account. Models with daily measured data used, has proved to be suitable for water quality forecasts at a fixed point of cross-sectional area or for river stretches with uniformly water flow. They were found to be sufficient for simulations and predictions in order to make an assessment of their self-purification potential.

For all cases, the parameters can be estimated by ordinary least squares or by recursive least squares estimation procedures [92, 365, 366]. The quality of fit of a linear regression function (simple regression or multiple regressions) can be checked by statistical measures [347]:

1. Performance index (coefficient of determination) $B = R^2$.
2. Residual sum of squares is calculated as follows: $S_R = (y_i(t) - y_i * (t))^2$ where $y_i *$—estimated model output.
3. Residual variance $s^2 = S_R/(n - (m + 1))$ where n—number of variables, m—number or parameters for $n > m + 1$.

The multiple linear regression model of DO given above will be expanded by nonlinear terms of the state variables, since the relationships within the water body concerning the DO budget are of nonlinear nature. Polynomials up to the third order have proved to be suitable for the description of rivers. The following nonlinear approach is considered as complete and obtained on the base of the above given simple linear model:

$$DO = a_0 + a_1 T + a_2 Q + a_3 BOD + a_4 T^2 \\ + a_5 Q^2 + a_6 (BOD)^2 + a_7 T^3 + a_8 Q^3 + a_9 (BOD)^3. \qquad (2.66)$$

The model now looks for is to describe linear and nonlinear relationships. It should not be too comprehensive, since model output will suffer from too many parameters owing to the risk of including unimportant variables of higher order. Therefore, the relatively voluminous nonlinear model is reduced stepwise by removal of unimportant variables. The performance index B was used as decision criteria. It results in the following nonlinear DO model:

$$DO = a_0 + a_1 T + a_2 Q + a_3 BOD \\ + a_4 T^2 + a_5 Q^2 + a_6 (BOD)^2 + a_7 T^3. \qquad (2.67)$$

The result of model quality assessment by means of the performance index characterises this model as the best one for the purpose at hand (Table 2.2). However,

Table 2.2 Goodness of fit of static DO models for a river in a hilly region

Model state variable	B (%)	Comment
T, Q, BOD	71.6	Linear model valid for flow speed $v_x = 0.5\,\text{m/s}$
T, Q, BOD, T^2, Q^2, $(BOD)^2$, T^3, Q^3, $(BOD)^3$	64.9	So-called complete model, low estimation quality because of consideration of unimportant variables, weak convergence of algorithm
T, Q, BOD, O^2, T^2, $(BOD)^2$, T^3	73.5	Important variables considered with sufficient accuracy; sufficient estimate quality
T, Q, BOD, Q^2	65.7	Deterioration of estimate quality compared to linear model by inclusion of unimportant variables

Table 2.3 Correspondence between weighting, K, and goodness of fit

Weighting, K	1.00	0.98	0.95	0.93	0.90	0.88	0.85
Residual sum, S_R	1.9393	1.4694	1.1619	0.9361	1.0521	1.7107	2.2716

interpretations of the nonlinear terms of input variables are often very harmful and problematic. They express the strength of influence onto the goal variables qualitatively but quantification is not possible. Material transfers within a water body are controlled by other components of the freshwater ecosystem (including state variables, driving variables, forcing functions, control functions, constants, and auxiliary variables). Therefore, further enhancement of model quality will now be possible only by choice of a proper parameter estimation procedure.

The recursive regression estimation procedure allows the formulation of regression type models under consideration of time dependent parameter changes (quasi-dynamic models). The new parameter value at discrete time point (k) is computed on the base of its "old" value at discrete time point $(k-1)$ by addition of a valuated difference (error) between new system output at time point (k) and estimated model output at $(k-1)$ multiplied by the old parameter vector. K_k denote a weighting factor at time stroke k, where k is equal to the number of experimental data:

$$a_k = a_{k-1} + K_k(y_k - x_k^T a_{k-1}). \tag{2.68}$$

Model results depend from the choice of the (exponential) weighting factor, K, contained within the recursive parameter estimation algorithm (Table 2.3). Best simulation results for DO models of Zwickauer Mulde River are obtained by weighting factor $K = 0.93$. For all other weightings the residual sum of squares increases.

The intensity of weighting will substantially depend on the rates of parameter variation on the extent of disturbances. These two influences must be given different weightings. The model quality depends on the value of the weighting function at time K_{k+1}. Hence, optimum weighting will be achievable only as a compromise. The effectiveness of such an approach will differ by the hydrodynamic characteristics of rivers. By applying the performance index in judging the model output with measured values, it can be seen from Table 2.4 that sufficient accuracy is obtainable even from

Table 2.4 Performance indices, B (%), of linear static DO models

River	Flow rate v (m/s)	B (%) NR	B (%) RR
Elbe	>0.5	90.0	90.6
Mulde	>0.5	62.7	71.6
Spree	0.2	45.3	69.5

Table 2.5 Interpretation of parameters of regression type models

Type of regression	Model equation	Interpretation of parameters
Linear	$y(t) = a_0(t) + a_1(t)x(t)$	a_0—initial value, a_1—mean rate of change
Parabolic	$y(t) = a_0(t) + a_1(t)x(t) + a_2(t)x^2(t)$	a_0—initial value, a_1—mean rate of change, a_2—mean process acceleration
Polynomial	$y(t) = a_0(t) + a_1(t)x(t) + \cdots + a_n(t)x^n(t)$	Interpretation is impossible
Exponential	$y(t) = y(0)e^{-rt} + E$	Kinetics of 1st order: $y(0)$—initial concentration value, r—rate of change, E—random quota

NR models for rivers with flow rate $v \geq 0.5$ m/s. An improvement of model quality is obtainable by application of RR in dependence of the hydrologic regime of the river under consideration. On the other hand, for low flow conditions no substantive improvement will be obtained by recursive regression method.

Consequently, the reliability of linear and nonlinear regression models depends not only from the available data base but also from the kind of estimation procedure used. For rivers with high flow velocities and, therefore, with highly time-varying changes of concentration levels of water ingredients, static regression models are not well suited for water quality management statements. But there is a valuable contribution of such models for estimation of changing water quality conditions regarding mean or low flow conditions in rivers. Using recursive regression type models with time-varying parameters the computed results can be interpreted as follows (Table 2.5).

From Figs. 2.8, 2.9, 2.10, 2.11 can be seen that regression models represent the spatial-temporal process behavior of water quantity and quality in running waters with different performances depending from process dynamics. As an example, the (physically determined) water flow of the Lower Havel River, Germany, changes by 100 % between gauges SPK0020 and Hv0190 (cf. Fig. 2.8). The polynomial approximation cannot follow the (dynamic) jump process in water mass. Therefore, this type of mathematical models describes more the static process behavior rather than a dynamic one. But such a static model can be used to forecast the values of variables under consideration in the case of uniform environmental conditions.

Another picture will be getting if chemical and/or biochemical processes dominate the water quality. Changes of BOD are well estimated by a 2nd order polynomial
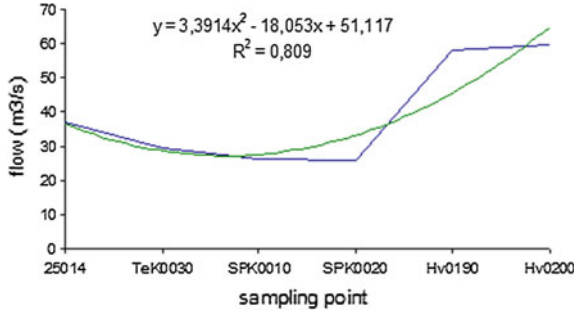
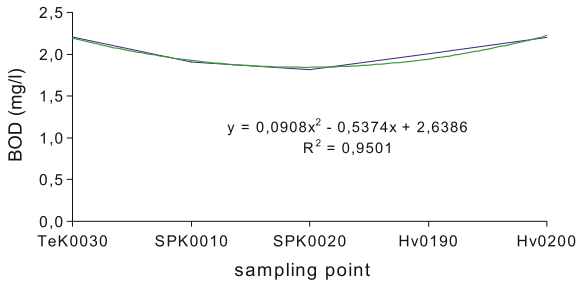**Fig. 2.8** Approximation of water flow by a 2nd order polynomial (Lower Havel River, Germany)

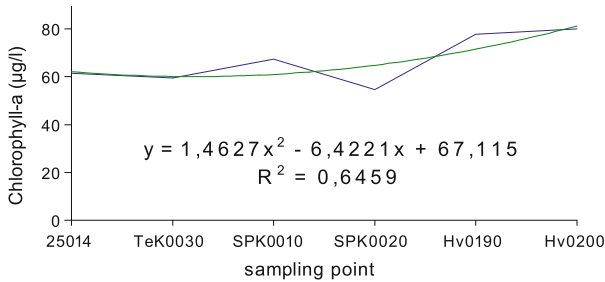**Fig. 2.9** Parabolic development of BOD concentration along a stretch of Lower Havel River

Fig. 2.10 Parabolic development of phytoplankton biomass along a stretch of the Lower Havel River

with a performance of 95 % (cf. Fig. 2.9). This water quality variable characterises the natural and anthropogenic pollution load with easily degradable organic substances. In opposite of hydrological conditions with increasing water flow between the gauges SPK0020 and Hv0190 no considerable changes of BOD concentration are observed. If concentrations of water quality indicators are characterised by influences of mixtures of natural drivers and processes as well as man-induced influences of their changes follow the dominant process. In the case of non-toxic drivers the algal biomass concentration lays out changes due to physical influences (transportation by water flow, residence time of water) as well as by biological and chemical reactions (nutrient uptake, algal growth).
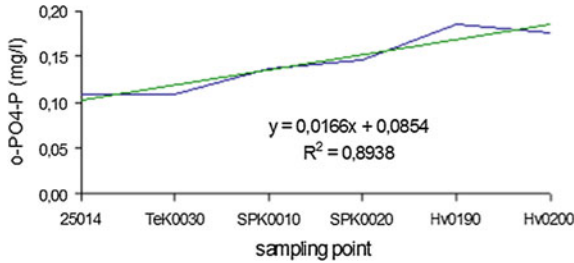
Fig. 2.11 Linear trend of orthophosphate phosphorus along a stretch of the Lower Havel River

As can be seen from Fig. 2.10, changes in phytoplankton biomass concentration follow mainly the hydrological conditions accompanied by phosphorus uptake for phytoplankton growth. The mathematical trend functions equalises all dynamic influences. It can be interpreted as a medium behavior of biomass balance.

The spatial-temporal trend of such a phytoplankton nutrient follows the dynamic changes of phytoplankton biomass overlaid by a physical component (water flow) (cf. Fig. 2.11). In running waters these changes are mostly influenced by hydraulic conditions of rivers [229].

Table 2.6 contains results of regression models for different water quality indicators observed in a low flow river. The signs in the last column indicate the fulfilment of 95 % level of significance of estimated model output. It can be seen from the value of performance index that some of the regression functions are not valid. This means,

Table 2.6 Regression type models of water quality indicators of Lower Havel River, Germany

Water quality indicator	Regression model	R^2	$P(95\%)$
Water temperature	Polynomial	0.6177	+
Conductivity	Polynomial	0.1971	−
Chloride	Polynomial	0.0382	−
DO	Polynomial	0.3858	+
BOD	Polynomial	0.9501	+
COD	Polynomial	0.7611	+
NH4-N	Exponential	0.5669	+
NO2-N	Exponential	0.4879	+
NO3-N	Exponential	0.4746	+
o-PO4-P	Exponential	0.8938	+
TP	Exponential	0.0822	−
SiO2	Exponential	0.8888	+
Suspended matter	Polynomial	0.0227	−
Chlorophyll-a	Polynomial	0.6459	+
Inorganic part of biomass	Polynomial	0.6742	+
Loss of organic matter	Polynomial	0.1418	−

that internal and external driving forces influence the concentration levels of water quality indicators very strongly.

For water quality management forecasts, polynomial and exponential functions forces of 2nd order are often suitable. Higher order polynomials may be accompanied by negative model results which do not agree with reality cf. [304]. Model parameter values diminish strongly along with rising order.

2.2.3.2   Dynamic Experimental Models

Dynamic experimental models of freshwater quality, generally, can be estimated in terms of a weighting function of a water quality indicator under consideration or as parameters of difference equations. Mostly, they will be solved by parameter estimation procedures [304] or numerically. They are also known as time series or regression type models and include the history of a water quality process. Their general structure is given by:

$$Y(t) = -\sum a_i Y(t-i) + \sum b_{ij} X(t-i), \qquad (2.69)$$

where Y represents the goal variable, and X represents a set of influence variables with time delay $(t-i)$. The variable $Y(t-i)$ describes the history of the water quality process variable under consideration.

Difference equation models are comparable with analytical water quality models formulated as differential equations and provide more flexibility for the mathematical representation of dynamic water quality processes. Analogous to advanced static experimental models the prediction power of such models is also limited. By using the same variables as in static experimental modeling the following second-order difference equation model for the DO concentration was applied to predict the DO concentration:

$$\begin{aligned}
DO(t) = {} & -a_1 DO(t-1) - a_2 DO(t-2) + b_{11} T(t-1) \\
& + b_{12} T(t-2) + b_{21} Q(t-1) + b_{22} Q(t-2) \\
& + b_{31} BOD(t-1) + b_{32} BOD(t-2), \qquad (2.70)
\end{aligned}$$

where a_i and b_{ij} are parameters estimated from real data, DO—dissolved oxygen concentration, T—water temperature, Q—water flow, BOD—chemical oxygen demand. As an example, the maximum prediction interval of the River Spree was given by 9 days.

Such dynamic experimental water quality models must be considered as precursors for deterministic descriptions of matter balances in running waters. According to the availability of measured data, loading variables of an upper gauge can be used as input variables and concentration data at a lower gauging station constitute the output of the given system (or model). Hence, equidistant data have to be measured at both gauges at identical time intervals and must be kept synchronised not less than

ten days [125]. The time shifting between input and output signals is separated by a time-delay. The possible outputs of dynamic experimental models depend on the quality of the data available. Model quality will be lower in response to the use of daily measurements (increase of mean model error), since changes with high frequencies are no longer recordable. When mixed data are used for modeling (e.g. continuous DO and water temperature data, daily measured water flow and BOD values) oscillations of the models parameters are caused by recursive estimation procedures [125]. Further studies in a stream revealed periodic water temperature variations in a 24 h rhythm, while the trend movement of DO was caused by variations of water flow. Highly frequent DO variations were caused by variations of BOD and other disturbance variables (meteorological and environmental effects other driving variables).

Another dynamic experimental method will be derived from control theory. Reference [275] adapted the description of a continuous dynamic process by a time discrete model applying the z-transformation on a difference equation:

$$G(z) = B(z^{-1})/A(z^{-1}) + \xi(z).$$

For discrete water quality data of the Elbe River the so-called Stochastic Transfer Method was used to predict the biomass content of the water body:

$$CHA(t) = f_0(t) + f_1(t)T + f_2(t)DO + f_3(t)pH$$

where f_i are parameters of z-transformation function.

2.2.3.3 Mathematical Analytical Models

Water quality processes take place in a chemical-physical environment. Dynamic river water quality models are state-space models by virtue of their mathematical form [133]. They are known in practice as modified Streeter–Phelps models. It has often been problematic to apply such models to experimental data, because the stochastic effects of natural and artificial driving forces are inadequately covered by them. Differential equations include derivatives of the state variables by independent variables (time, depth, distance, etc.) by small differences of the independent variables. They allow to model changes of water quality in a continuous manner. The equations are considered to be parameterised, if real values are assigned to the coefficients in the equations concerned. The solution (or integral) of such an equation will be defined as analytical. It is an algebraic equation giving the values of state variables at time-coordinate t or space-coordinate r. Mostly, high sophisticated water quality models cannot be solved in a closed, analytical manner. They have to be solved by numerical procedures where numerical solutions have been proposed for the majority of water quality models [170]. Consequently, this means that mathematical simplifications lead to losses of information [228].

Analytical water quality models are based on mass balances which are derived from the continuity equation. They describe the longitudinal and transversal distributions of conservative and non-conservative substances in the water body concerned [234, 272]:

$$\partial c/\partial t = 1/A(x,t) \cdot \partial/\partial x \cdot (Q(x,t) \cdot c) + S(c,x,t), \qquad (2.71)$$

where c—concentration of suspended or dissolved ingredient of water, A—cross-sectional area of river, Q—freshwater flow, and S—sources and sinks. The following assumptions are valid for one-dimensional running waters with water flow as the dominant driving variable:

1. The dispersive component of the flux is small compared with the advective one.
2. The concentration of the substance considered is assumed to be uniform in the lateral and vertical directions. That means, the water body is assumed as well mixed.
3. The freshwater flow and the cross-sectional area may vary in space and time.
4. Sources and sinks of water ingredients are functions of time and space, and of its concentrations or functions of concentrations of other substances.
5. The terms of the general model equation for specific running water are determined by hydraulic and geomorphologic characteristics as well as by hydrological and meteorological and climatic conditions of the watershed.
6. The water quality status of running water under consideration is determined by various physical, chemical and biological conditions as well as by wastewater input and site influences.

Longitudinal mixing of water ingredients is largely based on longitudinal dispersion which is described by an equation of the translation-diffusion type with D_x as dispersion coefficient [102]. The dispersion coefficient, D_x, represents not only the action of longitudinal dispersion but all other disturbance processes which act in the same direction [354]. Theoretical models are, basically, applicable to all kinds of rivers, but they are inaccurate for the specific case, since the stringent preconditions are usually not satisfied and disturbances must be neglected [22]. An error range of something between 50 and 100 % has been claimed for theoretical models by [100, 101]. Longitudinal mixing has often been neglected in models for stationary discharges, as it plays a role only in time-dependent discharges [233]. This has greatly simplified the models [170, 316, 325].

Dissolved oxygen is one of the most important water quality indicators for freshwater ecosystems. Therefore, most of water quality models of rivers are derived from the simple balance model of dissolved oxygen deficit, which has been proposed by [306] based on the assumption of a first-order reaction:

$$dD/dt = K_1 L(t) - K_2 D, \qquad (2.72)$$

where $D = DO_S - DO(t)$—the DO deficit (mg/l), DO_S—temperature dependent saturation concentration of DO (mg/l), DO(t)—dissolved oxygen concentration at

time t (mg/l), K_1—decay rate constant (d^{-1}), L(t)—organic pollution (organic matter) at time t (mg/l), K_2—re-aeration rate constant (d^{-1}).

In this equation only carbon degradation and atmospheric aeration is covered, while other substantive oxygen balance terms are neglected [128, 234, 272, 314]. Then, the equation of dissolved oxygen deficit following a flow time t is related to the origin of pollution by a point source:

$$D(t) = K_1 L_0/(K_2 - K_1) \times (e - {^{K_1^t}} - e^{-K_2^t}) + D_0 e^{-K_2^t}. \qquad (2.73)$$

Using the flow velocity v, the independent variable t can be transferred to distance $x = v \times t$ in flow direction. For computing the dissolved oxygen profile in flow direction the following assumptions will be made:

1. Complete mixing of waste water input with river water,
2. Constant flow rate in longitudinal direction over the cross sectional area of the river segment under consideration,
3. Chemical reactions including biodegradation and re-aeration are considered as first order reactions.

The DO concentration after discharge of waste water can be calculated by the following formula for mixing [279]

$$DO = (Q(W) \times C(W) + Q(R) \times C(R))/(Q(W) + Q(R)) \qquad (2.74)$$

where Q(W)—waste water flow (m^3/s), Q(R)—river water flow (m^3/s), C(W)—DO concentration in waste water (mg/l), C(R)—DO concentration in river water (mg/l).

Organic pollution of running waters by waste water with easily degradable organic substances is indirectly measured as the amount of the DO concentration which is required for bacterial decomposition of these substances. This amount can be expressed by BOD (biochemical oxygen demand). In the case that only chemical reactions are taken place data of COD (chemical oxygen demand) have to be analysed. Time variations of BOD depend on both the intensity of organic pollution and water temperature but they are independent of the DO concentration yet, under the assumption that a sufficient amount of dissolved oxygen is present in the water body. The variation of the deficit over time is proportional to the amount of organic pollution:

$$dD/dt = K_1 L. \qquad (2.75)$$

Integration results in

$$L(t) = L_0 e^{-K_1^t} \qquad (2.76)$$

where L_0—initial pollution at a fixed point of a river. Related to base e, the term K_1 will be determined, whereas $k_1 = K_1/2.303$ is related to base 10. Reference [306] used the following Arrhenius equation to express the temperature dependence of K_1 where Θ is a parameter with values depending from water temperature:

$$K_1(T) = K_1\Theta^{(T-20)}. \tag{2.77}$$

In rivers atmospheric aeration is often more intensive than biogenic aeration. The K_2-value depends on water temperature as well as on temperature-sensitive variables, such as molecular diffusion, kinematic viscosity, and surface tension. Following Fick's first law the dissolved oxygen deficit is described according to the equation for K_1 analogously:

$$dD/dt = -K_2 D. \tag{2.78}$$

Integration results in

$$D(t) = D_0 e^{-K_2 t}. \tag{2.79}$$

According to the determination of K_1-value the following Arrhenius expression is valid for rivers with an ice-free water surface:

$$K_2(T) = K_2\Theta^{(T-20)}. \tag{2.80}$$

Findings of computational and experimental determination of K_2-values have been presented by several authors in the past (see [170]). Values of Θ are presented in Table 2.7 to calculate K_i—parameter rate constants expressing the temperature dependence of chemical and biochemical reactions in freshwater ecosystems.

Most of empirical models used to determine K_2 are of the following non-linear regression type [61]

$$k_2 = a \times v^m \times \cdot z^{-n} K_2 = 2.303 k_2,$$

Table 2.7 Θ—values for kinetic parameter estimation

Kinetic parameter $K_i(\mathrm{d}^{-1})$	Temperature class (°C)	Θ
Decay rate constant K_1	4–20	1.135
	5–15	1.109
	5–25	1,05
	10–30	1.047
	15–30	1.042
	20–30	1.056
	30–40	0.967
Re-aeration rate constant K_2	5–22	1.0241
Nitrification rate constant K_3	5–25	0.877
	10–22	1.06–1.08
	22–30	1.097
Benthic oxygen demand rate constant K_4	5–20	1.072
	5–30	1.04–1.15

Table 2.8 Parameter values for calculation of $K_2 = 2.303\,k_2$ (modified from [304])

Flow rate v (m/s)	Mean depth z (m)	a	m	n	Reference
0.50–1.5	0.65–3.5	2.18	0.969	1.673	[61]
0.03–1.5	0.12–3.4	3.00	0.730	1.752	[241]
0.55–1.5	0.65–3.5	2.06	1.000	1.503	[161]
0.55–1.5	0.65–3.5	2.30	0.924	1.705	[184]

where a—regression factor, v—mean flow rate (m/s), z—mean depth (m) of water body. Table 2.8 contains a list of parameter values of empirical models presented in the literature. These models are more closely adjusted to specific situations and provide often accurate results. But they can hardly be generalised.

The dissolved oxygen supply of rivers in hilly or mountain regions is almost exclusively physical, whereas rivers in flatlands are typical representatives of shallow water bodies which are characterised by high photosynthetic oxygen input. Comparisons of experimentally and computationally determined K_2—values have been shown that the empirical results were often in fairly good agreement with tracer experiments. It was also found a correlation to exist between the values obtained from tracer experiments and the slope of the river stretches. Hydraulic indices like Chezy's formula, longitudinal dispersion coefficient, D_x, and Froude's number were used by some authors for simple estimation of K_2 (cf. [161]).

The longitudinal dispersion rate, D_x, in rivers is usually determined by tracer measurements [102, 225], evaluated by means of the routing procedure. For the Zwickauer Mulde River variations of K_1 and K_2 were computed for approximately constant flow rate, v_x, for an assessment of the effects of D_x on changes in the dissolved oxygen deficit (Table 2.9). Increasing values of D_x were accompanied by growing estimates of K_1 and K_2 with constant value of water temperature with the magnitudes of the K_2-values depending on different hydraulic conditions (e.g. variation of turbulence).

An increase of water flow causes changes of K_2-values. An increase of the mean temperature from 8 to 20°C, with constant water flow, however, causes K_1-values and K_2-values to go down in parallel with rising D_x due to several factors depending on water temperature (organic pollution is decayed, atmospheric aeration is reduced; degradation is reduced due to higher dispersion per unit volume).

Practically useful results are obtainable from simple segmentation of the river under consideration [96]. Incorporation of nitrification, sedimentation, adsorption, oxygen consumption by resuspension of sediments, oxygen demand of sessile organisms, and respiration of phytoplankton are the most common approaches to the expansion of dissolved oxygen models which are mostly restricted to oxygen-consuming processes. Advancing along these lines had often been undertaken in the past by case studies. Therefore, complex river water quality models cover additional environmental variables as photosynthetic oxygen input [234, 288] and phytoplankton dynamics [21], oxygen demand due to nitrification process [329], nutrient circulations

Table 2.9 Effects of changes in D_x on estimates of K_1 and K_2 for a river in a hilly region

D_x (cm^2/s)	T(°C)	Q(m^3/s)	K_1 (d^{-1})	K_2 (d^{-1})
1	8	14.5	1.43	47.44
	8	14	0.46	9.76
	20	14	0.14	5.20
3	8	14.5	1.43	47.53
	8	14	0.74	15.34
	20	14	0.09	4.48
5	8	14.5	1.43	47.76
	8	14	0.78	16.54
	20	14	0.09	4.56
7	8	14.5	1.47	47.90
	8	14	1.01	20.40
	20	14	4.28	4.28
10	8	14.5	1.47	48.36
	8	14	1.29	25.70
	20	14	0.05	3.78

(Sandoval et al. 1976), sediment oxygen demand due to point and non-point pollution [79, 229] as well as well as temperature-dependent and meteorology-dependent effects [299] and hydrodynamic influences [170]. The daily photosynthetic input of dissolved oxygen can be estimated according [327] by

$$DO = a \times \mu \times CHA \times \Theta^{(T-20)} \times LILIM, \tag{2.81}$$

where a—ratio DO (mg/l)/phytoplankton ($\mu gCHA/l$), μ—growth rate of phytoplankton [56], CHA—phytoplankton concentration ($\mu gCHA/l$), $\Theta = 1.066$, $LILIM$—light limitation of phytoplankton growth with $LILIM = 2.718 \times f \times LIAT/\varepsilon \times z$ and f—photoperiod (duration of day-light (hours/24)), $LIAT$—light attenuation with $LIAT = e^{-b} - e^{-c}$, and $b = I_0 \times e_m^{-\varepsilon \times z/I}$ and $c = I_0/I_m$ where I_0—average solar radiation at water surface during the day, I_m—light at which phytoplankton grows at maximum rate, ε—light extinction coefficient (m^{-1}), and z—(mixing) depth (m). Further models of water transparency and light extinction are presented by [304]. The phytoplankton respiration $RESP$ can be calculated by

$$RESP = 0.1 \times a \times CHA \times \Theta^{(T-20)} \tag{2.82}$$

where $\Theta = 1.08$ [182].

Estimates for sediment dissolved oxygen demand (SOD) can be calculated by an empirical equation

$$SOD = CDO/z, \tag{2.83}$$

where *CDO*—content of DO (g DO/m^2) at T $= 20\,°$C, z—depth of water body. The conversion to other water temperatures an be done following an Arrhenius equation. Reference [315] presented *SOD*-values for different soil conditions.

Other variables of water quality are important in the context of various uses of a water body are suspended matter, heavy metals, chloride, or organic carbon compounds like PAH, PAK or other chemicals. Specific models had to be developed for them (see [168]). The present problems in establishing mass balance models are attributable to difficulties in formulating the source and loss terms correctly. Many of these processes involved cannot be measured or only indirectly determined, which explains at least some of the uncertainties in the model results. General forecasts of trends and magnitudes are often sufficient for practical purposes and the model is required to be valued for the longest possible period of time. An effective water quality management will be carried out only in the case of practicable comparable results obtained from long-term simulation runs, because such simulation activities will make different management strategies comparable. Any prediction of the DO concentration at a fixed point of a river requires reliable parameter estimates in the model equations. Model parameters can be expanded by more accurate coverage of sewage characteristics, hydraulic variables, and concentrations of diffuse pollution (cf. [229]). The development of water quality models by improvement of their structure and by more accurate determination of the model parameters is twofold. The first topic covers the types of variables and their representations in a water quality model. The latter is achievable by inclusion of complex dependencies. But this would not necessarily lead to an improvement, since more parameters would increase uncertainty of model outputs and result in lower convergence of estimating procedures.

The validity of DO–BOD based water quality models has been tested in the past by numerous authors [21, 23, 81, 172, 183, 233, 315, 319]. Summarising accounts of the models have been given by [132, 188, 229, 272]. Current water quality models are developed in combination with decision making procedures (DSS) for different purposes. They will be applied to solve spatio-temporal water management problems, and to forecast time-dependent strategies of water quality management [358]. Actually, applications of water quality models are developed within the following fields of interest:

1. Solving dynamic simulations of point and non-point source pollution by conventional chemicals,
2. Simulation of water quality state due to storm water overflows and floods,
3. Impact of improved wastewater treatment plants operation and control,
4. Extreme pollution events due to accidents and spills of chemical tanks,
5. Improve assessment of anthropogenic influenced rivers,
6. Administrative applications concerning river basin planning and control.

The parameters of water quality models are not universal. It is not possible to describe different freshwater ecosystems with the same set of parameter values. Hence, site-specific model parameters must be obtained by calibration to experimental data. Therefore, a subset of parameters must be selected that can yield a

well-calibrated model for a given application of the model to a real river. For water quality modeling some important aspects has to be considered:

1. Prior knowledge on parameter values, their universality, and uncertainty.
2. Initial conditions and layout of measurements for data collection (which variables are measured at which locations and at which points in time).
3. Availability of sampled data.
4. Identifiability of subsets of model parameters from data. Measures of identifiability are given by sensitivity measures, by collinearity index, and by the measure of the extension of the confidence region.

Uncertainty analysis is mostly done by two procedures. The advantage of linear error propagation is its computational efficiency. If the sensitivity functions have already been calculated for identifiability analysis, no further simulations are required to get an error estimate. If model non-linearities are significant within the uncertainty range of the parameters, the results of linear error propagation are inaccurate. Monte Carlo simulation is a simple technique to consider the non-linear behavior of simulation results. But this technique is computationally very demanding because of the very large number of simulations required.

River water quality modeling has a long history. The *QUAL2*—model family belongs to the most comprehensive river water quality models based on the assumption of complete mixing of a water body [91]. It is an extension of the *QUAL1* water quality model [33, 86], and describes the longitudinal matter transport by advection and dispersion and constant hydraulic conditions within a certain river segment and a simulation time horizon. The enhanced water quality models *QUAL2E* and *QUAL2E-UNCAS* were intended as planning tools for water quality management [44]. Besides of water temperature the dissolved oxygen concentration, BOD_5, algal biomass, organic nitrogen, ammonia, nitrite, nitrate, organic phosphorus, dissolved orthophosphate phosphorus, coliforms, any non-conservative substance, and three conservative substances are taken into consideration. Multiple waste water inputs, multiple water withdraws and tributaries are considered within the model structure. Simulation runs can be carried out as steady-state or dynamic simulations where daily variations of DO and different meteorological conditions will be regarded. Actually, the models of this family are used to simulate the following processes: Degradation of organic material, growth and respiration of phytoplankton, nitrification, hydrolysis of organic phosphorus and nitrogen, re-aeration, sedimentation of algae, organic phosphorus and organic nitrogen, release of nitrogen and phosphorus from sediments. All these processes consider the effects on dissolved oxygen, total phosphorus and total nitrogen. The main difference between *QUAL2E* and other models of this family is the consideration of the eutrophication process characterised by the variables phytoplankton and macrophytes and its implications for DO concentration and nutrient cycles. By means of the *QUAL2E-UNCAS* model sensitivity analyses, first order error analyses and Monte Carlo simulations can be carried out.

The *WASP* (Water Quality Analysis Simulation Program) modeling and simulation framework [4, 5] was originally developed to simulate 1D, 2D and 3D processes of fate and transport of contaminants in surface waters. It consists of the three sub-

models *DYNHYD*, *EUTRO* and *TOXI* which are used to simulate steady and unsteady flows, wind, and tidal cycles (*DYNHYD*), to forecast conventional water quality processes as DO-BOD interactions, phytoplankton growth, nutrient transformations in sediment and free water (*EUTRO*), and to predict dissolved and adsorbed chemical concentrations in sediment and in free water (*TOXI*). The latter sub-model couples kinetic models derived from *EXAMS* (Exposure Analysis Modeling System) with the *WASP* transport model. Besides of transport processes of chemicals and biota in sediments and within the free water column the following water quality related processes are modelled explicitly in *WASP*:

1. Dissolved oxygen balance by Streeter–Phelps or modified Streeter–Phelps model, or by full linear or nonlinear DO balance including re-aeration, CBOD, nitrification/denitrification, settling of BOD, phytoplankton growth, respiration and death, and SOD;
2. Eutrophication by simple and intermediate eutrophication kinetics (the latter with benthos) covering phytoplankton kinetics, stoichiometry and uptake kinetics, phosphorus cycle, nitrogen cycle, DO balance, benthos-water column interaction;
3. Sediment transport;
4. Chemical tracer transport;
5. Simple toxicants including simple transformation kinetics, equilibrium sorption, transformations to daughter products;
6. Organic chemicals covering ionisation, equilibrium sorption, volatilisation, hydrolysis, photolysis, oxidation, biodegradation, extinction.

Due to these options, in the past *WASP* was used for water quality managment of rivers [53, 141, 147, 196, 198, 257, 348] (Warwick et al. [345]), lakes [165], and reservoirs [178, 326, 360] as well as coastal areas [331, 343]. In parallel to *QUAL2E-UNCAS* a High Level Architecture based (HLA) uncertainty analysis was carried out within *WASP* by [197].

The dynamic water quality model *QUASAR* [355] belongs to the class of extended Streeter–Phelps type models. Based on the results of some water management studies for the Bedford-Ouse River system [352, 351, 353, 357], it describes time varying changes of water flow and concentrations of water quality state variables. A set of ODE's is used to model water quality changes within the river which is divided into segments of different length', and each segment is considered as a CSTR [356]. For each segment, flow input from tributaries, flow abstractions, point and non-point pollutant inputs and effluent discharges can be taken into account. Water quality simulations with *QUASAR* can be carried out in the dynamic ODE-mode for operational water management actions or in a stochastic MC-mode for planning purposes. *QUASAR* requires data on the hydrodynamic structure of the river basin, water flow and water quality data of each river segment, as well as process rates for the biological and chemical processes of matter changes. To run the model daily, weekly or monthly data should be available.

The *RWQM1* was developed by an IWA Task Group on River Water Quality Modeling [270]. Goals of this process oriented software tool are the presentation of a complex biogeochemical conversion model for river water quality modeling in

parallel to the *ASM1* to *ASM3* model development of IWA [149], and to present a more or less complete set of mathematical models of water quality processes that run under sufficient DO or anoxic conditions within the water body [269]. For specific water management tasks the adequate sub-models may be selected and applied. The following processes are considered in the model:

1. Aerobic growth of heterotrophic organisms utilising organic substrate, DO and nutrients,
2. Loss of biomass of heterotrophic organisms due to aerobic endogenous respiration,
3. Anoxic growth of heterotrophic organisms with DO gained by denitrification,
4. Loss of biomass of heterotrophic organisms due to absence of DO by endogenous respiration with nitrate,
5. Growth of 1st and 2nd stage nitrifying bacteria,
6. Growth of phytoplankton biomass by primary production,
7. Loss of phytoplankton biomass,
8. Growth of consumers by grazing on phytoplankton, on autotrophic and heterotrophic organisms, and on particulate organic matter,
9. Loss of biomass of consumers,
10. Hydrolysis of slowly degradable particulate organic matter to dissolved organic matter by catalysis of heterotrophic biomass,
11. Six chemical equilibriums,
12. Adsorption and desorption of phosphate phosphorus.

Case studies of the model are carried out for the River Glatt by [270] and for the River Lahn by [33] and [270].

The *MIKE11* model family [74] is a modern powerful software tool for simulation of water flow and water level, of water quality and sediment transport in estuaries, rivers, flood plains, irrigation channels and other freshwater ecosystems. It is based on a modular structure with the hydrodynamic engine as core module (cf. Table 2.10). Additional modules and a GIS software extension allow the application of *MIKE11* in the various fields of water quality management.

MIKE11 Studio (restricted river modeling, limitation to 250 lateral profiles and structural elements) and *MIKE11 Enterprise* (detailed river modeling, no limitation of the number of lateral profiles and structural elements of the river under consideration) are predefined software packages for water management. *MIKE11* can be combined with other software tools as *MIKE21* (flood modeling), *MIKE SHE* (integrated surface and groundwater modeling), *FeFlow*® (subsurface flow and mass transport), *MOUSE* (integrated urban catchment modeling), and *Visual MODFLOW* (groundwater flow and contaminant transport).

Some of important models applied for river water quality simulation and management are listed in Table 2.11.

More general software tools for modeling and simulation of river water quality processes can be applied by using *AQUASIM* [269] or *STREAMPLAN* [209]. *AQUASIM* was developed for data analysis, and identification and simulation of

Table 2.10 Basic and add-on modules of *MIKE11* for river water quality modeling

Add-on module (short name)	Characteristics
Hydrodynamics (HD)	Core module, hydrodynamic simulation based on non-linear Saint-Venant equation, computation of surface runoff, unsaturated infiltration, evapotranspiration, aquifer as linear storage
Rainfall-runoff (RR)	Contains different rainfall-runoff models
Structure operation (SO)	Simulation of operation of sluices, weirs, pumps, culverts and other construction elements along the course of a river
Dam break (DB)	Tools and models to simulate dam breaks
Advection-dispersion (AD)	Transport und distribution of conservative substances and heat
Cohesive sediments (ACS)	Models of layered river bed, contains a quasi 2D erosion model
Non-cohesive sediments (ST/GST)	Transport, erosion and deposition of non-cohesive sediments, simulation of river morphology
ECO Lab	Numerical water quality and freshwater ecology models
AUTOCAL	Calibration of parameters
MIKE11 Stratified	Models of temperature and salinity stratification of water bodies
MIKE11 Real time	Simulation of operational flood forecasting with GIS front-end, real-time updating of data and Kalman filtering
GIS Extension	Interface to ArcMAP including features for river basin delineation using cross-sectional and DEM data, pollution load estimates and visualisation as 2D maps

water quality processes at EAWAG Zürich. The spatial structure of the river system of interest is designed as a set of linked compartments describing water flow, matter transport and change in open channels. Other types of compartments are CSTRs, biofilm reactors, plug-flow reactors with and without dispersion, saturated soil columns with sorption and pore water exchange, and lakes with stratification, matter transport and changes within the free water column and in adjacent sediment layers. All compartments can be connected by two types of links. The user has to specify a set of state variables and water quality processes active within the compartments. The model equations as formulated by the water quality manager will be solved by the software. State variables and initial parameter values can easily be changed. The outputs of this software are simulation runs as well as sensitivity evaluations and parameter estimations based on measured real data.

STREAMPLAN is a spreadsheet tool for river environment assessment management and planning. It was designed in 1996 at IIASA to foster the analysis and selection of alternative water quality management strategies on a river basin level [212]. The goal of this software development was to compare and to support decisions concerning policy oriented water quality management options related to national and international water quality standards, socio-economic conditions, and financial budgets in a river basin. A river basin is considered as a set of certain number of river segments of the main river, of tributaries, and of bifurcations connected with another together with a set of point pollution sources along these segments.

Table 2.11 Selected river water quality models

Model	State variables	Hydrodynamics	Reference
DOSAG-I,	T, DO, BOD	1D, steady-state	[33]
DOSAG-M	T, DO, BOD, coliforms, benthic BOD	1D, steady-state	[11]
QUAL1,	T, DO, BOD, nitrogen, phosphorus,	1D, steady-state,	[87, 91]
QUAL2,	T, DO, BOD, phytoplankton, N, P, coliforms, benthic BOD, any non-conservative substance, three conservative substances	1D, steady-state	[274]
QUAL2E, QUAL2E-UNCAS	T, DO, BOD, phytoplankton, TN, TP, coliforms, benthic BOD, any non-conservative substance, three conservative substances	1D, 2D, steady-state or quasi dynamic	[44]
WASP (including *DYNHYD, EUTRO* and *TOXI*)	DO, BOD, N, P, phytoplankton,	1D, 2D, steady-state, dynamic	[4, 5, 79]
QUASAR	DO, BOD, NO3, NH4, T, pH, conservative substances	Steady state CSTR, non-steady flow	[194, 289, 355]
RWQM1	T, DO, BOD, N, P, phytoplankton, zooplankton, bacteria,	1D, steady-state, dynamic	[270]
MIKE11	T, DO, BOD, N, P, Si, bacteria, phytoplankton, zooplankton, benthic algae	1D, quasi 2D, steady-state, dynamic	[74]
CE-QUAL-RIV1	T, DO, BOD, N, P, Si, phytoplankton, zooplankton, bacteria,	1D, steady-state, dynamic	[54]
QSIM	T, DO, BOD, N, P, Si, pH, phytoplankton, zooplankton, suspended matter, sedimentation, benthic algae, macrophytes, benthic filtrators	1D steady-state, dynamic	[285]
ATV	T, DO, BOD, P, N, Si, phytoplankton, zooplankton, benthic algae	1D, 2D, steady-state, dynamic	[12, 221]
HEC5Q	T, DO, BOD, N, P, phytoplankton, bacteria	1D, 2D, steady-state, dynamic	[145]

Point pollution sources are specified either in agricultural, industrial or in municipal controllable sources. Non-point pollution sources are considered as point sources at specific locations where the pollution is discharged from the sub-watershed to the river basin. Also uncontrollable background pollution is considered as a point source. For each segment steady and uniform flow with complete mixing of all water
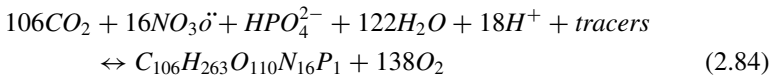
quality constituents as DO, CBOD, NH_4-N, NO_3-N, TP and any non-conservative substance is supposed. *STREAMPLAN* has a modular structure with hydraulic, water quality, socio-economic and optimisation models as basic elements. The EXCEL-based tool works with 6 modules (called workbooks) which are named Main, Static, Designs, Scenario, Model and LP. An optional WWTP workbook can be linked to the Designs workbook to generate effluent wastewater quality and economic information of various wastewater treatment alternatives in the river basin. A graphical interface allows visualisations of input data and output results. *STREAMPLAN* was successfully applied to rivers in central and Eastern Europe [167, 293].

Other useful software tools for modeling and simulation of water quality processes are *STELLA®* [254] or *MATLAB®/SIMULINK®* [359]. *STELLA®* is graphical oriented software tool and can be applied easily for steady-state modeling of population dynamics and other biological processes taking within freshwater ecosystems. The user has to draw a conceptual diagram of the water quality problem to be solved and to formulate the process equations. The differential equations appertaining to the problem are made by the software. Applications for water quality processes are presented by [170]. In opposite of that, *MATLAB®/SIMULINK®* is a general development software tool for identification, analysis, modeling and simulation of linear and nonlinear dynamic systems. Applications of *MATLAB®/SIMULINK®* based water quality models are widespread used (cf. [120, 122] and others).

2.2.4 Water Quality Models for Lakes and Reservoirs

In this sub-chapter, emphasis is laid on water quality models related to eutrophication process of lakes and reservoirs. Understanding the eutrophication process as a natural process taking place over geologic time interval this process is accelerated drastically by human activities [328]. Eutrophication describes the status of primary productivity (which is given by the photosynthetic process of green plants) within the water body:

Production $\rightarrow$

$$106CO_2 + 16NO_3\ddot{o} + HPO_4^{2-} + 122H_2O + 18H^+ + tracers$$
$$\leftrightarrow C_{106}H_{263}O_{110}N_{16}P_1 + 138O_2 \tag{2.84}$$

$\leftarrow$ *Respiration*

Easily measurable indicators of ongoing eutrophication process are phytoplankton biomass (chlorophyll-a), inorganic total nutrient concentrations (mostly P and N), transparency of water (so-called Secchi depth), organic nutrient forms (mostly N and C), and deep water level DO depletion [341]. For the development of water quality models the detailed hydro-biological structure of a freshwater ecosystem under consideration regulating chemical and suspended matter change processes within the water body will be neglected. The functioning of freshwater ecosystems and the water uses for drinking water supply, for industrial production and agricultural practices

are affected by natural and man induced influences. External inputs as industrial wastewater pollution, agricultural and forestry nutrient pollution, atmospheric dry and wet deposition as well as internal inputs due to nutrient remobilisation from sediments affect the water quality of freshwater ecosystems. While natural pollution is mostly small compared with the nutrient input due to land erosion and intensive anthropogenic activities in a river basin industrial and agricultural pollutions force the eutrophication processes in lakes and reservoirs. In the past, enhanced input of phosphorus into water bodies due to intensive use of mineral fertilizers on agricultural areas, or orthophosphate in laundry detergents, as well as intensive inputs of sewage effluents has led to exceptionally high loads of phosphorus and nitrogen into lakes and reservoirs [330]. The eutrophication process has several undesirable direct and indirect impacts on water quality resulting in decreased water transparency (light diminution), anoxic conditions in the deep water layer, loss of biodiversity as well as to taste and odour problems and, therefore, restricted water uses [327]. These impacts caused shifts from oligotrophic (nutrient poor) to eutrophic (nutrient rich), and to hypertrophic (extremely nutrient rich) freshwater ecosystems. Nutrient releases to lakes and reservoirs due to anthropogenic activities are caused by point and non-point sources. Point sources can easily be controlled either by waste water treatment or by other control devices. Non-point pollution of freshwater ecosystems is caused by precipitation, by storm water runoff, by agricultural runoff, by sewer overflow, and by middle-term or long-term flood events. Despite of reduction of external sources since the late 1980s the intended goal of reduced nutrient levels in the water body have not been achieved. Now it has become clear, that the sediments have been accumulated nutrients over several decades that they now function as internal nutrient sources [79]. Actually, eutrophication is now more sustained by internal than by external sources [127]. Therefore, water quality models of lakes and reservoirs have to consider external and internal effects on water quality.

Models for lakes and reservoirs can be broadly classified as empirical or analytical. In general, empirical models are based on observations and real data. They deal with simplifications and as well as with averaged conditions in space and time. They do not simulate dynamic biochemical processes explicitly, and contain simplified representations of hydrodynamics. Freshwater ecosystems may be seen be seen as black box, grey box or white box systems. In dependence of the number of input variables and the number of output variables where SIMO, MIMO, SISO and MISO systems will be distinguished. In opposite of analytically derived dynamic eutrophication and water quality models empirical models have relatively low data requirements. Empirical models for lakes and reservoirs can be divided into two classes [304, 341]:

1. Nutrient balance models which relate the nutrient level of the water body of interest to external nutrient loadings, to water basin morphometry expressed by the mean depth, and hydrologic conditions expressed by hydraulic residence time. For modeling, a lake or reservoir is assumed as CSTR at steady-state. All chemical reactions follow kinetics of 1st order. Simple nonlinear functional expressions are used to represent nutrient balances of lakes and reservoirs.

2. Eutrophication response models which describe the relationships between eutrophication indicators within a lake or reservoir. This type of models is represented by linear and nonlinear regression functions where additional input variables, control variables, and response variables are added. Mainly P and N are assumed to control phytoplankton growth and other eutrophication related water quality conditions.

The right balancing of lakes and reservoirs as well as forecasts of water quality depend on a concise analysis of the functional and structural relations between the major variables decisive for water quality. Mostly, the intensity of processes of mass conversion involved in a matter balance depends strongly on the given hydraulic conditions. Analytical models involve direct simulations of physical, chemical, and biological processes superimposed by hydrodynamic processes [304]. Generally, these models are characterised by extensive requirements in input data, computer facilities, and scientific expertise. They have to be distinguished in diagnostic and predictive models. Diagnostic models provide frameworks for analysis and interpretation of monitored data of a given water body. Yields of such models are statements on eutrophication-related water quality conditions and their controlling variables. Then, water quality assessments can be made in absolute terms with respect of national objectives, criteria, or standards, or in relative terms with respect to regional comparisons of water quality. Predictive models deliver suggestions for future water quality conditions in existing lakes and reservoirs or in planned impoundments. These types of models project steady-state responses to changes in controlling variables explicitly represented in the model which can be used for evaluations of water quality control strategies. On the other hand, a predictive model in combination with a chemical analysis of the water body under investigation acts as an initial extrapolation for the further water quality development [341] which may be a helpful baseline for water quality management of lakes and reservoirs.

2.2.4.1   Empirical Models for Lakes and Reservoirs

The identification of water quality of lakes and reservoirs by empirical models means the determination of the depth-dependent and time-dependent behavior of the water body on the basis of evaluations of stochastic water quality variables [114]. Relations have to be found to exist between input variables (from the watershed or internal pelagic processes) and output variables of a freshwater ecosystem (mainly biomass production), with the processes involved acting directly or indirectly on the output variable as they are given by phytoplankton biomass and TP or TN. Compared with the development of self-purification models for rivers Vollenweider's report on eutrophication [335] pushed the development of a lot of empirical models worked out to predict the biomass production or the DO content (as indicator of biomass production) of lakes and reservoirs [189, 265, 336]. In this context, two classes of general models have to be considered:

1. The class of Hammerstein models [92] includes water quality processes which may be represented as series circuit of a non-linear and a linear component with memory.
2. In opposite of that, in Wiener's model an order of linear and non-linear series circuit is assumed.

Mostly, a subdivision of the pelagic region of the water body may be helpful in making linear water quality models suitable for the prediction and simulations relevant to water quality management. For this reason, [304] divided pelagic water bodies of lakes and reservoirs into several strata of low thickness (e.g. 5 m) to present linear localised sub-models of water quality, and to bypass the difficulty of having to reckon with distributed parameters. If a water quality model is to be commensurate with real time, the parameters have to be estimated in real time for which purpose both static and dynamic methods of model construction may be used. A "finite memory" will then be assigned to the algorithms by differentiated exponential weighting of the data records. The amount of weighting will have to depend strongly on two aspects: The rates of parameter variations, and the intensity by which the disturbances act on the freshwater ecosystem of interest. These two influences must be separately evaluated, and so an optimum weighting will always be a compromise between the rate of parameter change and disturbance intensity. As a first step, linear MISO models should be constructed since no detailed information is available on the cause-effect relationship between a goal variable, or the output variable, and the input variables represented by measured data. Of course, the dynamic behavior of water quality processes may be described with sufficient accuracy by non-linear models. The changes over time of the system variables will then be expressed by the time variations of the associated parameters which can be estimated by recursive regression method. When it comes to autoregressive water quality models (inhomogeneous Markov models), the system outputs at previous time points $(t - i)$ are considered as pseudo-input variables at time point t. This will then be a model to describe the water quality in dependence on its "historical" development.

Empirical water quality models of lakes and reservoirs can be constructed in the same way as for rivers stretches (see Sect. 2.2.3.1). The effects of lake morphometry, primarily of average depth, on trophy have been widely studied, beginning with [335, 337]. A logistic relationship exists between average chlorophyll-a levels in summer and phosphorus concentrations in spring. The plateau for shallow and transparent water bodies is higher than that for deep or coloured lakes. Investigations of the action of mixing depth z or extinction coefficient gave rise to the conclusion that the extinction depth is decisive for the photosynthetic capacity of phytoplankton [303]. Therefore, static linear models should be formed with depth-dependent and time-varying parameters in keeping with subdivision of the pelagic region. A clear-cut change in the action of the influence variables on the goal variable is recordable at the so-called meta-limnion layer (approximately about 10–15 m).

For stratified freshwater ecosystems linear models are quite sufficient for an appraisal of influences of various depth levels. An appropriate selection of initial parameters for recursive estimates, in order to speed up convergence of the estimation method is also obtained. In parallel to water quality models of rivers, parameter

estimations for normal and weighted recursive regression may be obtained by using the least-square method. Performance index, residual variance, or residual sum of squares is used for an appraisal of model quality. The water quality indicator DO of a stratified lake or reservoir can be described by a MISO model

$$DO(t) = a_0(t) + a_1(t)T + a_2(t)BOD$$
$$+ a_3(t)SM + a_4(t)CHA + a_5(t)NO_3 - N$$
$$+ a_6(t)COD + a_7(t)PO_4 - P + a_8(t)TRANS, \qquad (2.85)$$

where T—water temperature, BOD—biochemical oxygen demand, SM—suspended matter, CHA—phytoplankton biomass, NO_3-N—nitrate nitrogen, COD—chemical oxygen demand, PO_4-P—orthophosphate phosphorus, and TRANS—transparency of water. Changes of parameter values of empirical models with depth-dependent variables indicate not only thermal and chemical changes within the water body also hydrodynamic influences (Table 2.12). Therefore, an intensive analysis should lay out the causative explanations for these data-based results. As can be seen from Table 2.12, some parameters indicate changing physical and chemical conditions in the so-called meta-limnion layer.

Another effect on empirical model output is caused by consideration of variables. For the model given above, the influence of variable orthophosphate phosphorus on model output was investigated (Table 2.13). The effect of the variable orthophosphate phosphorus at the water surface is lower than in consecutive deeper layers, which

Table 2.12 Depth dependent parameter changes of eutrophication models (Data from Saidenbach Reservoir)

Depth (m)	$a_0(t)$	$a_1(t)$	$a_2(t)$	$a_3(t)$	$a_4(t)$	$a_5(t)$	$a_6(t)$	$a_7(t)$
0	12.39	−0.138	0.206	0.051	0.021	−0.413	0.067	−0.186
10	12.72	−0.348	−0.0490	0.334	0.016	−0.065	0.009	−0.155
35	17.00	−1.400	0.700	0.088	−0.011	0.090	0.100	−0.519

The parameter $a_8(t)$ exist for the upper layer model only ($a_8(t) = -0.146$) and is neglected in the table

Table 2.13 Comparison of model quality for different parameter sets

Depth (m)	B (%) with PO_4-P	B (%) without PO_4-P
0	60.7	57.7
5	65.3	52.5
10	66.8	60.6
15	70.2	55.9
20	61.4	50.3
25	60.1	48.3
30	58.6	31.0
35	57.5	29.4

is attributable to the rapid uptake of orthophosphate phosphorus by phytoplankton. The congruence of performance indices of models with and without orthophosphate phosphorus, visibly at water surface is lost along with depth. The influence of orthophosphate is increased at the same time. In deep water, the orthophosphate proved to be a variable with indirect action upon the DO concentration (goal variable). This variable is found to be the result of growth processes in the pelagic region and degradation of biomass as well as re-suspension of orthophosphate phosphorus from the sediment. However, the model output would be distorted, if this variable is neglected.

The computation of linear and/or non-linear time-dependent empirical water quality models for lakes and reservoirs leads often to unsatisfactory simulation results with low performance (Table 2.14). Regression type models cannot follow rapid changes in chemical and biological composition within the water body.

Gradual adaptation of the model to the freshwater ecosystems state, and, consequently, improvement of the model could be achieved by weighted recursive regression estimations where deviations between recursively and normally estimated model outputs were recordable form the parameter curves. But, high retention times of the water body respective hydrodynamic effects as well as short-term and long-term changes (e.g. seasonal changes, climate changes) cause dynamic variations which influence the water quality. Mean parameter values estimated by normal regression proved to be hardly suitable for an appraisal of acute situations in water quality management. Changes of sign of parameters in the course of time indicate a change to the direction along which the influence variable acts upon the output variable. This would mean, for any interpretation of parameter curves, that with negative parameters values high values of the influence variable and vice versa. With positive parameter vales, on the other hand, high values of the influence variable will correspond to high values of the output variable. Long-term parameter trends were recordable from both surface water and deep water models, though real-time modeling proved to be more effective in the latter case. The water surface is more strongly exposed to external disturbances. This made the perception by means of regression models of long-term

Table 2.14 Performance of regression-type models of freshwater ecosystems

Freshwater ecosystem/goal variable	Linear model, B (%)	Non-linear model, B (%)
Lowland ponds/DO	50–55	60–70
Shallow lake/total nitrogen	12	25
Shallow lake/suspended matter	30	50
Shallow lake/DO	52	63
Saidenbach reservoir/DO	65	75
Kliava reservoir/suspended matter	63	75
Neunzehnhain reservoir/DO	72	84

trends more difficult, but it could be offset by stronger weighting of the deep water quality model as compared to the surface water quality model.

Empirical models should be used only with care and under consideration of hydro-dynamic conditions to forecast eutrophication in shallow water bodies. Autocorrela-tion among measured variables usually is strongly pronounced due to relatively high residence times. Inclusion of past records of eutrophication process variables at time points $(t - i)$ has proved to be favourable for an improvement in model quality and better convergence behavior of the algorithm. These variables may be considered as pseudo-input variables in respect of the model output. For water quality models of eutrophic water bodies the variables $T(t), T(t-1), T(t-2)$ as well as the phytoplank-ton biomass, global radiation, and nutrients are of great impact upon the behavior of the model output.

2.2.4.2 Analytical Models of Lakes and Reservoirs

The eutrophication models discussed in this paragraph belong to the class of ana-lytical, purely deterministic models of first order dynamics. Freshwater ecosystems are described by means of ordinary, coupled non-linear differential equations with fixed structure. No allowance is made in these models for adaptive mechanisms, but feedback mechanisms are considered. In general, analytical eutrophication models can be subdivided according to hydrodynamic and biological complexity [304]. A hydrodynamic one-layer model (fully mixed water body), just as multi-layer models, may be biologically simple or complex. The biological complexity of a model can be assessed by the number of biotic elements or feedback mechanisms involved [170]. According to the process of primary production (cf. Sect. 2.2.4) phosphorus has proved to be the most important growth-limiting nutrient in freshwater ecosystems in temperate regions [301, 327]. Therefore, phosphorus-phytoplankton relations are often in the focus of eutrophication models.

Examples of a hydrodynamic simple one layer eutrophication models are given by [303, 304]. The model *AQUAMOD 1* with the state variables phosphate phospho-rus, phytoplankton (expressed by chlorophyll-a), and filtrating zooplankton reflects a fully mixed water body of a lake or reservoir. The processes of primary production are described in detail while zooplankton processes are described by simple balance terms. Phytoplankton growth is limited by light and phosphate phosphorus, with growth rates depending on temperature. Negative balance terms are export of phyto-plankton biomass and sedimentation depending on sedimentation rate and turbulent mixing. The phosphate phosphorus balance consist of the positive terms of phosphate import, return flow of phosphate by living and dead phytoplankton as well as releases of phosphate phosphorus through filtrating zooplankton and of the negative terms of phytoplankton phosphate phosphorus uptake and export of phosphate. Phytoplankton is consumed by zooplankton. The consumption rate depends on filtrating intensity as well as on the amounts of zooplankton and phytoplankton biomass. The degree to which phytoplankton is consumed for an effective zooplankton growth tends to decrease along with growing phytoplankton biomass concentration. The mortality

of zooplankton is considered as a constant fraction of the zooplankton population. The ODE balance equations used in the eutrophication model *AQUAMOD 1* have the following form:

Phosphate phosphorus, $P(mgP/m^3)$

$$dP/dt = Q/VE(PIN - P) + FRZ \times A \times Z \times (1 - AZP) \times KSA/(KSA + A)$$
$$+ RESP \times TEMP \times A - G \tag{2.86}$$

Phytoplankton, $A(mgCHA/m^3)$

$$dA/dt = G - RESP \times TEMP \times A - FRZ \times CR \times Z \times A - UA \times A \times f(t), \tag{2.87}$$

where

$$G = (2 \times FOTOP \times A \times PMAX(T)/EPS \times ZMIX)$$
$$\times (arctan(I/(FOTOP \times 2 \times IK))$$
$$- arctan(I \times exp(-EPS \times ZMIX)/FOTOP \times 2 \times IK) \times P/(P + KP)),$$
$$PMAX(T) = 0.0193 \times exp(0.09 \times TEMP) \tag{2.88}$$

Filtrating Zooplankton, $Z(mgP/m^3)$

$$dZ/dt = FRZ \times Z \times CR \times C \times AZP \times KSA/(KSA + A) - MORT \times Z + Z(0) \tag{2.89}$$

Water body specific environmental variables

$$EPS = 0.2, Q/VE = 0.01, Z(0) = 10^{-4}, PIN = 100, ZMIX = 4 \tag{2.90}$$

Water body specific disturbance variables

$$I(J/cm^2 \times d) = 1840 + 1673\sin(t + 240),$$
$$TEMP(°C) = 12 + 10 \cdot \sin(t + 220), \tag{2.91}$$
$$FOTOP(h) = 12 - 4\cos t, f(t) = 0.8 + 0.25\cos t - 0.12\cos 2t$$

Model-specific parameter values

$$AZP = 0.6, IK = 1.25, KSA = 60, MORT = 0.075, \tag{2.92}$$

$$FRZ = 0.9 \times 10^{-3}, KS = 100, UA = 0.05, RESP = 0.005 \tag{2.93}$$

Complex eutrophication models are to some extent identical with the above formulated model *AQUAMOD 1*, in that only three state variables are used to describe the water quality. In multilayer models the number of feedbacks is higher, for example the density dependence of photosynthesis in response to growth of biomass, the diur-

nal and depth integral of photosynthesis, self-shading of algae, increased return flow of phosphate phosphorus via living and dead phytoplankton and zooplankton, and release of phosphorus stored in sediment. Darkness, low temperature, increased sedimentation of phytoplankton, and absence of zooplankton growth should be modelled for the deep water layer as well as the phosphorus exchange between hypolimnion and sediment. The phosphate phosphorus, dissolved in interstitial water of sediment is released from settled phytoplankton and coupled to sediment-fixed phosphorus through processes of chemical fixation and liberation (cf. Sect. 6.4). Reference [280] performed an eutrophication model for Lake Ontario where phytoplankton biomass was proved to be controlled in spring and fall by physical variables (radiation and mixing), in summer by chemical variables (silicon and phosphorus), and in late summer by biotic variables (zooplankton grazing).

A short overview on water quality models for lakes and reservoirs (respective eutrophication models) is presented in Table 2.15 where the models differ by their ecological and hydrodynamic complexity. The hydrodynamic and water quality submodels are connected to one another by direct coupling. However, the techniques of numerical computation required by hydrodynamic models usually differ from those needed for water quality models. Both models types are originated from different disciplines and show different trends of development. In this context, reference can be made to the biologically detailed model *CLEANER* [248] and the two-layer version called *MSCLEANER* [247] containing 31 state variables. The eutrophication model

Table 2.15 Selected eutrophication models

Reference	No. of state variables	Biol./hydrodyn. structure layer	Nutrients	Nutrient ratio	No. of species
[167], *MODEL* 2	12	Simple, 1D, 2	P, N, C	Constant	0
[298], *AQUAMOD* 1	3	Simple, 1D, 1	P	Constant	2
[160], *DYRESM-WQ*	13	Simple, 1D, 1	P, N	Constant	6(n)
[120] *CEUS*	5	Simple, 1D, 1	P, N	Constant	2
[299], *AQUAMOD* 2	5	Simple, 2D, 2	P	Constant	3
[267], *SALMO*	3	Simple, 2D, 1	P	Constant	2
[300], *AQUAMOD* 3	8	Simple, 2D, 3	P	Constant	3
[292], *BEM*	9	Simple, 3D, 1	P, N	Variable	4
[203], *BLOOM*	14	complex, 1D, 1	P, N	Constant	11
[317], *LAKE* 2	15	Complex, 2D, 1	P, N, C	Constant	5
[248], *CLEANER*	40	Complex, 2D, 1	P, N, C, Si	Constant	16
[247], *MSCLEANER*	31	Complex, 2D, 2	P, N	Constant	11
[63], *CE-QUAL-W2*	11	Complex, 2D (pseudo 3D), 2	P, N, C, Si	Constant	5
[56]	33	Complex, 3D, 1	P, N, C	Constant	13
[318], *LAKE* 3	15	Complex, 3D, 1	P, N	Constant	5

by [56] has shown that changes of nutrients and of populations of organisms are closely related to hydrodynamics in all layers. A comparison between the results obtained from simulation studies shows at least that a higher number of state variables is not necessarily a guarantee for realistic simulations [168]. Also no improvement in model quality can be expected a priori from the use of parameter optimisation [121]. Simulations of several water bodies were carried out with good success by the *SALMO* model (six state variables) [28, 267]. Much attention is recently given to quantify the degree of inaccuracy and uncertainty of eutrophication models.

In eutrophication modeling major emphasis is laid on pelagic processes. A precise forecast of water quality of a special lake or reservoir would provide a complete theoretical platform for a proper assessment of pelagic processes. But, some of direct and indirect correlations between various influence variables are insufficiently investigated. The complexity of water quality problems, especially socio-economic effects are inadequately met by the existing models. Various studies have been introduced into processes of the benthal region, of phytoplankton sedimentation and in sediments which act as buffers upon changes in the free-water zone. Hardly any information is available on the role played by the littoral zone in nutrient accumulation. Their representations in the structure of equations are incomplete. ODE models are important tools for the assessment of eutrophication . Global climate change impacts on freshwater ecosystems cause changes of the biological structure and the functioning of the ecosystem. Water quality will change during transition from one trophic state to another one as well as in response to physical and/or chemical changes in the system (e.g. morphometry, transparency, organic compounds). This variability has not been considered in the models so far constructed. Hydrodynamic models have so far been unsatisfactorily coupled with chemical and biological models. The action of various hydrodynamic microstructures on chemical and biological processes has been hardly elucidated. The conclusions of every model are to be used with caution, taking into account the limitations of the model, possible inadequacies of its formulation and the incompleteness of the input data.

2.2.5 Water Quality Models for Surface Water Management

Sustainable management decisions to control the water quality of freshwater ecosystems can only be achieved by using powerful simulation tools as they are represented by mathematical models. For water quality management of river basins a great variety of static and dynamic procedures are used for time series analysis, trend estimation of water quality indicators, as well as for water quality process modeling and simulation. Direct and indirect interrelations exist not only between trophic levels, but also between different ecosystem components. The management of lakes and reservoirs is closely coupled with the management of the respective watershed. Some of the watershed problems might become serious only in instances when the watershed includes a lake or a reservoir. For water quality management the problem of eutrophication creates far higher problems in standing than in flowing waters. Some eutrophication

models contain optimisation procedures to get optimal results. The use of combined simulation-optimisation procedures to manage the water quality of rivers, lakes and reservoirs is an approach promising more theoretical understanding of complicated natural processes and software engineering methods [358]. On one hand, water quality management operations follow some questions like: How to extract the pollution from the watershed, how to clean waters, or how to prevent water pollution [229]. On the other hand, practical questions arise on which eco-technological procedures should be applied, which one is the best one, which one is much less costly, and which one is more perspective than others?

Mostly, water quality problems in watersheds originate from following areas:

1. Organic pollution with easily degradable matter,
2. Eutrophication due to high nutrient inputs,
3. Acidification,
4. Salinisation,
5. Heavy metal pollution,
6. Pollution by organic hydro-carbons,
7. Bacterial and viral contaminations,
8. Nitrate contamination,
9. Water-borne diseases,
10. Erosion,
11. Siltation (sediment transport),
12. Agro-chemicals,
13. Pollution with toxic chemicals,
14. Hydrodynamic changes within the river basin,
15. Ageing of water bodies.

One way to cope with the requirements for a sustainable water quality management of surface water systems is to apply mathematical models of different complexity, or water quality information systems based on meta-models [117, 333]. Reference [302] distinguished water quality management models based on different theoretical methodologies:

1. Prescriptive models simulate the outcome of different management options by means of a scenario analysis.
2. Management or optimisation models include procedures for choosing the best suitable management option according to a set of criteria appropriate to the water quality situation. Major components are the management objective, goal functions (optimisation criteria) and constraints, costs for applying of each management option, an optimization algorithm for selecting the various optimal parameter combinations in the sense of the goal functions and constraints.
3. Static or empirical models are based on the black-box approach.
4. Dynamic water quality models with simple kinematics based on processes governing the water quality problem in question.
5. Deterministic models use average values of parameters and neglect the stochastic variability of events in nature.

6. Stochastic models predict the confidence band, within which is the system state to be expected.
7. Long-term horizon prediction models are used for water quality planning and management.
8. Operational models for water quality management under the assumption that the model is being constantly updated on the basis of measurements of the actual freshwater ecosystems state and short-term predictions of input values.
9. Knowledge based systems which guide the user toward relevant statements for water quality management.
10. Model based decision support systems including GIS to combine important water quality features with geographical based information.

Models for water quality management have to consider anthropogenic activities within the watershed, resulting in the disposal of domestic and industrial waste water, agricultural waste water, runoff of nutrients, organic and toxic compounds such as pesticides and herbicides used in agriculture and forestry, and organic hydro-carbons and pharmaceutical chemicals. Therefore, another classification of water quality models can be given following the type of water quality management activities in watersheds:

1. Water quality models dealing with water pollution within the watershed or with the consequences of water pollution,
2. Water quality models dealing with management activities in the water body,
3. Water quality models dealing with management activities at the outflow of a lake or reservoir.

In the past, water quality models are reviewed in a lot of well-known books by [170, 186, 238, 304, 305]. Other overviews are presented concerning non-point pollution by [27], on the use of DSS including GIS for water quality management by [148], and on eco-technological water quality models by [303]. Water quality models concerning acidification, salinity, turbidity, high sophisticated hydrodynamics (like *FeFlow*®) are of high actuality but they need consideration and will not discussed here. Additionally, the developments of DSS for water quality management need special considerations because of the power of these informatic tools (cf. Chap. 5).

Pollution sources in a watershed are introduced into models as inputs [231]. They are divided into point and non-point sources. Agricultural point pollution can be traced from large animal farms with in-house cultivation of animals as well as from deposits of fertilizers and organics used for plant protection. However, often it is not possible to separate between both categories of pollution sources. Mostly, agricultural pollution is considered as a non-point pollution source with organic matter from animal house cultivations with toxic ammonia concentrations, from fertiliser storages, and washout of chemicals during application. The losses during application depend on weather conditions during application, on soil and groundwater characteristics, on the ability of the vegetation cover in the application period to take up nutrients. Models of agricultural pollution are reviewed by [110, 273].

Eutrophication of freshwater ecosystems influences their water quality mainly by excess production of phytoplankton biomass due to high nutrient inputs. But it is

also affected by natural driving forces and other anthropogenic activities within the watershed. Some of these external and internal influence variables can be managed by eco-technological means. Therefore, four types of eutrophication models can be applied for water quality management:

1. Vollenweider type models which are represented by empirical relations of in-water body phosphorus concentration to external phosphorus load. The hydraulic load, the mixing depth of the water body, and the transparency of water are additional variables for water quality management.
2. Vollenweider type models which are represented by empirical relations of phytoplankton biomass (given as chlorophyll-a concentration) and total phosphorus concentration. These models are widely used for water quality management of lakes and reservoirs. There is one critical comment to this model type: The growth of phytoplankton biomass cannot increase infinitely with increasing phosphorus concentration. The relationship shows a saturation effect which has consequences for management operations. Above critical phosphorus concentration of about $50 \, \text{mg PO}_4\text{-P/m}^3$ or $100 \, \text{mg TP/m}^3$ a reduction of phosphorus concentration input does not correspond with a proportional decrease of phytoplankton production. Additional variables to influence the water quality are again the water transparency, and the zooplankton biomass for bio-manipulation.
3. Generalised dynamic eutrophication models of different biological and hydrodynamic complexity (see Sect. 2.2.4.2 and Table 2.15).
4. Ecological eutrophication models coupled with hydrodynamic models (see Table 2.15).

Water quality models dealing with methods for in-water body management are mostly oriented to management options where the eco-technological procedures are devoted to changes of natural and artificial drivers. Water quality models dealing with the manipulation of lake or reservoir outflow are often tied to the eco-technological procedures. The quality of the out-flowing water is directly related to the horizontal and vertical distribution of the water quality within the lake or reservoir. Water quality problems in the downstream river may arise if the water comes directly from hypolimnion. It is mostly deoxygenated and contains high concentrations of phosphorus, of organic compounds, and iron and manganese. The knowledge of processes decisive for water quality changes in surface waters is mainly derived from investigations of some components taken out of the context of freshwater ecosystems. The consequence is that within surface waters the process may run rather differently due to variables not considered in the experiments. The capability of organisms for adaptation to new environmental conditions is neglected. Moreover, the same difficulties like in the empirical field observations do exist due to the multivariate character of the processes, the synergetic effects of variables are difficult to study and therefore known inadequately. From a methodological point of view there are many inadequacies not only in management model formulations but also in model solutions. This is particularly valid for optimization problems, where the numerical approaches are

rather cumbersome and biased. Their transition to automated operational management alternatives is still difficult due to immaturity of both the specific water quality models and mathematical and informatic instruments.

2.3 Groundwater Modeling

Oliver Krol and Thomas Bernard

The modeling of groundwater in the context of water resources management requires another approach than the usual modeling of groundwater aquifers within the topic of transport modeling of groundwater ingredients for instance. This is up to the fact that usually bigger areas are taken into account such that a detailed modeling of the geological realities is not possible. Here immediately occurs the problem that a lot of necessary information is not directly available and most measurements are only valid for locally limited domains. This implies that measurements of hydrogeological parameters can only be a clue and have to be transformed to data representing regional realities. This topic will be the focus of this section and we like to present methods to come over the lack of information such that sufficient and satisfying results with respect to the requirements of water resources management can be gained.

In order to point out which data are relevant to determine within the groundwater modeling we start with the derivation of the governing equations in groundwater modeling. In the end we obtain a partial differential equation (PDE) describing an initial boundary value problem (IBVP). The key for the quest of finding a set of input data and parameters is the creation of a water budget that summarizes the main water fluxes in the considered area. It is the frame that ensures consistency and completeness of all required data and allows the close of information gaps by sound standing estimations based on indirect methods. It is the fundament for a more or less realistic estimation of the spatial distribution of hydrogeological parameters. By incorporating additional information also the input data like exploitation and groundwater recharge and the boundary conditions (groundwater inflow, horizontal groundwater recharge) can only be defined by means of the water budget.

In general, the resulting spatially distributed and dynamic model is very complex and in general quite cumbersome since usually a set of hundreds of thousands degrees of freedom has to be numerically solved. In the framework of water resources management where the question for a optimal control should be answered such a entity is not useful. Therefore, model reduction methods were applied that allow the incorporation of the groundwater model into an optimisation procedure with an acceptable performance. The crux of the matter is that the spatial distributed information can be more or less retained.

2.3.1   Governing Equations in Groundwater Modeling

Groundwater flow: We start with a short derivation of the governing equations for the description of groundwater flow. The basics are the balance of mass and of linear momentum. The general structure of balance equations is given by

$$\int_{\Omega_t} \left[\frac{d(\rho \Psi)}{dt} + \text{div } \mathbf{q} \right] dv = \rho Q. \tag{2.94}$$

whereby in the context of the mass balance equation the flux term becomes $\mathbf{q} = \mathbf{0}$ and Ψ is simply 1. Taking the Reynolds transport theoreme into account we obtain the local formulation of the continuity equation

$$\frac{\partial (\rho)}{\partial t} + \text{div } (\rho \mathbf{v}) - \rho Q_\rho = 0. \tag{2.95}$$

Here $\mathbf{v}$ denotes the flow velocity, ρ is the density of the fluid and Q_ρ summarizes all external quantities like exploitation or groundwater recharge. Since groundwater flow takes place through porous media such that only a part of the considered volume is water. The porosity is defined by

$$\varepsilon = \frac{V_p}{V_t} = \frac{V_f + V_a}{V_t} = \frac{V_t - V_s}{V_t} = 1 - \varepsilon_s \tag{2.96}$$

where V_t is the total volume of interest, consisting of the partial volume of the fluid V_f, the partial volume of the solid sceleton matrix material V_s and the partial volume of air V_a, which is the third phase, that in general has to be taken into account with respect to the unsaturated zone. In the context of groundwater flow that we consider subsequently this contribution can be neglected, but nevertheless we have to keep it in mind. ε_s describes the volume fraction of the solid matrix material. Thus taking the effects due to porous media into account and assuming saturated conditions we have to rewrite the mass balance equation for groundwater flow as

$$\frac{d(\varepsilon \rho_f)}{dt} + \text{div } (\varepsilon \rho_f \mathbf{v}) = \varepsilon \rho_f Q_\rho. \tag{2.97}$$

Neglecting any thermal effects or chemical interactions between matrix material and fluid, the only remaining influence is given by the hydraulic head such that the time derivative consists of

$$\varepsilon \frac{\partial \rho_f}{\partial t} = \varepsilon \frac{1}{\rho_f} \frac{\partial \rho_f}{\partial h} \rho_f \frac{\partial h}{\partial t} = \varepsilon \rho_f \gamma \frac{\partial h}{\partial t} \qquad \Rightarrow \qquad \gamma = \frac{1}{\rho_f} \frac{\partial \rho_f}{\partial h} \tag{2.98}$$

whereby γ corresponds to the fluid compressibility and

$$\rho_f \frac{\partial \varepsilon}{\partial t} = \rho_f \frac{1}{\varepsilon_s} \frac{\partial \varepsilon}{\partial h} \varepsilon_s \frac{\partial h}{\partial t} = \rho_f \Gamma (1 - \varepsilon) \frac{\partial h}{\partial t} \quad \Rightarrow \quad \Gamma = \frac{1}{\varepsilon_s} \frac{\partial \varepsilon}{\partial t} \quad (2.99)$$

where Γ denotes the sceleton compressibility. Summarizing these definitions in the mass balance equation we finally obtain

$$\frac{d}{dt}(\varepsilon_f(h)\rho_f(h)) = \rho_f(\varepsilon\gamma + \Gamma(1 - \varepsilon)) \frac{\partial h}{\partial t} = \rho S_0 \frac{\partial h}{\partial t} \quad \Rightarrow \quad S_0 = (\varepsilon\gamma + \Gamma(1 - \varepsilon))$$
$$(2.100)$$

Here S_0 corresponds to the specific storage coefficient that governs the time behavior of the system.

The linear momentum equation for fluid flow through porous media can be written as

$$\varepsilon \frac{\partial(\rho_f \mathbf{v})}{\partial t} + \text{div}\,(\varepsilon\rho_f \mathbf{v} \otimes \mathbf{v}) + \text{div}\,(\varepsilon\boldsymbol{\sigma}) = \varepsilon\rho_f \mathbf{g} \quad (2.101)$$

where $\mathbf{g}$ is the gravity acceleration and $\boldsymbol{\sigma}$ determines the internal forces that can in general be divided into an volumetric and an deviatoric part such that we obtain

$$\varepsilon\boldsymbol{\sigma} = \varepsilon p\mathbf{I} + \varepsilon\boldsymbol{\sigma}^{dev} \quad (2.102)$$

Applying the divergence operator to this expression and introducing an additional term $\boldsymbol{\sigma}_{fric}$ describing frictional effects we finally obtain

$$\varepsilon \frac{\partial(\rho_f \mathbf{v})}{\partial t} + \text{div}\,(\varepsilon\rho_f \mathbf{v} \otimes \mathbf{v}) = \varepsilon\rho_f \mathbf{g} - \varepsilon\,\text{grad}\,p + \text{div}\,\varepsilon\boldsymbol{\sigma}^{dev} + \varepsilon\boldsymbol{\sigma}_{fric} \quad (2.103)$$

For being able to simplify this complex equation we have incorporated the following assumptions:

1. Since in general the flow velocity $\mathbf{v}$ is quite low the inertia terms can be neglected

$$\varepsilon \frac{\partial(\rho_f \mathbf{v})}{\partial t} + \text{div}\,(\varepsilon\rho_f \mathbf{v} \otimes \mathbf{v}) \approx \mathbf{0} \quad (2.104)$$

2. We consider water as incompressible, such that

$$\text{div}\,\mathbf{v} = 0 \quad (2.105)$$

3. Assuming that the deviatoric part of $\boldsymbol{\sigma}$ is given by

$$\boldsymbol{\sigma}^{dev} = 2\mu \left[\mathbf{d} - \frac{1}{3}\mathbf{I}\,\text{div}\,\mathbf{v} \right] \quad (2.106)$$

where μ is the dynamic viscosity coefficient and

$$\mathbf{d} = \frac{1}{2}\left[\text{grad } \mathbf{v} + \text{grad }^t\mathbf{v}\right] \tag{2.107}$$

represents the symmetric strain rate tensor. Due to the symmetry the complete deviatoric stress finally disappears.

4. The internal friction depends on the flow velocity

$$\boldsymbol{\sigma}_{fric} = -\mu\mathbf{k}^{-1}[\varepsilon\mathbf{v}] \tag{2.108}$$

whereby $\mathbf{k}$ denotes the permeablity tensor.

Applying all these assumptions to the linear momentum balance equation we finally obtain the following expression for the velocity field in terms of pressure

$$\varepsilon\mathbf{v} = \frac{1}{\mu}\mathbf{k}\left[\text{grad } p - \rho_f\mathbf{g}\right] \tag{2.109}$$

This equation can be transformed into a formulation in terms of the hydraulic head h by applying the equation for the static pressure

$$p = \rho_f g[h - z] \tag{2.110}$$

to Eq. 2.109 and after performing the gradient operator this finally yields

$$\varepsilon\mathbf{v} = -\mathbf{K}_f\left[\text{grad } h + \frac{\rho_f - \rho_{f0}}{\rho_{f0}}\mathbf{e}_z\right] \tag{2.111}$$

whereby here the definition of the hydraulic conductivity

$$\mathbf{K}_f = \frac{\rho_{f0}g}{\mu}\mathbf{k} \tag{2.112}$$

was incorporated already. Inserting this expression into Eq. 2.97 we finally obtain the governing partial differential equation describing groundwater flow

$$S_0\frac{\partial h}{\partial t} - \text{div}\left[\mathbf{K}_f\text{grad } h + \frac{\rho_f - \rho_{f0}}{\rho_{f0}}\right] = \varepsilon\rho_f Q_\rho \tag{2.113}$$

For completion the boundary conditions have to be appended as well. Assuming the boundary of the domain consisting of two disjunct portions Γ_1 and Γ_2 of the total boundary $\partial\Omega_t$, whereby following two types of boundary conditions can be defined

$$h = \bar{h}$$
$$-\mathbf{n}\left[\mathbf{K}\text{grad } h\right] + a(h - \tilde{h}) = b \tag{2.114}$$

The first type represent a standard Dirichlet boundary condition. The second boundary condition is of Robin-type that corresponds to a Neumann boundary condition if a becomes zero and where $\mathbf{n}$ represents the normal vector on Γ_2. If $b = 0$ is valid we obtain a Cauchy boundary condition. As we derived before there are two parameters which determine the behavior of the groundwater flow, and which subsequently have to be determined by measurements and recursive estimation methods. The specific storage coefficient describes the dynamic behavior, since due to this quantity is determined how fast the hydraulic head increases or decreases at a particular point caused by exploitations for instance. The second parameter, the hydraulic conductivity tensor determines the flow velocity with respect to all directions. This means that in general an aquifer is an anisotropic entity which can have different properties in different directions. Subsequently in Sect. 2.3.5 we like to sketch how a good estimation of these parameters can be achieved.

Finally, we have to define the right hand side of Eq. 2.113. In the context of groundwater modeling we have the groundwater recharge Q_{GWR} as a source and the exploitation Q_{Expl} describing the sink term. Inclduing these terms in Eq. 2.113 we obtain

$$S_0 \frac{\partial h}{\partial t} - \mathrm{div}\, [\mathbf{K}_f \mathrm{grad}\, h] = Q_{GWR} - Q_{Expl} \tag{2.115}$$

Here we also skipped the second term within the divergence expression describing density alterations. In the context of large-scaled groundwater models such effects can not be resolved in detail and therefore they can be neglected and assumed to be covered by the remaining terms. In general, in the context of the large-scale groundwater models, the resulting quality of the groundwater model will never match reality exactly, but the model must be sufficient to describe the main effects and trends within the groundwater system. Therefore it is reasonable to keep the model as simple as possible, but on the other hand as accurate as necessary.

In the subsequent sections we are going to relate to the simplified formulation in Eq. 2.115, especially the description of the model reduction bases on this equation.

2.3.1.1 Unsaturated Zone

The modeling of the unsaturated zone requires the consideration of three phases that makes things much more complex and exceeds the goal of this chapter. Furthermore in the context of water resource management the unsaturated zone usually is neglected since the corresponding parameters cannot be determined reasonably for such large areas. Nevertheless the main relations should be sketched here. The common approach for modeling water flow in the unsaturated zone is the Richards equation that is usually formulated in terms of a piezometric head

$$\frac{\partial \theta}{\partial t} = \frac{\partial \theta}{\partial h_p} \frac{\partial h_p}{\partial t} = C(h_p) \frac{\partial h_p}{\partial t} = \frac{\partial}{\partial z} \left[K_r(h_p) \left(\frac{\partial h_p}{\partial z} \right) \right] \tag{2.116}$$

where $C(h_p)$ denotes the specific water capacity that represents the relation of the current water content θ and the pressure head h_p. $K_r(h_p)$ represents the hydraulic conductivity in the unsaturated zone where we have to notice here, that it is not constant but depends on the piezometric head. Both quantities behave highly nonlinear and the empiric relations can only be approximated by analytical functions. One empiric approach for the description of volumetric water content is the van Genuchten model that states the following constitutive relation

$$\theta(h_p) = \theta_r + \frac{\theta_s - \theta_r}{[1 + |\alpha h_p|^n]^m} \tag{2.117}$$

where θ_s corresponds to the saturation and θ_r is the residual water content. α, m and n are free fitting parameters without physical meaning. The specific water capacity corresponds to the derivative of Eq. 2.117 with respect to the pressure head. For the hydraulic conductivity we assume

$$K_r(h_p) = K_f \left[\sqrt{\theta_e} \left[1 - \left[1 - \frac{1}{\theta_e} \right]^m \right]^2 \right] \tag{2.118}$$

Here K_f corresponds to the constant hydraulic conductivity of the saturated case and θ_e is the effective saturation that is defined by

$$\theta_e = \frac{\theta - \theta_r}{\theta_s - \theta_r} \tag{2.119}$$

where θ_e becomes 1 if θ tends to saturation and K_r reduces to K_f. A more detailed discussion of these equations is given in [33, 78]. In the latter work especially the numerical realisation is considered since the numerical standard time integration methods have to be modified. Otherwise singularities can occur during computation.

2.3.1.2 Transport of Solutes in Groundwater Systems

For the derivation of the groundwater transport equation we start from Eq. 2.94 again and replace $\rho\Psi$ by the concentration c_i of the ith component and $\mathbf{q}_c$ represents the components flux. Sinks and sources within a representative volume element occur due to chemical or biochemial reactions and should be denoted by r_c. By taking Eq. 2.105 into account the transport equation of the ith component can be written as

$$\frac{\partial c_i}{\partial t} + \text{div}\,(c_i\mathbf{v}) + \text{div}\,\mathbf{q} = r_i \tag{2.120}$$

There are different physical effects that can cause a movement of chemical solutes within fluids. These transport mechanisms should be discussed subsequently.

Advection: The most important transport mechanism, that is denoted by advection, that is the passive movement of particles due to the fluids flow. It corresponds to the movement of leaves on a rivers surface, for instance. This transport mechanism is represented by the second term in Eq. 2.155

$$\mathbf{q}^{adv} = c_i \mathbf{v} \tag{2.121}$$

Diffusion: Another transport mechanism, results from the natural attempt of solutes to achieve a homogenous distribution in the fluid. This temperature-dependent process is caused by a difference of concentration of a solute between two points that leads to movement that is proportional to concentration gradient. This effect is called diffusion and can be described by

$$\mathbf{q}^{dif} = -\mathbf{D}^{dif} \operatorname{grad} c_i \tag{2.122}$$

whereby $\mathbf{D}_{dif}$ is the diffusion coefficient and in general a tensor. It depends on the fluid and the considered solute. In most cases of groundwater modeling this contribution can be neglected since it takes place on a molecular scale and is of a very small order. Nevertheless, it should be kept in mind.

Dispersion: The last transport mechanism is the dispersion which is described by the analogous mathematical structure and which also depends on the concentration gradient

$$\mathbf{q}^{dis} = -\mathbf{D}^{dis} \operatorname{grad} c_i, \tag{2.123}$$

but it covers a completely different physical phenomenon. In the voids of the groundwater body usually one find a very heterogenous velocity profile. Due to viscosity the velocity at the voids border is much smaller than in the middle of the void. In addition every void has a different geometry and therefore the velocity profile is different as well. Two particles which are originally next to each other get apart from each other due to the different velocities. The effect of tortuosity amplifies this effect, since the particles follow different paths through the porous media. In analogy to diffusion the solute tends to equilibrium of concentration but these effects take place on a macro-scale level. In contrast to the diffusion coefficent the dispersion tensor $\mathbf{D}_{dis}$ is specific for a particular matrix material and depends on the flow velocity of the considered fluid and the longitudinal dispersion length and transversal dispersion length (dispersivities), α_l and α_t. Finally the components of the dispersion tensor can be determined by

$$D_{ij}^{dis} = \alpha_t |\mathbf{v}| \delta_{ij} + (\alpha_l - \alpha_t) \frac{v_i v_j}{|\mathbf{v}|} \tag{2.124}$$

The coefficents α_l and α_t are scale-dependent that means they are changing with the size of the considered model area. Usually it's a hard task to determine the longitudinal and transversal dispersion lengths, since in general they are specific for the corresponding location and can only be determined at the site of interest. A detailed discussion about the determination of the parameters is given in [152]. In

general the diffusion and dispersion are superposed and the transport modeling is performed by the dispersion-diffusion-coefficient **D** containing both effects.

2.3.1.3   Chemical Reactions and Biological Degradation

In general, the solutes within the fluid can react with each other whereby the chemical reaction is described by

$$\nu_A A + \nu_B B \rightleftharpoons \nu_C C + \nu_D D \tag{2.125}$$

where ν_i are the stoichiometric coefficents of the corresponding components (reactants and products).[1] Chemical reactions at a particular temperature T and pressure p usually are characterized by the chemical equilibrium of reaction where the sum of the chemical potentials μ_i tends to zero

$$\sum_i \mu_i \nu_i = 0 \tag{2.126}$$

whereby the reactants chemical potential have negative signs. The chemical potential of an ideal gas has to be derived from state equations which can be calculated by a reference state $\mu_{0i}(p^+, T)$ and the integration to the current state parameters, such that we obtain

$$\mu_{0i}(p, T) = \mu_{0i}(p^+, T) + \int_{p^+}^p RT \frac{dp}{p} = \mu_{0i}(p^+, T) + RT \ln\left[\frac{p}{p^+}\right] \tag{2.127}$$

R denotes the ideal gas constant. For the description of real gases this approach has to be modified by the introduction of the fugacity coefficient φ_i

$$\mu_{0i}(p, T) = \mu_{0i}(p^+, T) + RT \ln\left[\frac{\varphi_i p}{p^+}\right] \tag{2.128}$$

that is specific for a particular component. For liquids this approach is continued, by calculating the chemical potential up to the saturation vapor pressure p_{0is}. In the transition zone from the vapor to liquid phase at a particular temperature the chemical potential can be assumed as constant $\mu_{0i}^L(p_{0is}, T) = \mu_{0i}^G(p_{0is}, T)$. Finally, the chemical potential of the liquid component is given by

---

[1] In order to keep it as simple as possible but as general as necessary we restrict our considerations to two reactants and two products. The subsequent derivations are also valid for an arbitrary number reactants R_i and products P_i

$$\nu_1 R_1 + \nu_2 R_2 + \cdots + \nu_k R_k \rightleftharpoons \nu_{k+1} P_1 + \nu_{k+2} P_2 + \cdots + \nu_{k+n} P_n$$

.
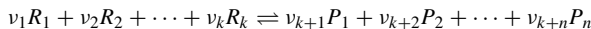
$$\mu_{0i}^L(p, T) = \mu_{0i}^G(p^+, T) + RT \ln \left[\frac{\varphi_i p_{0is}}{p^+} \right] + \int_p^{p_{0is}} V_{0i}^L dp \qquad (2.129)$$

but in order to obtain the same mathematical structure as in Eq. 2.127 the so-called Poynting-correction is introduced that yields chemical potential by

$$\mu_{0i}(p, T) = \mu_{0i}(p^+, T) + RT \ln \left[\frac{f_i^L}{p^+} \right] \qquad (2.130)$$

where f_i^L is the fugacity that describes the deviation of the real reactant from the ideal behavior. The fugacity can not be measured but has to be calculated by

$$f_{0i} = \varphi_{0is} p_{0is} \exp \left[\int_{p_{0is}}^p \frac{V_{0i}^L dp}{RT} \right]. \qquad (2.131)$$

Within a mixture of components the determination of the chemical potential is anlogous to Eqs. 2.127–2.129, but the pressure has to be replaced by the partial pressure p_i of the component i. Introducing the mole ratio x_i the fugacity of the components can be expressed by

$$f_i = \varphi_i p_i = \varphi_i x_i p \qquad (2.132)$$

and relating this to particular standard conditions p_0, T we can define the activity a_i of the ith component

$$a_i = \frac{\varphi_i x_i p}{p_0} \qquad (2.133)$$

With this at hand we can write the chemical potential of a real gas within a mixture as

$$\mu_i = \mu_{0i} + RT \ln a_i \qquad (2.134)$$

where μ_{0i} is the chemical potential of the component at standard conditions p_0 and a particular temperature T. Inserting this expression in to the equation of chemical equilibrium 2.126, we finally obtain

$$\sum_i \nu_i \mu_i = \sum_i \nu_i \mu_{0i} + \sum_i \nu_i RT \ln \prod (a_i^{\nu_i}) = \Delta_r G_0 + RT \ln K_a = 0 \qquad (2.135)$$

where $\Delta_r G_0$ corresponds to the standard enthalpy

$$\Delta_r G_0 = \nu_A \mu_{0A} + \nu_B \mu_{0B} - \nu_C \mu_{0C} - \nu_D \mu_{0D} \qquad (2.136)$$

and K_a denotes the reaction constant as it yields from the law of mass action

$$K_a = \frac{a_C^{\nu_C} a_D^{\nu_D}}{a_A^{\nu_A} a_B^{\nu_B}} = \exp \left[-\frac{\Delta_r G_0}{RT} \right]. \qquad (2.137)$$

This constant defines where the equilibrium of a particular reaction lies. In the context of liquids the reaction constant can be also expressed in terms of concentrations c_i

$$K_c = \frac{(\gamma_c c_C)^{\nu_C} (\gamma_D c_D)^{\nu_D}}{(\gamma_A c_A)^{\nu_A} (\gamma_B c_B)^{\nu_B}} \tag{2.138}$$

or in terms of partial pressures p_i

$$K_p = \frac{(\gamma_c p_C)^{\nu_C} (\gamma_D p_D)^{\nu_D}}{(\gamma_A p_A)^{\nu_A} (\gamma_B p_B)^{\nu_B}}, \tag{2.139}$$

if real gases are considered. The constant(s) of chemical equilibrium can be interpreted as the proportion of reactants and products where no further netto energy flux takes place. If the standard reaction enthalpy is known the corresponding constant of chemical equilibrium can be calculated. A detailed discussion can be found in [368].

The knowledge about chemical reactions and their equilibrium is not sufficient for the modeling of transport processes in groundwater flow. The question is how the derived equations can be related to the transport balance in Eq. 2.155. We remember that we introduced the terms r_i denoting sources and sinks of a certain component. Indeed those terms describe the rate of a component that means a change of concentration per time

$$r_i = \frac{dc_i}{dt} \tag{2.140}$$

This topic concernes the velocity of chemical reactions which is described by the kinetics of chemical reactions. For the systematic description of the reaction rate different types of reactions are classified. We want to discuss three types of reaction subsequently, namely reactions of

- 0th order (constant reaction rate)
- 1st order (radioactive decay)
- 2nd order (monod rate)

The simplest case is the reaction of 0th order of the reactant $A \longrightarrow B$ that is completely independent of the current reaction state, such that the temporal change of the concentration c_A is constant

$$-\frac{dc_A}{dt} = \frac{dc_B}{dt} = K_0 \tag{2.141}$$

The half-value period can be determined by integration

$$t_{0.5} = \frac{c_A}{2K_0} \tag{2.142}$$

which is an important parameter to characterize a chemical reaction since it gives an idea of how fast a reactions takes place. The reaction of first order depends on the remaining concentration c_A

$$\frac{dc_A}{dt} = -K_1 c_A \tag{2.143}$$

such that the reaction proceed in a exponential manner

$$c_a = c_{A_0} \exp[-K_1 t] \tag{2.144}$$

The half-value period is given by

$$t_{0.5} = \frac{\ln 2}{K_1}. \tag{2.145}$$

A reaction type which can be observed within biological degradation of organic matter can be described by the Michaelis–Menten-kinetics. During this kind of reaction an intermediate state developes forming a complex of substrate and enzymes before the reactant can be transformed into the product

$$E + A \rightleftharpoons EA \rightleftharpoons E + B \tag{2.146}$$

This reaction is governed by the production of the EA-complex as long as A available sufficiently. Only if A gets scarce the reaction depends on the current concentration c_A. Therefore the reaction rate can be described by

$$-\frac{dc_a}{dt} = \left[\frac{dc_a}{dt}\right]_{max} \cdot \frac{c_A}{K_M + c_A} \tag{2.147}$$

Here $\left[\frac{dc_a}{dt}\right]_{max}$ denotes the maximum reaction rate that corresponds to the state of full availability of the substrate A. In this case the c_A is very high and the second term in Eq. 2.147 tends to 1. As soon as c_A gets small the second term tends to K_M^{-1} and we obtain a first order kinetic. This means that the Michaelis–Menten reaction represents the transition from a 0th order reaction to a first order reaction. The reaction rate of 2nd order reactions with two reactants A and B reacting by

$$A + B \rightleftharpoons P \tag{2.148}$$

depend on the concentrations of both reactants

$$r_A = K \cdot c_A(t) \cdot c_B. \tag{2.149}$$

Assuming different start concentrations c_{A_0} and c_{B_0} the consumption of both reactants must be the same and the current concentration of the component B can be expressed by

$$c_B(t) = c_A(t) + (c_{B_0} - c_{A_0}) = c_A(t) + \Delta c_0 \tag{2.150}$$

Inserting this relation into Eq. 2.149 the reaction rate of component A can be written as

$$r_A = -\frac{dc_A}{dt} = c_A(t)[c_A(t) + \Delta c_0] \tag{2.151}$$

The integration yields the time dependent concentration function of the component A

$$c_A(t) = c_{A_0} \frac{\Delta c_0}{c_{B_0} \cdot \exp[\Delta c_0 \cdot K \cdot t] - c_{A_0}} \tag{2.152}$$

A more detailed discussion of chemical reactions in the context of groundwater flow can be found in [76, 77, 216, 253].

It is clear that if different solutes react with each other the transport equation has to be formulated for each component that is involved in the corresponding process and we obtain a system of coupled partial differential equations. The coupling affects the performance of the corresponding numerical solution method. In addition every transport equation of the form of Eq. 2.155 contains the current velocity field such that every transport equation is at least coupled with the groundwater flow equation.

2.3.1.4 Sorption

While the former considerations were focussed on chemical reactions of solutes with each other sorption denotes the physical and chemical interaction of solutes at solid surfaces as they can be found in porous matrix material of aquifers. The term sorption summarizes different effects and it includes adsorption, absorption and ion-exchange. An extensive overview is given in [99]. If the total concentration of the specific component is considered it consists of the part that is solved in the fluid and the part that is sorbed by the matrix material. The total mass of this component can be calculated by

$$m_i = c_i^f \cdot n_e + c_i^s(1-n) \cdot \rho_s \tag{2.153}$$

where c_i^f denotes the concentration of the solved component and c_i^s the sorbed one. n_e is the volumetric water content, n is the porosity and ρ_s describes the density of the soil. The key idea is that changes of the solutes concentration must be the same as changes in the concentration of the sorbed part, such that we obtain

$$\sigma_i = \frac{dc_i^f}{dt} = \frac{\rho_d}{n_e} \frac{dc_i^s}{dt} \quad \text{with} \quad \rho_d = (1-n)\rho_s \tag{2.154}$$

whereby we incorporated the dry mass density ρ_d. This term describes the process of sorption and can be added to the transport Eq. 2.155 as a sink term with respect to the considered solute with the corresponding negative sign

$$\frac{\partial c_i}{\partial t} + \text{div } (c_i \mathbf{v}) + \text{div } \mathbf{q} = r_i - \sigma_i \tag{2.155}$$

For the time-dependent behavior of c_i^s different approaches can be chosen. The most important approaches are

1. Henry sorption
2. Freundlich isotherme
3. Langmuir isotherme

where the first two approaches are empirical ones and the Langmuir approach is physically motivated. The equlibrium between the concentrations of the sorbens and the solute is usually reached under isothermal conditions. Therefore the relation between both concentration is usually represented by the isothermes. The Henry sorption assumes a linear relationship

$$c_i^s = K_H \cdot c_i^f \quad \rightsquigarrow \quad \frac{dc_i^s}{dt} = K_H \frac{dc_i^f}{dt} = \overline{K_H} \frac{dc_i^f}{dt} \tag{2.156}$$

where K_H denotes the Henry distribution coefficient that describes the ratio adsorbed and resolved concentration. The relation of Henry is only for small concentrations a sufficient approximation and should only be applied in this range. But with respect to numerical aspects this approach is very simple and easy to implement.

The Freundlich description assumes that the sorption isotherme can be represented by a power function

$$c_i^s = K_F(c_i^f)^n \quad \rightsquigarrow \quad \frac{dc_i^s}{dt} = K_F n(c_i^f)^{n-1} \frac{dc_i^f}{dt} = \overline{K_F} \frac{dc_i^f}{dt}. \tag{2.157}$$

where the K_F corresponds to the Freundlich distribution coeeficient and n is a constant parameter. If Eq. 2.157 is transformed to the logarithmic form it describes its parameters can be derived by linear regression.

The Langmuir approach assumes that all sorption places at the surface are energetically equivalent and can only be occupied by a monomolecular laminate. Furthermore no chemical interactions between the particles take place. The Langmuir equation is given by

$$c_i^s = b \frac{K_L c_i^f}{1 + K_L c_i^f} \tag{2.158}$$

where K_L is the Langmuir distribution coefficent and b is the maximum load at the surface. In contrast to the Freundlich and Henry approach the Langmuir isotherme covers the finite place at the surface and that there takes place a saturation effect at very high concentrations. The time derivative is given by

$$\frac{dc_i^s}{dt} = \frac{bK_L}{[1 + K_L c_i^f]^3} \left[1 - \frac{K_L c_i^f}{1 + K_L c_i^f} \right] \frac{dc_i^f}{dt} = \overline{K_L} \frac{dc_i^f}{dt}. \tag{2.159}$$

Inserting this in Eq. 2.155 and bringing the time derivatives on the right hand side we can rewrite the balance equation as

$$\frac{\partial c_i}{\partial t} = \frac{1}{R}\left[r_i - \text{div}\,(c_i\mathbf{v}) + \text{div}\,\mathbf{q}\right] \quad \text{with} \quad R = [1 + \frac{\rho_d}{n_e}\overline{K}] \qquad (2.160)$$

where $\overline{K}$ can be replaced by the corresponding expression in accordance to the applied approach ($\overline{K} = [\overline{K_H}, \overline{K_F}, \overline{K_L}]$). Here it easy to see how the transport is influenced by sorption: the higher R gets the slower will be the transport velocity of the considered solute.

2.3.2 Numerical Aspects

In general, there does not exist an analytical solution for the partial differential Eq. 2.113. Therefore, it has to be solved by numerical approximation methods like the finite difference method (FDM), the finite volume method (FVM) or the finite element method (FEM). An overview over the before mentioned numerical methods is given in [259]. A very common numerical software tool that is quite often used in groundwater modeling is MODFLOW, that bases on the finite difference method and is very widespread. In the subsequent discussion we like to deal with the finite element method, that is discussed in detail by [157, 268]. In the presented context the commercial software package FeFlow® was used. It provides certain possibilities of modeling and in the sequel we like to present the instruments which are relevant in the considered context [77].

The finite element method represents a numerical solution method that allows to calculate approximated solutions that in general converge to the exact solution with an increasing refinement of the finite element mesh. This method can not be applied to the partial differential equation directly, but it has to be transformed to an appropriate form: the weak form. Starting from Eq. 2.113 the equation is multiplied by a test function η and integrate it over the integration domain, such that we obtain

$$\int_{\Omega_t}\left[\eta S_0\frac{\partial h}{\partial t} - \eta\left[K_{ij}h_{,j}\right]_{,i} + \eta\left[K_{ij}\Theta_j\right]_{,i} - \eta\varepsilon\rho Q_\rho\right]dv = 0 \qquad (2.161)$$

By means of partial integration we can rewrite the second term in Eq. 2.161 as

$$-\int_{\Omega_t}\left[\eta\left[K_{ij}h_{,j}\right]_{,i}\right]dv = -\int_{\Omega_t}\left[\left[\eta K_{ij}h_{,j}\right]_{,i} + \left[\eta_i\left[K_{ij}\right]_{,i}\right]\right]dv \qquad (2.162)$$

If we apply the Gauss-Theoreme and take the boundary conditions from Eq. 2.114 into account we finally obtain

$$-\int_{\Omega_t} \left[\eta \left[K_{ij}h_{,j} \right]_{,i} \right] dv = -\int_{\partial\Omega_t} \left[\eta \left[K_{ij}h_{,j} \right] n_i \right] da = \int_{\Gamma_2} \eta[b + a[h - \tilde{h}]] da \quad (2.163)$$

Inserting all this in 2.161 and sorting the terms the weak form is given by

$$\int_{\Omega_t} \left[\eta S_0 \frac{\partial h}{\partial t} + \text{grad }{}^t\eta \cdot \mathbf{K} \cdot \text{grad } h \right] dv + \int_{\Gamma_2} \eta a h da$$

$$= \int_{\Omega_t} \eta[\text{div} \left[\mathbf{K} \cdot \Theta \right] + \varepsilon\rho Q_\rho] dv + \int_{\Gamma_2} \eta[a\tilde{h} - b] da \quad (2.164)$$

The next step after the derivation of the weak form is the spatial discretization, that means that the continous domain of consideration is approximated by a finite number of subdomains

$$\Omega_t \approx \Omega^h = \bigcup_e \Omega_e \quad (2.165)$$

Following the isoparametric concept we chose the following approach to describe the hydraulic head h and the weighting function η

$$h_e = \sum_i^{nnd} N_i h_i \implies \nabla h = \sum_i^{nnd} \nabla N_i h^i on\Omega_e$$

$$\eta_e = \sum_i^{nnd} N_i \eta_i \implies \nabla \eta = \sum_i^{nnd} \nabla N_i \eta^i on\Omega_e \quad (2.166)$$

whereby N_i are form functions. For the solution of groundwater flow problems linear approaches for the form functions are sufficient. Inserting these approaches into the weak form of Eq. 2.164 the set of partial differential equations can be rewritten as

$$\mathbf{M} \cdot \dot{\mathbf{h}} + \mathbf{K} \cdot \mathbf{h} - \mathbf{F} = \mathbf{0} \quad (2.167)$$

with

$$\mathbf{M} = M_{ij} = \sum_{e=1}^{nel} M_{ij}^e = \sum_{e=1}^{nel} \int_{\Omega_e} S_0 N_i N_j dv$$

$$\mathbf{K} = K_{ij} = \sum_{e=1}^{nel} K_{ij}^e = \sum_{e=1}^{nel} \left[\int_{\Omega_e} \Delta N_i \cdot [\mathbf{K}_f \cdot \nabla N_j] dv + \int_{\Gamma_2^e} a N_i N_j da \right]$$

$$\mathbf{F} = F_i = \sum_{e=1}^{nel} F_i^e = \sum_{e=1}^{nel} \left[\int_{\Omega_e} N_j \left[\text{div} \left[\mathbf{K}_f \cdot \Theta \right] + \varepsilon\rho Q_\rho \right] dv + \int_{\Gamma_2^e} N_i[a\tilde{h} - b] da \right]$$

$$(2.168)$$

For the time discretization we want to apply the implicite Euler integration scheme since it is completely stable and of first order accuracy. The time derivative for the hydraulic head is given by

$$\frac{\partial h}{\partial t} = \frac{h_{n+1} - h_n}{\Delta t} \quad \text{with} \quad h_{n+1} = h(t_n + \Delta t) \tag{2.169}$$

Applying this approach to the vector of hydraulic heads in Eq. 2.167 and solving it for primary unknown h_{n+1} we get

$$[\mathbf{M} + \Delta t_n \mathbf{K}] \, \mathbf{h}_{n+1} = \Delta t_n \mathbf{F}_{n+1} + \mathbf{M} \mathbf{h}_n \tag{2.170}$$

As mentioned before the implicite or backward Euler integration scheme combines very positive properties, but it requires more computation time since for every time step several iterations have to be computed depending of the size of the time step. Equation 2.170 represents the implemented form of the groundwater flow problem. In the sequel we like to summarize which data and information is required for setting up the finite element model and the corresponding data could be derived.

In order to model groundwater aquifers of large-scaled regions in the end we only require the following input data for the groundwater system as depicted in Fig. 2.12, namely,

- inflow\outflow in and out of the aquifer,
- groundwater recharge (sources)
- the exploitation from groundwater (sinks)
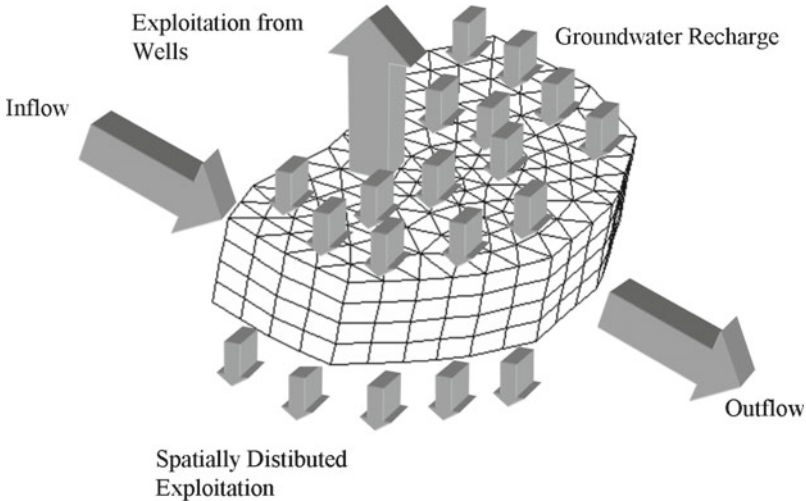
Fig. 2.12 Input data of a finite element groundwater model: horizontal inflow\outflow, groundwater recharge and exploitation

The three quantities have to be implemented in different ways and in the sequel we briefly discuss the corresponding realization within the FeFlow® Software. We start with first quantity the *inflow\outflow* into and out of the model area which is implemented by boundary conditions. FeFlow® knows 4 types of boundary conditions

- hydraulic head boundary conditions (Dirichlet type),
- flux boundary conditions (Neumann-type),
- transfer boundary conditions (Cauchy type) and
- single well boundary conditions

In general, one tries to use the hydraulic head boundary conditions since they are directly measurable and very easy to implement. But in general for considerations in the context of water resource management the dynamics of the groundwater system plays a crucial role. Usually the data base with respect to hydraulic head measurements is as good as it is required to represent the dynamical effects sufficiently. In order to implement the boundary conditions on base of the water budget values (m^3/d) which can not easily transformed into an exact hydraulic head representation, we recommend the use either of the flux boundary conditions or the well boundary conditions. However we have to mention here that at least at one boundary node of the finite element mesh a hydraulic head boundary condition has to be implemented for mathematical reasons, otherwise no unique solution can be found. Since in the end the boundary conditions should be scaled in dependency of the precipitation for instance, the best experience was made by using the single well boundary conditions and using them as injection wells.

The *groundwater exploitation* can be modelled by well boundary conditions as well and it is the common way to do so. But for the modeling of exploitations on a regional scale, like for agricultural exploitations, they can only be represented by a spatial distribution. The appropriate instrument for the implementation of spatially distributed quantities is the 'inflow on top\outflow on bottom'—option provided by FeFlow®. This option allows the user to define a spatially distributed outflow on the lowest layer of the finite element model. This does not correspond to reality, but it is an admissable procedure in modeling. In the context of water resource management both kinds of exploitation modeling are used. Since the location and exploitation rates of wells or well fields are well-known the modeling by single well boundary conditions will be the right choice. In order to model the agricultural exploitation due to irrigation the 'outflow on bottom'—option should be used.

In analogy to the spatially distributed exploitation rates the *groundwater recharge* is a spatially distributed quantity as well and therefore it can be implemented by the 'inflow-on-top'-option provided by FeFlow®. The groundwater recharge rates can not be measured directly but it can only be calculated by considering the water balance. A prerequisite for this, however, is the derivation of a water budget that allows the estimation of all input data and the quantification of the boundary conditions.

2.3.3 Water Budget

The first task in setting up models covering the water resources of a certain area a water budget has to be constructed after the model area was defined, especially if a very big model area is considered. Hereby the water budget is a theoretical device that supports structuring the water resource system and identifying the most important water fluxes. Here fluxes into and out of the system has to be collected as well as the water fluxes within the model area. The intension must be to realize the relation of all important water fluxes to each other, to quantify them, separating the more important from negligible water flows and to estimate the error that happens due to neglecting them. Of course, in some cases the separation of different flows is artificial that should support the identification of relations between different components and sometimes it helps to quantify them. Since most of the quantities in the water budget are not independent from each other, the quantification of the water budget must be an iterative process.

Some of the quantities have to be derived from others or at least they can be confirmed or disclaimed by them. But before we can quantify the water fluxes it has to be defined how the different fluxes are related to each other by a qualitative description.

The water fluxes determining the water resource system can be divided into two groups whereby the first one describes the interaction of the system with the ambient environment and the second group are water flows within the system. Following the idea of a system the latter group would not appear in the investigation. The required input data describing the water amounts flowing into and out of the system are

- precipitation and evaporation/evapotranspiration
- surface water inflow/runoff
- groundwater inflow/runoff
- waste water runoff

whereby here we want to assume that the anthropogenic structures like fresh water channels belong to the surface water system. The only exception is the waste water flow here, which should be treated separately since in the sequel the impacts on the system due to waste water should be considered more detailed.

As mentioned before the structuring of the water flows within the system sometimes includes that a theoretical distinction of water flows is made that in reality can not be distinguished, like the horizontal and vertical groundwater recharge, that can not be measured separately. Also the effects on the vertical groundwater recharge rate due to precipitation or irrigation can only be separated in theory. In reality, if it was measured the result is always the superposition of several effects. Nevertheless, it makes sense to resolve the problem qualitatively as good as possible since sometimes also information can be gained from partial knowledge or at least a better estimation can be won. Therefore, for instance, we have to distinguish between irrigation from groundwater, surface water or treated waste water. All of them effect the groundwater recharge rate beside precipitation or the surface water bodies. Due to this distinction
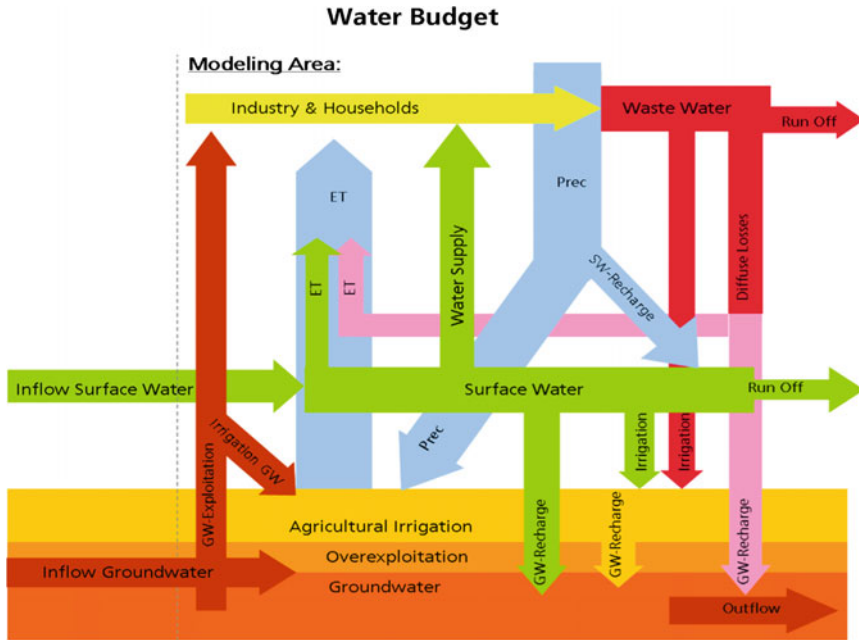
Water Budget

Fig. 2.13 Water budget

a better comprehension of where deviations between measurements and calculated results come from and a correction of input data or parameters can be performed.

Figure 2.13 represents the attempt to structure all the before mentioned effects and quantities by different colors representing subsystems. Due to arrows the impact of different quantities on each other should be pointed out. The first group represents the natural fluxes due to precipitation P and evapotranspiration/evaporation ET. Hereby, we have to take into account, that a part of the precipitation contributes directly to the surface water system that should be denoted by surface water runoff Q_{SWR}.

The next group summarize the surface water system and here we have to take into account an inflow $Q_{SW_{in}}$ from the ambient catchment areas. It is reasonable to distinguish an explicit contribution from surface water bodies to the groundwater and an implicit contribution due to irrigation from surface water that also infiltrates and also end up in the groundwater. But estimating these contributions separately could be easier. Parts of the surface water are taken for industrial or domestic purposes (EXP_{SW}) and a not negligible part evaporates. Balancing all these components (including Q_{SWR}) yields the surface water runoff.

The next subsystem covers the industrial and domestic user groups that are either supplied by surface water or by groundwater and from which emerges the waste water, whereby here it is assumed that the whole waste water is treated the same.

The last part is summarizes all components that are related to the soil and groundwater. Here we have to consider the infiltration that is fed by precipitation, irrigation

Q_{Irr} and/or diffuse losses Q_{DFL} from the urban water network and is divided into the evapotranspiration and the groundwater recharge Q_{GWR}. By the irrigation also the last and in most cases biggest user group, namely the agriculture is taken into account within the water budget. In total we distinguish three user groups or customer groups, respectively, namely domestic user, industry and agriculture.

For the supply of the three customer groups in principle three available resources can be chosen, namely surface water, groundwater or reused waste water, whereby in the sequel it is assumed that the reused waste water is only taken for the agricultural irrigation.

If we like to quantify the identified fluxes within the system we have to define where the balance has to be evaluated. Since we like to map all the information on the model area represented by a map showing a projection of the soil surface and some of the fluxes take place "above" or "under" the soil surface it seems reasonable to balance the water fluxes at the soil surface. Furthermore we assume with respect to the groundwater that the unsaturated zone can be neglected, that means that its property of storing big amounts of water and causing a delay between infiltration and groundwater recharge is ignored.

In principle, there are three possibilities to receive data:

1. Direct Method: it means the direct measurement of data and should be the best, if no principal mistakes are made.
2. Indirect Method: That requires a good knowledge about the relation between different quantities within the system and also another set of measured data from which the required data can be derived or computed.
3. Estimations or assumptions: Sometimes the only way to get parameters for any models is to estimate them, whereby these estimation usually are also based on other so-called *meta-information* or *soft information* which are measured themselves or derived, but which either can not be related to the searched data directly or the amount of measurements is not sufficient and have to be generalized.

The first kind of information is the best one of course, whereby also here always the correctness of the measurements have to be checked with respect to plausibility. The second and third kind are quite similar, whereby the main difference is that estimations and assumptions can only be verified iteratively by calculating the system and making some assumptions and checking wether the results fit to primary data which were collected by measurements. In this case the relation between the assumed data and the known data is not completely clear in contrast to the case which is covered by the indirect method.

2.3.4   Determination of Input Data

The next step is the quantification of the water budget on a yearly base such that in the end the input data for the groundwater model can be derived. Of course, one starts with these data which are available by direct methods since this is the simplest way.

In general, the quantity that can be measured directly is the precipitation P. Usually there is a big number of gauging stations available, but since a set of data for the entire model area has to be determined, the measurements have to be interpolated. Established methods are the Kriging algorithm, Akima Algorithm or the inverse distance procedure.

Another quantity that is quite easy to determine is the domestic and industrial water supply since in general it is performed by public waterworks solely. But sometimes industrial organisations are allowed to exploit water themselves such that in case these information have to be organised extra. The information can be inserted into the water budget scheme and the sum of industrial and domestic water corresponds to waste water. However, the crucial question in this context is where the supplied water comes from. Usually there are waterworks for surface water and groundwater separately such that a defined assignment is given. Since in the waterworks the flow rate is captured by flow measurement devices it is quite simple to collect the data for the water budget.

A quantity which follows from the domestic and industrial water supply is the amount of waste water. So most of the water that is used in private households and industry becomes waste water. So theoretically if the total water supply is known for a certain region we also know the amount of waste water. The problem here is that in most cases diffuse losses take place due to leckage from the fresh water the waste water system. These leckage is usually the range of 20–30 % and thus it is not negligible.

The measurement of the flow rate of rivers and channels can in principle be performed directly as well, but in general not all rivers are measured, such that the inflow of the total surface water into the model area has to be estimated where the flow rates of bigger rivers give a clue for the estimation of the flow rate of smaller ones. It is not possible to determine the exact figures, but the total sum of inflow and outflow should be of the right order.

But the surface water system is not only supplied by the inflow, but also by the surface water recharge. Here we have to distinguish beteen the direct surface water inflow that means the precipitation that falls directly on the surface water areas and on the other hand the rainfall run off from the non-water areas. The direct surface water recharge, subsequently denoted by $Q_{SWR_{WA}}$ is equal to the precipitation rate and if we consider the volume rate it is proportional to the area the surface water system takes place. The latter contribution from the non-water areas ($Q_{SWR_{nWA}}$) can ony be estimated. There is a big amount of rainfall-runoff-models available by which the surface water runoff can be calculated. But, these models are too complex to apply them in the present context.

Therefore the approach we follow subsequently is to quantify the surface water recharge in dependency of land use/land cover classes, whereby a linear dependency on the precipitation rate is assumed. The surface water recharge is estimated by

$$Q_{SWR}(\mathbf{x}, t) = w_{SWR}(\mathbf{x}) \cdot P(\mathbf{x}, t) \tag{2.171}$$

Table 2.16 Classes of land-use, groups and weighting factors for surface water run off and groundwater recharge

Land-use class	Group	$w_{swr}(\%)$	$w_{gwr}(\%)$
Urban areas	$\mathbb{U}$	25	10
Rural residential pl.	$\mathbb{U}$	25	10
Paddy fields	$\mathbb{I}$	15	20
Irrigated areas	$\mathbb{I}$	15	20
Orchards	$\mathbb{I}$	15	20
Woodland	$\mathbb{I}$	15	20
Shrubbery	$\mathbb{O}$	15	20
Meadows	$\mathbb{O}$	15	20
Open woodland	$\mathbb{O}$	15	20
Ephemeral water ar.	$\mathbb{W}$	100	45
Perennial water ar.	$\mathbb{W}$	100	45

This procedure automatically gains a spatial distribution and it is also applied to quantify the groundwater recharge rate later on. Table 2.16 shows some proposals for the percentual contribution of surface water recharge for different land use/land cover types.

If the values of Table 2.16 is related to the corresponding areas of a landuse map by a GIS we obtain a weighting map. By means of this weighting map and a precipitation map of the considered region Eq. 2.171 can be evaluated pointwise such that a map for the surface water run off is generated. If the model area is plain enough the discussed approach is sufficient. For more mountainous regions the weighting map can be merged with a corresponding map containing the slope, rescaling the weighting map for the surface water recharge. This yields run off higher surface water recharge rate in regions where the slope is quite small. In regions where the slope is big the runoff is higher and the surface recharge as well. But of course these maps have to be calibrated.

In the sequel, the parameters we like to discuss can not be measured anymore but we have to estimate and calculate it by balancing considerations. This should be done in a regionalized manner that means we will evaluate the balance equation step by step for the different land use types. In order to simplify the subsequent discussion we summarize some of the land use classes in Table 2.16 and treat them by the same regulations. In general the subsequent balance equations have to be evaluated for every land use/land cover class. The problem in this context is to find the correct rates for every class.

In total the Table 2.16 consists of eleven classes that are were summarized by four groups: non-cultivated areas, urban areas, agricultural irrigated areas and water areas. The last group contains rivers, lakes and reservoirs. The land use map in Fig. 2.14 shows a sample for the spatial distribution of the landuse classes in the Beijing region. For each of these groups the balance equation has to be formulated and evaluated differently. For simplicity we start with the non-cultivated areas, since there no side
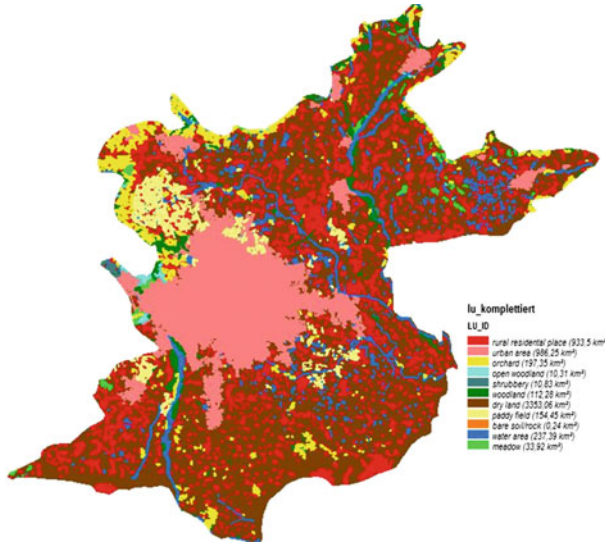
Fig. 2.14 Classes of land-use and their spatial distribution in the Piedmont plain

effects have to be taken into account. The general balance equation for non-cultivated areas is given by

$$P = Q_{Inf} + Q_{SWR} \tag{2.172}$$

where Q_{Inf} denotes the infiltration. Here any antropogene side effects are neglected. But on the left hand side the source terms are written whereas on the other hand the sink terms are summarized. Bearing this distribution in mind it is easy to introduce additional quantities, like irrigation for instance, at the right place. A further point we have to take care of is that the evaluation follows a certain order. The idea is that the rain water runs off much faster than it infiltrates. Therefore, it makes sense to introduce the effective precipitation that is defined by

$$P_{eff} = P - Q_{SWR} \tag{2.173}$$

If we subsequently calculate with effective precipitation it includes automatically that the surface water recharge is allready considered.

Non-cultivated Areas: We start the discussion of the balance equation for the different land use/land cover types with the non-cultivated areas since there no antropogene effects have to be considered, such that the balance is given by

$$P_{eff} = Q_{Inf} \tag{2.174}$$

that corresponds to Eq. 2.172 whereby Eq. 2.173 was incorporated. Furthermore, the infiltration can be divided into two further parts

$$Q_{Inf} = Q_{GWR} + ET \tag{2.175}$$

where Q_{GWR} denotes the groundwater recharge and ET is the evapotranspiration rate. The determination of both quantities is a very hard task since they are not measurable directly, at least not area-wide. In addition to that both quantities depend on a big number of variables, such that their indirect derivation from other quantities is difficult as well.

Especially, with respect to the evapotranspiration a lot of models were developed to quantify the evapotranspiration rate. Evapotranspiration is the sum of evaporation from water and the transpiration from plants. Since both effects usually occur simultaneously they are summarized by the evapotranspiration. Moreover, one distinguish the *potential evapotranspiration* potential evapotranspiration ET_{pot} and the *real evapotranspiration*indexreal evapotranspiration ET_a. Potential evapotranspiration is the amount of water that could evapotranspirate under certain conditions if enough water was available. The real evapotranspiration is the actual evapotranspiration that could be measured under certain conditions. There are a lot of approaches and some of them are only valid for particular climatic regions. An empiric model was developed by *Haude* for Germany that calculates the potential evapotranspiration by

$$ET_{pot}^{Haude} = kp_s \left[1 - \frac{1}{F} \right] \quad \text{with} \quad p_s = 6.11 \exp \left[\frac{17.62T}{243.12 + T} \right] \tag{2.176}$$

He introduced a particular Haude-factor k that specify the influence of different plants. This model is quite simple since it only depends on the saturation vapour pressure p_s, that is a function of the temperature T and relative humidity F. All quantities are easy to measure.

Another approach that was developed by Penman also considers energetic influences and aerodynamical effects calculates the potential evapotranspiration by

$$ET_{pot}^{Penman} = \frac{s}{s + \gamma} \cdot \frac{R_n - G}{L} + \frac{\gamma \cdot f(v) \cdot [p_s(T) - p]}{s + \gamma} \tag{2.177}$$

with

$$[p_s(T) - p] : \text{deficit of the saturation vapour pressure}$$
$$G : \text{soil heat flux}$$
$$\gamma : \text{psychrometric constant}$$
$$L : \text{specific vapourisation heat}$$
$$f(v) : \text{wind velocity}$$
$$s : \text{slope of saturation vapouration pressure}$$
$$R_n : \text{radiation balance}$$

The netto radiation balance R_n that depends on the global radiation R_G, the relative sunshine duration S/S_0, the absolute air temperature T_{abs} and the vapour saturation pressure and it is described by the subsequent expression

$$R_n = (1 - \alpha)R_G - \sigma \cdot T_{abs}^4 \cdot [0.34 - 0.044\sqrt{p}] \cdot \left[0.1 + 0.9\frac{S}{S_0}\right] \qquad (2.178)$$

This approach was enhanced by Monteith for the estimation of real evapotranspiration introducing biological characteristics to be able to cover the specific conditions on the area of consideration. The result of the modifications is given by

$$ET_a^{PM} = \frac{1}{L^*} \cdot \frac{s[R_n - G] + \frac{\rho_a c_p}{r_a}[p_s(T) - p]}{s + \gamma\left[1 + \frac{r_s}{r_a}\right]} \qquad (2.179)$$

Here ρ_a is the density of the air and c_p corresponds to the heat capacity of the air. L^* is the specific vapourisation heat and r_a denotes to the aerodynamical resistance that is assumed to be dependent on the crop height $f_c(h_c)$ and the wind velocity v_z at a certain measurment height z

$$r_a = f_c(h) \cdot v_z \qquad (2.180)$$

Additionally, a stomata resistance r_s was introduced which is a measure for the actual water supply of the crop. If this value becomes zero Eq. 2.180 only describes the interception effect that is the evaporation of water at the leafes surface. Then Eq. 2.179 represents the evaporation from free water surfaces. The Penman–Montheith evapotranspiration model is one of the widespreaded and most important scientific ones. The FAO recommends a particular application which is the so-called grass-reference evapotranspiration. As the name of this method tells already it is an application to a well defined grass area with a certain height and without water stress. By introducing crop coefficients the evapotranspiration of other can be calculated. A detailed discussion of this method would go to far at this place and the interested reader is referred to [2].

In order to calculate the evapotranspiration for a bigger area for the purpose of water resource management the quantification of the evapotranspiration by the before mentioned methods is too complex and in most cases the required data are not available for area-wide investigations. Therefore, we have to use simpler approaches that cover the reality in a sufficient manner. In the subsequent context we assumed that the evapotranspiration depends on groundwater recharge in linear way and we introduced a weighting factor in analogy to the computation of the surface water recharge, such that the groundwater recharge can be computed by

$$Q_{GWR}(\mathbf{x}, t) = w_{gwr}(\mathbf{x}) \cdot ET(\mathbf{x}, t) \qquad (2.181)$$

In Table 2.16 some values are listed for the different land use/land cover types. With this at hand we can rewrite Eq. 2.175 only in terms of the evapotranspiration and

obtain

$$Q_{Inf} = [1 + w_{gwr}] \cdot ET \tag{2.182}$$

The groundwater recharge weighting factor has to be quantified for every specific case, thus it depends on very many variables. In general the range can be asssumed between 0–40 %. But in case of carst regions, for instance, one can imagine that the contribution to groundwater recharge is higher. Furthermore it is straight forward that the groundwater recharge rate in paved areas must be much lower than somewhere else.

Agricultural Areas: The situation is getting much more complex if the water consumption (irrigation) of agricultural used areas has to be quantified. Here, especially with respect to bigger model areas, the problem is that not for all agricultural farms the correponding figures of water use can be obtained. Therefore, other ways have to be found to quantify the water use of agriculture in the corresponding model area. In order to get a sufficient good estimation for the agricultural water use, land use maps representing the agricultural production can be incorporated for calculating the required amount of water. For instance, the production of summer corn and winter wheat requires about 870 (mm/a) of water. In a region of about 590 (mm/) of precipitation per year an additional amount of water of about 280 (mm/a) would be necessary. Since not the whole precipitation is available for the agricultural production, but bigger parts becomes surface water recharge we have to insert the effective precipitation here and the required additional irrigation is even higher and is given by

$$Q_{Irr} = D_{Agr} - P_{eff} \tag{2.183}$$

Here, D_{Agr} denotes the agricultural water demand which contains not only the amount of water that is required by the crops for growth (crop water need *CWD*/crop evapotranspiration) but also all the groundwater recharge. That means that the D_{Agr} corresponds to the infiltration as defined in Eq. 2.175 but only in the context of agricultural areas. From an agricultural point of view the groundwater recharge has to be considered as 'losses' since they do not contribute to the biomass production, but usually it only can be avoided if drop irrigation is applied. It is a hard task to determine the corresponding rates of D_{Agr} for different crops. In order to compute the D_{Agr} we have to apply Eq. 2.181, whereby the weighting factor has to be quantified for every crop type as well as the evapotranspiration must be specified for the considered crop. In the current context where we discuss the quantification of budget data on a yearly base the order of different crops during the year is of less interest. However, as soon as we consider smaller time periods (time resolution) like monthly timesteps the order of the crops is very important. Therefore, in time resolved consideration the D_{Agr} is a time series considering the different stages of growth requiring different amounts of water. A more detailed discussion of determination of the crop water need is given in Chap. 4 in the context of water demand modeling. An entire theoretical and practical discussion with some representative figures for crop evapotranspiration can also be found in [41].

Urban Areas: In urban areas certain conditions have to be taken into account. At first due to the paved areas in those regions and the effort to lead the precipitation as quick as possible into the water network it is reasonable to assume lower groundwater recharge rates and higher surface water run off rates whereby the water pipe system is understood as a part of the surface water system.

A further assumption is that a certain amount of water always gets lost due to leakages in the fresh and waste water network. These 'diffuse losses' can only be estimated and do not contribute to the surface water run off, but only to the infiltration. Therefore we have to modify the balance equation by a new term Q_{DFL} describing the diffuse losses as an additional source term on the rhs:

$$P_{eff} + Q_{DFL} = Q_{Inf} \tag{2.184}$$

The diffuse losses can not be avoided and in european cities a loss of about 10 % seems realistic. In real mega-cities, the rate can be assumed much higher, since they grown-old and the the water infrastructure is old as well and an estimated rate of up 30 % can be realistic. The exact amount of losses can only be estimated. Since the diffuse losses do not contribute to the surface water run off the infiltration consists of a precipitation part and a contribution from diffuse losses. It is reasonable to apply different weighting factors for the computation of the groundwater recharge rate for the two contributions, because before the precipitation can seepage a bigger part will evaporate since the water is at the surface for a longer time. In contrast to this the diffuse losses are already in the soil and the evaporation only takes place due to capilar effects.

Water Areas: A more complex matter is the quantification of input data from water areas since ephemeral and perennial water bodies have to be distinguished here which show a different time dependent behavior. Especially in aride and semi-aride regions due to the climate change perennial water bodies change to ephemeral ones during longer dry periods and ephemeral ones run dry completely. Therefore, the total size of the water bodies reduces during a period of several dry years, especially if the surface water abstraction is not reduced. The problem here is that it can not be forecasted where the changes take place.

In order to take these climatic effects and the reduction of the water areas into account the easiest way is to update the land use/land cover map in a regular manner. If this is not possible one approach can be to scale the water areas in dependence of the yearly precipitation rate. Hereby the long term mean precipitation rate can be assumed as a reference value. By relating the precipitation rate of the current year c and the last n year(s) before to the long term mean value $\overline{P}$ a scaling factor can be calculated by

$$s = \frac{P_c \cdot P_{c-1} \cdot \cdots \cdot P_{c-n}}{\overline{P}^{n+1}} = \frac{\prod_{i=c}^{c-n} P_i}{\overline{P}^{n+1}} \tag{2.185}$$

that describes the reduction of the surface water areas. If we assume a start configuration of all water areas in the model area as $120\,\text{km}^2$ that corresponds to 100 %

whereby $80\,km^2$ are perennial and the rest are ephemeral water areas. With a particular long term mean precipitation rate of $600\,(mm/a)$, for instance, and a precipitation rate of the current year and the year before of about 550 and $500\,(mm/a)$ we obtain a scaling factor of

$$s = \frac{500 \cdot 550}{600^2} = 0.76 \qquad (2.186)$$

that corresponds to a reduction of $76\,\%$. This factor was applied to the perennial water areas and the remaining $24\,\%$ become ephemeral water bodies. After this the computed factor was applied once more to the total ephemeral water areas including the additional (former) perennial areas. With the before defined data we finally obtain a $60.8\,km^2$ perennial water areas, $45\,km^2$ ephemeral and the remaining $14.2\,km^2$ becomes non-cultivated areas like meadows.

For being able to solve the balance equation we have to make assumptions about the groundwater recharge rates and the evaporation rates on water areas which can be taken from literature. With this at hand we have to calculate the balance equation for the water areas whereby we have to take the surface water run off from the non water areas ($Q_{SWR_{nWA}}$) into account as an additional source term on the left side. The balance equation for water areas can be written as

$$P + Q_{SWR_{nWA}} + Q_{SW_{in}} = Q_{GWR} + ET + Q_{SWR} + Q_{SW_{out}} + Q_{Expl_{SW}} \qquad (2.187)$$

whereby a total inflow $Q_{SW_{in}}$ and outflow $Q_{SW_{out}}$ and the total surface water abstraction $Q_{Expl_{SW}}$ have to be determine as well either by measurements or estimations. Furthermore we have formally written the precipitation and the surface water recharge on the left and on the right hand side of the balance, respectively. But, since the precipitation becomes completely surface water both contributions cancel each other and the the effective precipitation gets zero and both. Therefore, the balance equation reduces to

$$Q_{SWR_{nWA}} + Q_{SW_{in}} = \overline{Q_{GWR}} + \overline{ET} + Q_{SW_{out}} + Q_{Expl_{SW}} \qquad (2.188)$$

Since the perennial and ephemeral water areas often can not be distinguished very well in maps a representative weighted mean value for the groundwater recharge $\overline{Q_{GWR}}$ and evaporation rate $\overline{ET}$ from water areas can be calculated, whereby the both classes contribute according to the size of the areas. Of course, the values change in correspondance to the reduction of the areal contributions. Moreover, in the context of water areas both contribution can not be summarized by the infiltration since the processes take place at different locations. Nevertheless, formally both quantities can be summarized by an artifical term $Q_{SW_{in,min}}$ that denotes the minimal required surface water inflow that would be necessary to ensure the expected evaporation and groundwater recharge rates. The real surface water inflow finally can be computed by

$$Q^*_{SW_{in}} = Q_{SW_{in,min}} + Q_{Expl_{SW}} - Q_{SWR_{nWA}} \qquad (2.189)$$

whereby we introduced here the netto surface water inflow $Q^*_{SW_{in}}$ for simplification and which is the required information for completion of the water budget. With respect to the groundwater model only the stated groundwater recharge rate is of interest.

Technical Remarks: Theoretically the considered balance equations are evaluated for every point of the model area. In fact the computation is performed on the base of grids with a finite resolution which influences the results of course. Therefore, the resolution of the grids have to be chosen in an appropriate way since it also effects the performance of the calculation tool. The computation results are maps for the groundwater recharge which have to by mapped on the finite element mesh, whereby a finite element usually contains more than one grid point. Therefore, an mean value for every finite element is calculated.

2.3.5 Parameter Estimation

The determination of the model parameters is one central task of modeling. It requires narrow coworking of the modeller and the corresponding experts. Subsequently we like to restrict the discussion to the determination of the hydrogeological parameters K_f and S_0, since these are the central parameters of groundwater modeling in the context of water resource management.

The problem of determining those parameters is that they are only measured on single places and in general these measured values are only valid for a quite narrow radius. On the other hand, the model requires spatially distributed data for the whole model such that in the end the required data sets has to be derived from single points by interpolation. There is a big number of appropriate interpolation procedures but nevertheless the original data should be representative for a bigger regions before they are interpolated. This requires a lot of experience and knowledge of geologists and hydrologists and permanent feedback between modeller and expert.

Of course, the described problem exists in modeling generally but in material science, for instance, one usually considers homogeneous bodies or bodies with well-defined inhomogenities. In geo-related problems the considered domains show always more or less variance in their parameters and the behavior can change from one place to the other. Thereby, the observed changes can happen continuosly or in a discrete manner and it depends on the modellers experiences what is assumed in the model: usually an continuous behavior is assumed. But, such things can be responsible for strong deviations of simulation results and real measurements. There are two principle approaches to overcome this problem, namely either to improve the measurements and trying to get more information of the soil by using special methods like remote sensing for instance or to develope methods which give better interpolation results.

In this book, we want to sketch a procedure how a complete and consistent set of parameters can be generated from incomplete information. The first step is the

estimation of the aquifer depth. This can often be derived from geological maps and from borehole data which can be collected in a different context, but nevertheless they can give information about the structure and thickness of the considered aquifer. Once the shape of the domain of interest including the third dimension is defined the parameters have to be determined. The modeller will discretize the domain in finite domains (finite elements) and with respect to geo-related problems also in different layers representing the structure of the considered aquifer system in the third dimension. The chosen horizontal discretization limits the maximum required resolution of the parameters. The resolution of in vertical dimension depends on the structure of the aquifer. But, it should be kept as simple as possible, since it determines the simulation performance directly.

Now the hydrogeologist must start to collect data of boreholes, observation wells, geological maps and all information he can get helping him to derive the corresponding parameters of interest. What is written here in some sentences can be a matter of weeks and months. Once the required data are defined the model has to be fed by those data. In a parallel task also the dynamic input data and boundary conditions have to be defined. A first draft of these data could be taken from the water budget for instance including all its simplifications like homogeneous spatial and temporal distribution of boundary conditions, groundwater recharge and exploitation. But, by means of this and a first estimation of the parameters a simulation run can be performed and first results can be produced in terms of hydraulic heads. Now the results can be evaluated by comparing the simulations results with measurements of the hydraulic heads at particular points or the whole groundwater surface that yield from interpolation of a big number of measurements at different places for instance.[2] Due to the evaluation of the deviation between measurement and simulation the regionalisation of the parameters and the input data can be pushed on. But now the problem occurs that the reason for the deviation is not unique. It can either be effected by wrong parameters or by incorrect input data and here the before-mentioned feedback loop starts. At first the regions of the biggest deviations have to be identified and the range of input data and parameters have to be proved and corrected. Normally, the effect of these quantities on the system is highly nonlinear and requires a lot of repetitions for each subregion until the maintaining mean error is sufficiently small. In the context of water resource management where real big model areas are taken into account mean error could be in the range of some centimeters up to some meters. It depends on the required accuracy and the possibilities of improvement due to additional data. The described procedure is depicted in Fig. 2.15.

Of course, in principle the described procedure can be automated and there is already a big number of software tools that can be applied to these problems. FeFlow® provides an interface to the parameter estimation software PEST that allows an iterative search of parameters for a finite number of subregions. But it requires a lot of simulations and it assumes that the used input data are correct (if the hydrogeological

---

[2]In this case, it must be ensured that the measurement points cover the whole model area, otherwise the missing data are derived by extrapolation that often yields big errors and therefore it is not admissible.
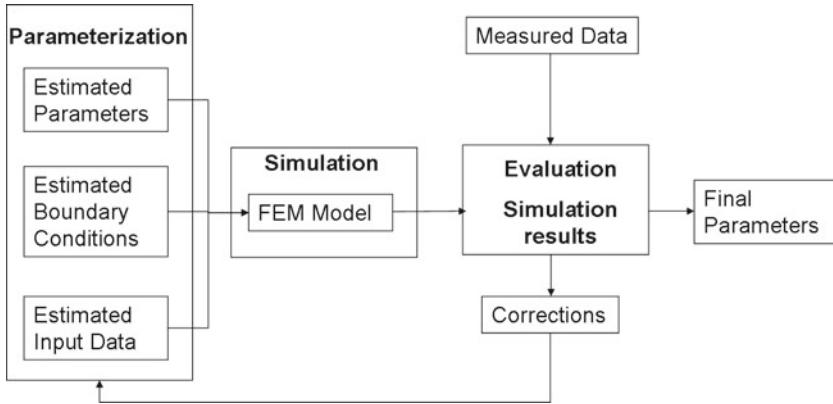
Fig. 2.15 Procedure of parameter estimation

input data are the unknown variables). Of course one can also choose the input data (exploitation and groundwater recharge) define as the searched variables, but then a set of parameters have to assumed to be the right one. Otherwise the mathematical problem becomes under-determined and therefore not solvable. In the before mentioned context where the parameters are as unsure as the used input data such parameter estimating tools at least have to be used very carefully. But, in a context where one of these quantities are well-known these tools could be very helpful and save a lot of time.

2.3.6 Initial and Boundary Conditions

In Sect. 2.1.2 we already described the numerical implementation and realisation of the governing partial differential equations and we learned that the mathematical problem is only well-defined as far as initial values and boundary conditions are given (beneath the required parameters). Also, here the corresponding data have to be defined in a geological and hydrogeological context. How this can be done is the objective of the present subsection.

The initial conditions represents a moment of the temporal development of the considered system. For simulations in material science, for instance the initial values usually correspond to a resting state and can be implemented quite easiliy. In modeling of geo-related problems the initial values have to be taken from reality and should represent a real system state. For a large-scale system of several hundreds or thousands of square kilometers this requirement is a challenge. In the context of groundwater modeling the required initial values are measurements of the hydraulic heads at observation wells with the same time stamp. Hereby the correct measuring is very important, since confined conditions for instance can yield mistakes. A

description and discussion of the measuring principles can be found in [109] and the correct description of the right performance is usually defined in national standards like the standard sheets of the German DVGW (German Gas and Water Association).

Once these data are available the information has to be prepared since from the point-wise information a spatially distributed dataset has to be derived by interpolation. Here, often the problem that arises is that the interpolated (and in some cases even extrapolated) information at the boundaries do not fit to the boundary conditions which were gained from different measurements. Here, the consistency can only be reached by a good cooperation of modeller and the hydrologist/hydrogeologist and good results can only achieved by an iterative procedure where the model is adopted step by step due to comparison of simulation results and measured data. Here, the water budget should support the search for the right data by giving an idea of which order the boundary conditions have to be if no further information about the inflow is available. If better information about the boundary are available the water budget has to be corrected. But, the experience shows that there is a lack of information about the inflow\outflow. Finally, the model must be test again by an independent test run with independent test data.

2.3.7 Reduced Groundwater Models

Groundwater models can be used on the one hand for the simulation of defined scenarios ("what would happen, if"). On the other hand, with groundwater models optimal withdrawal strategies can be calculated. E.g. in the case of water scarcity, the groundwater resources have to be managed in an optimal way in order to avoid overexploitation of the groundwater storages. Unfortunately, the simulation of groundwater models is in general relatively time consuming, as the spatial distributed models in general are implemented as 2-D or 3-D Finite Element models. 3-D Finite Element models in many cases contain more than 100.000 nodes, which corresponds to a simulation time of several minutes for a long term simulation horizon (e.g. 10 years). As for the optimization of withdrawal strategies it may be necessary to run the model several thousand times, the need for reduced groundwater models with drastically reduced calculation time is obvious (Fig. 2.16).

In the next subsection an overview of methods for model reduction is provided. And afterwards a special method for model order reduction of groundwater models is introduced which allows the reduction of complex 3-D models to linear state space models with about 50 states. Finally the application of this method to the model reduction of a large scale groundwater model is presented.
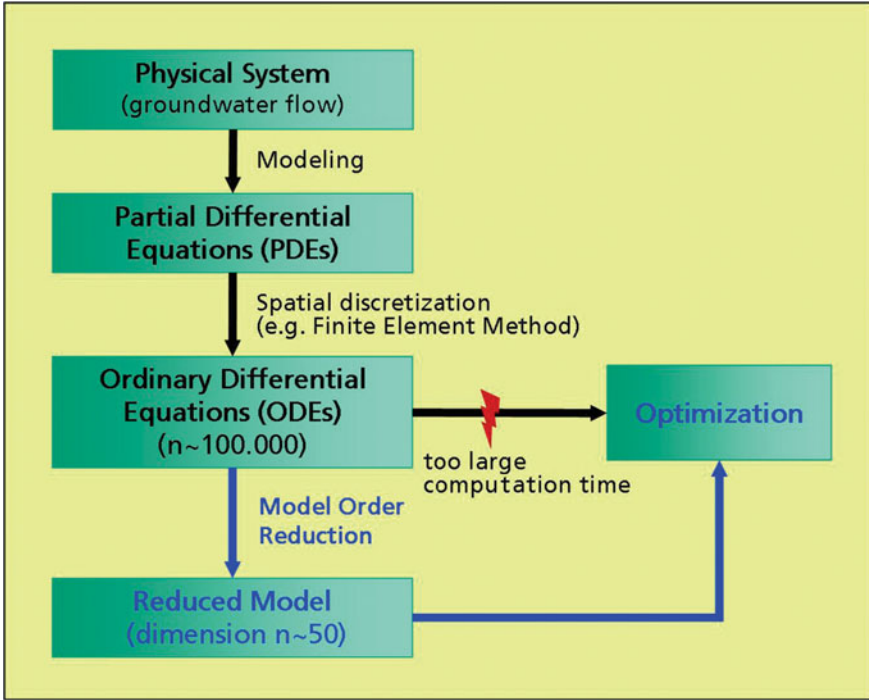
Fig. 2.16 Reduced groundwater models are necessary if optimal strategies have to be calculated

2.3.7.1 Problem Formulation of Model Order Reduction

Model Order Reduction (MOR) is a branch of system and control theory, which studies properties of dynamical system in application for reducing their complexity, while preserving (to the possible extent) their input-output behavior.

Generally the system under investigation will be modelled by means of a set of first-order coupled differential equations, together with a set of algebraic equations:

$$\Sigma : \begin{cases} \frac{dx(t)}{dt} = f(x(t), u(x)) \\ y(t) = h(x(t), u(t)) \end{cases} \tag{2.190}$$

This mathematical model is called *State space representation*. For simplicity, we will use the following notation:

$$\Sigma = (f, h), \qquad u(t) =\in \mathbb{R}^m, \qquad x(t) \in \mathbb{R}^n, \qquad y(t) \in \mathbb{R}^p \tag{2.191}$$

In this setting, Σ denotes the system, u is the input or excitation function, x is the state and y is the output. The complexity of Σ is defined as the number of states n. For linear, time invariant systems, Eq. 2.190 can be represented by

$$\Sigma : \begin{cases} \frac{dx(t)}{dt} = Ax(t) + Bu(t) \\ y(t) = C(x(t) + Du(t)) \end{cases} \tag{2.192}$$

where $A \in \mathbb{R}^{n \times n}$ is the state matrix, $B \in \mathbb{R}^{n \times m}$, $C \in \mathbb{R}^{p \times n}$, $D \in \mathbb{R}^{p \times m}$, and x^0 is the initial state of the system. The associated transfer function matrix (TFM) obtained from taking Laplace transforms in Eq. 2.192 and assuming is:

$$G(s) = C(sI - A)^{-1}B + D \tag{2.193}$$

The problem of model reduction is to simplify or approximate the system Σ with another dynamical system $\hat{\Sigma}$,

$$\hat{\Sigma} = (\hat{f}, \hat{h}), \qquad u(t) = \in \mathbb{R}^m, \qquad \hat{x}(t) \in \mathbb{R}^n, \qquad \hat{y}(t) \in \mathbb{R}^p \tag{2.194}$$

The reduced model $\hat{\Sigma}$ should meet these following criteria:

1. The number of states (i.e. the number of the first-order differential equations) of the approximated system $\hat{\Sigma}$ is much smaller than in the original system Σ, i.e. $k \ll n$.
2. The approximation error should be small (the existence of a global error bound).
3. Stability and passivity should be preserved.

2.3.7.2 Overview of Methods for Model Reduction

Basically, three main classes of methods for model reduction can be identified [7], namely

(a) methods based on singular value decomposition (SVD),
(b) Krylov based methods and
(c) iterative methods combining aspects of SVD and Krylov based methods.

Figure 2.17 provides an overview about some important methods [8]. SVD based methods are suited for linear systems and nonlinear systems of an order $n < 500$ (e.g. balanced truncation for linear systems, proper orthogonal decomposition (POD) for nonlinear systems). Most of these methods have favourable properties like global error bounds and preservation of stability. Krylov based methods are numerically very efficient as only matrix multiplications and no matrix factorization or inversion are needed. Hence they are also suited for large-scale systems. Unfortunately, global error bounds and preservation of stability cannot be guaranteed. Hence actual research is focused on the development of concepts which combine elements of SVD and Krylov based methods.

Fig. 2.17 Overview of methods for model reduction [8]

2.3.7.3 Identification Based Approach for Model Reduction

All of the approaches discussed in the previous section have in common that they aim to approximate the state vector x with respect to a performance criterion, e.g. minimize the deviation between original system and reduced system for a given test input. As for the purpose of groundwater management and withdrawal optimization in many cases a black box input-output model is sufficient, there is no need to approximate the whole state vector x. Furthermore, the dimension n of a reduced model which approximates the whole state space vector x (which has usually a dimension of 10.000 or even > 100.000) would be in most cases $n > 100$. With a dimension for the given optimization problem the solution time would be unacceptably high ($\sim$hours). Last but not least the use of commercial software like FeFlow$^®$ in many cases prevents the application of e.g. a Krylov based method as the model representation (e.g. state space model) can not be exported by the software.

2.3.7.4 Basic Idea: Trajectory and Identification Based Approach

Hence a method is necessary which is only based on input and output data of the simulation model and—for model validation—the corresponding measured values. In control theory the experimental system identification is a standard method. In order to identify a dynamical system, the dynamic response of a system to a test signal (e.g. step-like change or sine signal as input) is analyzed. The result of system identification is a model, represented by a ordinary differential equation resp. an equivalent transfer function, where the parameters of the model are optimized so that the model reproduces the measured values as good as possible.

The basic idea is sketched in Fig. 2.18. We assume the existence of a reference scenario which means that the time dependent input parameters $\mathbf{u}_{ref}(t)$ of the FEM groundwater model (especially groundwater exploitation Q_{Expl} and recharge Q_{GWR})
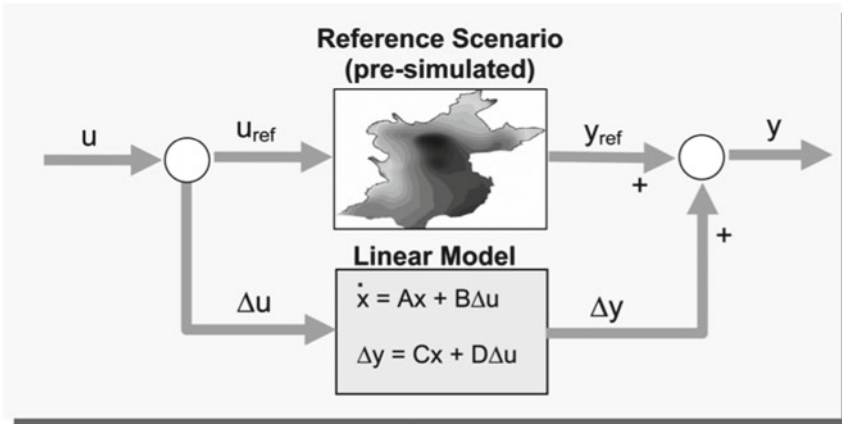
Fig. 2.18 Basic idea of the trajectory and identification based concept: Linear state space model in combination with a pre-simulated reference scenario

are determined for the whole optimization horizon. In practical cases these reference scenarios are mostly available or can be generated by plausible assumptions. Hence the task consists in the derivation of a model which approximates the behavior of the full FEM model in the case that the input parameters **u** differ from $\mathbf{u}_{ref}(t)$. This model is gained by identification techniques: Test signals (e.g. steps) are added to the reference input $\mathbf{u}_{ref}(t)$ (dimension p) and the corresponding deviations from the reference output $\mathbf{y}_{ref}(t)$ (dimension q) are identified. Doing this separately for every component of the input-/output vectors **u** and **y**, we finally merge the $(p \cdot q)$ single input-single output SISO models to a multi input-multi output MIMO model. For the groundwater model, the input parameters are e.g. cumulated (e.g. spatially integrated) exploitation of certain regions or cumulated exploitations of large well fields. The output parameters of the groundwater model are the hydraulic head at representative points ('observation wells').

In the project "Beijing Water" (see Sect. 6.2) 14 inputs and 13 output parameters have been defined by the users: The inputs consist by 9 counties and 5 well fields, the 13 output parameters are 12 observation wells and the mean hydraulic head of the whole area of the water supply system (see Fig. 2.19 for the definition of the inputs and outputs).

As the slow stream groundwater flow can be interpreted as diffusion process (cf. Eq. 2.115) only nearby located input and output parameters (e.g. regions/well fields and the correspon-ding observation wells) have some correlation and a SISO model with these input-/output combinations can be gained. Due to this physical reason the number of relevant SISO models is relatively small and hence the resulting MIMO model of relatively low dimension ($n < 50$) which is appropriate for the optimization problem. The proposed approach can be called trajectory and identification based model reduction. The main steps of this identification based concept for model reduction are summarized as follows:
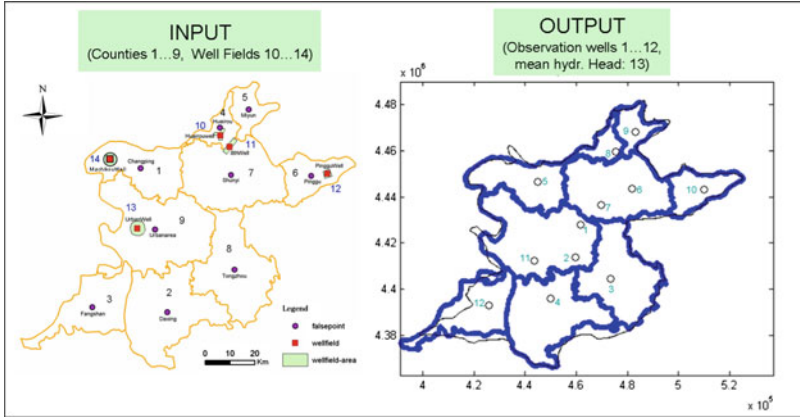
Fig. 2.19 Definition of the inputs and outputs of the reduced groundwater model in the project "Beijing Water"

Step 1: Definition of the input variables (e.g. exploitation of several counties) and output variables (e.g. hydraulic head of several observation wells) of the reduced groundwater model.

Step 2: Definition of a reference scenario regarding input variables. Simulation of the references scenario with the full FEM model, storage of the results of the output variales (which is the reference trajectory).

Step 3: Step-like increase (or other variations) of the input variables and simulation with the full FEM model (simulate the input variations separately). Storage of the output variables of each simulation run.

Step 4: Identification of the parameters of a state space model with defined max. number of states which describes the variation of the reference scenario.

Step 5: Evaluation of the performance of the reduced model. If the model performance is unsatisfactory, step 4 has to be repeated with a different model structure (e.g. greater number of states).

2.3.7.5   Description of the Algorithm

The steps of the algorithm of the trajectory and identification based model reduction concept is discussed in detail in the sequel.

Step 1: Definition of input and output variables

The first step of trajectory and identification based model reduction consists in defining the inputs and outputs of an Input/Output model (I/O model). Comparing with a FEM model representation which provides a nearly exact solution of the PDE in the whole space by using numerical technique, I/O model representation is in many cases sufficient for decision support, control and optimization. Therefore defining

input and output parameters is the first important step of model order reduction. The output of the system are in general the values which are of note (e.g. hydraulic head of selected observation wells or mean hydraulic head of several counties). The parameters which have an impact to the output variables and which can be varied are defined as the input of the system in the sense of manipulated variables.

Step 2: Definition and simulation of the reference scenario

The resulting reduced model is assumed to be linear, hence the superposition principle is applicable. As a consequence, one key idea of the proposed model reduction concept is the use of a 'reference' input and output data as information storage (cf. Fig. 2.18). The reference input time series reflect e.g. a nominal or assumed exploitation over the simulation or prediction horizon. Figure 2.20 shows an exemplary reference time series for one input (e.g. exploitation of one county). In the reference input time series assumptions regarding climate behavior, industrial or agricultural development can be considered.

By means of the full FEM model and the reference input time series the corresponding reference output time series are generated and stored. These output data are called "reference trajectory". It suggests that the complex spatial distributed model is 'linearized' about the reference trajectory. Mathematically this is not true as the PDE of slow groundwater flow in general is linear, hence also the ODEs, which are obtained by spatial discretization, are linear.

Fig. 2.20 Exemplary reference input time series for one input variable
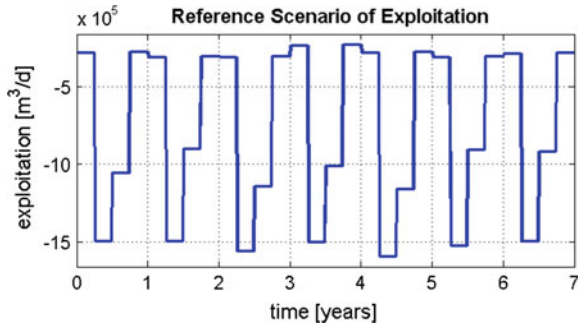
Fig. 2.21 Exemplary refernce input time series (*blue*) and added step-like function (*red dashed line*) for one input variable
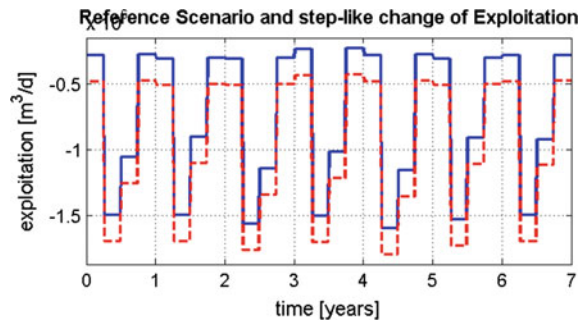
Step 3: Step-like increase of the input variables and simulation with the full FEM model

Now a stimulation function usti(t) is added to each of the reference input time series uref(t) (e.g. step function). An exemplary resulting time series is shown in Fig. 2.21 (red dashed line). The magnitude of the stimulation function usti(t) has to be chosen in a way that at least one of the output variables is modified significantly compared to the reference scenario. All input variables are modified separately by a stimulation function and accordingly simulated with the full FEM model. This means that for m input variables m simulation runs with the full FEM model are necessary.

Step 4: Identification of the parameters of a state space model with defined max. number of states which describes the variation of the reference scenario

The next step after defining I/O parameter and generating reference trajectory is to find all the individual single input–single output (SISO) models. For the assumed m input variables and p output variables $(m \cdot p)$ SISO models have to be determined. Only the impact of the stimulation function is needed for the identification of the SISO models. Therefore the output data for estimating the parameter is:

$$y_{id} = y_{sti} - y_{ref} \tag{2.195}$$

Hence the necessary data for the identification of the SISO models are

$$Z^N = [\mathbf{u}_{sti}, \mathbf{y}_{id}], \quad \mathbf{u}_{sti} = [u_{sti_1}, u_{sti_2}, u_{sti_3}, \ldots, u_{sti_n}]^T, \quad \mathbf{y}_{id} = [y_{id_1}, y_{id_2}, y_{id_3}, \ldots, y_{id_n}]^T \tag{2.196}$$

This batch of data is the starting point of an iterative identification procedure which aims searching the best SISO models iteratively for the given data set.

The multi input–single output (MISO) model, which is the summation of each SISO model over all input parameters, has the following general representation:

$$A(q)y(t) = \sum_{i=1}^{nu} \frac{B_i(q)}{F_i(q)} u_i(t - nk_i) + \frac{C(q)}{D(q)} e(t) \tag{2.197}$$

where denotes the number of inputs.

Reducing the number of states in each SISO model is also reducing the size of the MISO model. There are two alternatives for this purpose. One is applying the SVD-based reduction method to the SISO models. The other is eliminating the SISO model having small effect on output. Since the *balanced truncation* (BT) can provide an efficient result and less computational cost compared to the *optimal hankel norm approximation (HNA)*, BT is applied to reduce the model.

Finally, all MISO models are combined to a multi input–multi output (MIMO) model, as shown in Fig. 2.22. With this MIMO state space model, an approximation of the full FEM model with less computational effort is available, which was the aim of the model reduction.
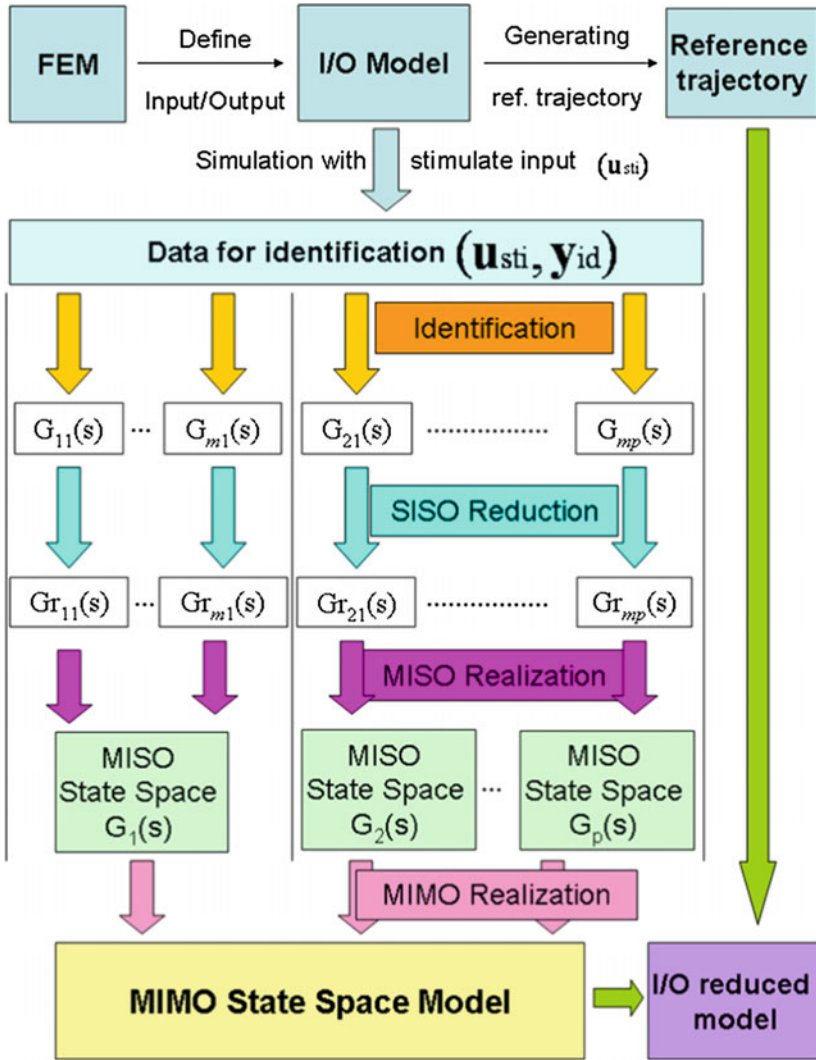
Fig. 2.22 Illustration of the model reduction scheme

Step 5: Evaluation of the performance of the reduced model

The performance of the reduced model has to be evaluated, e.g. by defining maximal limits for allowed deviations between reduced model and full FEM model. If the performance of the reduced model is unsatisfactory, step 4 has to be repeated with a different model structure (e.g. greater number of states). Figure 2.22 summarizes the proposed trajectory and identification based model reduction scheme.
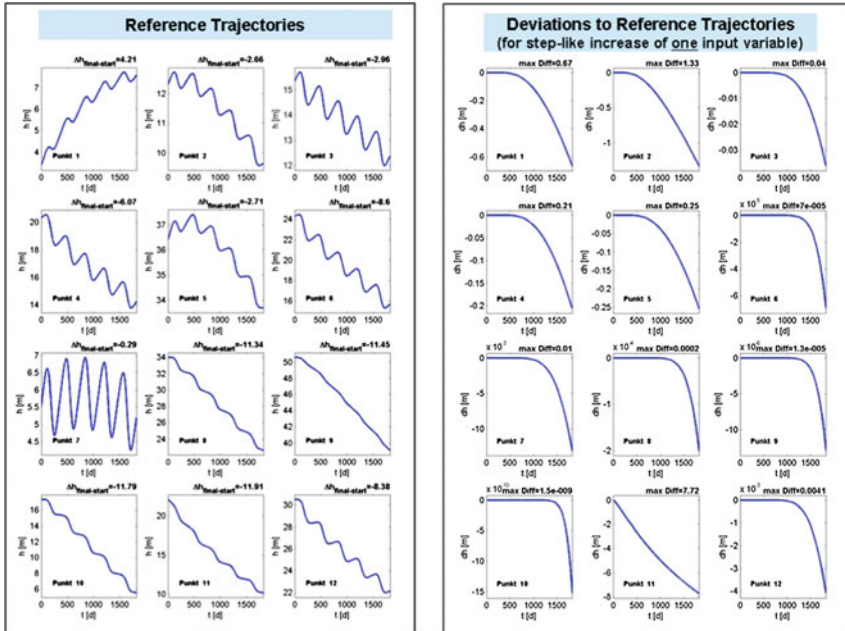
Fig. 2.23 *Left* Reference trajectories at 12 observation points of the groundwater system for a time horizon of 5 years (1825 days). *Right* deviations of the output variables with respect to the reference scenario, when one input is changed by a step-like increase as stimulation function

2.3.7.6   Exemplary Result for Reference Trajectory and Impact of Stimulation Function

In Fig. 2.23 (left), an exemplary time plot of the output variables (hydraulic head of 12 observation points) in a defined reference scenario are shown. The plot in Fig. 2.23 (right) shows the deviations of the output variables with respect to the reference scenario, when one input is changed by a step-like increase as stimulation function over a time horizon of 5 years. Obviously only at some observation points a strong impact of the stimulation function can be seen. At points 1, 4, 5 the amplitude of the deviations is in the interval 0.2 and 1.5 m, while the amplitude of the deviations at point 2 and 11 is greater than 1 m.). At all other points the deviations are smaller than 1 cm. The time plot of the deviations shows a negative exponential characteristics with dead time (due to transport processes). An application of the proposed model reduction concept is presented in Sect. 6.2 (project "Beijing Water").

2.4   Coupling of Groundwater and Surface Water Models

Torsten Pfützenreuter

2.4.1   Interaction Types and Coupling Scheme Selection

According to the hydrologic cycle that describes storage and movement of water above, on and below the earth's surface the different water resources are continuously interacting; this applies of course to groundwater and surface water. For both of them a number of simulation models and simulator engines exist that are specialized for their intended usage. Typically, ground water and surface water are simulated with different engines, the interaction between them is neglected or emulated with fixed or time-dependent flow rates. This may be sufficient for the multiplicity of applications, but not for long-term simulations and optimizations. In this section two different coupling schemes are described that are suitable for the most important interaction types between ground water and surface water. Beforehand, the most important information on this interaction will be resumed.

From the ground water's point of view, the interaction with the surface water depends of the altitude of the ground water table:

- If the altitude is higher than a stream of lake surface, ground water is transformed into surface water (Fig. 2.24).
- A altitude lower than a stream of lake surface results in gains of ground water, surface water is transformed into ground water (Fig. 2.25). Such loosing streams or lakes can be separated from ground water table by unsaturated zones with

Fig. 2.24 Stream or lake gaining water
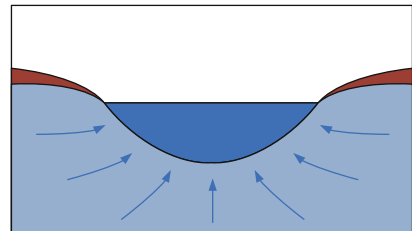
Fig. 2.25 Stream or lake loosing water
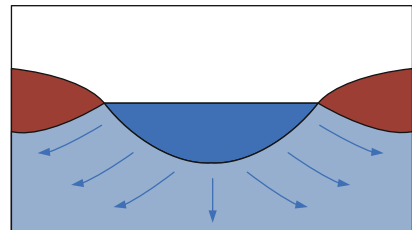
Fig. 2.26 Stream or lake
with unsaturated zone to
ground water table
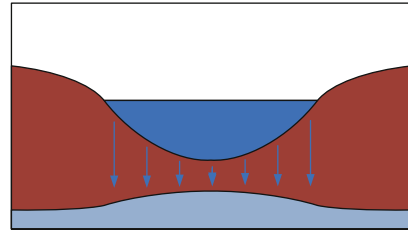
very different thicknesses (Fig. 2.26). See Sect. 2.3.1.1 for more information on
unsaturated zones.

- Wetlands typically have complex hydrological interactions with ground water.
  They have periodically changing water levels (seasonal or tidal changes) that influ-
  ence the flow direction (from or to ground water).

The coupling scheme suitable for modeling the interaction can be determined
by observing the interaction's flow direction: If the direction is expected to change
never in the simulation horizon, the simple sequential coupling scheme can be used.
If the flow direction changes, for instance seasonally or periodically, the time-step
coupling is the proper scheme. Both will be described in the next chapters.

2.4.2 Time-Step Coupling Scheme

Time-step coupling implements a tight connection between surface water and ground
water simulations. Typically, one simulator is the master for the coupled simulation
run, the other acts as the slave. The master prepares the input data for the slave,
controls its time step execution and collects the desired output data to create the
input data for the master's model. This requires a time-consuming coordination of
both simulator systems, but achieves the most accurate results.

The decision on the right simulation master is mainly influenced by the simula-
tion software systems and the desired application software. For the Beijing project
described in Sect. 6.2 the numerical computing environment MATLAB is the basis for
the graphical user interface and the surface water simulation. Therefore, MATLAB
was selected as simulation master.

During simulation, two different simulation modes can be used, the decision
depends on the selected time step length of both simulation models. The time steps
in turn are dependent on the system dynamics. Typically, the surface water model
works with smaller steps than the ground water model. This is the most common
situation since the groundwater processes are slowly compared to the surface water
dynamics.

If the time steps of both models are equal, the synchronous mode exchanging
information at every time step is the mode of choice (Fig. 2.27). In asynchronous
mode, the step size of the surface water simulation model is shorter than of the

Fig. 2.27 Synchronous
simulation mode
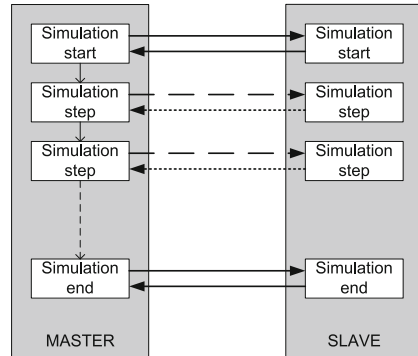
Fig. 2.28 Asynchronous
simulation mode
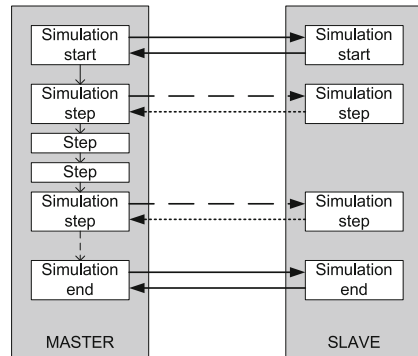
groundwater system. In this mode, the input data for the ground water simulator are
taken from the last valid time step of the surface water system and are constant for
the whole time step of the groundwater simulation (Fig. 2.28).

2.4.3 Sequential Coupling Scheme

The sequential coupling is the simpler method to establish a connection between
two simulation systems. In this case, surface water and groundwater simulations are
executed sequentially. Firstly, the simulator with no dependencies is executed. In
case of disconnected surface water and ground water systems as shown in Fig. 2.26
the sequence starts of course with the surface water simulation. For a sequential
coupling scheme also two modes exist:

- The one-step mode executes the whole simulation horizon with the independent
  simulator (Fig. 2.29). Afterwards, the other simulation run is started. The second
  simulator gets a time series of input data from the first simulation (e.g. seepage
  time series for streams or lakes).
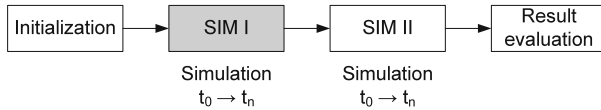
Fig. 2.29 Sequential coupling: one-step simulation
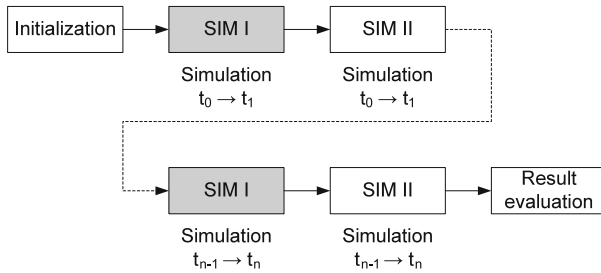
Fig. 2.30 Sequential coupling: multi-step simulation

• The multi-step mode divides the simulation horizon into smaller pieces to get time series back into the simulator running firstly (Fig. 2.30). This may be for instance of interest if the altitude of the ground water table is used to control ground water pumping stations that are simulated as part of the surface water model. It should be clear that the information from the ground water simulation can only be used in the subsequent time step of surface water simulation.

For the sequential coupling is it necessary to save the internal state (e.g. hydraulic heads, pressures, flow rates) of both simulators between the subsequent runs since the two simulators are working alternately. If this is not possible or desired, the time-step coupling scheme must be used.

Chapter 3
Transportation

Thomas Rauschenbach, Thomas Westerhoff and Buren Scharaw

3.1 Models for Describing Courses of Rivers and Reservoirs

Thomas Rauschenbach

The simulation of the behavior of rivers and reservoirs presuppose the analytical description of them. For controlling it, it is sufficient to have knowledge of the behavior at the gauges regarding flow and water level. Up to now, the design just as the implementation of control concepts for influencing a reservoir or also for controlling reservoirs cascades in a coordinated way have been carried out on the basis of control-engineering models or black box models. However, these models are not suited to describe the non-linear unsteady behavior with sufficient accuracy. Models based on the Saint-Venant-equations, in which the course of the river is partitioned into several model sections, can better fulfill the requirements for control tasks [227]. However, due to the fact that many complex calculations are necessary to solve the system of differential equations, these models are not able to guarantee the simulation time required for online optimization [138, 177, 199, 218]. Furthermore, they make it also difficult to model retention areas or also the backflow behavior in the case of tributaries flowing into the river. Therefore, in this chapter a synthesis of both model set-ups, the HDCE models (hydrodynamic-control-engineering models), is being presented which fulfills the requirements with regard to accuracy and fast simulation.

T. Rauschenbach (✉) · T. Westerhoff · B. Scharaw
Fraunhofer IOSB-AST, Ilmenau, Germany
e-mail: thomas.rauschenbach@iosb-ast.fraunhofer.de

T. Westerhoff
e-mail: thomas.westerhoff@iosb-ast.fraunhofer.de

B. Scharaw
e-mail: buren.scharaw@iosb-ast.fraunhofer.de

It is common practice to provide models for control systems in the form of difference equations. In the following paragraphs, it will be shown how difference equation set-ups have been derived from the Saint-Venant equations and how the parameters of the set-ups have been determined.

Furthermore, partial models for different structures and hydrological quantities of a river section or also of a reservoir are set up. These models can be easily put together in a modular way to form the model of a river section.

3.1.1 General Model Set-Up of a River Section

The aim of the modeling of a river section for control tasks is to determine the time series of the water level and the flow rate at those levels which are important for the control. This, however, is only possible if all special features of the river which have an effect on the time series are described in the model. Figures 3.1 and 3.2 show a possible course of a river containing the most important effects which are to be taken into consideration for modeling. At first, some partial models must be available as basic models by means of which the time series of the water level and the flow rate can be determined at any point of the course of the river. Special attention has to be paid to the unsteady behavior, for example in the case of rising high water. The surface curve developing in a wedge-shaped way must be taken into consideration for both water level and flow determination. Otherwise, no satisfying modeling will be possible. Also, the water level is changing during damming up at the weir and must therefore be taken into consideration in the models [10, 17, 35, 89].
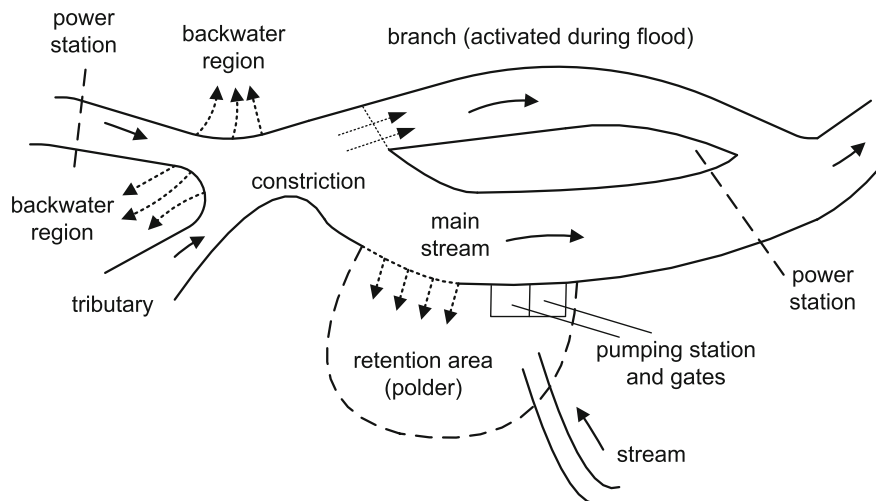
Fig. 3.1 Effects to be taken into consideration for river sections
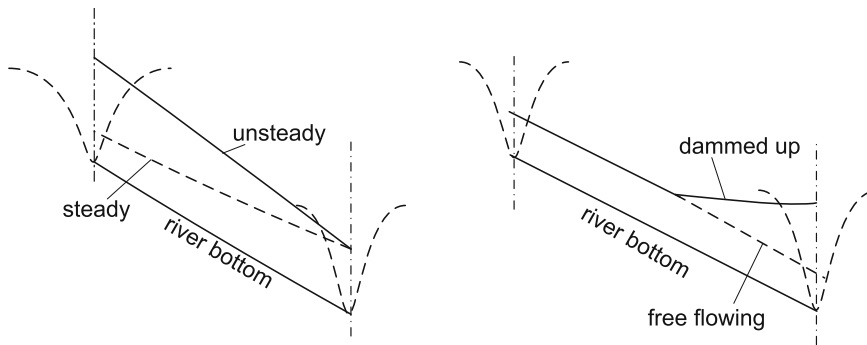
Fig. 3.2 Water tables to be taken into consideration for river sections

In addition to these models, a number of further partial models are necessary for an overall description. One of them is the backwater model. At the mouths of tributaries with a narrow point in the main stream, backwater will flow into the adjacent fields when the water levels are rising, which essentially changes the behavior of the flow and water level curves. Thus, this effect must not be neglected. The water level of a river having reached a certain height, spills into branches or other retention areas often occur. For this, a model must be set up by means of which the flow through these areas can be determined. In this respect, it is necessary to be able to describe the flow behavior within these retention areas. Here, two different kinds are to be told apart: On the one hand, there are those branches which need to be taken into consideration only in the case of high water. They often lead the water past power stations, thus influencing the flow balance considerably. To guarantee an active flood control, flooding regions, so-called polders, are installed alongside the course of the river. For those models which shall describe the time series of the water level and the flow rate well enough in the case of high water, the modeling of these regions is absolutely necessary [14, 18]. They are not only flooded by the main stream having reached a well-defined water level, but also creeks from the surrounding area (intermediate area) contribute to their filling. Thus, the retention behavior can be significantly influenced. Furthermore, the polders are often isolated from the main stream by pumping stations and gates. They exert an influence on the water level in the polder according to a fixed regime and, therefore, must also be taken into consideration for modeling. In the following chapters, the derivation of these models from the Saint-Vernant equations will be explained.

3.1.2 The Saint-Venant Equations and Their Discretization for Time and Place

In order to obtain models which are as exact as possible, the unsteady flow in a river is described by means of the one-dimensional Saint-Venant equations [39, 59]. Furthermore, the newly developed models in the form of difference equations are based on the work of Zielke [153].

The one-dimensional equations are:

$$\frac{\partial q}{\partial x} + \frac{\partial A}{\partial t} = 0 \tag{3.1}$$

$$\frac{\partial h}{\partial x} + \frac{1}{g}\left(\frac{\partial v}{\partial t} + v\frac{\partial v}{\partial x}\right) + I_R - I_S = 0 \tag{3.2}$$

with

q: Flow
h: Water depth v: Velocity of flow
A: Cross-sectional area I_R: Friction slope
x: Distance alongside the river axis I_S: Bed slope
t: Time g: Acceleration due to gravity.

Using the relations

$$v = \frac{q}{A}, \quad \mathrm{d}F = b \times \mathrm{d}h, \quad \bar{h} = \frac{A}{b} \tag{3.3}$$

with b = surface width of the conduit, the following equations will be obtained:

$$\frac{\partial q}{\partial x} + \frac{\partial h}{\partial t} = 0 \quad (3.4)$$

$$\frac{\partial h}{\partial x}\left(1 - \frac{v^2}{g \times \bar{h}}\right) + \frac{2v}{g \times \bar{h} \times b} \times \frac{\partial q}{\partial x} + \frac{1}{g \times \bar{h} \times b} \times \frac{\partial q}{\partial t} + I_R - I_S = 0 \quad (3.5)$$

The expansion of I_R into a Taylor series according to the Manning formula yields
with

$$I_R = a \times q^2 \times h^{10/3} \tag{3.6}$$

and

$$a = \frac{1}{(k_s \times b)^2} \tag{3.7}$$

the relation

$$I_R = a_1 + a_2 q' - a_3 h' + a_4 \left(q'\right)^2 - a_5 q' h' + a_6 \left(h'\right)^2$$
$$- a_7 \left(q'\right)^2 h' + a_8 q' \left(h'\right)^2 - a_9 \left(h'\right)^3 + \cdots \tag{3.8}$$

with k_s being the coefficient of roughness.

Here, $a_1 = I_{R0}$ represents the value of the function at the point (q_0, h_0), and the values a_i $(i \geq 2)$ are the partial derivatives for q and h at this point. The variables q'

and h' are operating point-related quantities, i.e., the relations $q' = q - q_0$ and $h' = h - h_0$ hold. For the partial derivatives of these quantities, the following relations hold true:

$$\frac{\partial q}{\partial x} = \frac{\partial q'}{\partial x}, \quad \frac{\partial q}{\partial t} = \frac{\partial q'}{\partial t} \tag{3.9}$$

$$\frac{\partial h}{\partial x} = \frac{\partial h_0}{\partial x} + \frac{\partial h'}{\partial x}, \quad \frac{\partial h}{\partial t} = \frac{\partial h'}{\partial t} \tag{3.10}$$

After substituting (3.8) and (3.10) into (3.4) and (3.5), the relations

$$\frac{\partial q'}{\partial x} + b \times \frac{\partial h'}{\partial t} = 0 \tag{3.11}$$

and

$$\frac{\partial h_0}{\partial x}\left(1 - \frac{v^2}{g \times \bar{h}}\right) + \frac{\partial h'}{\partial x}\left(1 - \frac{v^2}{g \times \bar{h}}\right) + \frac{2v}{g \times \bar{h} \times b} \times \frac{\partial q'}{\partial x} + \frac{1}{g \times \bar{h} \times b} \times \frac{\partial q'}{\partial t}$$
$$+ a_1 + a_2 q' - a_3 h' + a_4 \left(q'\right)^2 - a_5 q' h' + a_6 \left(h'\right)^2$$
$$- a_7 \left(q'\right)^2 h' + a_8 q' \left(h'\right)^2 - a_9 \left(h'\right)^3 + \cdots - I_S = 0 \tag{3.12}$$

will result. At the point (q_0, h_0), all terms with q' and h' vanish. Thus, the following relation holds:

$$\frac{\partial h_0}{\partial x}\left(1 - \frac{v^2}{g \times \bar{h}}\right) = I_S - a_1 \tag{3.13}$$

If the point (q_0, h_0) is fixed such that q_0 and h_0 nearly assume the value zero, then—from a physical point of view—v in (3.13) approaches zero, thus the water level slope approaches more and more the bed slope, and the friction slope I_{R0} approaches zero. Thus, the terms in (3.12)

$$\frac{\partial h_0}{\partial x}, \quad I_S, \quad a_1 \tag{3.14}$$

cancel each other out, and q' approaches q, h' approaches h. Then, (3.11) and (3.12) read:

$$\frac{\partial q}{\partial x} + b \times \frac{\partial h}{\partial t} = 0 \tag{3.15}$$

and

$$c_1 \frac{\partial h}{\partial x} + c_2 \frac{\partial q}{\partial x} + c_3 \frac{\partial q}{\partial t} = -a_2 q + a_3 h - a_4 q^2 + a_5 qh - a_6 h^2$$
$$+ a_7 q^2 h - a_8 qh^2 + a_9 h^3 + \cdots . \tag{3.16}$$

The systems of equations (3.15) and (3.16) represent the basis for all further steps made in the following.

In order to realize the setting up of the model by employing equations which are as simple as possible but also sufficiently exact, (3.15) and (3.16) are now discretized. For this, the continuous quantities $q(x, t)$ and $h(x, t)$ are transformed into discrete quantities in a mathematically exact way by applying the z-transformation for space and time twice [137, 211]. Here, a method shall be presented which is less complicated but equally efficient. The discretization for time, i.e. the transition of all variables from continuous to discrete quantities involves that changes of the variables within the sample time cannot be detected any more. As in the most cases of application, the sample time lies in the range of minutes, the loss of information is low in view of the slow speed of the processes.

The discretization for space, i.e. the transition from infinitely short path sections to finite path sections—in this case the distance between the existing gauges—implies that any differences in the coefficient of friction, in the profile can only be detected on average. However, it is not possible to make any general a-priori statements about whether this is admissible in and whether this effects accuracy too much or not. Later, admissibility has to be proved by means of simulation results [260].

For discretization, the following agreements are made: Let the argument for the loci x be $j \in (0, 1, 2, m - 1, m, m + 1)$. Let the argument for the time t be $i \in (0, 1, 2, k - 1, k, k + 1)$.

Thus, the following relations hold: $q(x, t) \Rightarrow q[j, i]$
$$h(x, t) \Rightarrow h[j, i].$$

For a well-defined locus j and a well-defined point in time i, it also holds:

$$
\begin{aligned}
& h(x, t) \Rightarrow h[m, k] \\
& q(x, t) \Rightarrow q[m, k] \\
& \frac{\partial h}{\partial t} \Rightarrow \frac{h[m, k] - h[m, k - 1]}{\Delta T} \\
& \frac{\partial q}{\partial t} \Rightarrow \frac{q[m, k] - q[m, k - 1]}{\Delta T} \\
& \frac{\partial h}{\partial x} \Rightarrow \frac{h[m, k] - h[m - 1, k]}{\Delta L} \\
& \frac{\partial q}{\partial x} \Rightarrow \frac{q[m, k] - q[m - 1, k]}{\Delta L}
\end{aligned}
\tag{3.17}
$$

Here, ΔT is the sample time and ΔL the length of the river between two gauges. On the basis of these agreements, (3.15) and (3.16) change to:

$$
\frac{q[m, k] - q[m - 1, k]}{\Delta L} + b \times \frac{h[m, k] - h[m, k - 1]}{\Delta T} = 0
\tag{3.18}
$$

and

$$c_1 \frac{h[m, k] - h[m-1, k]}{\Delta L} + c_2 \frac{q[m, k] - q[m-1, k]}{\Delta L} + c_3 \frac{h[m, k] - h[m, k-1]}{\Delta t}$$
$$= -a_2 q[m, k] + a_3 h[m, k] - a_4 q^2[m, k] + a_5 q[m, k] h[m, k]$$
$$- a_6 h^2[m, k] + \cdots. \tag{3.19}$$

These equations constitute a system of non-linear difference equations of the 1st order, which is solved by the transposition for the desired variables, with (3.18) always being substituted into (3.19). The parameters of the system are determined through the least squares method. The speed-dependent parameter c_1 is treated as a constant in the regression (least squares method). In how far this is admissible must be decided on the basis of the results obtained regarding the hydrographs. The parameters c_2 and c_3 do not have any influence on the results as the terms (forces of inertia) connected with them do not emerge as essential from the regression in several application cases. The criterion to be applied here is the standard deviation [260, 261].

3.1.3 Difference Equation for the Flow Rate

On the basis of Eqs. (3.18) and (3.19), which were derived from the Saint-Venant equations, a model is developed which permits the prediction of flow q at any point of the river. The basic idea of the model draft was adopted from Becker and Sonsnowski [24]. In this book, a linear parabolic differential equation is derived on the assumption that the flow loop referring to a certain level is the addition of a steady flow and an unsteady supplementary flow (cf. Fig. 3.3). In deriving this relation, Becker starts out from the assumption that the flow at a specific point is composed of:

$$q = q_{steady} + q_{unsteady} \tag{3.20}$$

Fig. 3.3 Flow rate—water level relation
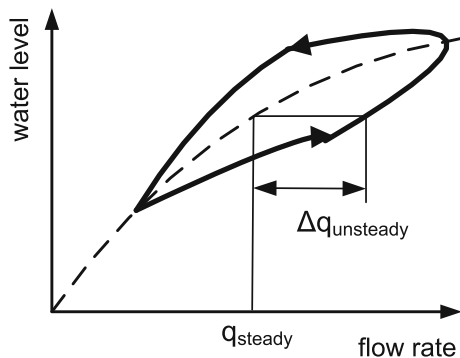
For the steady portion, the following relation holds true:

$$q_{steady} = k_1 h \tag{3.21}$$

with h being the water depth and B the water-table width as well as the parameters k_1 and k_2. The unsteady portion is described by the equation

$$q_{unsteady} = -k_2 B \frac{\partial h}{\partial x} \tag{3.22}$$

Thus, on the whole the following relations hold true:

$$q = k_1 h - k_2 B \frac{\partial h}{\partial x} \tag{3.23}$$

or also Thus, on the whole the following relations hold true:

$$q = a_1^* h - a_2 \frac{\partial h}{\partial x} \tag{3.24}$$

From (3.21), it can be seen that—for the steady case—the relation between the height h and the flow q is regarded as linear, which can be assumed for flow ranges around the working point.

The relation (3.24) can be directly derived from (3.15) and (3.16) and, thus, from the Saint-Venant equations. As in the case of large rivers c_2 and c_3 take on very small values ($=10^{-4}$), the forces of inertia can be neglected, with (3.16) assuming the following form:

$$c_1 \frac{\partial h}{\partial x} = -a_2 q + a_3 h - a_4 q^2 + a_5 qh - a_6 h^2$$
$$+ a_7 q^2 h - a_8 qh^2 + a_9 h^3 + \cdots . \tag{3.25}$$

By a selection of the essential terms of the right-hand member, the following relation is obtained:

$$c_1 \frac{\partial h}{\partial x} = -a_2 q + a_3 h. \tag{3.26}$$

After transposing, the relation

$$q = c_1^* h - c_2^* \frac{\partial h}{\partial x}. \tag{3.27}$$

results. Equation (3.27) has the same structure as Eq. (3.24). By a partial differentiation of (3.27) for t, the following form is obtained:

$$\frac{\partial q}{\partial t} = c_1^* \frac{\partial h}{\partial t} - c_2^* \frac{\partial^2 h}{\partial x \partial t}. \tag{3.28}$$

By using the known continuity relation (3.15),

$$\frac{\partial h}{\partial t} = -\frac{1}{B}\frac{\partial q}{\partial x} \tag{3.29}$$

can be set in (3.28). Assuming that the water-table width B is constant, one gets the following relation:

$$\frac{\partial q}{\partial t} = -\frac{c_1^*}{B}\frac{\partial q}{\partial x} - c_2^* \frac{\partial^2 h}{\partial x \partial t}. \tag{3.30}$$

If the discretized terms, which were determined before, are substituted into (3.30), the following expression results:

$$\begin{aligned} q(m_{out}, k) - q(m_{out}, k-1) = c_1' &[q(m_{out}, k-1) - q(m_{in}, k-1)] \\ &+ c_2'[h(m_{out}, k) - h(m_{in}, k) - h(m_{out}, k-1) + h(m_{in}, k-1)] \end{aligned} \tag{3.31}$$

with

k: point in time
m_{in}:   locus of inflow in river section
m_{out}:   locus of outflow from river section.

As $q(m_{in}, k)$ can be composed of several tributaries which flow into at different points along the river section and which present different travel times, the following relation can be admitted, too:

$$q(m_{in}, k) = q(m_{in1}, k - k_1) + q(m_{in2}, k - k_2) + \cdots. \tag{3.32}$$

If (3.32) is substituted into (3.31) and transposed for $q(m_{out}, k)$, the following difference equation is obtained:

$$\begin{aligned} q(m_{out}, k) = aq(m_{out}, k-1) &+ b_1 q(m_{in1}, k - k_1) + b_2 q(m_{in2}, k - k_2) \\ &+ \cdots + c[h(m_{out}, k-1) - h(m_{in}, k-1) - h(m_{out}, k-2) + h(m_{in}, k-2)]. \end{aligned} \tag{3.33}$$

Here, the h-values have been shifted by one time unit length. The term $c \times [\,]$ represents the unsteady flow portion. Further studies have shown that the other terms contained in the equation of motion can be neglected [263]. The parameters a, b_i and c are estimated by means of the least squares method on the basis of original flow data.

3.1.4 Difference Equation for the Water Level

This model is based on the equation of motion by Saint-Venant

$$\frac{\partial h}{\partial x} + \frac{1}{g}\left(\frac{\partial v}{\partial t} + v\frac{\partial v}{\partial x}\right) + I_R - I_S = 0. \tag{3.34}$$

After transforming this basic equation, the following relation holds true:

$$\partial h = I_S \partial x - I_R \partial x - \frac{v}{g}\partial v - \frac{1}{g}\frac{\partial v}{\partial t}\partial x. \tag{3.35}$$

The discretization of time and place results in:

$$\Delta h = I_S \Delta x - \frac{v_{mean}^2(k)}{k_{st}^2 r_{hy,mean}^{4/3}}\Delta x$$
$$- \frac{v_{mean}(k)}{g}[v_2(k) - v_1(k)]$$
$$- \frac{1}{2Tg}[v_2(k) - v_2(k-1) + v_1(k) - v_1(k-1)]\Delta x. \tag{3.36}$$

Here, the index 1 is always assigned to the higher profile (upstream), whereas the index 2 is assigned to the lower profile. When calculating the speed v, the continuity equation is taken into consideration via $q = v \times A$. In this case, q is calculated on the basis of models which have been derived from the continuity equation. As a substitute for I_R, the Manning-Strickler formula is used in (3.36) [20, 35]. Equation (3.36) can be simplified by using the piezometer level difference Δhp instead of the water depth difference Δh (cf. Fig. 3.4):
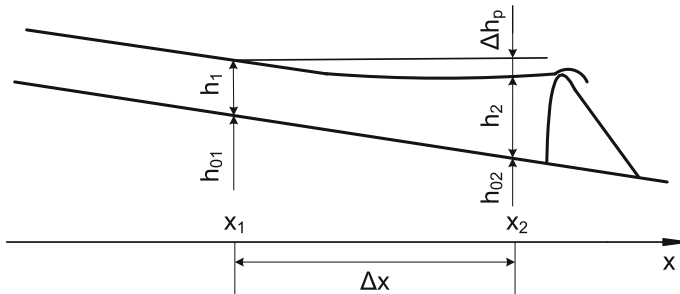
Fig. 3.4 Parameters for applying the equation according to Bresse [35]

$$\Delta h_p(k) = -\frac{v_{mean}^2(k)}{k_{st}^2 r_{hy,mean}^{4/3}} \Delta x - \frac{v_{mean}(k)}{g} [v_2(k) - v_1(k)]$$

$$- \frac{1}{2Tg} [v_1(k) - v_1(k-1) + v_2(k) - v_2(k-1)] \Delta x. \qquad (3.37)$$

In [35], the formula for calculating the water level hydrographs according to Bresse is given as follows:

$$\Delta h_p(k) = -\frac{v_{mean}^2(k)}{k_{st}^2 r_{hy,mean}^{4/3}} \Delta x - \frac{v_{mean}(k)}{g} [v_2(k) - v_1(k)]. \qquad (3.38)$$

Here, the term from the mass inertia, which is contained in the equation of motion, is neglected towards (3.37). This simplification, however, is not adopted. Thus, the following conditional equation for the level h_1 of the river section results:

$$h_1(k) = h_2(k) + h_{02} - h_{01} - \Delta h_p. \qquad (3.39)$$

The implicit form of this equation requires the application of iterative procedures for determining the level. For this, the square difference of the level h_1 is minimized in two consecutive iteration steps:

$$h_1(k) = argmin \left\{ \left[h_1^i - h_1^{i-1} \right]^2 \right\}. \qquad (3.40)$$

3.1.5 Description of the Flow in the Case of Spills

Already existing retention areas on rivers represent an effective, sustainable means of flood protection. Depending on the profile of the river bank, the river spills into those areas when the water reaches a defined level. This effect must always be taken into account when modeling the time series of the flow rate. In the retention areas, the flow behavior differs greatly from that in the profile of the conduit as the flow and delay times are considerably longer due to the surface structure. For the splitting of the flow in the spill areas, a number of characteristic lines are known from model tests. These characteristic lines are approximated as polynomial function and filed in the simulation model. They model the flow portion in the river after the spill sections and the inflow into the retention areas. By means of the individual flow models for these two regions, the corresponding hydrographs are simulated (cf. Fig. 3.5).

Fig. 3.5 Splitting of the
flow in the case of spills
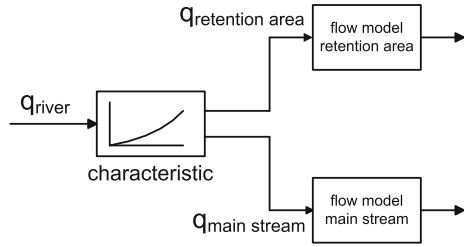
3.1.6 The Polder Model

Along the courses of rivers, polders can often be found which are activated in the
case of a flood. Their function is to lower the vertex flow of the flood wave and,
thus, the maximum water levels, which would minimize the damages due to flood in
this way [19]. Figure 3.6 shows the structure of the general polder model used. The
polder model has two inputs. On the one hand, it is the inflow q_{river} coming from the
river itself, and on the other hand, the inflow coming from the space areas $q_{space\ area}$.
The inflow from the space areas originates mainly from streams in the surroundings
of the polder (cf. Fig. 3.1). With the amounts of water they carry, they contribute to
the filling of the retention area and cannot be neglected in many cases.

In essence, the polder model consists of an integrator by means of which the
water volume in the polder is determined on the basis of the inflows. Thus, the water
level h_{polder} can be determined via the V-h characteristic. This characteristic is often
available in tabular form. For the integrator, three inflows act as entry (this, however,
is not the case for parallel flows, which will be explained afterwards). The first inflow
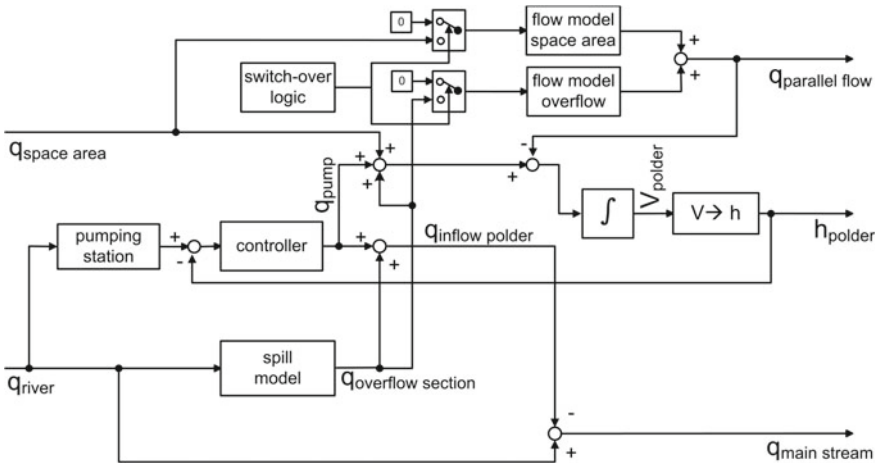
Fig. 3.6 General polder model

is $q_{overflow\ section}$, which corresponds to that portion which flows from the river into the polder through the overflow sections. It is determined by means of the above-described spill model. The second inflow which influences the water level in the polder is brought about directly by the water coming from the space areas, $q_{space\ area}$. The third inflow originates from the amount of water transported by the pump station (including also the sluices) into or also out of the polder. The function of the pump stations is to maintain a well-defined water level in the polder, depending on the flow rate prevailing in the main stream. In the case of a flood, however, the pump stations are not effective. They are of special importance for the pre-flooding of the polders when the water levels are rising. This is necessary in order to prevent the breaking of the dam. The model includes the water levels to be maintained as a function of the flow in the form of a characteristic. This characteristic fixes the reference input for a controller which sets the water level in the polder to the required values. Here, the pump flow q_{pump} serves as control variable, which can take both positive and negative values. The three mentioned flows are decisive for the water level in the polder. The sum of $q_{overflow\ section}$ and q_{pump} makes up the inflow $q_{inflow\ polder}$ which originates from the river and, therefore, must be deducted from its flow. In this way, the output of the polder model, $q_{main\ stream}$, is obtained which corresponds to the flow remaining in the river bed. When modeling the polder, attention has to be attached to a special effect: parallel flowing occurring after evening out the water levels between the polder and the river. By means of a switch-over logic, the inputs of the flow models "Space area" and "Overflow" are switched from zero to $q_{space\ area}$ and $q_{overflow\ section}$, respectively, when parallel flowing is achieved. By applying these two flow models, the run time and delay behavior in the case of parallel flowing is taken into account. The parameters are determined on the basis of flood events where parallel flowing occurs. Adding up the two model outputs yields $q_{parallel\ flow}$. This flow is available as output of the polder model and must be fed again into the river in accordance with the local conditions. Furthermore, $q_{parallel\ flow}$ is deducted from the input of the integrator as it equals a run-off out of the polder.

The switch-over logic evaluates the water levels in the polder and of the river, and switches over to parallel flowing when the two levels have reached the same height.

3.1.7   The Headwater Level Model

The impounding head (height measured at the headwater level) as well as the stored water volume as a measure for the storage effect are essential state quantities for a reservoir. There is a non-linear relation between these two quantities, which is available as volume characteristic for each storage region. The following relation holds true:

$$V = f(h_{headwater},\ q_{dam}) \tag{3.41}$$

The considerations regarding the setting up of a model shall be based on the behavior of a storage reservoir in the case of an inflow $q_{in,\ dam}$. Starting from an initial volume,

an inflow into the reservoir brings about an increase in its volume. Then, the system constitutes an integrator whose behavior can be characterized as follows:

$$\Delta V(t) = \int_0^t q_{in,\,dam}(\tau)\mathrm{d}\tau \qquad (3.42)$$

If a run-off occurs at the same time, only the difference between inflow $q_{in,\,dam}$ and outflow $q_{out,\,dam}$ will entail a change in the water volume:

$$\Delta V(t) = \int_0^t \big[q_{in,\,dam}(\tau) - q_{out,\,dam}(\tau)\big]\mathrm{d}\tau \qquad (3.43)$$

A resulting change in the impounding head can be determined via the volume characteristic, which can be found as a characteristic. For further considerations, however, it is necessary to derive an analytical description. Therefore, the characteristic is approximated in the form of a polynomial set-up. The following expression results:

$$V(h, q) = a_0 + a_1 q + a_2(h - h_0) + a_3 q^3 + a_4 q(h - h_0) + a_5(h - h_0)^2 \qquad (3.44)$$

with

q: being the flow at the dam,
h: being the headwater level above reference point
h_0: being the level of the conduit ground at the headwater level above reference point.

The coefficients a_i can be determined via direct regression from the interpolation nodes of the characteristic of the barrage to be examined. In order to determine the connection between the change of volume and the change of level, a Taylor series of (3.44) in the working point (h_{WP}, q_{WP}) is carried out. As only the dependence of the volume on the level shall be examined here, the run-off at the power station is regarded as being constant:

$$V(h, q_{WP}) = V(h_{WP}, q_{WP}) + \frac{\partial V(h_{WP}, q_{WP})}{\partial h}(h - h_{WP})$$
$$+ \frac{1}{2}\frac{\partial^2 V(h_{WP}, q_{WP})}{\partial h^2}(h - h_{WP})^2 + \cdots . \qquad (3.45)$$

A truncation after the linear portion and the use of the following relations

$$\Delta V = V(h, q_{WP}) - V(h_{WP}, q_{WP})$$
$$\Delta h = h - h_{WP} \qquad (3.46)$$

yields the following relation between ΔV and Δh:

$$\Delta V = \frac{\partial V(h_{WP}, q_{WP})}{\partial h} \Delta h \qquad (3.47)$$

Attention has to be paid to the fact that this relation is only valid for small changes towards the working point. Using the polynomial from (3.45) for the derivative in (3.47) results in (3.48):

$$V_h(h_{WP}, q_{WP}) = \frac{\partial V(h_{WP}, q_{WP})}{\partial h} = a_2 + a_4 q_{WP} + 2a_5(h_{WP} - h_0). \qquad (3.48)$$

This term constitutes a measure for the change of volume in the case of an occurring change of the headwater level. By applying the reciprocal of this relation, the following correction term for the level results:

$$\Delta h_{headwater} = \frac{1}{V_h(h_{WP}, q_{WP})} \Delta V \qquad (3.49)$$

By adding this change of level to h_{WP}, the impounding head is obtained as an essential state quantity of the barrage. In this way, the model for calculating the impounding head at the power station can be set up (cf. Fig. 3.7).

3.1.8 The Backwater Model

Backwater effects can occur on the mouths of rivers. These effects must be taken into consideration when setting up a model as they bring about a significant change in the time series of the flow rate. With increasing water level, an ever greater flow portion is removed from the river. This portion flows into the backwater regions where it is
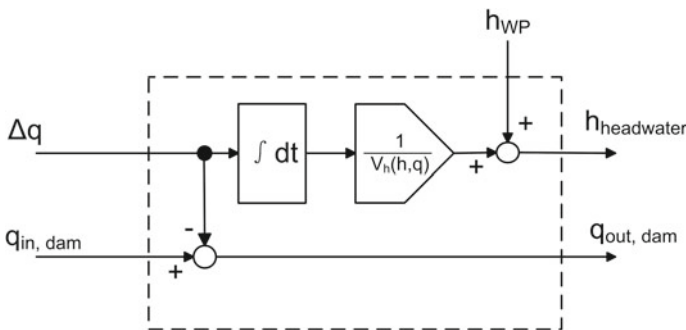
Fig. 3.7 General model for calculating the headwater level at a dam
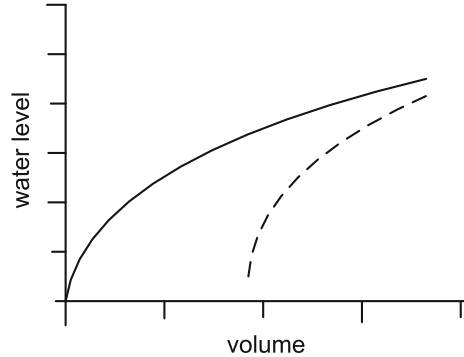
stored before it later returns to the river. The analysis of the volume balance between
the inflow into the backwater regions and the run-off out of them yields a difference.
This deficit is due to the absorbability of the soil and also due to the fact that a certain
amount of water remains in natural retention areas such as ponds (cf. Fig. 3.8).

For describing the h-V-characteristic branch during the filling of the retention
areas, the following relation is used:

$$h = a\sqrt{V} + h_0 \qquad (3.50)$$

with

h: being the water level (course of river) in the retention area,
V: being the volume flowing into the retention areas,
a: being the parameter (determined by means of the least squares method),
h_0: water level at which the filling of the retention areas sets in.

From (3.50), the relation for the calculation of the volume is obtained as a function
of the water level of the river. It holds:

$$V = \left(\frac{1}{a}(h - h_0)\right)^2 . \qquad (3.51)$$

Furthermore, when a linear storage with time constant T is assumed, a change of
flow Δq can be determined from a change of volume ΔV as follows:

$$\Delta q = \frac{1}{T}\Delta V. \qquad (3.52)$$

Using (3.51) and (3.52), the flow q into the backwater area or also out of it is calculated
at the time $(k + 1)$, starting from time k. The following relation holds true:

$$q(k + 1) = q(k) + \frac{1}{T}\left(V(k + 1) - V(k)\right). \qquad (3.53)$$

Furthermore, the gradient of the flow is used as input quantity for the backwater model. Thus, it is possible to simulate the hysteresis by switching from the filling characteristic over to the run-off characteristic at the time of the gradient change. For the run-off characteristic, the following description can be used:

$$h = a\,(V - \Delta V)^{\frac{1}{n}} + h_0. \tag{3.54}$$

Here, ΔV represents the volume remaining in the backwater area and n is a parameter determined by measured data. The term ΔV is situation-dependent and is calculated at the time of the switch-over (change of gradient) during simulation. The calculation starts out from the condition that the calculated levels of the filling characteristic and of the run-off characteristic are equal at the time of the switch-over. Thus, (3.50) and (3.54) can be equated. The following relation holds true:

$$a\sqrt{V} + h_0 = a\,(V - \Delta V)^{\frac{1}{n}} + h_0. \tag{3.55}$$

From this, ΔV results as follows:

$$\Delta V = V - V^{\frac{n}{2}}. \tag{3.56}$$

Thus, for the calculation of the volume in the case of the run-off characteristic, the following relation is obtained:

$$V = \left(\frac{1}{a}(h - h_0)\right)^n + \Delta V. \tag{3.57}$$

Thus, the flow can be calculated—by employing the volumes according to (3.51) and (3.57)—for the backwater behavior according to (3.53) both during the filling and the run-off phase.

3.2   Water Supply Systems

Thomas Westerhoff and Buren Scharaw

3.2.1   Introduction

Drinking water is the most important aliment for human being. The save supply of millions of people with drinking water is a great challenge for engineers in water supply. It needs to be 24 h a day and 365 days a year stable an with good quality. Water distribution systems are key elements of urban infrastructure and require a significant investment. As water demand grows, these systems become larger and more complex. Therefore, in order to optimize their operation costs it is appropriate to analyze them on a component basis. So the optimal control, the safe operating and the precise

planning of such systems is very important to guarantee low operational costs, system stability and good water quality and quantity. To achieve that goal without interruption of the running processes, engineers needs tools to model and simulate such complex distribution networks with all their hydraulic components like pipes, pumps, valves, tanks and others. With such hydraulic models predicted water demands engineers are able to design new supply areas, calculate the dimensions of pipes and pumps that are necessary to achieve the needed hydraulic grade. Also the handling of special situations like fire flow and leak location can be done with hydraulic models an special computational programs. In many countries water is a very valuable good because it is very rare. minimizing the water losses through leakages and evaporation is very important in such countries. Pumps need electric energy for operation that commonly is produced by fossil fuels yet. So the minimization of pumping energy by optimal pump scheduling can make a contribution to reduce the CO_2 emission to the atmosphere. Using different energy tariffs in pump schedule optimization can also reduce the costs for pumping and increase the profit of the water supplier. This additional profit can be used to reconstruct the network with new modern pipes or to decrease the water fee for customers.

3.2.2 Hydraulics of Pressurizes Networks

The flow in closed pressurized water distribution networks (WDS) in principle can also be simulated with the Saint-Venant-Equations. Since water supply networks nearly unexceptional are build with circular cross-section pipes there are a lot of simplifications possible that makes the simulation much faster and simpler. In the past a lot of different methods to do this where developed. The most common methods will be described in the following chapters.

3.2.2.1 The Reynolds Number

The flow of liquid through a pipe is resisted by viscous shear stresses within the liquid and the turbulence that occurs along the internal walls of the pipe, created by the roughness of the pipe material. This resistance is usually known as pipe friction factor f and is measured is feet or meters head of the fluid, thus the term head loss is also used to express the resistance to flow. The pipe friction factor depends on the so called Reynolds number. Reynolds number Re can be defined for a number of different situations where a fluid is in relative motion to a surface. These definitions generally include the fluid properties of density and viscosity, plus a velocity and a characteristic length or characteristic dimension. This dimension is a matter of convention—for example a radius or diameter are equally valid for spheres or circles, but one is chosen by convention. For flow in a pipe the internal diameter is generally used today.

$$Re = \frac{\rho v d}{\mu} = \frac{v d}{\nu} = \frac{Q d}{\nu A} \qquad (3.58)$$

with

v: mean fluid velocity [m/s]
d: hydraulic diameter of the pipe [m]
μ: dynamic viscosity of the fluid [Pa · s or N · s/m^2 or kg/m · s]
ν: kinematic viscosity [$\nu = \mu / \rho$) [m^2/s]
ρ: density of the fluid [kg/m]
Q: volumetric flow rate [m^3/s]
A: pipe cross-sectional area [m^2].

3.2.2.2 The Moody Diagram

The Moody chart is a graph in non-dimensional form that relates the pipe friction factor f, Reynolds number Re and relative roughness ε for fully developed flow in a circular pipe. It can be used for working out pressure drop or flow rate down in such a pipe. The basic chart plots Darcy-Weisbach friction factor against Reynolds number for a variety of relative roughnesses and flow regimes. The relative roughness being the ratio of the mean height of roughness of the pipe to the pipe diameter. The Moody chart can be divided into three regimes of flow: laminar and turbulent and a transient region.

For the laminar flow regime (Re < 2000), the Darcy-Weisbach friction factor was determined as a consequence of Poiseuilles Law simply as $\frac{64}{Re}$. In this regime roughness has no discernible effect (Figs. 3.9, 3.10, 3.11, 3.12).
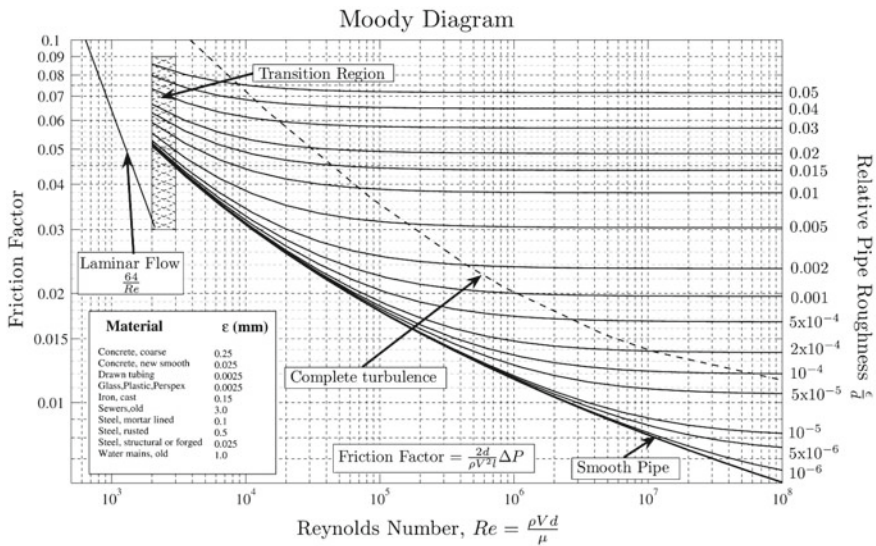
Fig. 3.9 Moody diagram
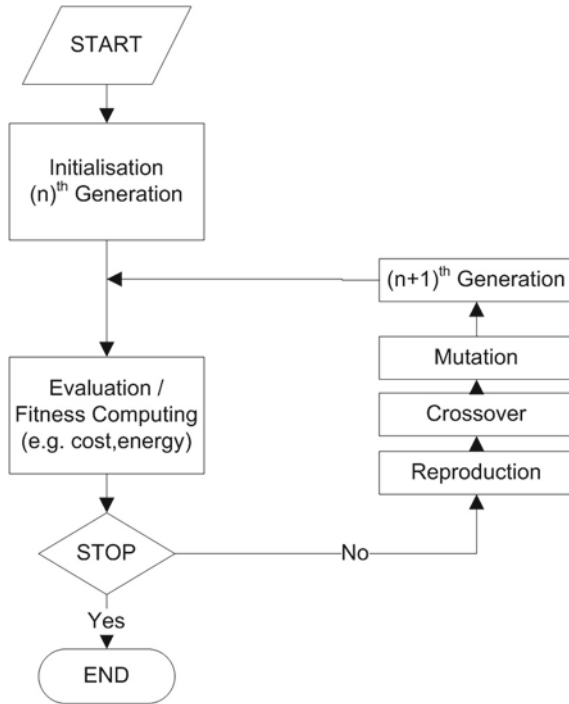
Fig. 3.10 Outline of the basic genetic algorithm
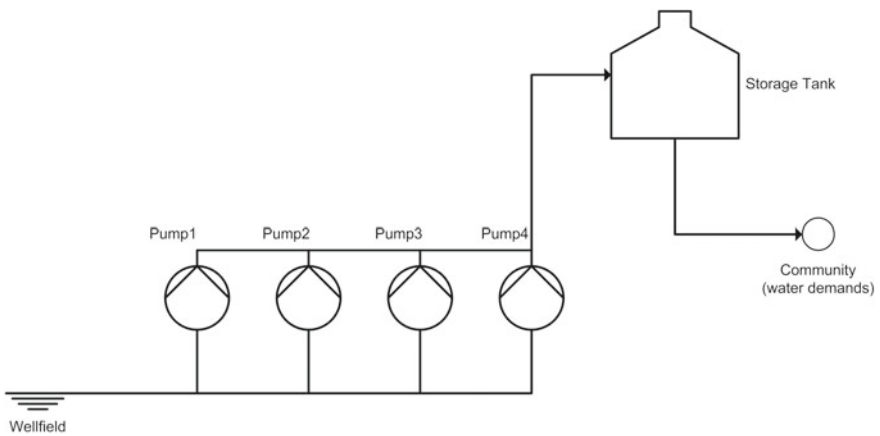
Fig. 3.11 Sample network for optimal pump scheduling

For the turbulent flow regime (Re > 4000), the relationship between the friction factor and the Reynolds number is more complex and is governed by the Colebrook-White equation which is implicit in f [88]:
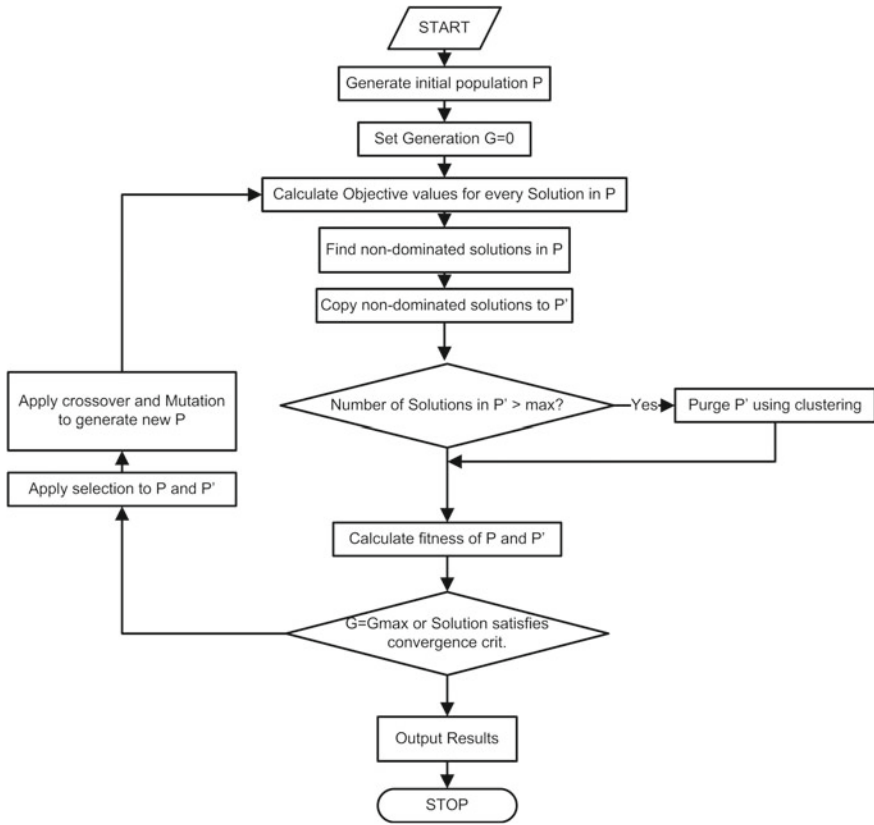
Fig. 3.12 Flowchart of SPEA

$$\frac{1}{\sqrt{2}} = -2.0 \log_{10}\left(\frac{\frac{\varepsilon}{d}}{3.7} + \frac{2.51}{Re\sqrt{f}}\right) \tag{3.59}$$

with

ε: pipe roughness factor [m]
d: pipe inner diameter [m].

Alternatively the Swamee-Jain equation can be used to calculate the Darcy-Weisbach friction factor directly for a full-flowing circular pipe. It is an approximation of the implicit Colebrook-White equation.

$$f = \frac{0.25}{\log_{10}\frac{\varepsilon}{3.7d} + \frac{5.74}{Re^{0.9}}} \tag{3.60}$$

with

ε: pipe roughness factor [m]
d: pipe inner diameter [m].

In the transition region (2000 < Re < 4000) the calculation of the friction factor can be done by a polynomial interpolation described by Dunlop [88].

$$f = (X_1 + R(X_2 + R(X_3 + X_4)))$$ (3.61)

where

$$R = \frac{Re}{2} 000$$
$$X_1 = 7F_a - F_b$$
$$X_2 = 0.128 - 17F_a + 2.5F_b$$
$$X_3 = -0.128 + 13F_a - 2F_b$$
$$X_4 = R(0.032 - 3F_a + 0.5F_b$$
$$F_a = (Y_3)^{-2}$$
$$F_b = F_a \left(2 - \frac{0.00514215}{Y_2 \cdot Y_3} \right)$$
$$Y_2 = \frac{\varepsilon}{3.7d} + \frac{2.51}{Re^{0.9}}$$
$$Y_3 = -0.86859 \ln \left(\frac{\varepsilon}{3.7d} + \frac{2.51}{1745.235} \right)$$

with

ε: pipe roughness factor [m]
d: pipe diameter [m].

3.2.2.3 The Darcy-Weisbach Equation

Many factors affect the head loss in pipes, the viscosity of the fluid being handled, the size of the pipes, the roughness of the internal surface of the pipes, the changes in elevations within the system and the length of travel of the fluid.

The resistance through various valves and fittings will also contribute to the overall head loss. A method to model the resistances for valves and fittings is described in Sect. 3.2.3.1.

In a well designed system the resistance through valves and fittings will be of minor significance to the overall head loss. Much research has been carried out over many years and various equations to calculate head loss have been developed based on experimental data.

In fluid dynamics, the Darcy-Weisbach equation is a basic equation, which relates the head loss due to friction along a given length of pipe to the average velocity of the fluid flow. Weisbach first proposed this equation we now know as the Darcy-Weisbach formula or Darcy-Weisbach equation. Head loss can be calculated with

$$h_f = f\frac{L}{d} \cdot \left(\frac{v^2}{2g}\right) \tag{3.62}$$

with

h_f: head loss [m]
f: friction factor
L: length of pipe work [m]
d: hydraulic diameter of the pipe (for a pipe of circular section, this equals the internal diameter of the pipe) [m]
v: velocity of fluid [m/s]
g: acceleration due to gravity [m/s^2].

Given that the head loss h_f expresses the pressure loss Δp as the height of a column of fluid,

$$\Delta p = f\frac{L}{d} \cdot \left(\frac{\rho v^2}{2}\right) \tag{3.63}$$

with

Δp: pressure loss [m]
ρ: density of the fluid.

The friction factor f or flow coefficient λ is not a constant and depends on the parameters of the pipe and the velocity of the fluid flow, but it is known to high accuracy within certain flow regimes. It needs to be evaluated for given conditions by the use of Moody chart describes in the previous section.

The Darcy-Weisbach equation is very often used in hydraulics simulation because it works well for all the possible flow regimes laminar and turbulent.

3.2.3   Simulation of Meshed Drinking Water Networks

With the formulas in the previous section it is possible to calculate the headloss in one single pipe, but in a real water supply network there are sometimes thousands of pipes connected to each other. To solve the hydraulic formulas for such a system the use of computers is essential because we have not a single equation but an equation system. In a network with N pipes one have N equations with $2N$ unknown variables (head at upstream and downstream node).

In the past a lot of methods where developed to solve such equation systems. One method to solve the flow continuity and headloss equations that characterize the hydraulic state of the pipe network at a given point in time is called the hybrid node-loop approach. Hamam and Brameller [142] call it the *Hybrid Method*. Other, similar approaches have been described by Todini and Pilati [323] as the *Gradient Method* and by Osiadacz [239] the *Newton Loop-Node Method*. All these approaches are in common the same. The only difference between them is the way in which link flows are updated after a new trial solution for nodal heads has been found. Because Todinis approach is the simplest, it often is used in most of the hydraulic computational programs today.

3.2.3.1 The Todini Pilati Method

The Todini Pilati method starts at nodes with fixed hydraulic grade like tanks, wells or reservoirs. Assume we have a pipe network with N junction nodes and N_F fixed grade nodes like tanks or reservoirs. The flow-headloss relation in a pipe between nodes i and j be given as:

$$H_i - H_j = h_{ij} = rQ_{ij}^n + mQ_{ij}^2 \tag{3.64}$$

with

H: nodal head [m]
h: headloss [m]
r: resistance coefficient
Q: flow rate [m/s]
n: flow exponent
m: minor loss coefficient.

The value of the resistance coefficient will depend on which friction headloss formula is being used (e.g. Darcy-Weisbach). For pumps, the headloss (negative of the head gain) can be described by a power law of the form

$$h_{ij} = -\omega^2 \left(h_0 - r \left(\frac{Q_{ij}}{\omega} \right)^n \right) \tag{3.65}$$

with

H_0:   shutoff head for the pump [m]
ω: relative speed setting
r, n: the pump curve coefficients.

The second set of equations that must be satisfied is flow continuity around all the nodes:

$$\sum_i Q_{ij} - D_i = 0 \quad \text{for} \quad i = 1, \dots, N. \tag{3.66}$$

with

$D_i p$:   flow demand at node i [m^3/s].

Now we introduce the convention, that flow into a node is positive. At all the fixed grade nodes the head is known and we seek a solution for all these heads H_i and flows Q_{ij} that satisfy Eqs. (3.64) and (3.66). The Gradient solution method begins with the initial estimation of flows in each pipe. This may not satisfy flow continuity. At each iteration of the method, new nodal heads are found by solving the matrix equation:

$$AH = F \qquad (3.67)$$

with

A: an (N $\times$ N) Jacobian matrix
H: an (N $\times$ 1) vector of unknown nodal heads
F: an (N $\times$ 1) vector of right hand side terms.

The diagonal elements of the Jacobian matrix are:

$$A_{ij} = \sum_j p_{ij} \qquad (3.68)$$

while the non-zero, off-diagonal terms are:

$$A_{ij} = -p_{ij} \qquad (3.69)$$

with

p_{ij}:   inverse derivate of Headloss in link between i and j.

For pipes we can calculate,

$$p_{ij} = \frac{1}{nr|Q_{ij}|^{n-1} + 2m|Q_{ij}|} \qquad (3.70)$$

while for pumps:

$$p_{ij} = \frac{1}{n\omega^2 r\left(\frac{Q_{ij}}{\omega}\right)^{n-1}} \qquad (3.71)$$

Each right hand side term consists of the net flow imbalance at a node plus a flow correction factor:

$$F_i = \left(\sum_j Q_{ij} - D_i\right) + \sum_j y_{ij} + \sum_f p_{if} H_f \qquad (3.72)$$

where the last term applies to any links connecting node i to a fixed grade node f and the flow correction factor y_{ij} is:

$$y_{ij} = p_{ij}\left(r|Q_{ij}|^n + m|Q_{ij}|^2\right)sgn(Q_{ij}) \qquad (3.73)$$

for pipes and

$$y_{ij} = p_{ij}\omega^2\left(h_0 - r\left(\frac{Q_{ij}}{\omega}\right)^n\right) \qquad (3.74)$$

for pumps, with $sgn(x)$ is 1 if $x > 0$ and -1 otherwise. Q_{ij} is always positive for pumps. After new heads are computed by solving Eq. (3.67), new flows are found from:

$$Q_{ij} = Q_{ij} - (y_{ij} - p_{ij}(H_i - H_j)) \qquad (3.75)$$

If the sum of absolute flow changes relative to the total flow in all links is larger than some tolerance (e.g. 0.001), then Eqs. (3.67) and (3.75) are solved once again. The flow update Eq. (3.75) always results in flow continuity around each node after the first iteration.

The Todini-Pilati approach is robust but also has disadvantages. The time to solve the whole equation system is rising exponentially with the number of the network elements. So this could be a problem when using it in an Genetic Algorithm for optimization purposes.

But there are also newer methods available where the calculation time not rises exponential but linear with the number of network elements like the SAMG (Algebraic Multigrid Methods for Systems) developed at Fraunhofer SCAI [307].

3.2.4 Optimization Methods for Water Distribution Systems

3.2.4.1 Genetic Algorithms

Genetic Algorithms (GA) are a part of evolutionary computing, which is a rapidly growing area of artificial intelligence. Genetic algorithms are inspired by Darwin evolution theory. Simply, solution to a problem solved by Genetic Algorithms is evolved. As described earlier, Genetic Algorithms can be used to solve problems that are non-continuously. So they are ideal for the solution of hydraulic problems because there is a non-continuity between laminar an turbulent flow regime. Also the model is non-linear in the turbulent flow regime. Another advantage of Genetic Algorithms is parallelism because each individuum can be solved in one separate thread of a simulation program or in one of the processor cores or in a multi processor environment. In the following chapter the basics of Genetic Algorithms and there usage for optimization problems will be explained.

Chromosome

All organisms consist of cells. In each cell there is the same set of chromosomes. Chromosomes are strings of DNA and serves as a model for the organism. A chromosome consist of genes, that are blocks of DNA. Each gene encodes a particular protein. One can say, that each gene encodes a trait, for example color of eyes. Possible settings for a trait (e.g. blue, brown) are called alleles. Each gene has its own position in the chromosome. This position is called locus. The complete set of genetic material (all chromosomes) is called genome. Particular set of genes in genome is called genotype. The genotype is with later development after birth base for the organism phenotype, its physical and mental characteristics, such as eye color, intelligence etc.

Encoding of a Chromosome

The chromosome should in some way contain information about the solution which it represents. The most used way of encoding is a binary string. This is for instance convenient if one want to find an optimal solution for pump scheduling where each pump can be switched on {1} and off {0}. The chromosome then could look like this:

Chromosome 1:	1101100100110110
Chromosome 2:	1101111000011110

Each chromosome has one binary string. Each bit in this string can represent some binary characteristic of the solution. Or the whole string can represent a number.

Of course, there are many other ways of encoding. This depends mainly on the solved problem. For example, one can encode directly integer or real numbers (see network calibration), sometimes it is useful to encode some permutations and so on.

Reproduction

During the reproduction, first occurs recombination (or crossover). Genes from parents form in some way the whole new chromosome. The new created offspring can then be mutated. Mutation means, that the elements of DNA are a little bit changed. This changes are mainly caused by errors in copying genes from parents. The fitness of an organism is measured by success of the organism in its life.

Crossover

After one have decided what encoding will be used, one can make a step to crossover. The crossover selects genes from parent chromosomes and creates a new offspring. The simplest way how to do this is to choose randomly some crossover point and everything before this point copy from a first parent and then everything after a crossover point copy from the second parent.

Crossover can then look like this (—is the crossover point):

Chromosome 1	11011—00100110110
Chromosome 2	11011—11000011110
Offspring 1	11011—11000011110
Offspring 2	11011—00100110110

There are some other ways how to make crossover, for example one can choose more crossover points. The crossover can be rather complicated and very depends on the encoding of chromosome. A specific crossover made for a specific problem can improve performance of the Genetic Algorithm.

Mutation

After a crossover is performed, mutation take place. This is to prevent falling all solutions in population into a local optimum of solved problem. Mutation changes randomly the new offspring. For binary encoding one can switch a few randomly chosen bits from 1 to 0 or from 0 to 1. Mutation can then be following:

Original offspring 1:	1101111000011110
Original offspring 2:	1101100100110110
Mutated offspring 1:	1100111000011110
Mutated offspring 2:	1101101100110110

The mutation depends on the encoding as well as the crossover. For example when one is encoding permutations, mutation could be exchanging two genes.

Crossover and Mutation Probability

There are two basic parameters of Genetic Algorithms—*crossover probability* and *mutation probability*.

Crossover probability says how often will be crossover performed. If there is no crossover, offspring is exact copy of parents. If there is a crossover, offspring is made from parts of parents' chromosome. If crossover probability is 100 %, then all offspring is made by crossover. If it is 0 %, whole new generation will be made from exact copies of chromosomes from the old population. The crossover is made in hope that new chromosomes will have good parts of old chromosomes and it may be that the new chromosomes will be better. However it is good to leave some part of population survive to next generation.

Mutation probability says how often parts of chromosome will be mutated. If there is no mutation, offspring is taken after crossover (or copy) without any change in the chromosome. If mutation is performed, a part of the chromosome is changed. If mutation probability is 100 %, whole chromosome is changed, if it is 0 %, nothing in the chromosome is changed. Mutation is made to prevent falling Genetic Algorithm into local extreme, but it should not occur very often, because then the Genetic Algorithms will in fact change to random search.

Basic Flow of Genetic Algorithms

Algorithm is started with a set of solutions (represented by a set of chromosomes) called population. Solutions from one population are taken and used to form a new population. This is motivated by the hope, that the new population will be better than the old one. Solutions which are selected to form new solutions (offspring) are selected according to their fitness—the more suitable they are the more chances they have to reproduce.

1. **Start**—Generate random population of n chromosomes (suitable solutions for the problem)
2. **Fitness**—Evaluate the fitness $f(x)$ of each chromosome x in the population
3. **New population** Create a new population by repeating following steps until the new population is complete

    3.1. **Selection** Select two parent chromosomes from a population according to their fitness (the better fitness, the bigger chance to be selected)
    3.2. **Crossover** With a crossover probability cross over the parents to form a new offspring (children). If no crossover was performed, offspring is an exact copy of parents.
    3.3. **Mutation** With a mutation probability mutate new offspring at each locus (position in chromosome).
    3.4. **Accepting** Place new offspring in a new population

4. **Replace** Use new generated population for a further run of algorithm
5. **Test** If the end condition is satisfied, stop and return the best solution in current population
6. **Loop** Go to step 2.

Other Parameters

There are also some other parameters of Genetic Algorithms. One also important parameter is the size of the population.

Population size says how many chromosomes are in population (in one generation). If there are too few chromosomes, the Genetic Algorithm have only a few possibilities to perform the crossover and so only a small part of search space is explored. On the other hand, if there are too many chromosomes, the Genetic Algorithm slows down. Research shows that after some limit (which depends mainly on encoding and the problem) it is not useful to increase population size, because it does not make solving the problem faster.

Selection

As one already know from the Genetic Algorithm outline, chromosomes are selected from the population to be parents to crossover. The problem is how to select these chromosomes. According to Darwins evolution theory the best ones should survive and create new offspring. There are many methods how to select the best chromosomes, for example *roulette wheel selection*, *Boltzman selection*, *tournament selection*, *rank selection*, *steady state selection* and some others.

Roulette Wheel Selection   The Parents are selected according to their fitness. The better the chromosomes are, the more chances to be selected they have. Imagine a roulette wheel where are placed all chromosomes in the population, every has its place big accordingly to its fitness function. Then a marble is thrown there and selects the chromosome. Chromosome with bigger fitness will be selected more times.

This can be simulated by following algorithm.

1. **Sum** Calculate sum of all chromosome fitnesses in population—$\sum S$.
2. **Select** Generate random number from interval (0,S)—r.
3. **Loop** Go through the population and sum fitnesses from 0—$\sum S$. When the $\sum S$ is greater then r, stop and return the chromosome where you are.

The first step is performed only once for each population.

Rank Selection   The previous selection will have problems when the fitnesses differs very much. For example, if the best chromosome fitness is 90% of all the roulette wheel then the other chromosomes will have very few chances to be selected. Rank selection first ranks the population and then every chromosome receives fitness from this ranking. The worst will have fitness 1, second worst 2 etc. and the best will have fitness N (number of chromosomes in population). After this all the chromosomes have a chance to be selected. But this method can lead to slower convergence, because the best chromosomes do not differ so much from other ones.

Steady-State Selection   This is not particular method of selecting parents. Main idea of this selection is that big part of chromosomes should survive to next generation. The Genetic Algorithm then works in a following way. In every generation are selected a few (good—with high fitness) chromosomes for creating a new offspring. Then some (bad - with low fitness) chromosomes are removed and the new offspring is placed in their place. The rest of population survives to new generation.

Elitism   When creating new population by crossover and mutation, we have a big chance, that we will loose the best chromosome. Elitism is the name of the method, which first copies the best chromosome (or a few of best chromosomes) to the new population. The rest is done in classical way. Elitism can very rapidly increase performance of Genetic Algorithms, because it prevents losing the best found solution.

Recommendations for Parameters of Genetic Algorithms

This should give you some basic recommendations if you have decided to implement your Genetic Algorithm. These recommendations are very general. Probably you will want to experiment with your own Genetic Algorithm for specific problem, because today there is no general theory which would describe parameters of Genetic Algorithms for any problem.

Recommendations are often results of some empiric studies of Genetic Algorithms, which were often performed only on binary encoding.

Crossover rate   Crossover rate generally should be high, about 80–95 % . (However some results show that for some problems crossover rate about 60 % is the best.)
Mutation rate   On the other side, mutation rate should be very low. Best rates reported are about 0.5–1 %.
Population size   It may be surprising, that very big population size usually does not improve performance of Genetic Algorithms (in meaning of speed of finding solution). Good population size is about 20–30, however sometimes sizes 50–100 are reported as best. Some research also shows, that best population size depends on encoding, on size of encoded string. It means, if you have chromosome with 32 bits, the population should be say 32, but surely two times more than the best population size for chromosome with 16 bits.
Selection   Basic roulette wheel selection can be used, but sometimes rank selection can be better. Check paragraph about selection for advantages and disadvantages. There are also some more sophisticated method, which changes parameters of selection during run of Genetic Algorithms. Basically they behaves like simulated annealing. But surely elitism should be used (if you do not use other method for saving the best found solution). You can also try steady state selection.
Crossover and mutation type   Operators depend on encoding and on the problem. Check chapter about operators for some suggestions. You can also check other sites.

3.2.4.2   Multiobjective Evolutionary Algorithms (MOEAs)

Often there is not only one objective that has to be minimized using Genetic Algorithms. Multiple, often conflicting objectives arise naturally in most real-world optimization scenarios. As Evolutionary Algorithms possess several characteristics that are desirable for this type of problem, this class of search strategies has been used for multiobjective optimization for more than two decades. Meanwhile evolutionary multiobjective optimization has become established as a separate subdiscipline combining the fields of evolutionary computation and classical multiple criteria decision making. In normal Genetic Algorithms we take a population of genomes (individuals) randomly scattered across state space and evaluate the fitness of the results. The best are then retained (selection) and a new population created (reproduction), incorporating mutation and crossover operations to gain a different set of possibilities (variation). Over many generations the population will search state space and hopefully converge on the best solution, the global optimum. In multiobjective Genetic Algorithms we do much the same, except that in this case we are trying to optimise not for one fitness parameter but against a collection of them. To achieve this we must generate an understanding of the overall fitness of the set of objectives, so that we can compare solutions and there are many ways of doing this. In traditional multiobjective optimisation it is usual to simply aggregate together (add in some way) all the various objectives to form a single (scalar) fitness function, which can then be treated by classical techniques such as simple Genetic Algorithms, multiple

objective linear programming (MOLP), multiple attribute utility theory (MAUT), random search, simulated annealing etc.

One of that multiobjective optimization problems is the problem of optimal pump scheduling in water supply networks that will be described later in this chapter. In the past some derivations of the standard Genetic Algorithm for multiobjective optimizations where developed such as

1. Strength Pareto Evolutionary Algorithm (SPEA) [369],
2. Non-Dominated Sorting Genetic Algorithm (NSGA) [296],
3. Non-Dominated Sorting Genetic Algorithm 2 (NSGA2)[71],
4. Controlled Elitist Non-Dominated Sorting Genetic Algorithm (CNSGA) [73],
5. Niched Pareto Genetic Algorithm (NPGA)[154],
6. Multiple Objective Genetic Algorithm (MOGA) [106].

Detailed information about each of these MOEAs can be found in referenced papers. However, it is important to remark the most important aspects of these algorithms. MOEAs produce a set of solutions, instead of a single one. In fact, in general, there is no single optimal solution in a multiobjective optimisation problem with contradicting objectives. In this case, the multi-objective search space is partially ordered in the sense that two arbitrary solutions are related to each other in two possible ways: either one dominates the other or neither dominates (they are non-dominated or non-comparable). Hence, the goal is to find a set of solutions (decision vectors) called the Pareto Optimal Set and its corresponding Pareto Optimal Front (objective vectors). Solutions in the Pareto Optimal Set are the ones that cannot be improved in any objective without causing degradation in at least one of the other objectives. MOEAs work simultaneously with a set of solutions (known as evolutionary population). Each algorithm processes its population differently, using random based genetic operators (as selection, mutation and crossover). Thus, it is expected that this set of solutions, improves from one iteration (generation) to the next one. In this way, the best possible approximation to the Pareto Optimal Set for a particular run is obtained from the final set of solutions (by the last iteration). SPEA, however, works with two populations, storing in the second one most of the best solutions found during calculations. Therefore, this second population is the one with the calculated Pareto Optimal Set at the end of the computation.

3.2.5   Network Model Calibration

Even though the required data have been collected and entered into a hydraulic simulation software, the modeler can not assume that the model is an accurate representation of the real system. A hydraulic simulation software simply solves the model equations using the supplied data. The quality of the data will dictate the quality of the model results. So the accuracy of the hydraulic model depends on the model calibration. A calibration have to be always be performed before a model is used for

decision-making. A well calibrated model is a prerequisite for a good simulation and optimization of the real system.

Calibration is the process of comparing the model results to field measured data and, if necessary, adjusting some model parameters until the model-predicted data reasonably matches the measured system data. The process of calibration can include the following changes:

1. Changing system demands,
2. Changing roughness factors of pipes,
3. Changing pump operating characteristics,
4. Changing other parameters that may affect the model results.

The parameter estimation is defined by the determination of system model parameters that will produce a minimum deviation between simulated and observed values when the simulation models are carried out under time varying conditions. Once that model parameters are accurately estimated, desired simulation results may be achieved. Mathematically, parameter estimation problem has been formulated by regression statistical theory. The general relation between observed and true values is:

$$y = f(\beta) + \varepsilon \tag{3.76}$$

with

y: observed values
$f(\beta)$: model estimate of y
β: model parameter vector
ε: random measurement error vector

The maximization of likelihood provides an argument known as common least-squares (LS) problem:

$$max\, L(\beta) = min\, \frac{1}{2}(y - f(\beta))^T C_d^{-1}(y - f(\beta)) \tag{3.77}$$

The parameter estimation problem is to determine the optimal values of roughness and emitter coefficients from a limited number of field observations (measurements) so that a certain criterion is optimized. If LS approach is used to represent the deviation between observed and simulated values, it is possible to express the objective function by:

$$min\, FO = \sum_{i=1}^{N}\left[\frac{\Delta P_i}{\frac{\sum_{i=1}^{N} P_i'}{N}}\right]^2 + \sum_{j=1}^{M}\left[\frac{\Delta Q_i}{\frac{\sum_{j=1}^{M} Q_i'}{M}}\right]^2 \tag{3.78}$$

with

P_i': a set of pressure values
Q_j': a set of flow values
ΔP_i: the difference of pressure between simulated and observed data

ΔQ_j: the difference of flow between simulated and observed data
N: number of monitored nodes
M: number of monitored pipes.

Data Requirements From the formula above we can start a discussion about data requirements and the reasons for discrepancies between modeled behavior and actual field measurements of a water distribution system. Variations can stem from the cumulative effects of errors, approximations and simplifications in the way the system is modeled; site-specific reasons such as outdated system maps and causes that are more difficult to quantify such as the inherent variability of water consumption.

In making comparisons between model results and field observations, the user must ensure that the field data are correct and useful.

Comparisons Based on Head When comparisons are made between field measurements and model results, there is no mathematical reason to use pressures instead of hydraulic grades. But pressure is just a converted representation of the height of the HGT (Hydraulic Grade Line) relative to the ground elevation. They are essentially equivalent for comparison purposes but for calibration purposes, there are several arguments for working with hydraulic grades rather than pressures:

1. Hydraulic grades provide the modeler with a sense of the accuracy and reliability of the data. If computed and measured hydraulic grade values are drastically different from one another, it should immediately alert the modeler that a particular value is wrong. Maybe an elevation was entered incorrectly.
2. Hydraulic grades give an indication of the direction of flow insight.
3. Hydraulic grades makes it easier to work with pressure measurements not taken exactly at node locations within the model. It is the elevation of the pressure gage, not the node, that is used to convert measured pressure into HGT.

Accordingly, the first step the modeler should complete upon collection of field data is to convert pressure and tank level data into the hydraulic grades. Comparisons should always be made between observed and modeled HGTs. There are some basic rules how to do field observations:

1. Head data for model calibration should generally be collected at a significant distance from known boundary heads (tanks, wells, reservoirs). Wrong roughness coefficients and demands affect the slope of the hydraulic grade line. If data are collected near the boundary nodes, the differences between the model and the field data may appear to be small because of the short distance.
2. There should be at least one flow measurement in each pressure zone and the number of flow measures should be proportional to the size of the pressure zone.
3. For point readings (single location at a specific time), samples should be collected at locations where the parameter being measured is steady so that the sample measurement is representative of the location over a long time period.
4. To get the most out of continuous monitoring (collecting data at a single location over time), the data should be collected from locations where the parameter being measured is dynamic.

5. In situations where a point reading must be made at a dynamic location, it is critical to carefully note the time and boundary conditions corresponding to the data point.
6. More tests will increase the confidence.

Roughness Values A great deal of research has been done in the area of estimating pipe roughness values. Meanwhile there are extensive tables available that documenting pipe C-factors for a wide variety of pipe materials, sizes and ages. The increase in pipe roughness as a function of water quality was also evaluated. The research determined that two pipes of the same size, material and age can have different effective diameters and roughnesses based on the quality of the water flowing through the pipe in the past.

Despite all of these variables, pressure data collected in the field can be used to select appropriate roughness values for the pipes. However, in calibrating a model, it is important to consider the potential for compensating errors; that is, fixing one inaccuracy by introducing another one into the network. When calibrating, the adjustments made to the variables should be appropriate for a range of operating conditions and not just the individual case being considered.

The water distribution modeling equations are based on the simplifying assumption that water is withdrawn at a network node. A source of error is related to how the demands change over time. Accurate measures of the demand pattern are necessary. It is conceivable that a model could incorporate all of the locations where water is withdrawn from the system by placing junction nodes. This approach, however, would significantly increase the number of pipes required in the model, thereby increasing its complexity. Grouping water usage at the junction nodes instead of at the actual locations where water is withdrawn from the system produces relatively minor differences between computer-predicted and actual field performance if the actual location of the customer demand is in close proximity to the assigned node. Incorrect demand will becomes problematic when demands from large customers are missed or assigned to nodes in the wrong pressure zones. In most cases, however, errors in allocating demands to exactly the right node are insignificant, especially when fire flows used in design are significantly greater than normal demands.

When making comparisons between the model and field measurements, it is important that the demands in the model correspond to the time that the field measurements were taken. The modeler should be take care of the calibration values. He should be skeptical of needing to assign unrealistic pipe roughness or unrealistically high or low nodal demands to achieve calibration. If demand values that are significantly different from historical records are needed to calibrate the model, then a logical explanation for this deviation should be provided. Maybe the swimming pool was being filled on the day pressures were measured or a large water-using industry was temporarily shut down during pressure testing.

3.2.5.1 Calibration Approaches

Identifying and addressing large discrepancies between predicted and observed behavior is critical in the calibration effort. This step, referred to as rough-tuning, is necessary to bring predicted and observed system parameters into closer agreement with one another. After that step efforts can be focused on fine-tuning. Fine-tuning involves adjusting the pipe roughness values and nodal demand estimates and is the final step in the calibration process.

The most important part of model calibration is making judgments regarding the adjustments that must be made to the model to match it with the field results.

The following is a approach that could be used as a calibration guide.

1. Identify the intended use of the model,
2. Determine estimates of model parameters,
3. Collect calibration data,
4. Evaluate model results based on initial estimates of model parameters,
5. Perform a rough-tuning or macrocalibration analysis,
6. Perform a sensitivity analysis,
7. Perform a fine-tuning or microcalibration analysis.

Identifying the intended use of the model is the first and most important step because it helps the designer establish the level of detail needed and the acceptable tolerance for errors between field measurements and simulation results. After this, the modeler can begin estimating model parameters and collecting calibration data. The model can then be evaluated and large discrepancies can be addressed simply by looking at the nature and location of differences between the model results and the field data. Next, a sensitivity analysis can be conducted to judge how performance of the calibration changes with respect to parameter adjustments. For example, if pipe roughness values are globally adjusted by 10 %, the modeler may notice that pressures do not change much in the system, thus indicating that the system is insensitive to roughness for that demand pattern. On the other hand, nodal demands may be changed by 10 % for the same system, causing pressures and flows to change significantly. In this case, time should be spent focusing on establishing good estimates of system demands. If neither roughness coefficients nor demands have a significant impact on system heads, then the velocity and therefore the headloss in the pipes may be too low for the data to be useful for this purpose.

The final step in the calibration process, fine-tuning, can be time-consuming, particularly if there are a large number of pipes or nodes that are candidates for adjustment.

3.2.5.2 Automated Calibration Approaches

Traditionally, model calibration was a manual task where the modeler makes changes to pipe roughness values or demands on a trial-and-error approach to achieve convergence between model and field values. But there are many potential combinations

of calibration parameters, so that finding the best set of parameters is a time expensive challenge to the modeler. Therefore, he can calibrate the system much more efficiently and consistently by using a computer-based, numerical optimization technique (Genetic Algorithms) that is able to identify the near-optimal combination of calibration parameters to achieve a match to the field data.

Often the computer based model calibration will be done with implicit models, that consists of optimization-based models. The calibration problem is represented as an optimization problem by introducing an objective function. The problem is solved implicitly, usually by minimizing the objective function. Three commonly used types of objective functions are

1. sum of squared errors,
2. sum of absolute errors,
3. maximum absolute error.

Errors are calculated as differences between measured and output variables computed by the hydraulic model. Typically the head and flow errors are used, but also other types of errors may be used too, such as tank level or head loss. Hydraulic models linked to optimization methods are steady-state models (single- or multiple-loading condition), extended-period simulation models, or unsteady (transient) models.

3.2.5.3 Optimization Problem Formulation

The model calibration with optimization methods search for a solution describing the unknown calibration parameters that minimizes an objective function, while simultaneously satisfying constraints that describe the feasible solution region. If the vector of the unknown parameters is given as x (roughness, demand, control status), the objective function may be given, derived from (3.78) as

$$min f(x) = \sum_{i=1}^{N} w_i [y_i^* - y_i(x)]^2 \tag{3.79}$$

with

f: objective function to be minimized
N: number of observations
w_i: weighting factors
y_i^*:   observation values (pressures, flows)
$y_i(x)$:   model predicted values (pressures, flows).

As an example, the y vector of observations and predictions would consist of a set of values such as '517 m, 34 l/s, and 510 m' where those values would be the measured head at a node, the flow in a pipe, and the head on the discharge side of a pump. The x vector of unknowns could consist of values such as '0.15 mm, 0.98 mm, 5 m^3/h, and open' where those values are the C-factors at two pipes, the demand at

a node, and the status of a pump. The values for *x* will vary by each iteration, but the values for *y* are constant for a given run. Weightings can be applied to reduce the influence of observations that are less accurate, to increase the influence of the other observations.

In vector notation, the preceding objective function (from (3.77)) becomes

$$min \ \ f(x) = [y^* - y(x)]^T W[y^* - y(x)] \tag{3.80}$$

with

y^*:	vector of observations
$y_i(x)$:	model predicted values
T:	transpose operator
W:	weighting operator.

The set of constraints associated with this problem are implicit hydraulic constraints, known initial conditions (device statuses and tank levels) and boundary conditions (reservoir levels). By the use of Genetic Algorithms for solving the optimization problem a standard hydraulics simulation can be used. This is easier than explicitly incorporating the equations of conservation of mass and energy into the optimization routine. The solution is passed back to the optimization routine, where the algorithm computes the objective function, evaluates the constraints and if necessary, updates the decision variables. New values of the decision variables are then passed to the simulation routine and the process is repeated until an acceptable calibration is obtained. Fitness is determined by comparing how well the simulated flows and pressures resulting from the candidate solution match the measured values collected in the field. Several steady state simulations are run to simulate a variety of demand conditions, including the operating conditions for minimum, maximum and average demands. At each measurement point and for each steady-state run, the differences between simulated and observed data (head and/or flow) are calculated and the objective function (an overall error value for the network) is computed. Different weightings between head and flow measurements can also be incorporated within the objective function. In addition to eliminating most of the routine and tedious aspects of the calibration process, Genetic Algorithms will generally achieve a better fit to the available data if the user can select the correct set of variables to be included in the solution and can establish the correct range of possible solutions.

3.2.5.4 Optimal Pump Scheduling

In conventional water supply systems, pumping of treated water represents the major fraction of the total energy budget. Optimising the pump scheduling has proven to be a practical and highly effective method to reduce operation costs without making changes to the actual infrastructure of the whole system. According to the number of variables and objectives considered, optimising a pump scheduling problem may become very complex, especially in large supply systems.

Typically, a pumping station consists of a set of some pumps of different capacity, that are used to pump the water to the reservoirs. These pumps work in combination with each other to pump the needed amount of water. While doing this, all hydraulic and also all technical constraints (such as maximum level in the tank and pump power) must be fulfilled. Thus, at a particular point in time, some pumps would be working but others would not. In this context, scheduling the pumps operation means choosing the best combination of pumps that will be working at each time interval of a scheduling period. A pump schedule is the set of all pump combinations chosen for every time interval of this scheduling horizon. An optimal pump schedule can then be defined as a pump schedule that optimises particular objectives, while fulfilling system constraints.

A lot of researchers have developed optimal control formulations to minimise the operating costs associated with water supply pumping systems. During the first studies, linear, non-linear, integer, dynamic, mixed and other kinds of programming were used to optimise a single objective: the electric energy cost [213]. Later the number of pump switches as an alternate way to evaluate the pumps maintenance cost, which became the second objective considered until that date, was introduced. In the past few years, techniques of Evolutionary Computation were introduced in the study of the optimal pump scheduling problem. Genetic Algorithms has been proven to be a powerful tool to solve optimal pump scheduling problems. Due to great advances recently achieved in the field of evolutionary multi-objective optimisation, their undoubted usefulness and the complexity of the pump scheduling problem, this work presents an analysis of an optimal pump-scheduling problem as a multi-objective optimisation and its solution using MOEAs. Some different algorithms can be implemented and combined with a heuristic method that handles problem constraints. Traditional optimisation methods often combine all objectives into a single figure of merit (combined cost). However, these MOEAs optimise e.g. four objectives simultaneously without aggregation. These objectives will be *electric energy cost*, *pumps maintenance cost*, *peak power* and *level variation in a reservoir*.

Multi Objective Optimal Pump Scheduling Problem

Lets have a look at a model of a simple water supply network. This model is composed of:

1. an inexhaustible water source: the potable water reservoir or ground water
2. a potable water pumping station with e.g. four pumps used to pump water from the source to an elevated reservoir
3. a main pipeline used to convey water from the pumping station to the elevated reservoir
4. the elevated reservoir, which supplies water demand from a city.

The only data considered outside of the proposed model is the water demand of the city. The pumping station is comprised of a set of *n* different constant velocity centrifugal pumps working in parallel association. Pumping capacities are supposed constant during every time interval. Therefore, for a time interval of 1 h, each pump combination was assigned a fixed discharge, fixed electric energy consumption and

fixed power. Nonlinearities in the combination of the pumps are considered through a table of pump combination characteristics. The reservoir stores water coming from the pumping station and it satisfies the cities water demand by gravity. An important aspect is the initial level, which has to be recovered by the end of the optimisation period because a final level above the initial one represents extra water in the reservoir and there is no need to store extra water in the reservoir if it is not going to be consumed by the community. This also implies a useless extra cost. A final level below the initial one represents lack of water for the next day. This lack of water has to be recovered the next day, affecting its schedule through a variation of the initial parameters and extra cost. The goal is to keep a periodical schedule if conditions in consecutive days do not change substantially. But is another issue that has to be kept on eye. The initial water level in the reservoir should be the maximum allowable level of that reservoir. So it would be possible to supply the community for some hours in the case of pump station fault. This gives more security of supply.

A mass balance mathematical model can be chosen. This model is based on the equilibrium between the amount of water that comes into the reservoir and the amount of water that comes out of it. Since water demand is an input data for this problem, it has to be obtained from reliable sources. The quality and applicability of an algorithms solution depends on the reliability of the predictions of the water demand. Data is obtained through a statistical study of the community's water demand during many years. Through these studies, an estimated water demand can be established, according to certain parameters.

In order to use Evolutionary Algorithms, a binary alphabet was used to code the optimal pump schedule. Each pump, at every time interval, is represented by a bit in a vector. In this string, a zero represents a pump that is not working (off) in a particular time interval, while a one represents a pump that is working (on).

Timestep	1h				...	24h			
Pump	Pump1	Pump2	Pump3	Pump4	...	Pump1	Pump2	Pump3	Pump4
Chromosome	1	0	1	1	...	0	1	1	0
Pump status	on	off	on	on	...	off	on	on	off

An optimisation period of one day can be divided into 24 intervals of one hour each. Pumps can be turned on or off only at the beginning of each time interval. Due to problems constraints, a lot of possible solutions are not feasible. In fact, not all solutions are expected to fulfil maximum and minimum level constraints. As a result, the search space is reduced from possible solutions to feasible solutions only, but the last quantity is still too big to be analysed with traditional methods. Under this condition, Genetic Algorithms has to be chosen because of their ability to deal with such huge search spaces efficiently.

As described before there are four objectives that have to be fulfilled in common pump optimization problem:

1. Reservoir level variation
2. Electrical energy cost
3. Pumps maintenance cost
4. Maximum power peak.

Reservoir Level Variation

There are three levels to be considered in the reservoir:

1. a minimum level that guaranties enough pressure in the pipeline.
2. a maximum level, which must not be exceeded in order to avoid pipeline losses.
3. an initial level that has to be recovered by the end of the optimisation period.

Maximum and minimum levels are considered as constraints. Hence, at the end of each time interval, water level must end up in some position between the maximum level h_{max} and the minimum level h_{min}. However, level variation between the beginning and the end of the optimisation period D_h is stated as another objective to be minimised, since small variations do not necessarily make a solution not acceptable, as shown in Eq. (3.82).

$$\Delta h = \sum_{i=1}^{24} \frac{[D(p_i) - d_i]}{S} = f_1 \tag{3.81}$$

$$h_i = h_{i-1} + \frac{[D(p_i) - d_i]}{S} \tag{3.82}$$

$$h_i \leq h_{max} \tag{3.83}$$

$$h_i \geq h_{min} \tag{3.84}$$

with

S: reservoirs surface (constant)
$D(p_i)$:   discharge at time i using pump combination p_i
d_i: water demand at time i.

There are some other constraints as follows:

1. amount of water supplied by water source
2. pipeline pressure constraints
3. valves in the system are not considered
4. pumps characteristics (are includes in the hydraulic model)
5. water demand.

Electrical Energy Cost

Electric energy cost is the cost of all electric energy consumed by all pumps of the pumping station, during the optimisation period. An important issue to be considered when analysing electric energy cost is the charge structure used by the electric power company. In most electricity supply systems, electric energy cost is not the same throughout the whole day. Often there is a charge structure available that is devides into day and night tarrifs like (example)

1. High cost: (C_H): from 5:00 AM to 6:00 PM
2. Low cost: (C_L): from 6:00 PM to 5:00 AM.

Electric energy costs can be substantially reduced if the optimal pump schedule establishes the smallest possible number of pumps working during the high cost period. Water already stored in the reservoir can be used during this period of time in order to satisfy the water demand. A different charge structure can also be considered if needed. The mathematical expression of electric energy cost E_C is given by Eq. (3.85).

$$E_c = C_L \sum_{i=1}^{5} c(p_i) + C_H \sum_{i=6}^{18} c(p_i) + C_L \sum_{i=18}^{24} c(p_i) = f_2 \qquad (3.85)$$

with

i: time interval
p_i: pump combination at interval i
$c(p_i)$:   electrical energy consumed by pump combination p_i.

Pumps Maintenance Cost

Pumps' maintenance cost can be as important as the electric energy cost or even more relevant. The concept of the number of pump switches is introduced as a way of measuring pumps maintenance cost. So, a pumps wear off can be measured indirectly through the number of times it has been switched on. A pump switch is considered only if the pump was not working in the preceding time interval and it has been turned on. A pump that was already working in the preceding time interval and continues to be in the same state or is switched off, does not constitute a pump switch for the algorithm. The total number of pump switches N_s is computed as sum of pump switches at each time interval. The number of pump switches between the last time interval of the preceding optimisation period (day before) and the first time interval of the day being analysed, will be also computed. Just half of that quantity is added to the total number of pump switches, in order to consider possible switches between two consecutive optimisation periods, supposing there is a certain periodicity between consecutive pump schedules, as shown in Eq. (3.86).

$$N_s = \sum_{i=2}^{24} \|max\{0, (p_i - p_{i-1})\}\| + \frac{\|max\{0, (p_1 - p_{24})\}\|}{2} = f_3 \qquad (3.86)$$

Maximum Peak Power

Many electricity companies charge their big clients according to a reserved power. This reserved power has a fixed charge, but an expensive additional charge will be added when this power is exceeded. Therefore, reducing such power peaks becomes

very important. The approach could be proposing a daily power peak P_{max} as another objective to be minimised. This is easily computed using Eq. (3.87)

$$P_{max} = max[P(p_i)] = f_4 \qquad (3.87)$$

with

$P(p_i)$:   Power of pump combination p_i at time i.

The Optimization Problem

With each of the four objectives defined, the multiobjective pump scheduling problem can be stated as follows

$$minf(x) = (f_1(x), f_2(x), f_2(x), f_2(x)) \qquad (3.88)$$

with

f_1:   Reservoir level variation Eq. (3.82)
f_2:   Electrical energy cost Eq. (3.85)
f_3:   Pump maintenance cost Eq. (3.86)
f_4:   Maximum peak power Eq. (3.87).

subject to:

$h_i = h(x_i) \le h_{max}$ for each time interval
$h_i = h(x_i) \ge h_{min}$ for each time interval
h_i Reservoir level at the end of time interval i.

Because the different objective values considered in this work, i.e., electricity cost and number of pump switches, are not comparable, one have to normalise the distance between two solutions s_i, s_j with respect to objective f_k as:

$$f_k^{nor} = \frac{(f_k(s_i) - f_k(s_j))^2}{(f_k^{max} - f_k^{min})^2} \qquad (3.89)$$

with

f_k^{max}:   known maximum value of the objective
f_k^{min}:   known minimum value of the objective.

Given N pumps and T time intervals, the number of possible solutions is 2^{NT} and the maximum number of switches per pump is $T/2$. The maximum electrical cost corresponds to a schedule where all pumps are operating during the whole simulation period, while the minimum electrical cost is zero. For the total number of pump switches, the maximum value when $T = 24$ h and $N = 4$ pumps is 48, while the minimum value is always zero.

After the normalization Eq.(3.88) can be transformed to

$$minf(x) = \sum_{k=1}^{4}(f_k^{nor}(x))$$

(3.90)

with

$f_k^{nor}(x)$ normalized objective.

In summary, this considers pumps' characteristics in order to satisfy water demand from a community, while fulfilling other constrains such as the maximum and minimum levels in the reservoir. At the same time, electric energy cost, pumps maintenance cost, maximum power peak and level variation in the reservoir between the beginning and the end of the optimisation period, are minimised. Baran and Luecken [15] found out that Strength Pareto Evolutionary Algorithm (SPEA) gives the best result for optimial pump schedule. Overall performance in the analyzed metrics used places SPEA as a better alternative for the optimal pump scheduling problem presented and the parameters considered in the test problem, while NSGA2 looks like a good alternative. Moreover, SPEAs set of solutions provides pumping station engineers with a larger number of optimal pump schedules to choose from. The engineers criterion is to be used to select the appropriate solution.

3.3 Long Distance Water Supply

3.3.1 Introduction

With the city development, the distance of water conveying will be longer and longer. Many large cities are located far away from their water resources so the transport of a huge amount of water over long distances will become more and more important. Sometimes the water needs to be transported over hundreds of kilometers, over mountains and lowlands with large elevation differences. This work will be done by Water Transportation systems (WTS). In opposition to Water Distribution Systems (WDS) they are mostly not meshed and contains of one ore more pipes in parallel with intermediate storage tanks, pumping stations and valves.

One of the largest pipeline projects worldwide is the *Great Man Made River Project* (GMMRP) in Libya. The Guinness World Records 2008 book has acknowledged this as the world's largest irrigation project. It consists of more than 1,300 wells, most more than 500 m deep and supplies 6,500,000 m^3 of freshwater per day to the cities of Tripoli, Benghazi, Sirt and other cities in the north of Libya. The GMMRP authority has been entrusted with the implementation and operation of this worlds largest pre-stressed concrete pipe project which, since it's conception in 1984 has grown to include almost 4,000 km of mainly 4 m diameter pre stressed concrete

cylinder pipe (PCCP). These dimensions show how much important modeling, simulation and optimal planning for such a system is. Another large pipeline project is the Shoaiba Water Transport System in Saudi-Arabia which is 344 Km long and transports drinking water from the Red Sea into the highlands of the country.

3.3.2 Types of Pipeline Systems and Problems

With the growing dimensions of long distance pipeline systems also the problems will grow. Also there are other types of problems to solve than in smaller supply networks in cities. Often the pipeline has a complex landform with large elevation differences. This means that the hydraulic grade and the pressure in the lowest parts of the pipeline system will be very large. In the GMMRP some pipelines has a elevation difference of more than 150 m. With today technology, fluids can be conveyed through pipelines efficiently and safely. When the product pumped is oil or gas, the reliability of supply and the potential risks for the environment are, however, major points of concern— and if the medium pumped is water, aspects of hygiene also have to be considered. From the point of view of hydraulics, pumping water poses a larger challenge, because it cannot be compressed like oil or gas. During start-up and shutdown, emergency stopping or a change of flow rate, pipelines—which can be miles long—can be affected by so-called transient flow conditions (a situation, between two periods of steady flow conditions, where the volume of the product flowing through a pipeline varies with time, i.e. is unsteady. Unsteady rates of flow always go hand in hand with pressure variations). To keep the resultant pressure waves within controllable limits, the system has to incorporate carefully-designed surge control equipment. In principle there exist two types of pipeline systems *open systems* and *closed systems*. In a so-called open system, the medium is pumped, section by section, from one reservoir to the next with a long distance in-between. The long distances are bridged by a multitude of reservoirs and pumping stations. So, in fact, the system consists of a series of individual systems which are not directly linked to each other hydraulically. The GMMRP in Libya is such a system. Furthermore, some parts of the system are not fully filled means, that they can not be simulated with the common closed network hydraulics model (e.g. Darcy-Weisbach). The system has to be dealth like open channel systems and so the Saint-Venant-Equations has to be used for simulation purposes. This makes the simulation more complex an needs extensive computation power.

Closed systems are altogether different. The intermediate pumping stations along the line form an integral part of the same pipeline. This type of system does not require buffer tanks at the intermediate pumping stations (so-called booster pumping stations) and it is therefore considerably cheaper to build than an open structure. There is no need for treatment facilities to remove biological impurities from the water, either and also no costs to be considered for maintenance and upkeep of the facilities. The lower hydraulic pressure losses and the resultant energy savings can also reduce total operating costs. One system of that category is the Shoaiba Pipeline

system in Saudi-Arabia where the water, produced in water desalination plants on the coast of the Red Sea, is pumped stepwise over some cascades into the middle of the country where the large cities Jeddah, Makkah und Taif are located. In that system the water is pumped with three stages over an elevation of more than 1744 m.

3.3.3 Pipe Dimensioning

The daily volume rate of flow forms the basis for designing a long distance water transport system. The following equation is used to calculate the possible nominal diameters of the pipeline for a number of different flow velocities.

$$DN = \sqrt{\frac{4Q}{\pi v}} \qquad (3.91)$$

with

DN: nominal diameter [m]
Q: Flow [m^3/s]
v: velocity [m/s].

Often the pipe cross-sections of long distance pipelines are dimensioned such that the velocity of the medium pumped will not exceed 2 m/s. At this rate of flow, the ratio that the hydraulic pressure losses bear to the initial investment costs of pumping stations and pipeline is positive. In the GMMRP the daily flow rate is about 6,500,000 m^3/d and this gives 74 m^3/s with a velocity of 2 m/s this will result in a diameter of 6.8 m. It often makes sense to divide the total volume rate of flow between two parallel pipelines of a smaller cross-section. This is true in particular for systems handling high day rates, in situations in which the reliability of supply is paramount, or where the topography of the terrain complicates matters. The problem of the selected pipes availability on the global market, in the huge quantities required, also has to be addressed during the planning phase. And, trivial as it may seem, transporting each section of a pipeline to the often difficult to reach construction sites must also be arranged. Because of this the main pipelines of the GMMRP consists of two parallel pipes with 4 m diameter each.

Optimal Pipe Diameter by Head Sections

Especially on long pipelines with high elevation differences it makes sense to divide the pipeline into sections of different pipe types depending on the static head in the corresponding section. This gives the engineer the possibility to minimize the cost of the project. Figure 3.13 illustrates the pressure sections in a sample pipeline. If a pipeline is divided in that way one will get the following sections. Often there is a selection of defined diameters (available on the market) possible. This could be the following 5 diameters in that example (DN2000, DN2500, DN3000, DN3500 and DN4000). With the roughness and the material of each type the headloss can
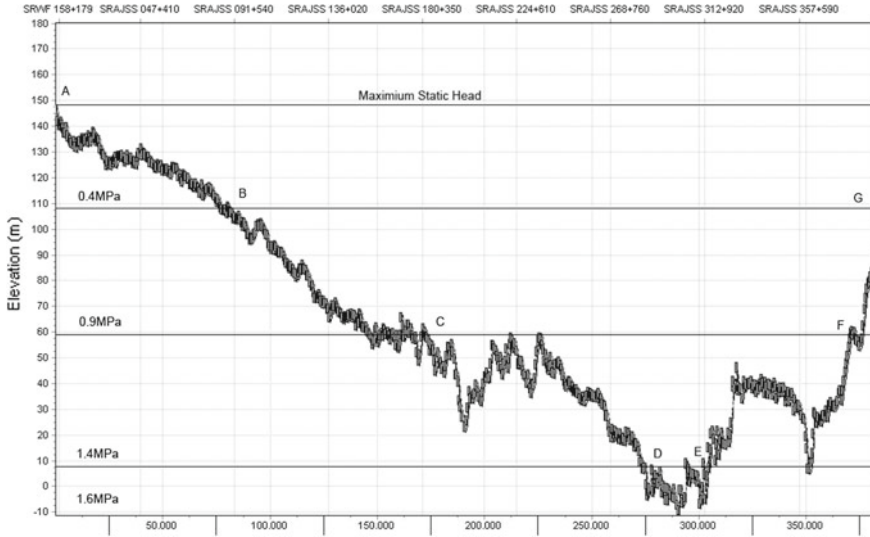
Fig. 3.13   Pressure rating of a pipeline

Table 3.1   Constraint condition for optimization

Working pressure (MPa)	Section/sect. No
0.4	AB/L_1
0.9	BC/L_2
1.4	CD/L_3
1.6	DE/L_4
1.4	EF/L_5
0.9	FG/L_6

be calculated with a hydraulic simulation program. With dividing this pipeline into six sections in Table 3.1 one will have six constraint conditions of length for the optimization problem.

$$L_i = \sum_{j=1}^{5} x(i,j) \qquad (3.92)$$

with

L_i: Length constraint of section i [m]
$x(i,j)$:   length of section i with pipe diameter j [m]
j: selectable pipe diameters.

The water head that can be utilized in this pipeline (head difference between the upper and the lower reaches of the pipeline) is $\Delta H = 37$ m. For fully utilize the head, the total headloss of the pipeline system equals to the utilize head

$$\sum_{j=1}^{5} x(i,j) * l(i,j) = \Delta H \qquad (3.93)$$

with

ΔH: total head loss [m]
$x(i,j)$:   length of section i with pipe diameter j [m]
$l(x,j)$:   head loss of section i with pipe diameter j [m].

The optimization problem will now give the following objective function

$$min \quad M = \sum_{i=1}^{6} \sum_{j=1}^{5} x(i,j)\dot{m}(i,j) \qquad (3.94)$$

with

ΔH: total head loss [m]
$x(i,j)$:   length of section i with pipe diameter j [m]
$m(x,j)$:   per km pipe length project cost of section i with pipe diameter j [currency].

This gives a linear optimization problem which does not need the use of Genetic Algorithms.

3.3.4 Transient Flows and Water Hammer

A one can imagine the amount (the mass) of water that move in a long thick pipeline is very large. When a mass is moved with a specific velocity then it will have a large kinetic energy that simply can be calculated with

$$E = \frac{mv^2}{2} \qquad (3.95)$$

with

E: kinetic energy [Nm]
m: mass of the fluid [kg]
v: velocity of the fluid [kg/m^3].

A pipe with a diameter of 1 m and al length of 1000 m contains 998,000 kg of water. It this mass moves with 2 m/s it will have a kinetic energy of 19.96 millon Nm. When a valve closes immediately this energy will produce a very large change of head and therefore the pipe can collapse. This example is only a simplification to show the amount of energy that is stored in moving water. For planning a pipeline system it is

more important to know how large a head change caused by flow change may be and how the valve or pump switching times needs to be adjusted to reduce these head changes.

In this chapter we want only calculate the amount of water hammer for dimensioning and planning purposes. Further information can be found in [342].

For a simple approach to calculate the amount of water hammer or the pressure change in the pipeline caused by a change in flow we want to have a look at a single frictionless horizontal and elastic pipeline. First the momentum equation is applied to a control volume at the wavefront following a disturbance caused by a downstream valve action. The following equation will express the pressure change in the upstream section

$$\Delta p = -\rho a \Delta v \tag{3.96}$$

$$\Delta H = -\frac{a}{g} \Delta v \tag{3.97}$$

with

Δp: change in pressure [Pa]
ρ: fluid density [kg/m^3]
a: characteristic wave celerity [m/s]
Δv: change in fluids velocity [m/s]
ΔH: change in head [m].

As we can see with that equation a valve opening action causing a positive velocity change will result in a negative pressure change. Conversely a closing valve will produce a positive pressure change on the upstream section. For the downstream section the equation changes to

$$\Delta p = \rho a \Delta v$$

$$\Delta H = \frac{a}{g} \Delta v$$

The characteristic wave speed can be calculated by applying the mass conversation equation to the entire pipeline for L/a seconds and combining with Eq. (3.97)

$$a = \sqrt{\frac{\frac{E_v}{\rho}}{1 + \frac{E_v \Delta A}{A \Delta p}}} \tag{3.98}$$

with

ΔA: change in cross-sectional area of pipe [m^2]
ρ: volumetric modulus of elasticity of the fluid [Pa]
a: characteristic wave celerity [m/s]
Δv: change in fluids velocity [m/s]

ΔH: change in head [m].

For a complete rigid pipe the change in pipes area ΔA is zero and the Eq. (3.99) will be reduced to

$$a = \sqrt{\frac{E_v}{\rho}} \tag{3.99}$$

The wave speed in a rigid pipe is about $1400\,\text{m/s}$. If there is a change in ΔA that is for elastic pipes, this speed will be reduces. As a is roughly 100 times larger than g, a $0.5\,\text{m/s}$ change in velocity can result in a $50\,\text{m}$ change in head. Because the change of velocity of several m/s can occur when a pump switches or a valve is closed one can see how large transients can occur in water systems. So it is very important to select the valve opening/closing time as long as the resulting transient don't exceeds the maximum pressure limit of the pipe. In the GMMRP in Libya valve closing times of about $45\,\text{min}$ are common.

3.3.5 Leak Detection

Often long pipeline systems where build through large uninhabited areas. In that areas it is often difficult to check the condition of the pipeline frequently. But like water distribution systems also long pipeline systems will not be untroubled by leakages. While in small systems leak detection can be done by placing some sensors (pressure logger, noise logger) within a very small area, in long WTS it will be too expensive to place a sensor every some hindered meters. So another method needs to be used to estimate the approximate position of the leakage.

In a common WDS there are customer demands. That will be at a minimum in the night hours between 2:00 AM to 3:00 AM. In that time the hydraulic of the network is dominated by the outflow of leakages. The network can be divided in several District Metered Area (DMA). Flow and head are measured in that area and in combination with a hydraulic model the amount of leakages in that DMA can be calculated. A Pipeline can also be treat as a simple DMA. The advantage of a pipeline is that it has an inflow and an outflow that needs to be the same value if there is no leakage. In the case of a leakage the leakage flow will be the difference between inflow and outflow (flow balance).

$$Q_{leak} = Q_{in} - Q_{out} - \sum_{i=1}^{n} nQ_T \tag{3.100}$$

with

Q_{in}:   Flow into the pipeline (e.g. from pump)
Q_{out}:   flow out of the end of the pipeline
Q_T: flow out of the pipeline from turnouts

n: number of turnouts (pumps).

For leakage amount and allocation calculation flow and head measurements at the beginning and the end of a pressurized pipe are necessary. The pipeline needs to be completely filled. These measurements can be taken automatically from the SCADA system (if available for this pipeline segment) or measured manually. Based on these measured data and by the use of hydraulic equations the approximate location of the leak is calculated with the method of Regula Falsi with interval nesting in the following way. The head loss is described by the Darcy-Weisbach equation Eq. (3.62). To determine the actual flow regime the Reynolds number is calculated with

$$Re = \frac{vD}{\eta} \tag{3.101}$$

with

η: kinematic viscosity of the fluid [m^2/s]
v: fluid velocity [m/s]
D: pipeline diameter [m].

Where the velocity of the water can be calculated as follows

$$v = \frac{Q}{A} = \frac{4Q}{\pi D^2} \tag{3.102}$$

with

D: pipeline diameter [m]
A: pipeline cross-section area [m^2].

While the system is in the laminar flow regime the friction factor is calculated simple by

$$f = \frac{64}{Re} \tag{3.103}$$

and the head loss from Eq. (3.62) resolves to

$$h_f = \frac{64\eta v}{D^2 2g} \tag{3.104}$$

now the velocity will be replaced with Eq. (3.102)

$$h_f = \frac{64\eta v}{D^2 2g} = \frac{64\eta 4Q}{D^2 2g \pi D^2} = \frac{128\eta Q}{\pi D^4 g} \tag{3.105}$$

For turbulent flow the friction factor can be determined by the Colebrook-White Eq. (3.59) By replacing f from Eq. (3.62) and the Reynolds number on gets the following equation

$$v = -2\sqrt{2gDh_f}\,\log\left(\frac{k}{3.17D} + \frac{2.51\eta}{D\sqrt{2gDh_f}}\right) \tag{3.106}$$

The final equation is created by replacing the velocity v

$$0 = \frac{4Q}{\pi D} + 2\sqrt{2gDh_f}\,\log\left(\frac{k}{3.17D} + \frac{2.51\eta}{D\sqrt{2gDh_f}}\right) \tag{3.107}$$

This equation is solved for h_f by a Regular Falsi method. When h_{f1} and H_{f2} are found for the pipeline parts before and after the leak, the leak location can be determined:

$$h_{f1} = \frac{h_1 - h^*}{x}$$

$$h_{f2} = \frac{h^* - h_1}{L - x}$$

$$x = \frac{h_1 - h_2 - Lh_{f2}}{h_{f1-h_{f2}}}$$

The leak allocation error depends on the water amount leaking, the errors in pressure measurements and flow measurements and the error of the pipeline roughness value. Lets have an example form GMMRP. The total flow at Benghazi is about 41,700 m³/h with a pressure of 72.62 m and the measured inflow is 45,833 m³/h with a pressure of 96.40 m. About 10 % of the water is leaking (difference between inflow and outflow of the pipeline. The errors of the pressure measurements are about 0.1 %. The errors of the flow measurements are about 1 %. The leak allocation is calculated to be at 69.5 Km with a maximum error of approximately 5.3 km. This location error can be reduced significantly when the calculation is run between turnouts along the pipeline (if exist), which are equipped with additional measurements. The leak allocation accuracy in this example is $1 - (5.3/140\,\text{km}) = 96.2\,\%$. The above leak allocation method only works for pipeline segments without turnouts. There is also the disadvantage that this method is very sensitive to measurement errors. Therefore a slightly different approach can be used.

By analyzing the pressure profile the pipeline segment between two turnouts with the leak has to be determined. For pipeline segments with turnouts leak allocation is also possible if the flow at all turnouts is measured too. In this case a different approach will be done to detect leak position. A fully hydraulic simulation will be done with a virtual leak (as additional demand) at position x and the leakflow calculated as described above. With several hydraulic calculations moving of x, the position x with the least mean square error between calculation and measurements will be found. This location with the least error will be the possible location of the leak (Fig. 3.14).
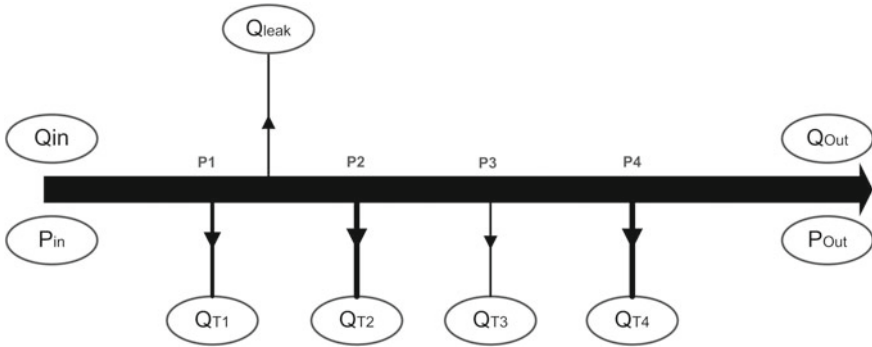
Fig. 3.14 Example of leak in pipeline with turnouts

From Eq. (3.100) the leak flow in this example will be calculated from the flow balance as e.g.:

$$Q_{leak} = Q_{in} - Q_{out} - Q_1 - Q_2 - Q_3 - Q_4 \qquad (3.108)$$

The algorithm now will search for the most probable allocation of the leak that will show the smallest difference between the simulated pressures and the measured pressures. Because the search space is very small there is no need to do this with a Genetic Algorithm like in meshed networks. The pipeline will be splitted into segments between the turnouts and leak allocation calculation for each segment. The leak is assumed in each pipeline segment. The flow in and flow out of the segment is calculated e.g. for the segment between P1 and P2:

$$Q_{S_{in}} = Q_{in} - Q_1$$
$$Q_{S_{out}} = Q_{out} + Q_2 + Q_3 + Q_4$$

and for segment between P2 and P3

$$Q_{S_{in}} = Q_{in} - Q_1 - Q_2$$
$$Q_{S_{out}} = Q_{out} + Q_3 + Q_4$$

Chapter 4
Water Use

Marco Jacobi

4.1 Overview

A water supply system is a composition of different elements which have to work together. Generally, there is a source, a distribution system and a consumer for water or any other resource. The water sources were explained in Chap. 2 and the distribution system in Chap. 3. This chapter shows different models and methods to examine and forecast the water consumption and demand. The actual and future water demand as well as the water consumption is essential for the planning and the operation of water resource systems.

This chapter examines the water demand of the customers in a water supply system. It presents techniques to model the general and regional distributed water demand of different customer types.

As seen in Fig. 4.1, the water consumption is an important part of a water supply system. From the cybernetic point of view, the water consumption is a kind of sink for the resource water, when water reuse and waste water are not regarded in the water system description.

The water system description contains the water sources with catchment areas (Sect. 2.1) and groundwater (Sect. 2.3), the water transportation system (Chap. 3) including reservoirs for storage (Sect. 3.1) and the water consumption (this chapter). In general, the water system is build for a reasonable and safe water supply for the consumers. Therefore, the amount of water which is consumed now and in the future is essential for planning and running the water supply system. To optimize such a system as presented in Sect. 5.3, the water demand is needed.

The prediction of the future water demand for a region or customer is also required to plan the future of the water supply systems. It is essential to know where and how much water is needed in the future, to build water transport systems, reservoirs etc.

M. Jacobi (✉)
Fraunhofer IOSB-AST, Ilmenau, Germany
e-mail: marco.jacobi@iosb-ast.fraunhofer.de
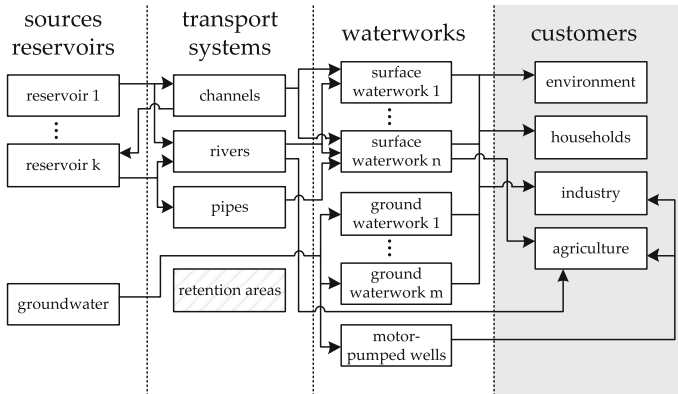
Fig. 4.1 Overview

Various models for the forecast of the water consumption exist for different consumer groups in the literature. There exist judging models which are based on knowledge [205], time series models [205], bi- and multivariate models [19], econometric demand models [19] and models based on component analysis [205]. This chapter introduces basic models and techniques to parametrize these models. It concludes with an overview of different applied models for the three major water consumer groups.

4.1.1 Forecasting

Definition 4.1 Forecasting is the identification/estimation of quantity and/or quality parameters of systems for the time span $t > t_0$ (future) and bases on models.

General methods for forecasting that are easy to use are:

- graphical extrapolation, which is similar to linear regression (Sect. 4.3.2),
- usage of the last measured value and
- extrapolation using the last two measured values, can be compared to AR-models (Sect. 4.2.1.3).

They are illustrated in Fig. 4.2.

This kind of forecasting can be used to get a draft overview of the current situation and is suited to do a fast forecast for the next time steps. It bases on the experience and knowledge of the user and is described in Sect. 4.2.3.
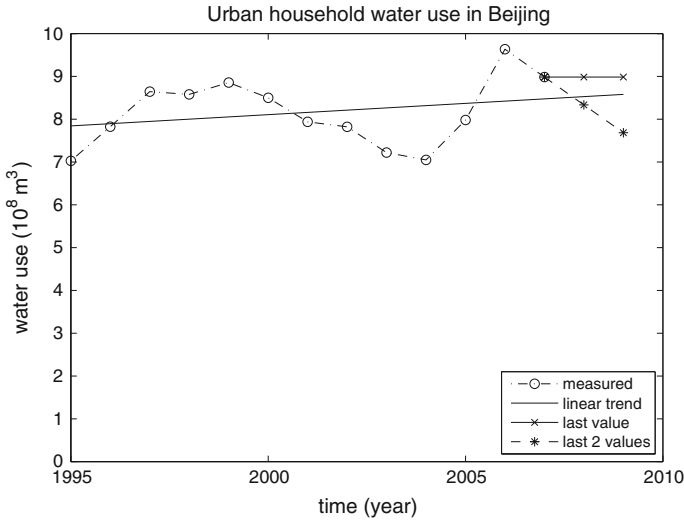
Fig. 4.2 Graphical forecasting

4.1.2   Model Based Forecasting

When using a mathematical model for forecasting, it is important to observe the time variant effects and/or the exogenous influences on the monitored variable. Such a variable can be described as a time series (Sect. 4.2.1).

The model development bases on the search for rules and correlations between the variable (here the water use) and the influencing variables (population, economic growth, etc.) as well as on patterns or cycles in the variable itself. The variation of the variable wd can be a compilation of time $f(t)$, external variables $wd_{ext.}(t)$, auto-correlated $wd_{ARM}(t)$, cyclic $wd_{cycl.}(t)$ and stochastic influences $wd_{stoch.}(t)$:

$$wd(t) = f(t) + wd_{ext.}(t) + wd_{ARM}(t) + wd_{cycl.}(t) + wd_{stoch.}(t) \qquad (4.1)$$

The general approach to create a model of a variable (water demand/water use wd) can be described as following:

1. Description of the forecasting problem.
2. Raw analysis of the forecasting variable and possible influences.
3. Collection of historical data, based on the analysis of point 2.
4. Detailed analysis of the forecasting variable and the influences with correction of measurement errors in the raw data and correlation tests etc.; usage of the collected historical data.
5. Division of the gained data in data sets for model training and for validation.
6. Identification of the model structure.
7. Identification of the model parameters with the training data set.

8. Model validation with the validation data set.
9. Forecasting with the gained model and
10. Improve the model, when new data is available.

4.1.3   Selection of the Forecast Method

When selecting a forecast method we need the correct balance between necessary accuracy of the forecast and the costs (for data acquisition, computing complexity etc.) [205]. An exact forecast reduces the wrong assignment of resources and permits to transact investments purposefully. Areas or sectors, which threaten water scarceness, can be identified with an exact forecast. Three basic principles for the selection of the correct forecast method have to be regarded [205]: The accuracy of the forecast should stand in relationship to the costs, which causes forecast errors. The forecast of a needed component, which constitutes a relatively small part of the total requirement, can be afflicted with high error, without increasing the gross error considerably. And the most important water requirement sectors should receive most attention.

Possible variables, which influence the water requirement, are e.g. total population, gross domestic product, temperature, precipitation or for the irrigation water requirement, water price, the kind of the cultivated cultures and managed surfaces.

4.2   Basic Models

Different approaches exist for forecasting. Two major concepts are the time series based forecast and the component based calculation. A combination of these two concepts can be useful for describing the water use and to forecast the future water demand.

This section describes these approaches, several of their modifications and concepts to handle nonlinearities.

4.2.1   Time Series

In general, a model describes the dependency of a variable (result or output) from other variables (inputs). For time series, the primary independent input variable is the time: $wd(t)$.
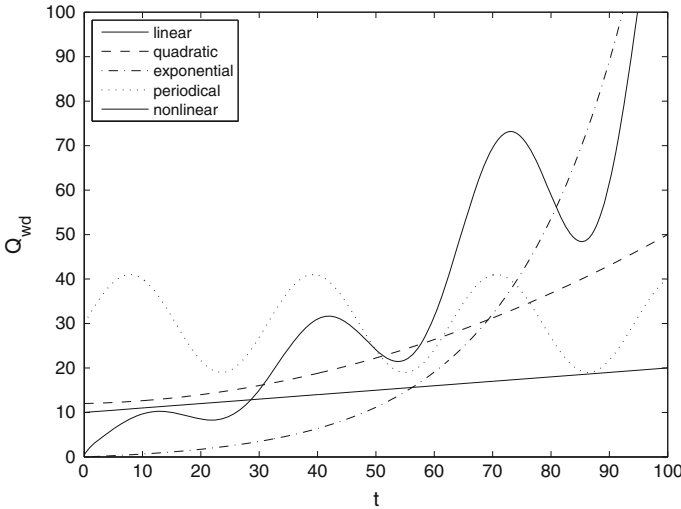
Fig. 4.3 Time based models

4.2.1.1 Basic Time Series Model

The *basic time series model* shows the dependency of the water demand *wd*, which is the resulting variable, from the independent variable time *t*. This dependency can be:

- trend/polynomial: $wd(t) = a_0 + a_1 t + a_2 t^2 + \cdots$,
- exponential: $wd(t) = b\, e^{a\, t}$ with a and b as parameters,
- periodical: $wd(t) = b\, \sin(a\, t) + \cdots$, with a and b as constants,
- nonlinear: $wd(t) = f(t)$, with $f(t)$ as nonlinear function or
- stochastic: $wd_k = \sum_{i=1}^{n}(a_i wd_{k-i}) + \varepsilon_k$ as AR process (Eq. 4.4).

The different time based models are illustrated in Fig. 4.3. When using the water demand $wd(t)$ as flow variable in the water transportation model (Chap. 3) the variable can be described with Q_{wd}.

The time is the only influence on the water demand for this model type; there are no dependencies on other factors such as population, water price etc. This model can describe simple trends, but it cannot react on exogenous changes and is not suitable for a direct prognosis of the future water demand. It is very useful for the prognosis of other factors which have influences on the water demand such as population growths.

4.2.1.2 Bivariate and Multivariate Models

This type of forecasting models describe the linear dependency of the resulting water demand value *wd* from one X_1, for the bivariate model, or from more, for the multivariate model, influencing values X_n, $n \in N$. The linear basic time series

model is a bivariate model with the time as independent value. The mathematical formulation for this model type is shown in Eq. (4.2).

$$
\begin{aligned}
wd(t) &= a_0 + a_1 X_1(t) + a_2 X_2(t) + \cdots \\
&= a_0 + \sum_{i=1}^{n} a_i X_i(t)
\end{aligned}
\tag{4.2}
$$

An example for a bivariate model is the water demand per capita; with wd for the water demand per year, the population P and the water demand per capita b:

$$
wd(t) = b(t) \cdot P(t)
\tag{4.3}
$$

The water demand and the population are time series.

4.2.1.3 Auto Regressive Models (AR-Models)

When the time series has a stochastic behavior it can be described as auto regressive process. The Eq. (4.4) describes such a process; in detail a n order autoregressive process $AR(n)$. The value ε_k characterizes white noise and wd_0 is the water demand at the initial measurement $k = 0$.

$$
wd_k = wd_0 + \sum_{i=1}^{n} a_i wd_{k-i} + \varepsilon_k
\tag{4.4}
$$

An autoregressive process uses at every step k its previous values $wd_{k-1}, \ldots, wd_{k-n}$ to describe its behavior.

4.2.1.4 Auto Regressive Models with Exogenous Influences (ARX-Models)

The ARX-process is generally the same such as an autoregressive process. Additional influences x_j affect the resulting value wd_k. Equation (4.5) describes an AR(n)X model which refers n time steps backwards.

$$
wd_k = wd_0 + \sum_{i=1}^{n} a_i wd_{k-i} + \sum_{j=1}^{m} b_j x_j + \varepsilon_k
\tag{4.5}
$$

4.2.2 Component Models

Component based models consist of different components compiled together. Hotels, for example, can calculate their water demand knowing how much guests they have.

They also know how much water the guests need for showering and using the toilet; for cleaning the room and so on. The specific water use, for example, for using the toilet is one component of the guest water use. With all the specific components and the information about the guest behaviors the hotel management can sum it up to the whole water need of the hotel.

The same can be done for the water use in general. Therefore, the components have to be identified, which is a lot of basic research. The components have to be monitored because they can differ by the time. It is also difficult to examine all the components for a model region with different customers, which can be for instance industrial companies, farmers, households or the municipal administration.

If the model area is small or there is only one customer type, the component model can be very accurate for water demand modeling. Such a component model is the irrigation model from the FAO.[1] It will be presented in Sect. 4.4.1.1.

4.2.3   Knowledge Based Models

This type of models is based on the subjective knowledge of one expert or of a group of experts. This kind of model is not suited for a detailed water demand forecast, but the expert knowledge is essential for selecting the parameters of a time series or component based model. The expert knowledge is also important for the formal validation of a model.

A further way to use the expert knowledge can be to extend time series and component models with extra causal dependencies. Therefore, the experts knowledge can be used with an expert system which can be based for example on fuzzy logic.

4.2.4   Partitioned Models and Sub-models

For modeling huge regions with different water users it is very effective to subdivide the model area in smaller *regions* and to use different models for different *customer groups*.

The resulting water demand is calculated via superposition. This means all the calculated results by the sub-models are summed up (Eq. 4.6). All sub-models must have the same time base, such as monthly, daily or yearly values.

$$wd(t) = \sum_{i=1}^{n} wd_i(t) \qquad (4.6)$$

---

[1] Food and Agriculture Organization of the United Nations.

4.2.4.1 Regions

When the model region is cut down in smaller regions differences in the structure and specific regional behaviors in the water use can be modeled in detail and the water demand projection can be more accurate.

The best way to divide the model region in smaller regions is to use the given circumstances such as administrative regions, different data sets for the sub-regions or different water consumers for the specific sub regions. Different customers can be agriculture with irrigation, a city or village and an industrial complex. For example, Fig. 4.4 shows a division of the model region Beijing in China. In this case, the administrative districts were used because for each district data sets with the past water use, population etc. were available.

4.2.4.2 Customer Groups

Different types of customers have a different water usage. This bases on the different behavior of each group. Customers with the same water usage behavior can be grouped together.

Fig. 4.4 Regional model areas (Example: Beijing, source: www.echinaexpat.com)
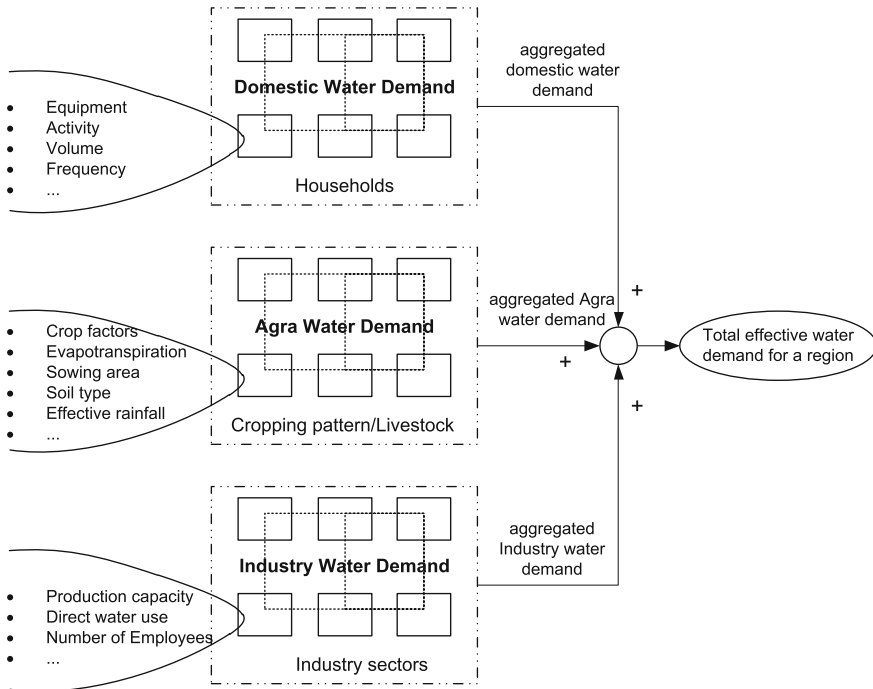
Fig. 4.5 Example for different water user groups

A different water usage has different reasons and requires different models. The information or data available for any customer group can also differ.

Figure 4.5 illustrates three customer groups: households, agriculture with farming and livestock and the industrial sector. Each group has its own influences on the water usage.

4.3 Parametrization

To parametrize a model, a set of data is necessary. The model quality and the predicted water demand depend on the chosen model as well as on the quality and quantity of the data, which is used for the training of the model.

To train the model usually historical data is used. It depends on the model type the forecast horizon and time steps, which kind of historical data is required. The time horizon can be short or long term; this has a direct impact on the forecast. Yearly data for the last 50 years cannot be used for an hourly forecast for the next three weeks. In this case, hourly measurements are needed. A daily data-set for one year can also not be used for a prediction for the next years, the time horizon of the training data

is to short. In summary, the selected model and the training data have to fit to the demands of the prediction.

When the historic data for the training is collected, the data set needs to be divided in two or more subsets for training and for validating the parametrized model.

The data which is collected usually has uncertainties because of measurement errors or unknown influences. To describe this issue a normal distribution with mean value and variance is assumed. The data sources can be measurements (e.g. from water meters) or statistics (e.g. population from the static yearbook).

This section describes the analysis of the influences of the different data-sets (e.g. water use, population, income, etc.) to each other using correlation tests. Linear regression with the least mean square algorithm and trend analysis will be used to calculate the model parameters using the historical data. And finally a method to prove the model quality will be presented.

4.3.1   Correlation

Most of the models presented in this chapter are linear. They describe the linear influence of the variables on the interesting variable. Here, the interesting variable is the water use. To test the linear dependency of one variable v_A to another v_B the correlation test is sufficient.

The correlation factor shows the linear dependency of these two variables

$$\rho(v_A, v_B) = \frac{cov(v_A, v_B)}{var(v_A)var(v_B)} \tag{4.7}$$

with $\rho \in [-1; +1]$. The value 1 describes a fully linear dependency of the two variables, -1 the inverse and 0 no linear dependency, which are illustrated in Fig. 4.6.

Correlation factors and significance tests such as the t-test (Sect. 4.3.3) can be used to determine the significant input values for the model. Figure 4.7 shows different
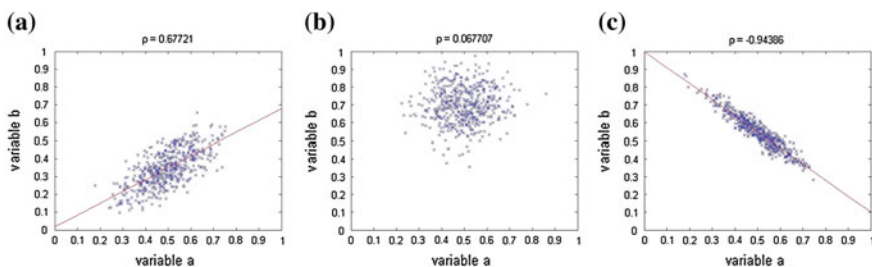
Fig. 4.6 Linear correlation scatter plots of data sets. **a** Positive correlated. **b** Uncorrelated. **c** Negative correlated
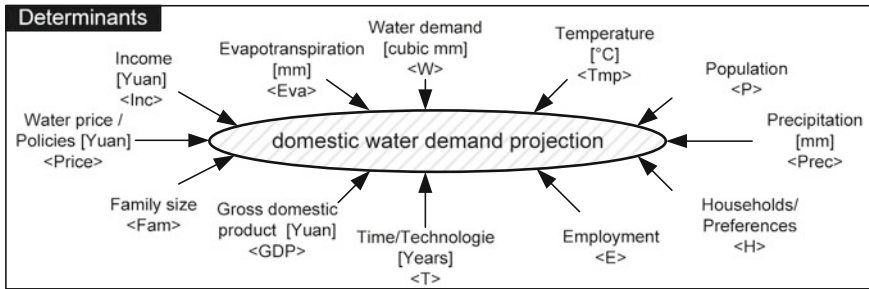
Fig. 4.7 Possible determinants for domestic water demand

Table 4.1 Correlation coefficients for the possible determinants

	T	P	GDP	H	Tmp	Prec	E	W	gdpc
T	1.000								
P	**0.934**	1.000							
GDP	**0.991**	**0.928**	1.000						
H	**0.993**	**0.947**	**0.996**	1.000					
Tmp	0.047	−0.199	0.079	0.002	1.000				
Prec	−0.546	−0.413	−0.489	−0.486	−0.243	1.000			
E	0.406	0.548	0.501	0.499	−0.133	0.069	1.000		
W	0.183	−0.016	0.078	**0.676**	0.332	−0.500	**−0.777**	1.000	
gdpc	−0.294	−0.537	−0.373	−0.384	0.382	−0.199	**−0.899**	**0.824**	1.000

influences on a water demand model. Such an analysis is done in [179], the results with the significances are presented in the Table 4.1.

The bold values in Table 4.1 are the significant determinants. It shows that not all possible determinants influence the resulting value, here the water demand, significantly. The model also gains more robustness when the possible model parameters are reduced.

4.3.2 Linear Regression and Trend

When the linear model is selected and the data set for parametrization the model is prepared linear regression can be used to gain the model parameters. This algorithm minimizes the least square error between the model and the training data set with the quality function Q (4.8).

$$Q = \|\underline{e}\|^2 = \sum_{k=1}^{n} e(k)^2 \tag{4.8}$$

$$y_{model}(k) = a_0 + a_1 u(k) + a_2 u^2(k) + \cdots + a_i u^n(k) \tag{4.9}$$

Table 4.2 Population of Beijing

Year $u(k)$	1996	1997	1998	1999	2000	2001	2002	2003	2004	2005
Population (10^6) $y_{data}(k)$	12.59	12.4	12.46	12.57	13.64	13.83	14.23	–	–	–
Population (10^6) $y_{model}(k)$	12.32	12.62	12.93	13.23	13.54	13.84	14.15	14.45	14.76	15.06
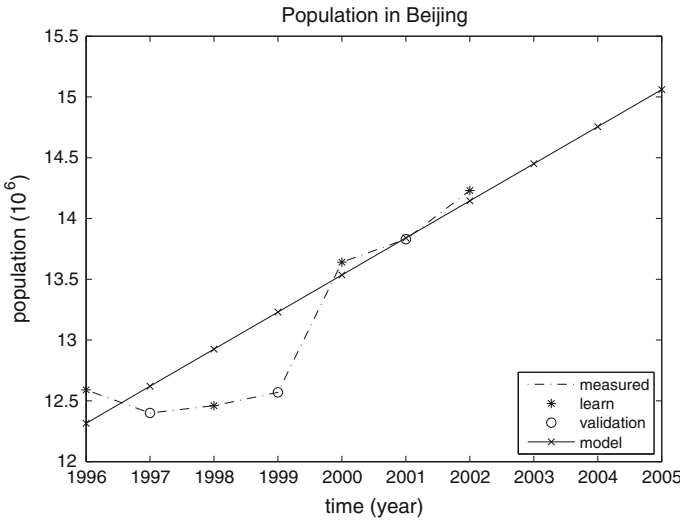
Fig. 4.8 Plot of the data from Table 4.2

When using a bivariate linear model (4.9) the resulting value $y_{model}(k)$ at measurement k from n measurements, can be calculated and compared with the measured value $y_{data}(k)$, which gives the modeling error e (4.10). The variables a_i with $i \in [0; n]$ are the model parameters and $u(k)$ is the input variable.

$$e(k) = y_{data}(k) - y_{model}(k) \tag{4.10}$$

The calculated model can be also interpreted as trend in the data-set when the time is the input value u.

The example in Table 4.2 illustrates the examination of the model parameters from the population time series from Beijing city. The model used for this example is $y_{model} = a_0 + a_1 u(k)$. The identified parameters are $a_0 = 12.315$ and $a_1 = 0.305$. The data from the measurements and the results of the model are shown in Fig. 4.8.

4.3.3 Model Quality

To prove if the calculated model approximates the measured data correct, it has to be validated. Therefore, different metrics exist. One of them is the sum of the quadratic

residuals S_R and another residual statistical dispersion s_R. The S_R is in the same way calculated such as Q in (4.8). The calculations of S_R and s_R are shown in formula (4.11) and (4.12).

$$S_R = \sum_{k=1}^{n} (y_{data}(k) - y_{model}(k))^2 \tag{4.11}$$

$$s_R = \frac{1}{n-l-1} S_R \tag{4.12}$$

with l as number of calculated parameters and n as number of measurements.

4.3.3.1 Modified T-Test

The modified t-test can be used to test the model parameters a_i for their significance and it utilizes the student's t-distribution.

In general, significance tests are done like this: First, the hypothesis is made, here the H_0-hypothesis. This means, it is assumed that the interested parameter is zero ($a_i = 0$) or not significant. Then, with formula (4.13) the t-value is calculated and finally compared with the $t_{\alpha,f}$-value from the distribution. The value α is the level of significance and f the degree of freedom.

$$t = \frac{|a_{i,model} - a_i|}{\sqrt{var(a_{i,model})}} \tag{4.13}$$

If the degree of freedom f is bigger than 30, the student's t-distribution can be approximated by a standard normal distribution.

4.4 Applied Models

The former two sections presented different fundamental model structures and concepts. They introduced a basic algorithm to identify linear model parameters and to validate them.

This section shows models applied for the water demand analysis and forecasts developed by different research and interest groups. In this section they are compiled together, modified and applications of these models for different customer groups are presented. All the previously discussed basic models are the foundation for these specific models:

The *International Model for Policy Analysis of Agricultural Commodities and Trade (IMPACT-Water)* was developed as framework to analyze the availability of water on food supply, demand and prices. Rosegrant describes this model framework in [275, 277].

WaterGAP 2.1 (Water—a Global Assessment and Prognosis) is a global water availability and use model and is described in [1, 72, 82–84]. It was developed to be able to evaluate the sustainability of water resources. This model is subdivided in a global hydrology model and in a global water use model. The model for the water use consists of models for households, industry and agriculture. It has a global approach and models the water demand of wide areas of the different continents.

The *FAO-Model for irrigation* is presented in [3], published by the Food and Agriculture Organization of the United Nations. The authors describe a component based method to calculate the irrigation water demand of an specific crop. It can also be used by the single farmer to calculate the their plantations directly.

The *IDWR-Model* was developed by the Idaho Department of Water Resources (IDWR). The publication [66] examines the situation of the Ada and Canyon counties, which had a significant population growth and an increasing demand of water. This situation is also applicable for developing regions such as Beijing.

The models described in this section are subdivided in their usage for the three main consumer groups: agriculture with irrigation and stock farming, industry and households. Not all models are described in detail for every customer group. Often, the water use cannot be subdivided in different kinds of users, especially when the people live and work on the same place. As mentioned in Sect. 4.2.4, when the data for different consumer groups are available, it is the best to introduce different models to reproduce the different water use behaviors.

4.4.1 Agriculture

Many regions with water shortage are located in arid or semi arid areas. A significant amount of water is used for food production. It is used to irrigate the plantings and for stock farming.

The water demand calculation for irrigation is suited for the use of component based models. Mostly, a crop consists of a single kind of plants which are grown. The farmers know usually in advance what will be planted in the next years. In this situation, a direct component based model, such as the FAO-model or the IMPACT model, is the best solution to estimate the water demand of these plantings.

4.4.1.1 FAO-Model

The main calculation steps of this model are summarized in Fig. 4.9 and described in detail in [43]:

- calculation of the water need for standardized crop (like grass),
- adapting the water need for the specific crop using scaling factors and
- compare the calculated water need with the rainfall to get the irrigation water need.
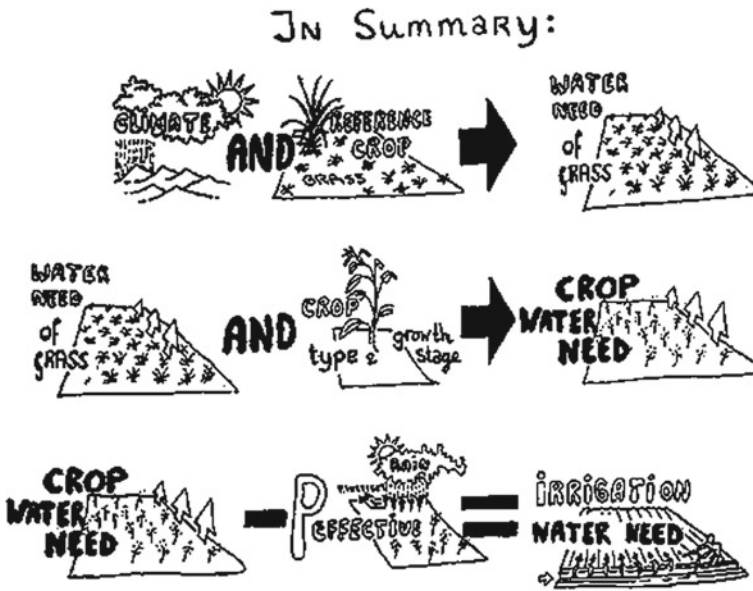
Fig. 4.9 FAO model calculation steps [41]

The first step is to calculate the water need or the evapotranspiration (=transpiration + evaporation) (Fig. 4.10) of the reference crop ET_0: By definition, it concerns thereby a large surface of green grass, which is 8–15 cm high, grows actively and does not suffer from water scarceness. The value for the evapotranspiration of the reference plant RT_0 results from the climatic condition, such as temperature, air humidity, duration of sunshine and wind velocity of the region. It can be gained from experiments like the pan evaporation method [42] or calculated using the Blaney Criddle method [313].

The Blaney Criddle method needs the monthly average temperature $\bar{\vartheta}$ as well as the mean daily duration of sunshine p in percent (%) for computation of ET_0 (Eq. 4.14).

$$ET_0 = p\left(0.46\bar{\vartheta} + 8\right) \text{ [mm/day]} \tag{4.14}$$

Table 4.3 lists the values for p, relevant for Beijing, which is a function of the degree of latitude. The monthly average temperature $\bar{\vartheta}$ can be gained from measurements in the regarded region, e.g. from statistical yearbooks. The temperature for the model region Beijing is shown in Table 4.3. Tables 4.5 and 4.6 show exemplary the temperature and the calculated ET_0 values for the Beijing area.

With the value for the evapotranspiration of the reference plant ET_0 the water requirement of the specific plant ET_{crop} can be calculated as the second step of the FAO-model. The water requirement ET_{crop} depends on the kind of plant, development stage as well as on the period between sowing and harvest. Because of that it is
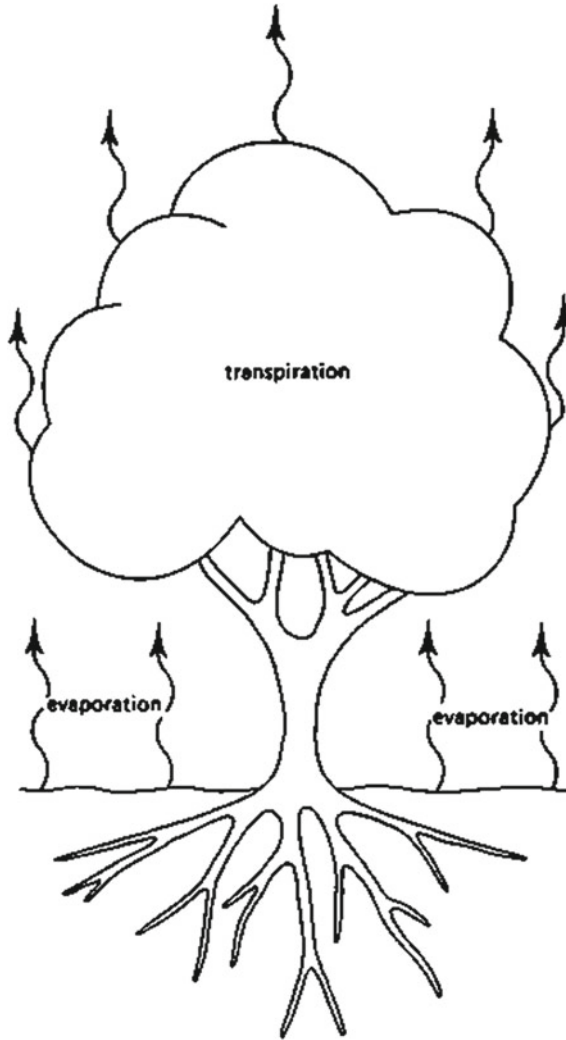
Fig. 4.10 Evapotranspiration [41]

Table 4.3 Daily portion of the annual duration of sunshine in % for the Beijing model region [43, 164]

	Jan	Feb	Mar	Apr	May	Jun	Jul	Aug	Sep	Oct	Nov	Dec
p	0.22	0.24	0.27	0.30	0.32	0.34	0.33	0.31	0.28	0.25	0.22	0.21
ϑ	−4.7	−1.9	4.8	13.7	20.1	24.7	26.1	24.9	19.9	12.8	3.8	−2.7
ET_0	1.28	1.71	2.76	4.29	5.52	6.58	6.60	6.03	4.80	3.48	2.14	1.42
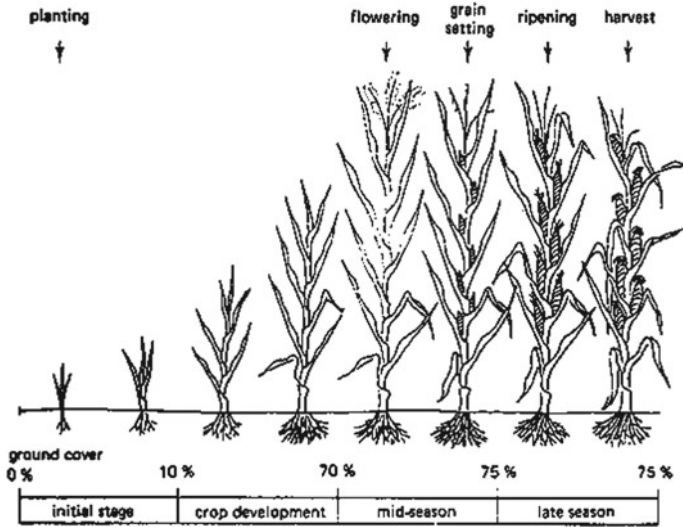
Fig. 4.11 Growth stages [41]

appropriate to define several growth phases (four phases in [43], shown in Fig. 4.11) for each plant and to assign a crop factor k_c for each single growth phase. The daily water demand of the plant ET_{crop} results from the product $k_c \cdot ET_0$. Table 4.4 shows exemplary crop factors for different plants.

The last step to determine the irrigation water requirement, is the determination of P_{eff}. In [43] the P_{eff} results from the monthly precipitation P in accordance with Eq. (4.15).

$$P_{eff}[\text{mm/month}] = \begin{cases} 0.8P - 25, P > 75\,\text{mm/month} \\ 0.6P - 10, P \leq 75\,\text{mm/month} \end{cases} \tag{4.15}$$

Since different growth phases can fall into one month, results the monthly value for k_c as average value of the k_c-values in this month of the growth phases, weighted by the length of each growth phase in the regarded month. The difference between the crop water need ET_{crop} and the effective precipitation P_{eff} results in the irrigation water requirement IWD_{FAO} (Eq. 4.16).

$$IWD_{FAO} = ET_{crop} - P_{eff} \tag{4.16}$$

To demonstrate the application of the FAO-model an example crop consisting of a plantation of corn is used. The sowing time is April 2001 in the area of Beijing.

The climatic data in Table 4.5, which correspond to average values of the model area, serves as basis for the water demand calculation. The monthly values for reference evapotranspiration ET_0 (Eq. 4.14) and the effective precipitation P_{eff} (Eq. 4.15) listed in Table 4.6 are obtained using the climate data from Table 4.5 and the

Table 4.4 Crop factors k_c for different plantations and growing phases [41]

Crop name	Month of sowing (1–12)	Length of phase 1 (days)	Crop factor of phase 1	Length of phase 2 (days)	Crop factor of phase 2	Length of phase 3 (days)	Crop factor of phase 3	Length of phase 4 (days)	Crop factor of phase 4
Rice	5	30	1.1	30	1.15	60	1.2	30	1
Winter wheat	11	30	0.35	140	0.75	40	1.15	30	0.45
Corn	4	30	0.4	50	0.8	60	1.15	40	0.7
Tubers	4	30	0.5	35	0.8	50	1.1	30	0.95
Soy bean	6	20	0.35	25	0.75	75	1.1	30	0.6
Cotton	3	45	0.45	90	0.75	45	1.15	45	0.75
Oil bearing crops	3	25	0.35	40	0.8	65	1.15	50	0.35
Vegetable	6	25	0.45	35	0.7	50	0.9	20	0.75
Melon	5	25	0.45	35	0.75	40	1	20	0.75
Forage	3	10	0.5	30	0.7	110	0.9	100	0.85

Table 4.5 Monthly average temperature ϑ and amount of precipitation P in Beijing

	Jan	Feb	Mar	Apr	May	Jun	Jul	Aug	Sep	Oct	Nov	Dec
ϑ in (C)	−4.7	−1.9	4.8	13.7	20.1	24.7	26.1	24.9	19.9	12.8	3.8	−2.7
P in (mm)	4	5	8	17	35	78	243	141	58	16	11	3

Table 4.6 Reference value of the evapotranspiration ET_0 and effective precipitation P_{eff}

	Jan	Feb	Mar	Apr	May	Jun	Jul	Aug	Sep	Oct	Nov	Dec
ET_0 in (mm/day)	1.28	1.71	2.76	4.29	5.52	6.58	6.60	6.03	4.80	3.48	2.14	1.42
P_{eff} in (mm)	0	0	0	0.2	11	37.4	169.4	87.8	24.8	0	0	0

Table 4.7 Crop factor distribution, water requirement of the plant and the irrigation water need (*IWN*) for corn

Month	Crop factor k_c	ET_{crop} (mm)	IWN (mm)
Apr	30 Days 0.4	51.48	51.28
May	30 Days 0.8	132.48	121.48
Jun	20 Days 0.8	180.95	143.55
	10 Days 1.15		
Jul	30 Days 1.15	227.7	58.3
Aug	20 Days 1.15	180.9	93.1
	10 Days 0.7		
Sep	30 Days 0.7	100.8	76
Sum		874.31	543.71

Eqs. (4.14) and (4.15). The crop factors for the four growth stages (Fig. 4.11) are taken from Table 4.11.

From the periods of the crops growth phases results the distribution of the k_c values, on whose basis the water requirement by corn ET_{crop} is determined. The last column in Table 4.7 contains the irrigation water requirement, thus of $ET_{crop} - P_{eff}$.

In the case of a cultivated area of 100,065.3 hectares, a total amount of $wd_{FAO} = 573.71 \, l/m^3 \times 100,065.5 \, ha = 5.74 \times 10^{11} \, l = 574$ billion m^3 water for irrigation is needed.

The Fig. 4.12 shows the yearly irrigation water demand for rice, corn and wheat in comparison. In the computation of the irrigation water demand by rice another characteristic has to be considered. Because the rice fields need a permanent water layer for weed control, a further term comes in addition to the irrigation water requirement, which results from the evapotranspiration of the plants. This serves the saturation of
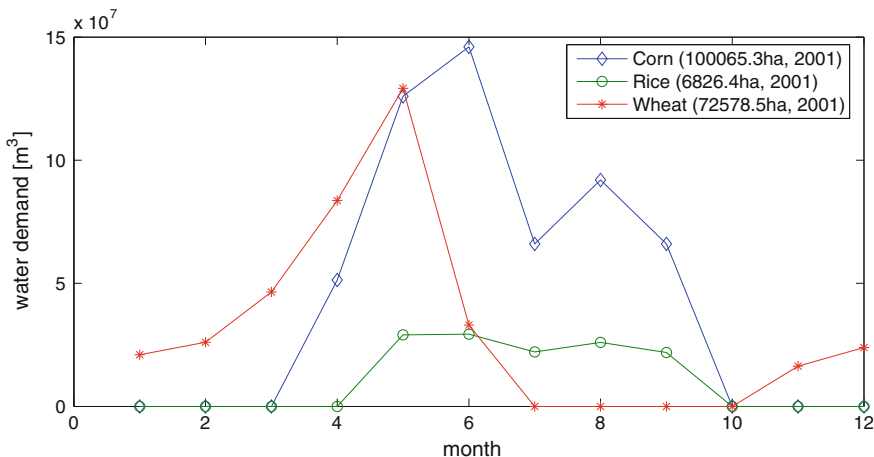
Fig. 4.12 Irrigation water demand for corn, rice and wheat

the soil with water and for the maintenance of the water layer. How this additional irrigation water requirement is calculated, can be read in [42].

4.4.1.2 IMPACT-Model for Irrigation

The IMPACT partial model for the irrigation water requirement [276] is based to a large extent on the model of the FAO, however still brings two extensions with itself. The Eqs. (4.17) and (4.18) contain the regulation for the computation of the irrigation water requirement *IWD*.

$$NIWD = \sum_{cp} \sum_{st} \left(k_c^{cp,st} ET_0 - P_{eff} \right) AI^{cp} \left(1 + LR \right) \tag{4.17}$$

$$wd_{irrigation} = NIWD/BE \tag{4.18}$$

First the net irrigation water requirement (*NIWD*) is computed. As in the case of the FAO model we use the crop factor k_c, the reference evapotranspiration ET_0 and the effective precipitation P_{eff}. The difference from the water requirement of the plant and the P_{eff} is multiplied by the irrigated area of arable land AI^{cp} as well as by a "salt leaching factor' *LR* [276] that depends on the salt content of the soil and the irrigation water. This must take place for all cultivated plants with their respective growth phases. Therefore, the summation over the crop index *cp* and the index of the growth phase *st*. The entire irrigation water requirement IWD results from the quotient of net irrigation water requirement and the Basin efficiency *BE*.

4.4.1.3 IMPACT-Model for Stock Farming

The IMPACT model contains also a suggestion on the computation of the water requirement of the livestock $wd_{livestock}$ (Eq. 4.19).

$$wd_{livestock} = QS \cdot w \qquad (4.19)$$

whereby QS, the number of livestock, is multiplied by the specific water consumption w. This simple model assumes that the specific water requirement for a agricultural product remains constant. Details like the growth condition of the animal or the kind of the watering places remain unconsidered.

4.4.2 Industry

The second large consumer group is the industry. When regarding different subgroups, such as mining, production, commercial, hotel etc. industrial sectors. It is the best to calculate the water demand for each group or sector separately and sum it up to get the whole water demand.

4.4.2.1 IMPACT-Model for Industrial Water Demand

The IMPACT water demand calculation model for the industrial water requirement wd_{ind} developed by [276] is a socio-economic model. This model depends on three variables: the gross domestic product per capita $GDPC$, the total population pop in the model area, as well as the time t (Eq. 4.20).

$$wd_{ind} = IWDI \cdot (GDPC \cdot pop) \qquad (4.20)$$

with

$$IWDI = \alpha + \beta \cdot GDPC + \gamma \cdot t \qquad (4.21)$$

The gross domestic product for each inhabitant $GDPC$[2] and the time variable t, which represents the technological progress, are measured variables of the industrial water demand density $IWDI$. The $IWDI$ is the water requirement standardized on the gross domestic product GDP (Eq. 4.21).

The parameters α, β and γ must be determined via regression (see Sect. 4.3) from the water requirement and the gross domestic product per capita $GDPC$ of the past. The parameter γ is usually negative, because it is assumed the industrial water requirement density decreases with increasing technological progress.

---

[2]Gross domestic product per capita.
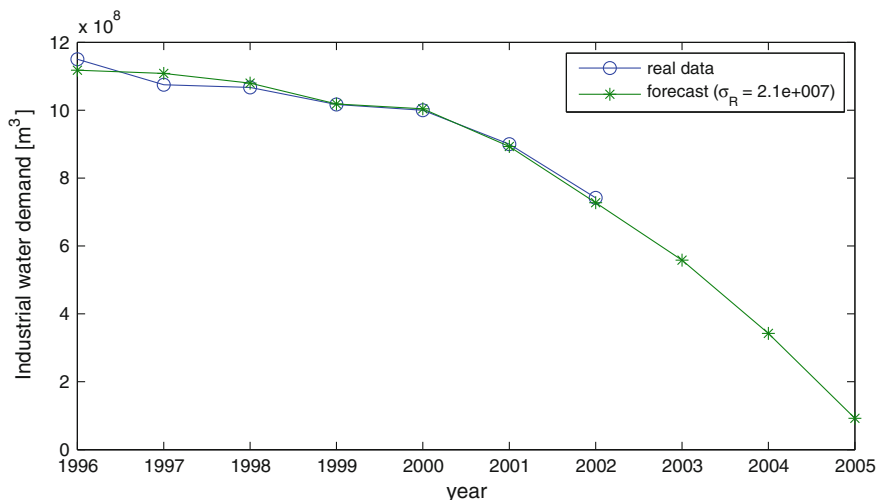
Fig. 4.13 Industrial water demand

Figure 4.13 shows the results of the model for the total industrial water demand of the model region Beijing. The model can also be used to forecast the water demand of the three different industrial sectors (primary, secondary and tertiary) as mentioned in Sect. 4.2.4.2.

The circles show the real values and the stars the calculated values from the model. The last two values are forecasted. The decrease in water demand is also due to the progress in technology and increase in water prices.

4.4.3 Domestic/Households

The water demand of this customer group is the most difficult calculable, especially in developing countries without detailed water metering of each household. Private water wells are also used for the water supply of the households. They cannot be measured by the water authorities and have a deep impact on the groundwater resources, when heavily used by many households of a specific region (see Sect. 2.3). A second difficulty evolves out of the situation that most of the water usage of households in developing countries cannot be separated in industrial and domestic water use because many families work and live at the same place.

Additionally, the high variability of the explicit water usage in the different households is the reason why direct modeling approaches cannot be used. The IWDR-model for domestic water demand calculation is an indirect model, the previous water demand and other influencing variables are used for forecasting (see Sect. 4.2.1).

4.4.3.1 IDWR-Model

The IDWR model, described in [67], inherits descriptions of water requirement models for the domestic water users: One of these model descriptions determines the water need of an average household. Another model, which is part of the IDWR model, examines the influence of the water price on the water requirement. And the third sub-model can be used for a long-term forecasts of the future household water requirement.

The initial description of all these three models is the Eq. (4.22):

$$w = f(p, y, D, g, k, v). \tag{4.22}$$

The water requirement w of an average household is a function of the water price p, the households income y, the residence density D, the customer preferences g, the number of persons in each household k and the weather v. But, for these parameters we usually don't get any complete data-set.

To reduce the number of input variables for the resulting model and to get a improved model stability a main component analysis with the examination of the correlation factors between the variable as described in Sect. 4.3.1 needs to be done. With the identified variables that have the most significant influences on the water requirement the model can be formulated and the parameters identified. The following example illustrates the identification of the most significant input variable and the resulting model description.

To apply the model, a data-set for the domestic water use form the city of Beijing is used. The input variables of the IDWR model are analyzed using the total, partial and multiple correlation coefficients. These correlation coefficients describe the linear dependency between each input variable among themselves and the water use as the output variable of the model. The variables to describe the weather influences are the annual average temperature and yearly precipitation.

The correlation coefficients were computed only for the variables water requirement DWD of the households, time, total population, gross domestic product GDP and the number of households. The results are shown in Table 4.8.

The analysis of the partial correlation coefficients shows that the values of the GDP and the time have the largest influence on the DWD. A simple and understandable regression model based on the connection between the water demand and gross

Table 4.8 Total (top left), partial (bottom right) and multiple correlation coefficients

	Pop.	DWD	GDP	Househ.	Time
Pop.		0.341	0.934	0.919	0.900
DWD	0.095		0.461	0.538	0.606
GDP	0.344	−0.620		0.994	0.984
Househ.	0.179	−0.410	−0.061		0.996
Time	−0.275	0.752	0.714	0.735	
Multiple	0.945	0.977	0.999	0.999	1.000
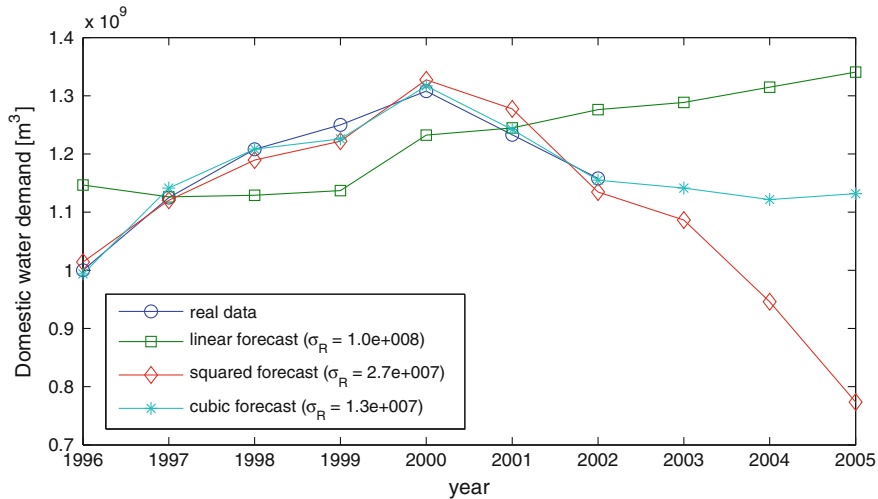
Fig. 4.14 Domestic water demand using different forecasting models

domestic product per capita can be developed: A polynomial approach of up to the third degree can be used as described in Eq. (4.23).

$$wd_{dom.}(t) = \alpha + \beta GDPC(t) + \gamma GDPC(t)^2 + \delta GDPC(t)^3 \qquad (4.23)$$

To apply the model identified by the component analysis and to compare the influences of the linear, quadratic and cubic terms three variations of this model are used to forecast the water demand: a linear forecast, an utilization of the squared relation between gross domestic product and water demand and finally, the usage of the third order dependency between GDPC and water requirement per capita.

The measured data used to train the models is plotted in Fig. 4.14 as circles. The resulting values are also shown as comparison in this figure.

The *linear forecast* of the domestic water demand is the simplest and in addition, a very robust method for estimating the future water requirement of the households. The entire water requirement of the households is for each year the product of estimated domestic water requirement per head and the estimated total population.

The only difference to the previous model implementation is that the water requirement is *squarely related to the GDPC*. The inhabitant-specific water requirement resulting from this model decreases however drastically as shown in Fig. 4.14. The square term is responsible for the strong decrease. For the given input values, this model appears quite unsuitable.

The *dependence of third order* between GDPC and water requirement per capita shows a very good adjustment of the model values up to the real water requirement. The future development of the water demand follows a "smooth" process. It has a smaller tendency to decrease than the square model, stagnated however not, as it is in the linear case.

4.5 Summary

A water supply system is a composition of different elements which have to work together. Generally, there is a source, a distribution system and a consumer for water or any other resource. The water sources were explained in Chap. 2 and the distribution system in Chap. 3. This chapter shows different models and methods to examine and forecast the water consumption and demand. The actual and future water demand as well as the water consumption is essential for the planning and the operation of water resource systems.

This chapter presented the need of water usage models to plan and operate water management systems. It is also an important input variable for optimizing water supply systems. Therefore, different basic models and modeling approaches were introduced. They are the foundation for the applied models such as the FAO, the IMPACT, the IWDR and the IMPACT-Water models, which were also discussed for the three main consumer groups.

Chapter 5
Model Based Decision Support Systems

Divas Karimanzira

5.1 Introduction

This chapter describes a decision support system framework specifically developed to meet the growing demands and pressures on water resources managers. A generic concept is designed to be applicable to a wide variety of specific water resources system configurations, institutional conditions, and management issues. The framework is based on a detailed model of the water resources system being simulated and include scenario planning in combination with state-of-the-art large scale network flow optimization algorithm. Issues from the demand-side such as water use patterns, costs, and water allocation schemes are considered equally well as supply-side issues such as reservoirs, and water transfers. The system applies integrated approach to simulating both natural (e.g., runoff, baseflow) and man-made components (e.g., reservoirs, groundwater pumping) of water systems. This allows the system user access to a more comprehensive view of the broad range of factors that must be considered in managing water resources for present and future use. The framework stresses out the sovereignty of the user, therefore features menu-driven graphics-based interfaces that facilitate user interaction and can be customized for water availability analysis, conjunctive surface and groundwater use, infrastructure planning, assessing irrigation potential and reservoir performance, estimating water supply capacity and to find equitable trade-offs among stakeholders requirements.

The issues in water resources management requiring rational decision making are increasing rapidly in complexity and thus such decisions are becoming more and more difficult, despite advances in methodology and tools for decision support in other areas of research. The following factors contribute to the increase of this complexity:

D. Karimanzira (✉)
Fraunhofer IOSB-AST, Ilmenau, Germany
e-mail: divas.karimanzira@iosb-ast.fraunhofer.de

1. Variability of the resource water in time and space. Almost all the consumable water emanates from precipitation (rain, snow, hail), which varies immensely over time and space. Most tropical and sub-tropical regions of the world are characterized by huge seasonal and annual variations in rainfall, often compounded by unpredictable short-term variations, e.g., in Beijing, 85 % of the rain falls between July and September. At times, 40–70 % of the rain falls within 3 days. Such variability manifoldly increases the demand for infrastructure development and the need to manage water demand and supply. The challenge in managing variability is clearly greatest in the poorest countries with financial and know-how scarcity to cope with the problem [237].
2. Water resources stakeholder[1] groups have very diverse, often conflicting goals and values, including interests in environment/ecology (e.g., control water pollution, provide for groundwater recharge, prevent damages from runoff), economy (e.g., obtain new water resources in order to increase food production, managing costs, improve navigation, generate hydroelectric power, providing for fishing and recreation opportunities), and control & protection (e.g., floods and drought control);
3. Many municipalities and water authorities often derive their water supplies from several sources, which may include surface reservoirs, rivers, groundwater wells or combinations of these sources. To identify the best combination of supply sources in the long term, or to determine the most effective way of managing existing systems, decision-makers need to handle a lot of information to account for all of the hydrologic, hydraulic, water quality, and economic relationships within the system;
4. The predictability of the boundary conditions under which water management has to perform is reduced by the increasing uncertainties due to climate and global change.

Traditional water management decision support systems emphasize on end-of-pipe solutions [244, 370], or command and control approaches [45]. As can be seen in [45, 370], limitations of these approaches are evident. The idea followed in this book is to achieve sustainability through the basic principles of efficiency, equity, and ecosystem integrity. Therefore, the following aspects are taken into consideration:

- Source control which is more in alignment with sustainable water management [237],
- Flexibility and adaptivity in management decision making,
- Participatory management and collaborative decision making [243, 244],
- More attention to management of human behavior,
- Common and shared information sources and
- Explicitly incorporating the environment in management goals [364]

---

[1]In this book stakeholder include all persons, groups and organizations with an interest or in an issue, either because they will be affected or because they may have some influence on its outcome. This includes individual citizens and companies, economic and public interest groups, government bodies and experts.

Several decision support systems for water resources management, which differ in complexity and completeness have been developed world wide [85, 158, 361, 364, 367]. RIBASIM [158], MIKEBASIN [158], IRAS (Resource Planning Associates, Inc.), IQQM (New South Wales Department of Infrastructure, Planning and Natural Resources, Australia [143] and WEAP (Stockholm Environmental Institute-Boston [364] are the most applied river basin management DSS's that incorporate most of the desirable attributes of a DSS.

A DSS and network flow model, MODSIM described in [191] and [361] is based on an optimization algorithm ensuring distribution of available water resources conform to physical, hydrological and institutional aspects of management. Initial model development at Colorado State University dates back to the 1970s. Since 1992 the U.S. Bureau of Reclamation Pacific Northwest Region has sponsored continued model improvement efforts. OASIS [159] developed by Hydrologics, Inc. is a general purpose water simulation model. Simulation is accomplished by solving a linear optimization model subject to a set of goals and constraints for every time step within a planning period. OASIS uses an object-oriented graphical user interface to set up a model, similar to ModSim. A river basin is defined as a network of nodes and arcs using an object-oriented graphical user interface.

Another complex DSS is WaterWare, which was developed through a European collaborative effort involving universities, research institutes, and commercial companies [98]. WaterWare is designed as a comprehensive decision support system for river basin planning that combines advanced technologies including geographic information systems, database technology, modeling techniques, optimization algorithms, and expert systems. WaterWare also utilizes rule-base concepts for developing operating criteria and policies, but is a proprietary modeling system requiring expensive licensing.

A reservoir and river basin simulation and optimization modeling environment ideal for evaluating operational policy, system optimization, water accounting, water rights administration, and long-term resource planning is RiverWare. It is under development since 1990 at the Center for Advanced Decision Support for Water and Environmental System, University of Colorado [367]. RiverWare is customized using the RiverWare Policy Language(RPL) for developing operational policies for river basin management and operations. A rule editor allows users to enter logical expressions in RPL defining rules by which objects behave, as well as interrelationships between objects for simulating complex river basin operations. As an interpreted language, RPL is far less computationally efficient than compiled code. Extensive, complex rule bases are required for priority-based water allocation in a river basin, and RiverWare is deficient in stream aquifer management tools for conjunctive use of surface and groundwater resources.

HEC-PRM [93] is a generalized computer program that performs deterministic network flow optimization of multi-reservoir systems. PRM "prescribes" optimal values of flow and storage over time by minimizing penalty functions at selected locations in the water resources network. Penalty functions associate a penalty or reward (benefit function) with designated levels of flow or storage. Because a given location (flow reach or reservoir) can have several competing objectives, a separate

penalty curve for each objective can be included in the model. Optimization with a Network Flow Programming with gains algorithm enables relatively fast run times for large systems but restricts constraints to capacity limits and mass balance at nodes. PRM has been applied to several large multi-reservoir river systems, such as the Columbia system, the Missouri system and the entire state-wide water resource network of California.

CalSim, as described in Draper [85], was developed by the California Department of Water Resources as a generalized river basin management DSS. Its specific application to joint operation of the Federal Central Valley Project (CVP) and the California State Water Project (SWP) is embodied in CalSim II. CalSim allows customized specification of objectives and constraints in strategic planning and operations without the need for reprogramming of complex models through use of an English-like modeling language called WRESL (Water Resources Engineering Simulation Language). CALSIM uses a mixed-integer linear programming solver to route water through the river network at each time step (in contrast to the traditional Out-of-Kilter algorithm of OASIS or the more efficient Lagrangian approach of ModSim). CALSIM lacks a comprehensive graphical user interface for constructing and editing the river basin system topology, as well as effective mechanisms for considering conjunctive use of surface and groundwater resources. Computations in CalSim are confined to monthly time steps without consideration of flow routing, and CALSIM is ill-suited for evaluating legal issues related to water and storage rights for priority-based water allocation.

These DSS's features very good quality for many applications regarding physical and hydrological nature of water resources system, but each lacks one or the other import characteristics of a DSS such as effective customization capability (particularly with respect to understandability, simplicity, vast data requirements), which limits the adaptability and therefore the applicability to unique river basin conditions.

5.2 Framework for the Model Based Decision Support System

The idea behind the framework of the model based decision system is to apply simulation models, optimization and forward looking scenario planning to make decisions.

5.2.1 Decision Making Models and Information System

In the framework, the DSS is divided into two parts. The first part provides the opportunity to evaluate "what if" scenarios through simulations (Fig. 5.1). In this scheme, the user enters different values for parameter of interest and then examining the values that are generated as output for making decisions. Several scenarios are
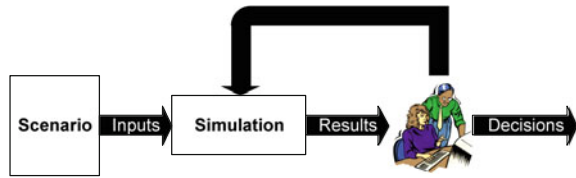
employed to assess future situations and prove various hypotheses. The analysis aims
to see the possible reasoning behind each scenario and how chosen scenario affects
final output of the model. One can change all or some of the conditions (i.e., rainfall
and water demand boundary conditions, options of flood control gates operations)
and compare the results of the various simulations. In this part attention is pared
more to the reproduction of the real system. Therefore, complex and detailed models
for surface water (Saint Venant equations) and groundwater (Finite Element models)
as decribed in Chap. 2 should used.

The second part of the framework supports a search process for the most attractive
decision option. In this case the role of the decision makers is essentially to specify
aspirations concerning the various interests, the desired attributes of the hydrologic
and water-resource management systems (such as minimum stream flow require-
ments or maximum allowed groundwater level declines). The model then supplies (if
possible), from a set of several possible strategies, a "how to" scenario that best meets
the desired attributes. This can be based on various analytical decision support tools,
including optimization algorithms or solvers, together with models in analytical form.
However, in some cases, the model may determine that none of the possible strategies
are able to meet the specific set of management goals and constraints. Such outcomes,
while often not desirable, can be useful for identifying the hydrologic, hydrogeologic,
and management variables that limit water resources development and management
options. The core of the second part is a coupled simulation model with a numerical
search method for optimizing decision variables as illustrated in Fig. 5.2. Here com-
putational effort for solving the optimization problem should be considered, hence
the detailed and time consuming models used in part 1 need to be reduced to have less
parameters. After the optimization process using the reduced models, the results can
then be verified using the detailed models. The decision process follow a nonlinear,
step-by-step process, with data entering the process, analysis being performed, and
decisions being taken in an almost continuous fashion [214].

The quality of the decisions depends principally on the information available
for decision making. Therefore, the decision support system consists primarily of a
high sophisticated information system. In a real world application, several sources
of information or databases, more than one problem representation or model, and a
multifaceted and problem oriented user interface, ought to be combined in a common
framework to provide realistic, timely, and useful information. Typical data required
by a water management DSS is listed in Table 5.1.

The models are linked to database and linkage between the models is by means
of time series of flow or water demand that summarize the output from one model as
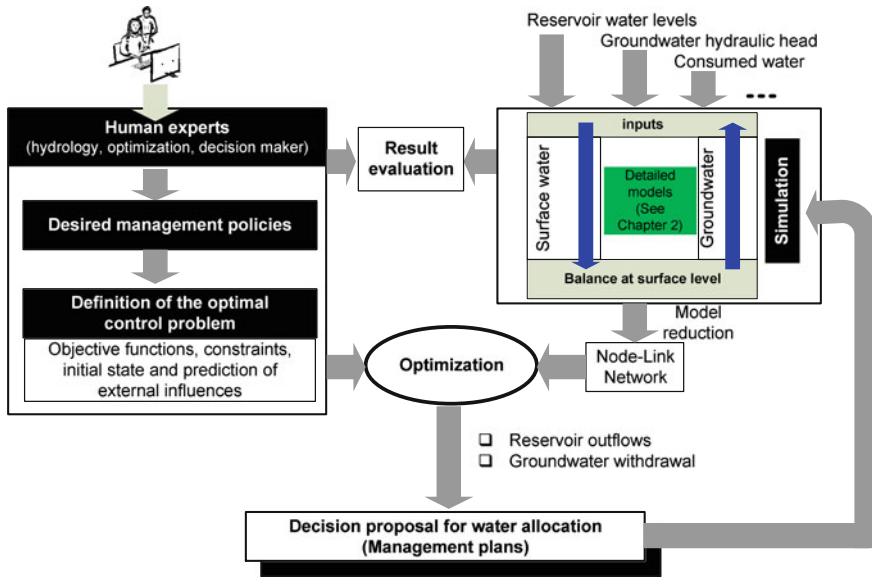
Fig. 5.2 The decision support model

Table 5.1 Typical data required by the decision support system

Category	Description
Institutional guidelines	Institutional guidelines in which management decisions are to be made, such as laws pertaining to the allocation of water to various users and the various standards (e.g., quality standards) set by public health and environmental agencies
Targets	Targets, specified from the manager of the hydrosystem (e.g., water supply, flood control, environmental protection, power production)
Time series	Water quantity and quality demands over time and space
Climatic factors	Climatic factors such as temperature, wind, solar radiation, and rainfall
Land-use and geomorphic information	Land-use and geomorphic information (e.g., slopes, drainage density, geology, soils, land covers, channel cross-sections, and groundwater depths)
Physical constraints	Physical constraints, due to project attributes (e.g., storage capacity)
Hydraulic and hydrologic data	Hydrologic data that include flows, water levels, depths, and velocities
Pollutant loads	Pollutant loads from point sources (e.g., cities, industries, and wastewater treatment plants that discharge their wastes into surface waters and pollutant loads from nonpoint sources that enter surface waters along an entire stretch of the river, channel or reservoir
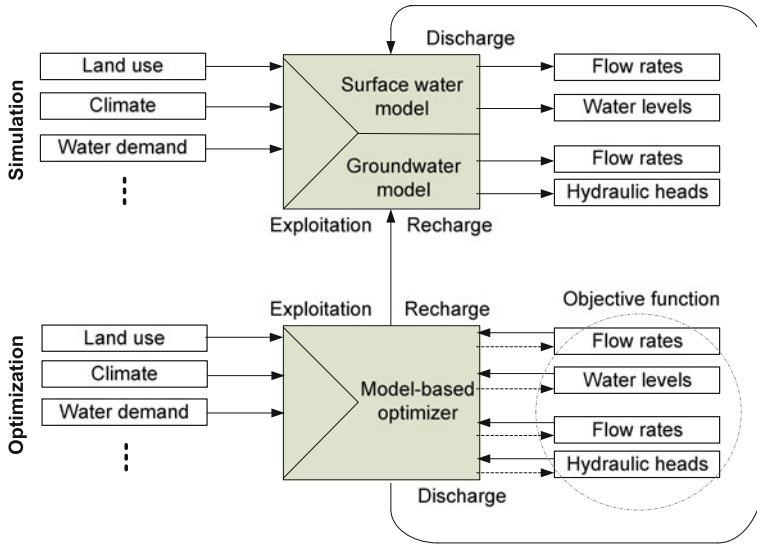
Fig. 5.3 Coupling the simulation and optimization models

boundary conditions and dynamic inputs for another. Surface water and groundwater models are coupled by means of quantifications of infiltration and groundwater recharge as well as the determination of spring yield from ground water recharge and abundance. The coupling between simulation and optimization allows the advantages of both modules to be retained within a single framework (see Fig. 5.3) and comprises two stages. Stage 1 involves the exchange of information shown in Fig. 5.3 between the reduced simulation models and the optimization algorithm during the optimization process. The second stages involves passing the optimization results to the detailed simulation models for verification.

5.2.2 Organizing Module and Scenario Planning

Besides the models and the database, the DSS framework also contains an orgainizing module (see Fig. 5.4), which holds responsibility for the overall organization and the decision process. This component is often implemented as part of the human machine interface and, therefore, usually it is not mentioned separately. The organizing module is composed of several logical components including components for database management logic, data assignment logic, model control logic, execution logic, reporting logic, feasibility check logic and organizational logic. The information to implement the logic for these components should be acquired during requirement analysis. The organizing module links together all other parts of the DSS using the information provided by the user in the HMI, is responsible for data handling (including access to data and archiving any information that a user may want to store)—controlled by the database management logic and the data
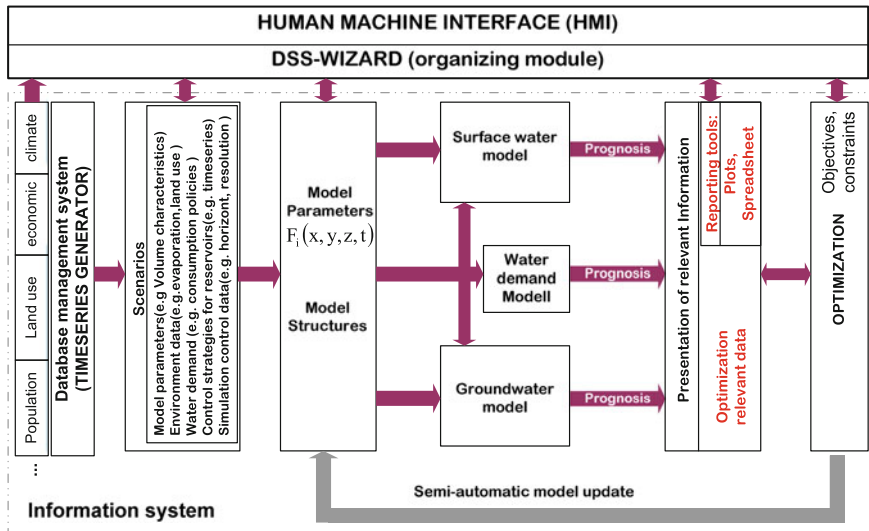
Fig. 5.4 The organizing module

assignment logic, and the order of using various other parts of the DSS controlled by the model control logic, organizational logic and the execution logic. In short, the organizing module has to check whether a particular module is required or can be used at a given stage of the decision process (e.g., if all steps that provide a consistent set of data have been executed), which is controlled by the pausability check logic (see Fig. 5.5). The organizing module is also used to assist model calibration and testing, the user can select partial running of the model chain (e.g., only simulation using the detailed models, or optimization and then simulation), providing flexibility to facilitate scenario assessment. Scenarios combine descriptions of situations with intentions or proposals for an optimal handling of such situations. As Fig. 5.4 shows, scenarios will be transformed into specific sets of input parameters for the existing models. With these parameters and possibly changes of model structures, the models will calculate prognosis data to be presented to the human decision makers. The human decision makers will then evaluate the proposals of the respective scenarios with regard to the detailed model outputs. The loop into the scenarios will close resulting in changes of the scenarios.

Because future events are unknown in advance, risk estimates (projections) are inherently uncertain, yet there is a need to take decisions and develop strategies that will impact on this uncertain future. The organizing module provides water managers with a powerful tool for scenario planning and dealing with future uncertainties to develop strategies that are robust to a range of potential future scenarios. Scenario planning examines important "What if...?" questions that involve large uncertainties in the external influences on water systems. Unlike strategic planning, which postulates a single future, scenario planning looks at several alternative versions of the future, any one of which may or may not come about. Their use in the DSS allows

Fig. 5.5 Organizatorial logic for scenario planing and execution
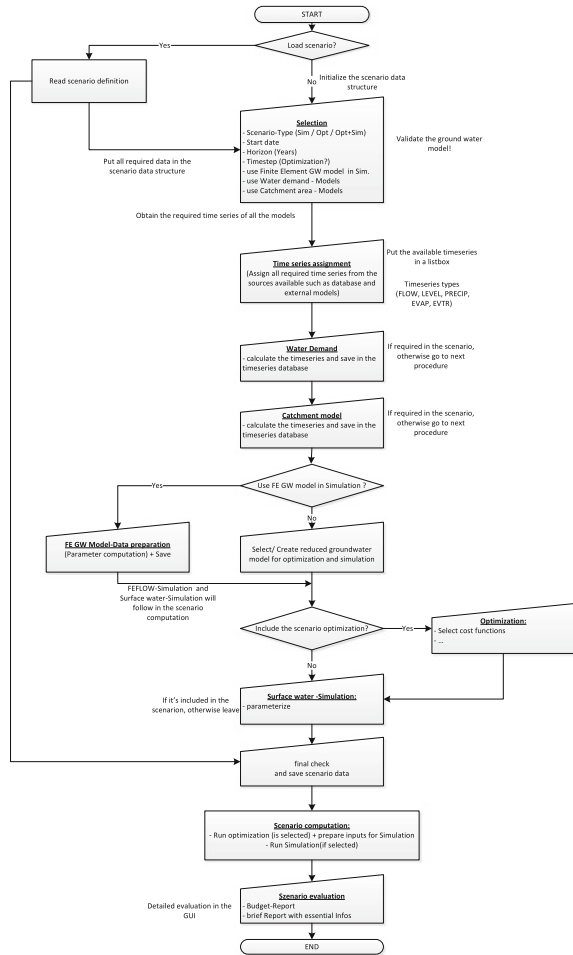
water managers to explore the likely nature and impact of potential changes to the urban water system in terms of changes both water resources quantity and quality.

Assessment of the applicability and the sensitivity of the DSS is also very important. Therefore, the scenarios should present typical problem situations that might evolve over the next years. Typical problem scenarios to be analyzed in water resources management should include (the current situation as baseline, climate change, demand change and supply change) [217]. The current situation is used as the starting point to compare other scenarios against and to explore the likely impacts of the current management practices. The climate change scenario is used to explore likely implications of global climate change on water resources using local climate change predictions, such as decrease in rainfall, increase in evaporation due to temperature changes. The demand change scenario explores the impacts of increased water consumption driven by rapid population growth, economic growth or changes in usage patterns. Last but not least, the supply change scenario is used

to explore infrastructural changes (addition or removal of reservoirs, water transfers, etc.), ground and surface water contamination. These four scenarios should be adapted depending on the characteristics of individual application region, case and in consultation with the key stakeholders involved in the study.

The following is an overview, which lean on the scenario-planning process presented by [146]. The stages in setting up and running scenarios in the DSS are:

1. Identification of issues and drivers, i.e., the definition of the parameters of the water resources system in the quantity and quality model. This includes climate inputs, land use, contaminant profiles of different flows, water usage patterns and population distribution. This can be accomplished through a brainstorming session involving a diverse group of staff members with the active involvement or tacit support of decision makers.
2. The participants should identify the potential issues that must be managed or overcome given the uncertainties involved.
3. After identifying the potential issues appropriate models from within the DSS and the model time period should be selected.
4. Lastly the DSS is executed and the results analyzed. To develop a more flexible, multidimensional view of the future, each scenario is considered equally likely to occur.

The transformation of tasks and applications into scenarios is the starting point and prerequisite of the decision support system framework. Table 5.2 shows an example of a scenario specification with goal definition, assumed impact, procedure and possible reactions.

Conclusively, application of scenario planning enables the potential impact of individual drivers on the water resources to be pinpointed, then the drivers can

Table 5.2 Example of a scenario description

Attribute	Description
Initial stage	Scenario of year 2006
Assumed impact	Precipitation drop from 600 mm in year 2006 to 400 mm in year 2007
Possible reactions	Increased exploitation of groundwater
	Increased waste water reuse
	Increased use of water from regional transfers
	Increased prices for household water use
	Decreased agricultural irrigation
Procedure	For each possibility, a scenario has to be formulated to derive the input for simulations and running simulations for the possibilities of the reaction
Decision support	Comparison of the simulation results
	Finding an optimum between these possibilities of reaction for a given goal function
Goal function	No limitations in water supply for the households and minimal costs

be combined to include a variety of outcomes including water re-use strategies, pro-active pipeline rehabilitation, relocation of current potable water extraction systems and upgrading current water restriction policies and treatment systems. In reality, individual drivers are coupled (can either compensate for or be additive to the effects of others) and therefore it is an advantage when elaborating a water management policy to be able to disentangle and quantify the relative effects of each component on water quantity and quality. The DSS is flexible and supports the selection and comparison of problem scenarios, which gives the end-user suggestions to find a best-practice response.

5.2.3   Human Machine Interface

In this DSS framework as in most other decision supports systems [214, 358, 361], an important aspect is that the user holds a sovereign position. In other words, the DSS should be seen as an aid tool which helps the users in various tasks. Thus the DSS must not substitute the user in any stage of the decision process. The user is the one who knows roughly what he/she wants, he/she defines the optimal control problem and selects the models to be used, therefore the final responsibility for the outcomes of the decision process rests with the users of the DSS.

The human machine interface (HMI) is an obvious main component of a DSS and is responsible for the communication between the user and the system. An example of such a GUI is shown in Fig. 5.6. The appropriate design of the user interface is a key
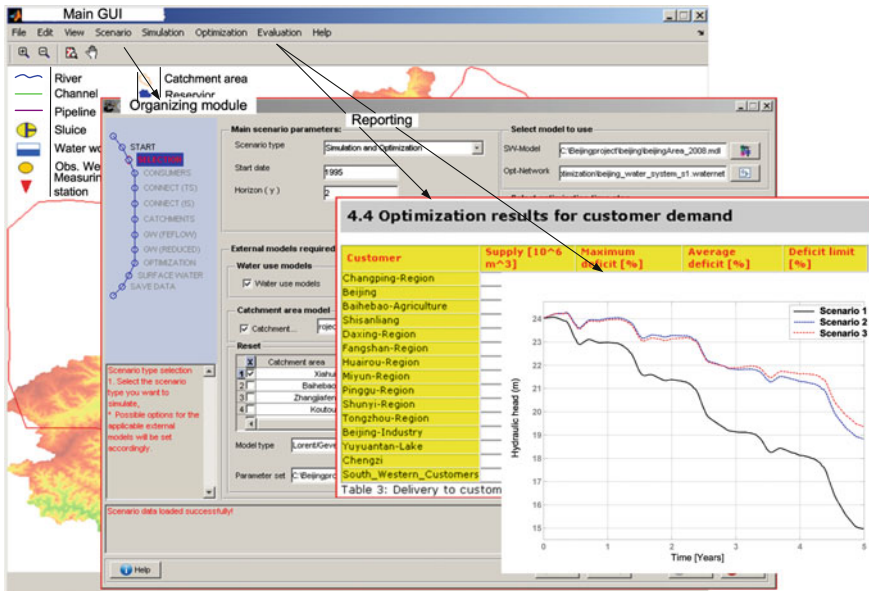
Fig. 5.6 Example Menu-driven GUI
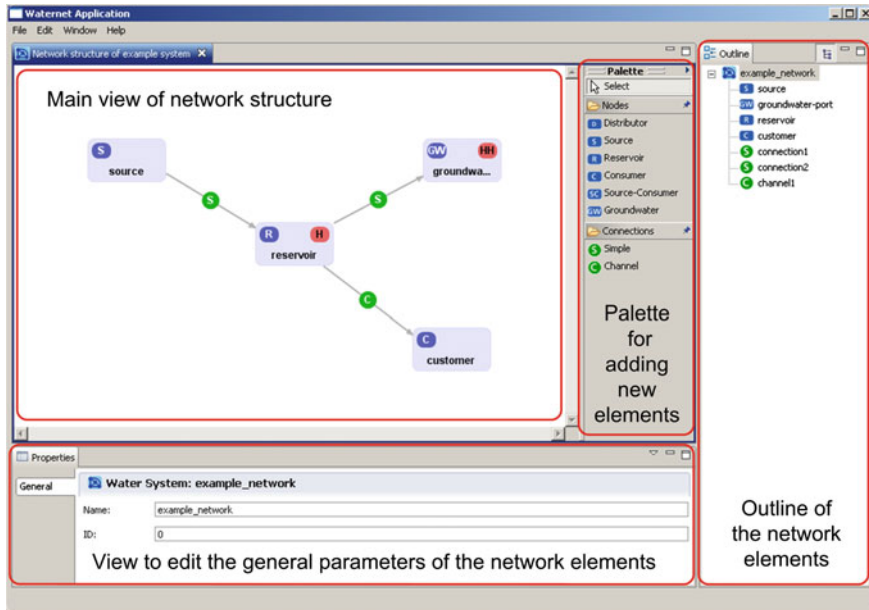
Fig. 5.7 Network editor

issue towards the successful implementation of the whole system, so as to ensure that the user can take full advantage of the analytical capabilities that the system provides. Advances in computer hardware and software have enabled user-friendly graphical user interfaces to serve this function. As the optimization is based on a network optimization formulation, therefore the GUI also include a portable dialog for river basin network creation by drag and drop of the network elements (nodes and arcs, see e.g. Fig. 5.7). The attribute data of the network elements are entered interactively with data consistency checks and linked to the network. The DSS generates as its results a large quantity of data. Therefore, the HMI is also integrated with a reporting tool. The reporting tool convert the large data sets according to some reporting logic defined by the user into comprehensible spreadsheets and images, which enable the users to recognize patterns, trends and anomalies inherent in the data with little effort.

5.3 Optimization of Water Resources Systems

As described in Chap. 2, the management of a water resources system follows operational rules.[2] Convenient and efficient mathematical expressions for quantitative and qualitative operation rules of a reservoir are based on the reservoir continuity Eq. (5.19) and the conservation law, respectively.

---

[2]An operation rule is a law that specifies how a component of a water resources system operates for various purposes (quantity, quality) as a function of system states and parameters [226].

The reservoir is operated let's say at a monthly basis. Rates of inflow, outflow, and spill for the reservoir are assumed constant during each time period.

Assuming that the operating rules and consequently all parameters of the system are known, according to Eq. (5.19) the desired storages S^k and releases from each reservoir R^k will also be known at the beginning of each time step k. It is clear that knowing the desired release values may not be sufficient for the specification of all system's flux variables (i.e., the actual releases and discharges) because of at least one of the reasons below:

- The discharge capacity is bounded to some value, therefore the actual releases may differ from the desired ones,
- There may be several water ways of different cost, via which the flows in the network can be conveyed,
- Multiple and contradictory operational targets have to be satisfied simultaneously;
- The total water availability is also bounded and may not cover the total water requirement.

Therefore, a discrete-time water flow allocation problem arises, demanding to strictly satisfy all the physical constraints of the system, handling all the operational targets according to a predefined priority series and minimize the total water conveyance cost and system's losses. At the same time the deviations between the actual and the desired releases have to be minimized in order to satisfy (or, if not possible, approach) the operation rules of the system.

Let a general discrete-time process model (state transition function describing the evolution of the state vector, from time k to time $k + 1$) be defined by

$$x^{k+1} = f^k\left(x^k, u^k, z^k\right), \quad k = 0, \ldots, N - 1 \tag{5.1}$$

$$f^k : \Re^n \times \Re^m \mapsto \Re,$$

where the vector x^k and u^k describes the n-dimensional state vector and the m-dimensional control vector at time k, respectively. State vector and control vectors denotes the vectors of network flow variables representing water flows, aquifer and reservoir storages, and pollution concentrations in link flows, aquifers or reservoirs; z^k is the vector of non-network type decision variables (side variables), which may be water prices, water transport costs, pollution control costs, crop types, irrigation areas, water priorities, and product prices; N is the optimization horizon; k is the stage number (the discrete time index $t^k = k \cdot \Delta t$).

Intuitively, if discretization is fine enough, then solutions found in discretized space are fairly good approximations to the original solutions. The accuracy of solutions found in discretized continuous Nonlinear Programming (NLP) has been studied in [36].

In the case of the process model in Eq. (5.1), we got a dynamic optimization problem, which can be represented as discrete optimal control problem as follows:

$$F^N\left(x^N\right) + \sum_{k=0}^{N-1} f_0^k\left(x^k, u^k, z^k\right) \;\rightarrow\; \min_{u^k,\; k=1,\ldots,K} \tag{5.2}$$

$$f_0^k : \mathfrak{R}^n \times \mathfrak{R}^m \mapsto \mathfrak{R},$$

$$F^N : \mathfrak{R}^n \mapsto \mathfrak{R}$$

subject to

$$x^0 = x\left(t_0\right), \tag{5.3}$$

$$g^N\left(x^N\right) \leq 0, \tag{5.4}$$

$$x^{k+1} = f^k\left(x^k, u^k, z^k\right), \tag{5.5}$$

$$h^k\left(x^k, u^k, z^k\right) = 0, \tag{5.6}$$

$$g^k\left(x^k, u^k, z^k\right) \leq 0, \tag{5.7}$$

where x^0 is the initial states vector; $h^k\left(x^k, u^k, z^k\right) = 0$ is a vector of m equality constraints (e.g. balance of non-storage nodes); $g^k\left(x^k, u^k, z^k\right) \leq 0$ is a vector of k inequality constraints(e.g. minimum (maximum) reservoir level); F^N is the terminal cost function; f_0^k is a strictly convex scalar objective function for time k given in terms of the vectors x^k, u^k and z^k and all discrete variables in x are finite. In general, functions $f(x, u, z)$, $g(x, u, z)$, and $h(x, u, z)$ are not necessarily differentiable and can be linear or nonlinear, continuous or discrete, and analytic or procedural. The search space X is the Cartesian product of discrete domains of all variables in x, u, z. Without loss of generality, we consider only minimization problems, knowing that maximization problems can be transformed into minimization problems by negating their objective functions.

It is assumed that F^N, f_0^k, f^k, g^k, g^N have continuous second derivatives. Also, it is assumed that constraints may contain fixed initial or final states, as well as simple bounds for state and control variables and, in general, linear and nonlinear constraints of a mixed or a homogeneous type.

Depending on the purposes of water management planning, objective functions can be formulated in various forms and should incorporate measures such as efficiency (i.e., maximizing current and future discounted welfare), survivability (i.e., assuring future welfare exceeds minimum subsistence levels), and sustainability (i.e., maximizing cumulative improvement over time) [190]. The criteria are economic, social and environmental issues. Some common types of objectives include:

- Maximizing the flow to downstream nodes,
- Maximizing the economic production,

(a)   **(b)**
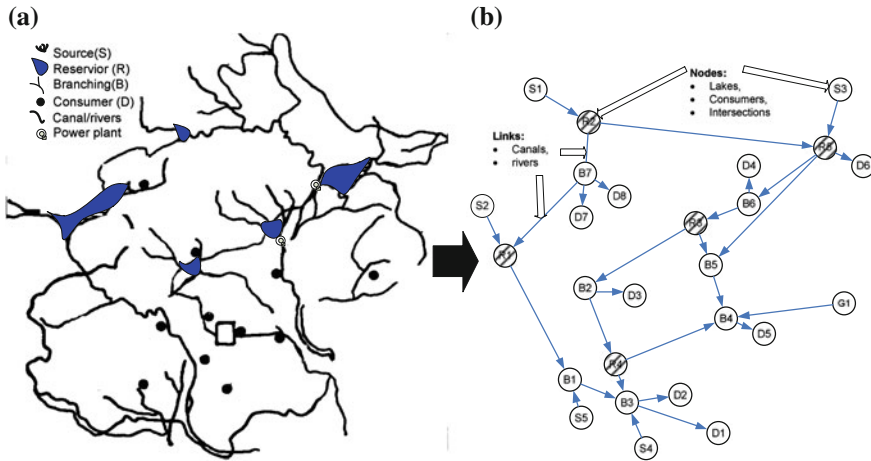
Fig. 5.8 Node-link water resources network. **a** Water supply system. **b** Node-link-Graph

- Minimizing the differences in water deficits among all demand sites, or
- Minimizing the pollutant concentrations at some locations,
- Minimizing deviations from the desired volume of storages

The dynamic optimization problem can be solved by formulating the mathematical model of the system as a network optimization problem, which is solved at each time step k, assuming that the system's components and attributes (system's spatial configuration) are represented in a capacitated digraph form (node-link), as shown in Fig. 5.8 [158, 344]. The equality and inequality constraints of the full discrete-time optimal control problem are composed of the constraints of the individual network elements (nodes and connections). The node-link representation enable node specific definition of the objective function, e.g. for a demand node the demand fulfillment need to be defined. The overall objective function is the weighted sum of all objectives defined in the network elements.

In the node-link water resources network, a node represents a physical component of interest such as watershed outflow, natural/man-made junction, intake structure, water or wastewater treatment plant, aquifer, reservoir, natural lake, dams, barrages flow control structures between modules (e.g. pumps, weirs, water gates, etc.) or aggregate water demand site. For the groundwater node a reduced model as described in Chap. 2 can be used. A link represents a natural or man-made water way such as a river reaches, canal, valves, turbines or pipeline between two different nodes, but can also stand for any flow of water such as the seepage between a demand site and an aquifer.

Let $G(V, L)$ be the directed network of a river basin, where $V = \{1, \ldots, v\}$ is the set of nodes, $L = \{(j_1, j_2) : j_1, j_2 \in V \& j_1 \neq j_2\}$ is the set of links of the network, and j_1, j_2 denotes the link from node $j_1 \rightarrow j_2$, then the water and substance balance equations for a general node j during each period t can be respectively written as

$$S(j, k) = S(j, k-1) + \sum_{(j_1, j \in L)} Q(j_1, j, k) - \sum_{(j_1, j \in L)} Q_l(j_1, j, k)$$
$$- Q_g(j, k) - Q_c(j, k) - \sum_{(j,k) \in L} Q(j, j_2, k), \forall j \in V \tag{5.8}$$

$$C_p(j, k) S(j, k) = C_p(j, k-1) S(j, k-1) + \sum_{(j_1, j) \in L} C_p(j_1, j, k) Q(j_1, j, k)$$
$$- \sum_{(j_1, j) \in L} O_{pl}(j_1, j, k) + O_{pg}(j, k) - O_{pc}(j, k)$$
$$- \sum_{(j, j_2) \in L} C_p(j, j_2, k) Q(j, j_2, k), \forall j \in V \tag{5.9}$$

where V is the set of nodes, L is the set of links, $S(j, k)$ is the storage volume for storage node (reservoir/aquifer) k. Note that $S(j, k) = 0$ for river and demand nodes, except for large storage nodes such as reservoirs and aquifers. $Q(j_1, j, k)$ is the flow from node j_1 to j during period k, $Q_l(j_1, j, k)$ is the conveyance losses because of evaporation, leakage and seepage of the flow from node j_1 to j, $Q_g(j, k)$ is the gain of inflow adjustment at node j during period k for discharges from small tributaries, local watershed drainages, river reach seepages or flows from other sources, $Q_c(j, k)$ is the water consumed at node j because of economic activities and evaporation, p is an index of pollutant types, $p \in P = \{1, 2, \ldots, \xi\}$, $C_p(j, k)$ is the concentration of substance p at storage node j at the end of period k, $C_p(j_1, j, k)$ is the concentration of substance p in the water flow from node j_1 to j during period k, $O_{pl}(j_1, j, k)$ is the conveyance losses of substance p in the water flow from node j_1 to j, $O_{pg}(j, k)$ is the total amount of substance p added to node j during period k because of inflow adjustment $Q_g(j, k)$ and of water use activities, and $O_{pc}(j, k)$ is the removal of substance p at node j.

Besides the general mass balance equations for each node, there are mass balance constraints for some natural physical response processes. These include link losses, node inflow adjustments, node losses, consumption and pollutant discharges, and outflows. For a typical water allocation problem, there are often several thousand constraints.

Constraints for water allocation formulated on a network structure can be classified into three kinds: physical, policy and system control constraints (complex social, economic and other constraints governing water allocation). Physical constraints consist of mass balances and capacity limits. The capacity limits, together with typical policy constraints, form the lower and upper bounds for storages, flows and qualities, such as:

- minimum and maximum water volume for a storage node j:

$$S_{\min}(j, k) \leq S(j, k) \leq S_{\max}(j, k) \tag{5.10}$$

- maximum allowed substance concentration in water volume of a storage node j:

$$C_p(j, k) \leq C_{p,\max}(j, k) \tag{5.11}$$

- minimum and maximum flow from j_1 to j:

$$Q_{\min}(j_1, j, k) \leq Q(j_1, j, k) \leq Q_{\max}(j_1, j, k) \tag{5.12}$$

- maximum allowed substance concentration from j_1 to j:

$$C_p(j_1, j, k) \leq C_{p,\max}(j_1, j, k) \tag{5.13}$$

5.3.1   Water Resources System Components

The Eqs. (5.8)–(5.13) will be applied to the common network elements and the resulting models will be described in the following subsection. Note that each node of the graph may have in general an unrestricted number of incoming and outgoing connections. The connections i weighed W_i denote the adjacency set $E(j)$ of a node j as shown in Fig. 5.9.

5.3.1.1   Models for Nodes

Mainly, there are eight types of network elements for nodes:

- Source/Supply nodes (S)
- Distributor nodes (DT)
- Confluence nodes (C)
- Reservoir nodes (R)
- Groundwater nodes (G)
- Hydropower generation nodes (P)
- Consumer nodes (D)
- Terminal nodes (T)

The source/supply node type is used to model the inflow into the water network, this could represent: a spring, an upstream catchment (which in turn can be simulated by the rain-runoff model, see Chap. 2), an inter-basin transfer, a major input

Fig. 5.9 Node model
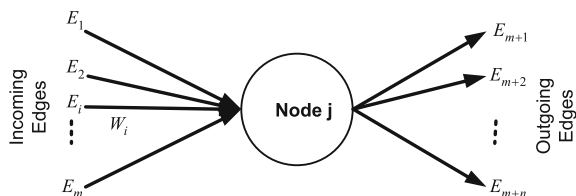
of groundwater to the surface water system. The source-consumer node type is a combination of a consumer and a source node and is an auxiliary or geometry node. This node should be used to simplify the network at hand. A simplification of the network is recommended if the connection between a source and a consumer node has no dynamic model for the flow process (simple connection). This will lead to a reduction of optimization variables and can therefore enhance the solver efficiency.

Distributor nodes represent branching of flow to several channels; it is characterized by more than one outflow and rules to distribute the flow. Abstractions to demand nodes may be described by diversions.

Confluence nodes which provide for the joining of several reaches that could represent natural tributaries or man-made conveyance channels. They are characterized by more than one inflow.

The reservoir node type has to be used to model natural or controlled storage elements of the water network. The balance equation describes the evolution of the storage volume as a function of the inflow where as the consumer node type has to be used to model customers (water demand for irrigation/environment, municipal water demands and water demands for industry) in the water network.

The groundwater node type serves as a connector to the reduced groundwater model within the full optimization problem. The exchange of water between the groundwater system and the surface water system at special points of interest (e.g. artificial recharge, withdrawal of water at well fields) have to be modeled using this node element. Each groundwater port of the surface water system is mapped to the input vector of the reduced groundwater model described in Chap. 2. Therefore, the number of groundwater ports and the number of inputs of the reduced groundwater model should be the same.

Terminal nodes are used to model outlets from the water network considered in the model, including outflow to the sea or inflow to lakes.

Network elements for connections can be divided into simple connection, to model a connection without regarding the dynamics of the flow processes (stationary behavior) and channel connection for a more complex description of the flow dynamics using lumped or distributed model approaches.

The optimization model-types for nodes and connections, which can be used will be described in the following sections.

Distributor Node (B) Models

For distributor nodes, the general model has no parameters and describes a node where the water from the incoming connections is distributed to the outgoing connections; see for example B5 in Fig. 5.8. The flow dynamics can be expressed as

$$\sum_{i \in E(j)} Q_i^k = 0 \tag{5.14}$$

where $i \in E(j)$ is the adjacency set of node j.

The substance flow balance dictated by the general Eq. (5.14) can be written as

$$\sum_{i \in E(j)} C_{p,i}^k Q_i^k = 0 \tag{5.15}$$

Source/Supply Node Models

For supply nodes, the supply model describes a node to which water is supplied to the network at a predefined rate, see for example S1 in Fig. 5.8. Its flow dynamics and the mass balance can be expressed as in Eqs. (5.16) and (5.17), respectively.

$$\sum_{i \in E(j)} Q_i^k + Q_{\text{sup},j}^k = 0 \tag{5.16}$$

$$\sum_{i \in E(j)} C_{p,i}^k Q_i^k + C_{\text{sup},i}^k Q_{\text{sup},j}^k = 0 \tag{5.17}$$

Another specialized supply model, often required in water resources for planning purposes, describes a node which delivers water to the network according to an annual maximum supply storage $S_{a\,\text{sup}}$. The distribution of the supplied water throughout the year is only restricted by maximum supply rate. It is assumed that the optimization horizon is starting at the first day of a year. Hence the flow dynamics can be expressed by Eq. (5.18)

$$S_{\text{sup},j}^k = \begin{cases} S_{\text{sup},j}^{k-1} + \Delta t^k q_{\text{sup},j}^k & year\left(t^k\right) = year\left(t^{k-1}\right) \\ 0 & year\left(t^k\right) > year\left(t^{k-1}\right) \end{cases} \tag{5.18}$$

subject to:

$$Q_{\min,j}^k \leq Q_{\text{sup},j}^k \leq Q_{\max,j}^k$$

$$S_{\text{sup},j}^k \leq S_{a\,\text{sup}}$$

Reservoir Node Models

For reservoir nodes, the storage model describes a reservoir storage based on a discrete-time volume balance equation expressed in Eq. (5.19) with stored volumes as state variables. Control variables are the spillage and also the productive outflow (outflow through the turbines) if the reservoir includes a hydropower station. The model includes time-varying constraints for the reservoir volume as well as an objective term to penalize deviations from a predefined reference trajectory for the volume content.

$$S_j^{k+1} = S_j^k + Z_j^k + \Delta t^k \left(\sum_{i \in E(j)} \left(Q_i^{k-\theta_i} + F_i^{k-\theta_i} \right) \right.$$

$$\left. + A_{O,j}^k q_{evpot,j}^k - q_{seep,j}^k + A_{O\,\max} q_{prec,j}^k \right) \qquad (5.19)$$

where $A_{O,j}^k = f\left(S_j^k \right)$.

Applying Eq. (5.9), the material balance Eq. (5.20) is simply an inventory of the mass of all materials entering, exiting, and accumulating in the reservoir and is described correspondingly by:

$$C_{p,j}^{k+1} S_j^{k+1} = C_{p,j}^k S_j^k + C_{z,p,j}^k Z_j^k + \Delta t^k \left(\sum_{i \in E(j)} \left(C_{res,p,j}^k Q_i^{k-\theta_i} + C_{o,p,j}^k F_i^{k-\theta_i} \right) \right.$$

$$\left. + A_{O,j}^k q_{evpot,j}^k - C_{inf,p,j}^k q_{seep,j}^k + A_{O\,\max} C_{prec,p,j}^k q_{prec,j}^k \right) \qquad (5.20)$$

The storage volume is denoted by S, the inflow into the reservoir by Z_j and the storage productive outflow is denoted by Q and discrete time step is denoted by Δt. The total evaporation from the reservoir depends on the water surface A_O and the potential evaporation q_{evpot}. The surface of the storage is modeled using a piecewise polynomial approach in dependence of the storage volume. Furthermore, the seepage q_{seep} from the reservoir to the groundwater as well as the direct inflow form precipitation q_{prec} can be specified. F denotes the spillage and θ the time delay. The volume of the storage can be scaled to enhance convergence properties of the optimization algorithm. $C_{p,j}$, $C_{z,p,j}$, $C_{res,p,j}$, $C_{inf,p,j}$ and $C_{prec,p,j}$ are substance concentrations in the reservoir, inflow, reservoir release, infiltration and precipitation, respectively. Evaporation terms do not usually enter the concentration balance as it is assumed that no substance concentration is contained in the evaporation liquid.

The previous Eqs. (5.19) and (5.20) are subjected to the following constraints,

$$S_{j,\min}^k \leq S_j^k \leq S_{j,\max}^k$$

$$S_j^0 = S_j\,(t_0)$$

$$C_{p,j}^k \leq C_{p,j,\max}^k.$$

The admissible range for the storage volume has to be specified using time-varying constraints and the evolution of the storage volume can be forced to follow a desired reference trajectory using a quadratic penalty term Eq. (5.21), where the penalty coefficient is denoted by ρ and the reference volume is denoted by S_{ref}.

$$J\left(V_j\right) = \rho_j \sum_{k=0}^{K-1} \Delta t^k \left(S_j^k - S_{j,ref}^k\right)^2 + \rho_j^K \left(S_j^K - S_{j,ref}^K\right)^2$$

$$+ \rho_{dS,j}^k \sum_{k=1}^{K} \Delta t^{k-1} \left(S_j^k - S_j^{k-1}\right)^2 \tag{5.21}$$

Groundwater Node Models

For the groundwater node, two models can be used. First model is a rough approximation of the storage model (compared to the FeFlow® model discussed in Chap. 2), which solely describes a storage based on a discrete-time volume balance equation which can be expressed in the simple form for two aquifers as:

$$S_1^{k+1} = S_1^k + \Delta t \left(Q_{in,1}^k - Q_{out,1}^k + Q_{12}^k\right), \quad S_1 = v_1 A_1 H_1 \tag{5.22}$$

$$S_2^{k+1} = S_2^k + \Delta t \left(Q_{in,2}^k - Q_{out,2}^k - Q_{12}^k\right), \quad S_2 = v_2 A_2 H_2 \tag{5.23}$$

$$Q_{12}^k = -K \left(H_1^k - H_2^k\right) \tag{5.24}$$

where, H is hydraulic head, A is the bottom area, K is the soil conductivity and v is the soil porosity, Δt is the time step, Q_{12} is flow from storage 1 to storage 2.

The second model which can be used is the reduced groundwater model described in Chap. 2.

Both models are governed by the constraints of the hydraulic head:

$$H_{\min}^k \le H^k \le H_{\max}^k$$

The evolution of the groundwater hydraulic head can be forced to follow a desired reference trajectory using a quadratic penalty term (Eq. 5.34),

$$J\left(H^k\right) = \rho^k \Delta t \left(H^k - H_{ref}^k\right)^2 \tag{5.25}$$

where the penalty coefficient is denoted by ρ and the reference hydraulic head is denoted by H_{ref}.

Hydropower Generation Node

Hydropower generation is computed from the flow passing through the turbine, based on the reservoir release or run-of-river streamflow, and constrained by the turbine's flow capacity. Note that the amount of water that flows through the turbine is calculated differently for local reservoirs, river reservoirs and run-of-river hydropower. For river reservoirs, all water released Q_{rel} downstream is sent through the turbines, but water pumped from the reservoir to satisfy direct reservoir withdrawals is not sent through the turbines. For local reservoirs, all linked demand sites are assumed to be downstream of the reservoir, so all reservoir releases are sent through the turbines.

For run-of-river hydropower nodes, the "release" is equal to the downstream outflow from the node.

The water flow Q_T that passes through the turbines is bounded by the minimum and maximum turbine flow. Note that if there is too much water, extra water is assumed to be released through spillways which do not generate electricity. If the release is less than the minimum turbine flow, then no electricity is generated. Otherwise, the turbine flow is the smaller of the reservoir release and the maximum turbine flow.

$$Q_{T,j} = \begin{cases} 0 & \forall Q_{j,rel} < Q_{T,j,\min} \\ \min\left(Q_{j,rel}, Q_{T,j,\max}\right) & \forall Q_{j,rel} \geq Q_{T,j,\min} \end{cases} \tag{5.26}$$

where $Q_{T,j,\min}$ is the minimum turbine flow for node j and $Q_{T,j,\max}$ is the maximum turbine flow for node j.

The amount of power generated is related to release rates and other pertinent factors as follows:

$$P_j^k = \begin{cases} e_j \cdot \sum_{j_2 \in (j_1,j_2)} Q_{j_1,j_2}^k \frac{\left\{\left[H_{j_1}^k + H_{j_1}^{k-1}\right] - tw_{j_1}\right\}}{2} & \forall j_1 \in \text{Nodes (Reservoirs)} \\ e_j \cdot pgc_j \cdot \sum_{j_1 \in (j,j_1)} Q_{j_1,j_2}^k, & \forall j_1 \in \text{Nodes (Rivers)} \end{cases} \tag{5.27}$$

subjected to constraints

$$P_{j,\min}^k \leq P_j^k \leq P_{j,\max}^k \tag{5.28}$$

where

$P(j,k)$: Hydropower generation node j at time k,
$H(j,k)$: Reservoir water level at time k,
$e(j)$: Hydropower generation efficiency,
$pgc(j)$: Power generation coefficient when a station, is a river node and power is assumed to be linear with flow through the river node,
$tw(j)$: Tail water elevation.

For reservoirs, the height that the water falls in the turbines is equal to the average elevation of the reservoir during the time period minus the tail water elevation and for run-of-river hydropower nodes, the drop in elevation is entered as data.

Consumer Node Models

Water demand is modeled as a set of diversion and instream flow targets for consumer nodes, the demand model describes a node from which water is extracted by a customer $Q_{dem,j}$, see for example D1 in Fig. 5.8. The governing flow and mass balance equations are described by Eqs. (5.29) and (5.30), respectively as follows:

$$\sum_{i \in E(j)} Q_i^k - Q_{dem,j}^k = 0 \tag{5.29}$$

$$\sum_{i \in E(j)} C_{p,i}^k Q_i^k - C_{p,dem,i}^k Q_{dem,j}^k = 0 \tag{5.30}$$

subject to the constraints:

$$Q_{min,j}^k \le Q_{dem,j}^k \le Q_{max,j}^k \;\; \left(= Q_{ref,j}^k\right)$$
$$C_{p,dem,j}^k \le C_{p,max,j}^k \;\; \left(= C_{p,ref,j}^k\right)$$

According to the management goal several objective functions can be defined for the demand model which penalizes the demand deficit of the consumer node j: A quadratic penalty term:

$$J_0\left(Q_j^k\right) = \rho_j^k \Delta t^k \left(Q_{dem,j}^k - Q_{ref,j}^k\right)^2 \tag{5.31}$$

A linear term with negative sign (to maximize supply from the node):

$$J_1\left(Q_j^k\right) = -\rho_j^k \Delta t^k Q_{dem,j}^k \tag{5.32}$$

A linear penalty term:

$$J_2\left(Q_j^k\right) = \rho_j^k \Delta t^k \left(Q_{dem,j}^k - Q_{ref,j}^k\right) \tag{5.33}$$

A normalized quadratic penalty term:

$$J_3\left(Q_j^k\right) = \rho_j^k \Delta t^k \frac{\left(Q_{dem,j}^k - Q_{ref,j}^k\right)^2}{\left(Q_{ref,j}^k\right)^2} \tag{5.34}$$

A normalized linear penalty term:

$$J_4\left(Q_j^k\right) = \rho_j^k \Delta t^k \frac{\left(Q_{dem,j}^k - Q_{ref,j}^k\right)}{Q_{ref,j}^k} \tag{5.35}$$

where $Q_{ref,j}$ is the demand of the consumer node j. These terms apply for every time step k within the optimization horizon.

Please note that the upper bound Q_{max} for the discharge from the node to the customer Q_{dem} needs to be adapted to the intended behavior of the node (see Chap. 4 on water demand modeling). For example, for irrigation, $Q_{dem,j}^k$ can be obtained as follows:

$$Q_{dem,j}^k = \frac{CWN_k - P_k}{c_u\left(1 - \varepsilon\right)} \tag{5.36}$$

where,

$$CWN_k = \alpha ET_{crop,k} \times A,$$
$$ET_{crop,k} = K_c ET_{0,k},$$
$$P_k = \alpha P_{eff,k} \times A,$$
$$P_{eff,k} = pl P_{tot,k},$$

CWN_k is the total area crop water need at time k, $ET_{crop,k}$ is the crop water need at time, $ET_{0,k}$ is the reference crop evapotranspiration at time k, based on climatic data, K_c is the crop coefficient, P_k is the total area effective precipitation at time k, $P_{eff,k}$ is the effective precipitation at time k, $P_{tot,k}$ is the total precipitation at time k, pl is the fixed percentage to account for losses from runoff and deep percolation. Normally $pl = 0.7 - 0.9$, ε is the conveyance loss coefficient, c_u is the consumptive use coefficient, A is the irrigation area [ha] and α is a unit conversion coefficient.

5.3.1.2 Models for Connection

Each arc/connection in Fig. 5.8 has three parameters: a weighting, penalty, or unit cost factor (relative priorities) c_{ij} associated with Q_{ij}; lower bound l_{ij} on Q_{ij}; and an upper bound U_{ij} on Q_{ij}. The requirement for lower and upper bounds results in the term capacitated flow network. The storage volumes of canals and barrages are so small that it is not necessary in most cases to calculate the effects of retention.

Source Connection Model

The source connection model enables a direct connection of a source node to a reservoir node and can be used to add an additional fixed (non-controllable) inflow to the reservoir. This model has no parameters.

Base Connection Model

The basic model for connections defines a time-varying lower and upper bound for the discharge and quality along the connection and is subjected to the following constraints:

$$Q_{i,\min}^k \le Q_i^k \le Q_{i,\max}^k$$

$$C_{p,i}^k \le C_{p,i,\max}^k$$

The basic model can be extended to a model which defines a time-varying lower and upper bound for the discharge along the connection as well as an objective term to attenuate discharge variations. The objective function can be expressed as in Eq. (5.37)

$$J\left(Q_i^k\right) = \rho_i \Delta t^k \sum_{w=1}^{W} \left(Q_i^k - Q_i^{k-w}\right)^2 \tag{5.37}$$

Please note that the objective term is associated with the introduction of auxiliary optimization variables according to the number of steps for considering the discharge variation penalty term. Therefore, only a few time steps should be considered in this term. In most cases one step will be enough for a sufficient attenuation of the discharge variation.

The previous model can also be extended to an additional objective term, which penalizes the deviation from a desired discharge along the connection. Hence the following objective function applies:

$$J\left(Q_i^k\right) = \Delta t^k \left(\rho_i \sum_{w=1}^{W} \left(Q_i^k - Q_i^{k-w}\right)^2 + \rho_{ref,i} \left(Q_i^k - Q_{ref,i}^k\right)^2 \right) \tag{5.38}$$

Minimum Flow Connection Model

Another important connection model is the minimum flow model, which is suitable for defining the environmental requirements concerning the discharge along the connection. The required discharge can go below the defined limit, but this is penalized by a special term of the objective function Eq. (5.39).

$$J\left(Q_i^k\right) = \Delta t^k \left(\rho_{i,l}^k \eta_i^k + \rho_{i,q}^k \left(\eta_i^k\right)^2 + \rho_{i,r} \sum_{w=1}^{W} \left(Q_i^k - Q_i^{k-1}\right)^2 \right) \tag{5.39}$$

The required behavior is modeled using soft constraints as follows:

$$Q_{i,\min}^k \le Q_i^k \le Q_{i,\max}^k,$$
$$Q_{i,\min,des}^k - \eta_i^k \le Q_i^k,$$
$$\eta_i^k \ge 0.$$

Low Slope Channel Connection Model

The third connection model is suitable for artificial channels with a very low slope. The model defines one state for the volume content of the channel. The channel outflow is restricted by an inequality constraint following a simple static impulse balance using the Chezy-Manning approach for friction [208]. The cross section of the channel is modeled using a trapezoid. The flow dynamics and the mass balance can be expressed as in Eqs. (5.40) and (5.41), respectively:

$$S_i^{k+1} = S_i^k + \Delta t^k \left(Q_{in,i}^k - Q_{out,i}^k - A_{O,i}^k q_{evpot,i}^k \right) \tag{5.40}$$

where $A_{O,j}^k = f\left(S_j^k\right)$;

$$C_{p,i}^{k+1} S_i^{k+1} = C_{p,i}^k S_i^k + \Delta t^k \left(C_{in,p,i}^k Q_{in,i}^k - C_{out,p,i}^k Q_{out,i}^k - C_{evpot,p,i}^k A_{O,i}^k q_{evpot,i}^k \right)$$

$$(5.41)$$

subject to:

$$S_{i,\min}^k \leq S_i^k \leq S_{i,\max}^k$$

$$C_{p,i}^k \leq C_{p,i,\max}^k$$

$$S_i^0 = S_i(t_0)$$

$$Q_{in,\min,i}^k \leq Q_{in,i}^k \leq Q_{in,\max,i}^k$$

$$Q_{in,p,i}^k \leq Q_{in,p,\max,i}^k$$

$$Q_{out,\min,i}^k \leq Q_{out,i}^k \leq \min\left(Q_{out,\max,i}^k, g\left(V_i^k\right)\right),$$

$$Q_{out,p,i}^k \leq Q_{out,p,\max,i}^k$$

where $g\left(V_i^k\right) = \frac{A_i^k \sqrt{S_{l,0}} \left(R_{H,i}^k\right)^{2/3}}{c_m}$.

The cross section of the channel is denoted by A, the hydraulic radius by R_H, the bottom slope of the channel by $S_{l,0}$ and the Manning friction coefficient by c_m.

Following the management requirements, the objective function J can be written as:

$$J(V_i) = \rho_{dS,i}^k \sum_{k=1}^K \Delta t^{k-1} \left(S_i^k - S_i^{k-1}\right)^2 \qquad (5.42)$$

Although not relevant for our studies, models for pumps, valves, etc., are usually required in operative water resources management. Therefore, for completion's sake we propose the following for further reading, please refer to [36, 46].

5.3.2 Solving the Dynamic Optimization Problem

One of the most widely used techniques in water resources management has been Linear Programming (LP) [6]. LP is concerned with solving problems in which all relations among the variables $f_0, \ldots, f_m$ are linear, i.e., satisfy $f_i(\alpha x + \beta y) = \alpha f_i(x) + \beta f_i(y), \forall x, y \in \Re^n$ and $\forall \alpha, \beta \in \Re^n$, both in the constraints and in the objective function to be optimized and it's application in water resources management vary from relatively simple problems of straightforward allocation of resources to complex situations of operation and management. Under certain assumptions, nonlinear problems can be linearized and solved. Planning aspects can be represented by linear optimization models by introducing simplifications and approximations, even if linear assumptions are not strictly adherent to real water resources systems. Depending on the nature of the nonlinearity, there are at least two methods for problem linearization.

The first approach, known as piecewise linearization converts the original nonlinear function to series of linear functions by defining additional variables. Sun et al. [310] use the piecewise linearization method in their implementation, which incorporate the nonlinear evaporation loss function of a reservoir in a water-supply-optimization model. The second method involves repeated applications of LP to solve a series of approximate problems in which the original objective function is linearized. Therefore, a widely adopted linearization scheme is based on the first order Taylor's series expansion of the nonlinear function about a given initial solution. This method is known as Successive Linear Programming (SLP) and is more general as it can cope with the introduction of additional variables. The main reasons of applying linear programming in optimization problems may include:

- Its ability to accommodate relatively high dimensionality with comparative ease (Megiddo et al. [215] demonstrated that the linear programming problem in d variables and n constraints can be solved in $O(n)$ time when d is fixed),
- It always achieves the optimal solution if one exists [215],
- No initial policy is needed (compared with DP and NLP) and
- Standard computer codes and solvers are readily available e.g., CLP, GLPK, LP-Solve, LP-Optimizer, Soplex, ExLP, Coin-OR, ABACUS, etc.

Dynamic programming (DP) is a procedure for optimizing a multistage decision process [25, 224]. It was largely formulated by Bellman and it's popularity and success in optimization of water resource systems can be attributed to the fact that the nonlinear and stochastic features which characterize a large number of water resources systems can be translated into DP formulation. With this method, highly complex problems with large number of variables can be decomposed effectively like in divide and conquer into a series of sub problems which are solved recursively. Bellman showed that the computation burden in discrete DP is dependent on the number n and discretization of the state variables m as $m \cdot n$. Therefore, the computational burden of DP increases exponentially with the number of state variables. Methods to overcome this dimensionality problem include Dynamic programming Successive Approximation Method (DPSA), which was first used by Trott and Yeh [324] in a water management system study. The method breaks up a problem containing several control variables into a number of sub problems containing only one control variable. Each sub problem has fewer state variables than the original problem; in the case where there are as many control variables as state variables, each sub problem has only one state variable.

In order to reach a more adequate level of adherence to the physical system more detailed models are resolved by taking into account nonlinearity in the objective function and constraints, which request a problem formulation as a constrained nonlinear programming problem (NLP). NLP is the most generalized deterministic mathematical programming techniques. In this section, we study the recent advances on the implementation and the models of NLP as they apply to water resources problems.

Several nonlinear programming formulations for the optimization of water resources systems exist. Diaz et al. [75] use SQP to find the optimal allocation of

power-plant releases during peak demand periods. They exploit the concave characteristic of the nonlinear objective function and show a rapid convergence to the global optimum. They tested their methodology on an existing multi-reservoir hydro-power system in Argentina and report very encouraging results. They also compare their results with SLP and report a faster rate of convergence for SQP. Fletcher [103] uses SQP for a highly nonlinear and non-convex problem.

GAMS/MINOS [40, 222] is one of the most successful software packages, which employs a projected Lagrangian on a sequence of linearly constrained sub problems to solve problem with nonlinear constraints and objective function. During the past decade, GAMS/MINOS has successfully been used for different applications of water resources problems e.g., in Pezeshk et al. [256], the author presents a nonlinear optimization model to minimize pumping costs for both a well field and a main water supply distribution system. They consider individual losses, pump efficiencies, and hydraulic losses in the pipe network. The NLP model is solved using the general nonlinear optimization program MINOS. Pezeshk et al. claim that for a given demand, the optimization procedure provides the best combination of pumps to meet the demand and in Ostfeld and Shamir [240], the authors develop a model based on MINOS for the optimal operation of a multi-quality water supply system, under steady-state conditions. The system contains sources of different qualities, treatment facilities, pipes, and pumping stations. The objective is to minimize total cost, while delivering to all consumers the required quantities at acceptable qualities and pressures. The steady-state example that they use consists of six consumers from three sources, two of them with treatment plants, and has three pumping stations and 10 pipes. The results demonstrate that the optimal solutions found by MINOS response to change in economic and operational conditions as expected.

There has been tremendous interest in the recent development of software based on Trust Region algorithms [65, 130]. Large and Nonlinear Constrained Extended Lagrangian optimization Techniques (LANCELOT) has been one of the successful software packages designed for the purpose of general nonlinear programming problems. The emphasis in LANCELOT is on problems which are significantly nonlinear, in the sense that they involve a large number of nonlinear degrees of freedom [65].

SISOPT [210], is developed for the management and operations of the Brazilian hydropower system. The system consists of 75 hydropower plants with an installed capacity of 69,375 MW, producing 92 % of the nation's electrical power and is one of the largest in the world. The system size and nonlinearity pose a real challenge to the modelers. The basic model is formulated in nonlinear programming (NLP). The authors compared the performance of SLP and NLP and NLP showed superior performance.

Arnold et al. [90] applied the optimization solvers IPOPT and HQP to find out optimal release strategies for a system of reservoirs with hydroelectric power-stations on the Zambezi river in southern Africa. State equations are derived from volume balance equations of the reservoirs with the volumes of stored water as state variables. Control variables are the productive outflow (outflow through the turbines) and the spillage. Arnold et al. [90] show in their results that the dynamic SQP solver and the IPOPT solver performed satisfactorily with high accuracy for all variations of

the Zambezi problem with varying time horizons, varying inflow scenarios and cost function parameters.

It is evident from the above literature review that a wide variety of techniques have been developed and applied to the optimization studies of water resources systems. Three different research areas mainly based on LP, DP and NLP have been reviewed. The fact that there are many applications of water resources problems with nonlinear objective functions and constraints has motivated our much interest in the use of NLP for our applications. The examples show that constrained NLPs can be solved by existing methods, such as sequential quadratic programming, huge quadratic programming or interior point, if they are specified in well-defined formulae, which have continuous variables and continuous and differentiable objective and constraint functions. However, only special cases can be solved when they do not satisfy the required assumptions.

As discussed before, the process simulation model Eq. (5.1) is composed of equations for hydro systems applications basically consist of the governing physical equations that describe a physical process such as conservation of mass, energy and momentum. These equations are typically large in number, sparse and nonlinear in terms of the decision variables. In some applications, there are finite difference expressions of the governing partial differential equations. Conceptually, the simplest approach is to have the optimizer directly solve the problem (Eqs. 5.2–5.7). Unfortunately, many of the real-world problems cannot be solved in this manner as a result of their size. An existing approach is to transform the discrete-time optimal control problem into a large scale, structured non-linear programming problem in the state and control variables (required by HQP or IPOPT [338])

$$\min_{y} \{J(y) \,|\, h(y) = 0; \, g(y) \leq 0\} \tag{5.43}$$

assuming that $J(y)$, $h(y)$ and $g(y)$ are twice continuously differentiable.

There exist two possible approaches for this conversion process

1. Formulation in the space of the control variables and
2. Formulation in the space of the state and control variables.

The first approach requires the elimination of the state variables and leads to an unstructured nonlinear programming problem of dimension $(K \times m)$ (K—number of time steps, m—number of control variables), which can be solved numerically with about $O\left((K \times m)^3\right)$ basic arithmetic operations. Simple bounds of the state variables turn to general constraints of the control variables:

$$x_i^k \leq x_{i,\max}^k \Rightarrow g\left(u^0, u^1, \ldots, u^{k-1}\right) \leq x_{i,\max}^k \tag{5.44}$$

The Hessian matrix as well as the Jacobian matrices of the equality and inequality constraints is in general full.

Using the second approach the vector of optimization variables y contains the state and control variables of all stages:

$$y = \begin{bmatrix} x^0 \\ u^0 \\ \vdots \\ x^{K-1} \\ u^{K-1} \\ x^K \end{bmatrix}, \qquad (5.45)$$

$$y \in \Re^{m_y}, \ m_y = K\,(m+n) + n$$

The process equations of the discrete-time optimal control problem are directly included in the nonlinear programming problem as equality constraints.

$$h(x) = \begin{bmatrix} f^0\left(x^0, u^0, z^0\right) - x^1 \\ f^1\left(x^1, u^1, z^1\right) - x^2 \\ \vdots \\ f^{K-1}\left(x^{K-1}, u^{K-1}, z^{K-1}\right) - x^K \end{bmatrix}, \quad h \in \Re^{m_h} m_h = K \cdot n \qquad (5.46)$$

To prevent infeasible optimization problems, slack variables η can be introduced in the system

$$x_{\min}^k - \eta^k \le x^k \le x_{\min}^k + \eta^k, \ \eta^k \ge 0 \qquad (5.47)$$

and constraint violations are penalized with an additional term in the objective function as follows:

$$\sum_{i=1}^{n} \left(\rho_{i,l}^k \eta_i^k + \rho_{i,q}^k \left(\eta_i^k\right)^2 \right), n = \dim\left(\eta^k\right) \qquad (5.48)$$

This results in $g(x) = \begin{bmatrix} g^0\left(x^0, u^0, z^0, \eta^0\right) \\ g^1\left(x^1, u^1, z^1, \eta^1\right) \\ \vdots \\ g^K\left(x^K, \eta^{K-1}\right) \end{bmatrix}, \quad g \in \Re^{m_g}, \ m_g = \sum_{k=0}^{K} r^k$ (52).

While the problem dimension $(K\,(n+m) + n)$ resulting from this formulation is higher (n- number of state variables), the advantage is the special sparsity structure with a block-diagonal Hessian-matrix and block-banded Jacobian matrices. The numerical solution effort is about $\mathrm{O}\left(K\,(n+m)^3\right)$ basic arithmetic operations. From simple considerations about the structure of the water resources allocation system at hand follow, that the second approach for transformation can lead to a significant lower computational cost. The IPOPT [338] solver is the currently most efficient, freely available optimization solver, which is suitable for large-scale, highly-structured problems and will from the mentioned theoretical foundations. This solver uses a nonlinear interior point algorithm to solve general nonlinear

programming problems. The main computational effort of this algorithm leads in the subsequent solution of large, sparse, linear equation systems. Therefore IPOPT[3] has interfaces to several sparse matrix solvers like MA27, WSMP or Pardiso und uses linear algebra packages like BLAS and Lapack.

Another optimization solver, which is specially suited for structured problems due to discrete-time optimal control problems and is also freely available, is HQP (Omuses) [282]. One important advantage of this solver is the special tailored problem interface, which allows for very efficient problem formulation process. Furthermore HQP [108] uses the automatic differentiation software Adol-C to compute numerically exact derivatives of the objective function and the equality and inequality constraints with respect to the optimization variables, which are necessary for gradient-based optimization algorithms. Therefore the problem interface of HQP is linked to IPOPT in order to take advantage from both software packages.

5.3.3 Examples of Formulating Dynamic Optimization Problems

For solution with standard methods/solver like IPOPT/HQP, the problem should be formulated in a specified format. The problem formulation basically involves the translation of verbal descriptions of the objectives and constraints into mathematical expressions in terms of decision variables and parameters. We will illustrate the discrete time optimal problem formulation on three typical water resources management problems, i.e., multi-purpose reservoir scheduling, simple water quality management, groundwater supply/demand management. Formulation and solutios of complex examples including all theses problems can be found in Chap. 6.

Example 1: Multi-purpose reservoir scheduling

A typical water resources management problem is reservoir scheduling and numerous investigations have examined methods to optimize reservoir policy decisions [90, 190, 210, 226, 258, 312]. Therefore, it is purposeful to illustrate the formulation of a discrete time control problem on such an example. In most cases reservoirs are multipurpose, i.e., they serve purposes of satisfying demand for irrigation and providing, flood control, hydroelectric power generation. Given as inputs the forecasts of water inflow from catchment areas and precipitation, irrigation needs and electric power rates, scheduling of such a system requires the solution of a discrete time optimal control problem.

As an example, we look at the problem of scheduling of a multi-purpose, five-reservoir Network, see Fig. 5.10. To lean on a real world network, we consider part of the Beijiang River Basin, a reservoir network in south china with the reservoirs,

---

[3]For the numerical solution of large scale non-linear programming problems interior point (IP) solvers have become popular during the last years because of their superior behavior for NLPs with many inequality constraints.
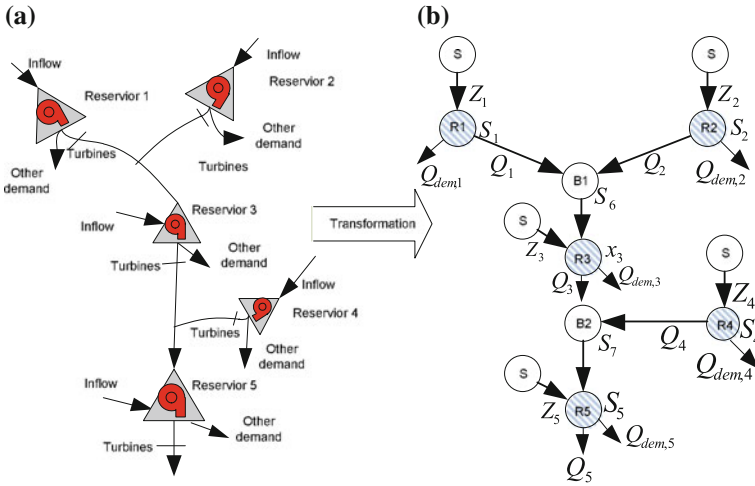
Fig. 5.10 Network of reservoirs. **a** reservoir System. **b** Node-Link-Graph

Nanshui (1), Mengzhouba (2), Baishiyao (3) Changhu (4) and Feilaixia (5). Each reservoir can deliver water to either the turbines or to a demand node (agriculture, household, industry and environment) and we raise the objective to meet all demand and use unallocated volume for electric power generation. Stream dynamics between the reservoirs (time delay θ_j) are modelled by linear difference equations with additional variables.

The variables and parameters in Fig. 5.10 for a given reservoir i for a given time period include, r^k the energy rate in period k, S^k the operative volume of water in reservoir at the beginning of period k, Z^k the inflow to reservoir from local watershed during period k, Q_{dem}^k the demand during period, η^k the turbine efficiency (function of flow rate), in period k and Δh^k the average pressure head at the turbine inlet during period k.

The cost function includes a nonlinear mixed state-control term (the outflow multiplied by the state dependent water height level). Other terms of the cost function result from the desired small deviations in time of the final water storage demands $A = \gamma \left(S_i^K - S_{ref,i}^K \right)^2 - \beta_E f_{e,i} \left(S_i^K \right)$ and the energy production $C = \varphi \left(Q_i^k - Q_{ref,i}^k \right)^2$, respectively.

$$ J = \sum_{i=1}^{5} \left\{ A + \sum_{k=0}^{K-1} \left\{ -\alpha Q_i^k \left(f_{h,i} \left(S_i^k \right) + f_{h,i} \left(S_i^{k+1} \right) \right) + C \right\} \right\} \qquad (5.49) $$

$f_{h,i}$ is the storage-water level relationship, $S_{ref,i}^K$ is the final reservoir volume reference value, $Q_{ref,i}^k$ is the reference trajectory for productive outflow, $f_{e,i}$ is the storage-potential electrical energy relationship, a function of energy production rate

r^k, turbine efficiency, pressure differential across the turbine, volume of water through the turbine and some conversion constant κ (height to power). and γ, β_E, α are weighting factors.

As mentioned in the node models for reservoirs and hydropower generation, constraints in the problem include bounds on reservoir levels and flows through the turbines. These are equivalent to constraints (Eqs. 5.3–5.7) and are also discussed in the section for reservoir node. Mass balance relationships describe the flow from one reservoir to downstream reservoirs as well as reservoir levels from one time period to the next. These may be viewed as the state transition Eq. (5.1).

After the problem formulation in the network programming format, the solvers IPOPT or HQP can then be applied to solve the problem.

Example 2: Water quality management

Water quality management problems can be formulated as a problem of minimizing treatment or pollution abatement costs while maintaining water quality standards. The dissolved oxygen (DO) concentration and the biochemical oxygen demand (BOD) of the wastes released to the stream can be used as appropriate measures of the water quality. Examples of such a problem are shown in [48, 64, 155, 206] among others.

Here as in [48] we consider a hypothetical water network system with P_i dischargers and R_j receptors (i.e., checkpoints, where water quality is measured) as depicted in Fig. 5.11. Relationship between the water quality indicator, (DO) at a receptor node and the treatment level upstream to that checkpoint is linear (based on Streeter-Phelps Equation) and is assumed to be available as well as data for streamflow, BOD loadings, travel times for various reaches of the river.

We consider the water quality maximization as the primary objective in a multi-objective optimization problem. Therefore, the optimization task can be formulated in terms of x_{ij}^k, the decision variable that represents the treatment, or removal fraction, at discharger i at time k, a_i the unit treatment cost for ith discharger, C_i^k the substance concentration loading to the treatment facility at source location i at time k, d_{ij}^k the transfer coefficient depicting the quality response at location j resulting from the release of a unit of pollution at source i and γ_j weighting factor to reflect the importance of quality at location j relative to the importance of quality at all other locations (for full problem description, see [48, 49]) as:

Fig. 5.11 Hypothetical water network with pollution source and receptor nodes
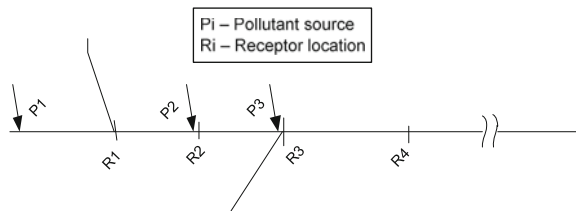
$$\min_{x} \sum_{j} \sum_{i} \gamma_j C_i^k d_{ij}^k (x_{ij}^k - x_{ij,ref}^k)^2 \tag{5.50}$$

where j is the index for the locations of water quality in concern and i is the index for the controllable sources of pollutant and $x_{ij,ref}$ is the reference treatment level.

In this example the constraints could include minimum and maximum treatment levels, budgetary considerations, and equity constraints. A sufficient satisfaction of water quality goals could be ensured by imposing constraints on the expected value of the quality response at each of the receptor locations. This would result in constraints of the form [48]:

$$\sum_{i \in I_j} C_i^k \left(1 - x_{ij}^k\right) d_{ij}^k \leq S_j^k - D_j \tag{5.51}$$

where I_j is the set of all sources that have a significant impact on receptor location j, S_j is the quality standard imposed at location j and D_j is the basis substance concentration at j due to non-controlled sources.

The set I_j will consist for a river basin of all dischargers that are upstream of receptor location j, but sufficiently close (in terms of travel time) to have a non-negligible impact on receptor j. To solve the problem any dynamic optimization solver can be taken into consideration, e.g., IPOPT, HQP.

Example 3: Groundwater supply/demand management

Let us look at simple, but practical groundwater problem. The objective of the optimization model is for example to maximize the total pumping rate from wells, while minimizing costs and subject to constraints on saltwater intrusion, sustaining baseflows, and maintaining regional gradients [13, 129, 180]. Since usually the purpose of wells is to supply water for drinking and irrigation, their salt concentrations must fulfill specified levels in the optimization models.

As in Gordu et al. [129], the decision variables z can be defined for each node and each well with s_i^k the drawdown at node i at time k (m), H_i^k the hydraulic head at node i at time k ($f(H_0, s_i)$), C_i^k the salt concentration at node i at time k, Q_j^k the pumping rate at well j at time k, $Q_{j,a}^k$ the pumping rate of well j that supplies water for demand area a and $Q_{w,i}^k$ the withdrawal rate from node i at time k.

Thus, to make it simple, for the optimization of the total cost of well pumping the objective function can be expressed as a function of pumping rates and cost. Further nonlinear terms, such as for cleanup times can be added to the cost function.

$$\min_{z} C_{tot} Q_{tot}^k = C_1 Q_1^k + C_2 Q_2^k + \cdots + C_N Q_N^k \tag{5.52}$$

where: Q_j^k is the pumping rate at well j at time k and $j = 1, \ldots, N$.
subject to:

The process model for drawdown s_i^k (Eq. 5.53) and change in substance concentration (Eq. 5.54) for each well, which can be expressed by the simplified Theis equation [13] as a sum of aquifer response to the pumping.

$$s_i = \frac{Q_j}{4\pi T} W(u) \tag{5.53}$$

$$C_i = \sum_i \varphi_{c,ij} Q_j \tag{5.54}$$

where $\varphi_{c,ij}$, which can be obtained from a finite element groundwater model denotes the factors for the aquifer response (transmissivity and storativity) to the pumping from the observation wells. T is the formation transmissivity, $W(u)$ is the well function for confined aquifers, $u = (Sr^2)/(4Tt)$, S is the formation storativity, r is radial distance from pumping well j, and t is elapsed time since pumping started.

In addition to the drawdown and concentration constraints which can be obtained using the response matrix technique, the model is subjected as well to the limitations of well capacity (Eq. 5.55),where $Q_{j,max}$ is the maximum capacity of well j, limitations in water demand (Eq. 5.56), where D_a is the amount of water required for demand area a, water distribution capacity from pumping wells to the demand areas (Eq. 5.57), avoidance of dewatering the well nodes (Eq. 5.58), where B_i is bottom elevation of the aquifer at node i below mean sea level.The purpose of this constraint is to ensure that hydraulic heads do not decrease below a level of 1 m above the bottom elevation of the aquifer at each node and the non-negativity constraints (Eq. 5.59):

$$Q_j^k \leq Q_{j,\mathrm{max}}^k \tag{5.55}$$

$$\sum_j Q_{j,a}^k \geq D_a \tag{5.56}$$

$$Q_j^k = \sum_a Q_{j,a}^k \tag{5.57}$$

$$H_i^k \geq B_i \tag{5.58}$$

$$Q_j^k, Q_{j,a}^k, C_i^k \geq 0 \tag{5.59}$$

5.4   Benefits and Applications of the Decision Support System Framework

All summed up, the decision support system is a very powerful tool in water resources management which can:

- generate new evidence in support of a decision through optimization,
- improve personal efficiency in decision making,
- expedite problem solving through complex modeling techniques and analysis algorithms,
- manage conjunctive use of surface and ground water,

- facilitate interpersonal communication between stakeholders of a water system,
- encourage exploration and discovery on the part of the decision maker through scenario planning,
- reveals new approaches to thinking about the problem space,
- helps automate the water resources managerial processes and give the possibility of directly incorporating institutional and legal governing water distribution,
- allow the simulation of synthetic or stochastic inflow and demand sequences generated by the time series generator included in the system,
- be used for long-term and short-term river basin management for preliminary chosen time step (day, week, month, year),
- allow simulating of river basins with complex configuration and not limited to branching or tree-like network structures,
- solve unstructured problems which require combining quantitative information with the decision-makers' judgement.

The DSS has a number of applications in the field of water resource management decision making and assessment, including:

1. Emergency management and water resources protection in case of

   a. natural disasters,
   b. terroristic attacks,
   c. accidents,
   d. water resources pollution.

2. Optimized adaptation of the water supply system to trends and changes

   a. evaluation and implementation of political decisions,
   b. adaptation to changes in economy, population and agriculture,
   c. handling climate changes and water quality degradation,
   d. evaluation of increased waste water reuse,
   e. strategies for sustainability of water use.

3. Support for planning tasks

   a. simulation and optimization of future technical structures,
   b. simulation and evaluation of resource recharge strategies,
   c. simulation and evaluation of strategies of demand reduction.

Chapter 6
Applications

**Torsten Pfützenreuter, Divas Karimanzira, Thomas Bernard,
Thomas Westerhoff, Buren Scharaw, Albrecht Gnauck
and Thomas Rauschenbach**

6.1 The Simulation and Control Toolbox "WaterLib"

Torsten Pfützenreuter

An engineer developing application specific simulation and optimization systems needs appropriate and handy tools for creating the right models. The toolbox "Water-Lib" for the block-oriented, dynamic simulation system Simulink of the numerical computing environment MATLAB is such a tool. It consists of the most important and commonly used modules for the construction of simulation models suitable for controller design and decision support systems. These modules where developed using the algorithms described in Chaps. 2 and 3.

T. Pfützenreuter (✉) · D. Karimanzira · T. Westerhoff · B. Scharaw · T. Rauschenbach
Fraunhofer IOSB-AST, Ilmenau, Germany
e-mail: torsten.pfuetzenreuter@iosb-ast.fraunhofer.de

D. Karimanzira
e-mail: divas.karimanzira@iosb-ast.fraunhofer.de

T. Westerhoff
e-mail: thomas.westerhoff@iosb-ast.fraunhofer.de

B. Scharaw
e-mail: buren.scharaw@iosb-ast.fraunhofer.de

T. Rauschenbach
e-mail: thomas.rauschenbach@iosb-ast.fraunhofer.de

T. Bernard
Fraunhofer IOSB, Karlsruhe, Germany
e-mail: thomas.bernard@iosb.fraunhofer.de

A. Gnauck
Environmental Informatics, Brandenburgische TU Cottbus Inst.-Senftenberg, Cottbus, Germany
e-mail: ah-gnauck@t-online.de

The first toolbox version started with simulation objects for run-of-river reservoirs and river sections, the second edition was enhanced with models for complex surface water systems and an interface to the finite element groundwater simulator FeFlow®.

6.1.1 Modeling Dynamic Systems with Simulink

The first version of MATLAB was written in the 1970s at the University of New Mexico as a numerical computing tool for matrix operations. A powerful and easy to learn scripting language is one reason for the commercial success of this tool. Another reason is Simulink, the completely integrated simulation and model based design environment. It consists of a graphical editor where simulation blocks of different domains can be combined to form a simulation or control system. A huge number of toolboxes support the application of Simulink in different areas (e.g. mechanical simulations, automotive or aerospace applications).

Simulation models in Simulink consist of a number of function blocks describing the input/output behavior of a separable system or subsystem. Blocks are connected among each other with directed lines (from outputs of one block to inputs of others or itself). Figure 6.1 shows a very simple dynamic system with a sinusoidal input signal and two first-order transfer functions. Simulating this system for 10 s produces the time series shown in Fig. 6.2.
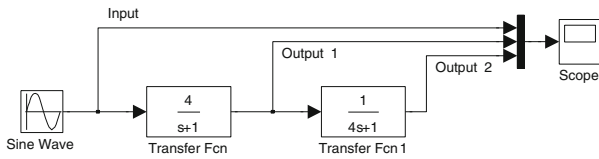
Fig. 6.1 Example simulation model

Fig. 6.2 Time series resulting from simulating the example model
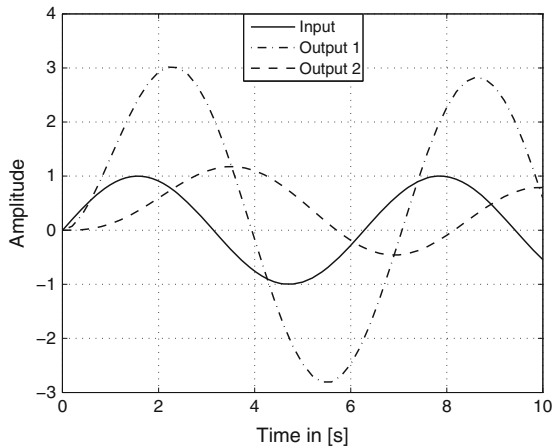
The simulation models of the "WaterLib" toolbox are created in a similar manner. Using the different model blocks presented in Sect. 6.1.2, a model of a complex surface water system can be developed in a very intuitive manner. For example, the simulation model of the Beijing region shown in Fig. 6.12 was created with the toolbox model blocks.

6.1.2 Toolbox Overview and Modules

Designing controllers for reservoirs or channels typically requires an analytical model of the system. Beside the mathematical calculation of the controller law and the associated parameters, simulations methods are often used to test and optimize control strategies. This requires a model of the controlled process. The toolbox "Water-Lib" contains models for the most important elements of surface water systems and was successfully used in different projects. Some of these projects are presented in sub sequential sections of this book. The toolbox consists of a number of modules (Fig. 6.3).

River-MOD contains flow models used for instance in highly dynamic run-of-river simulation models. All models rely on the analytical description of the hydrodynamic behavior of rivers and reservoirs presented in Sect. 3.1 (Fig. 6.4). With *River-MOD* the simulation of a river system with very high accuracy is possible.

Modeling a complex surface water system often results in a detailed simulation model with hundreds of parameters and a long simulation duration. The module *Complex-MOD* helps to reduce the modeling effort by using simplified simulation blocks (Fig. 6.5). Models created with these blocks are fast, reliable and sufficient for control and optimization tasks [262]. The library contains simplified models of the most important elements of a typical surface water system like reservoirs, river and channel sections, weirs, sluices, control gates with their dynamic behavior. Using these elements, major parts of surface water systems can be modelled very easily
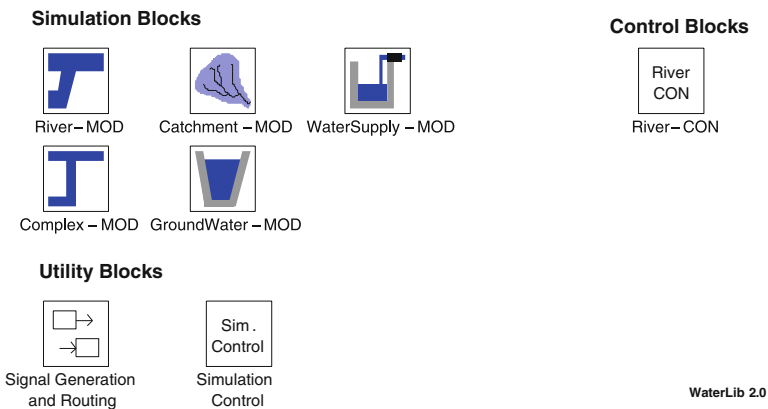
Fig. 6.3 Main library window of toolbox "WaterLib"
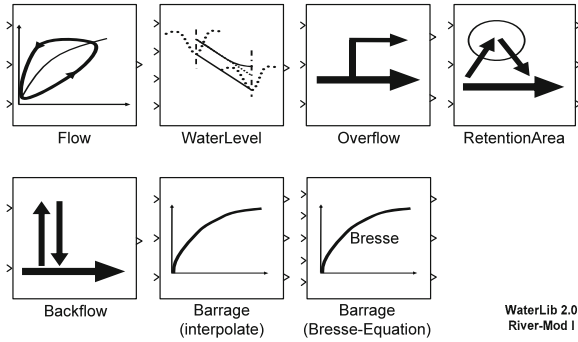
Fig. 6.4 Model elements for rivers and run-of-river reservoirs
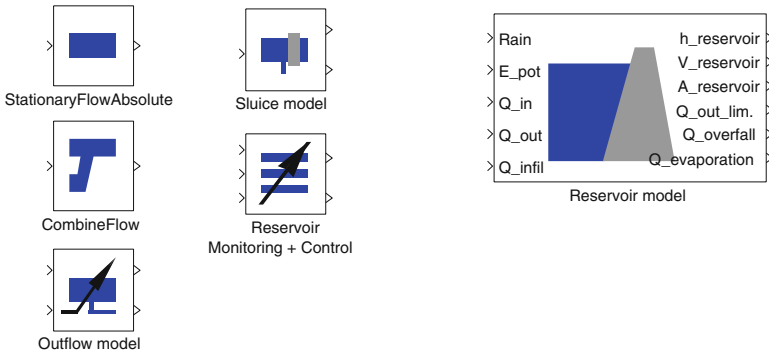
Fig. 6.5 Module Complex-MOD of toolbox "WaterLib"

with only a limited number of parameters. Typically, the data driven parametrization of the model blocks is done using optimization techniques.

Catchment-MOD includes different catchment area blocks to model the rainfall-runoff processes as described in Sect. 2.1 (Fig. 6.6). Simulation blocks to measure the performance of the different model types support the selection of the most appropriate type for the catchment that has to be modelled.

GroundWater-MOD contains a simple ground water storage block useful for isolated surface water simulations and the interface to the finite element groundwater simulator FeFlow® (Fig. 6.7). The FeFlow® interface follows the sequential coupling paradigm presented in Sect. 2.4.3. Coupling groundwater and surface water models requires to analyze the physical interconnection. Typically, the following most important interchange processes must be considered:

- groundwater withdrawal at wells,
- groundwater infiltration from rivers, lakes, reservoirs, irrigation,
- artificial recharge of groundwater at seepage fields.

The surface water simulation model computes all flow rates (withdrawal, infiltration, recharge) from its internal states. These time-dependent rates are transmitted
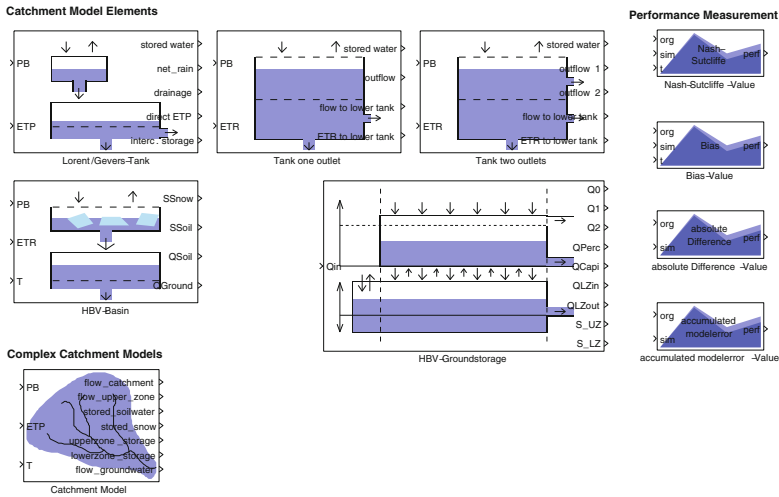
Fig. 6.6 Module Catchment-MOD of toolbox "WaterLib"

Fig. 6.7 Module
Groundwater-MOD of
toolbox "WaterLib"
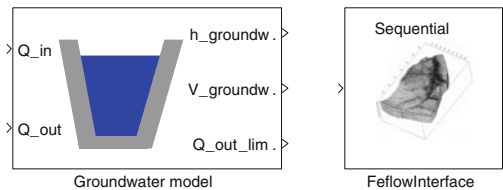
to FeFlow® and used for simulation of a predefined period. As output, FeFlow®
sends the hydraulic heads of all locations the surface water simulator is interested in.
During simulation, the surface water model is responsible for starting and controlling
the groundwater simulator as well as for the coordination of data transfer.

WaterSupply-MOD consists of simplified models for surface and ground water
works (Fig. 6.8). The groundwater works are controlled via the water level in a well
that is generated by the groundwater simulation model. If the water level is lower than
a given threshold, the demanded flow rate cannot be provided. In a similar manner
the surface water works are simulated: If the current inflow together with an optional
storage does not meet the demanded flow rate, the outflow is reduced.

River-CON comprises different run-of-river reservoir controllers and a coordi-
nation scheme for a chain of such reservoirs (Fig. 6.9). The algorithms used in this
module will be discussed in Sect. 6.5.

The *Utility Blocks* section includes signal routing blocks and simulation control
elements. Using signals in Simulink block diagrams opens up new opportunities
for model application: A signal may contain additional values beside the flow or
water level routed from source to destination block. Without changing the sim-
ulation model, the library "WaterLib" can be enhanced, for instance, with water

Fig. 6.8 Module
WaterSupply-MOD of
toolbox "WaterLib"

Groundwater works

Surface water works without storage

Surface water works
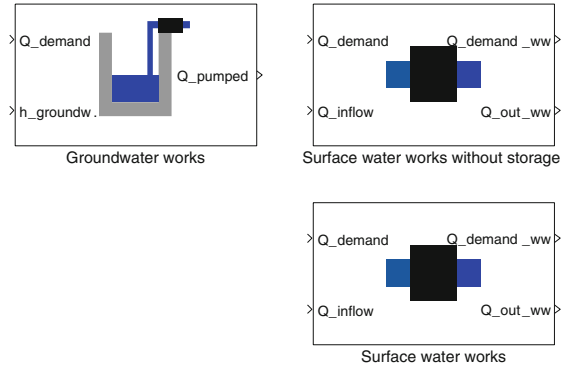
Fig. 6.9 Module River-CON
of toolbox "WaterLib"
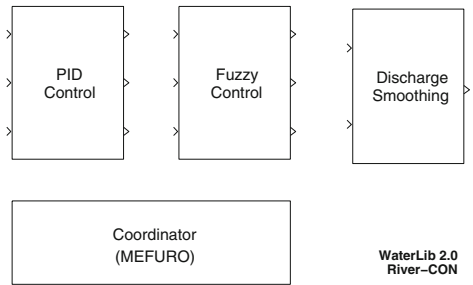
quality computations (for specific chemicals or as abstract quality classes) and the corresponding signal handling blocks. As result, the unchanged simulation model computes the water quality parameters starting with the next simulation run.

6.2 Application Example "Beijing Water"

Divas Karimanzira and Thomas Bernard

The municipal region, depicted in Fig. 6.10 of Beijing consists of $16,800\,km^2$ and is characterized by a continental climate with cold and dry winters, and hot summers that provide most of the annual precipitation under the influence of the south-east monsoon. Rainfall varies geographically, seasonally and yearly. Eighty-five percent of rainfall falls between July and September and at times, 40–70 % of rainfall falls within 3 days. Beijing has a very huge water demand contributed by the fast economic development in combination with a strong population growth. Beijing draws 50–70 % of its water from the ground, which is the most important source of water for the region. The quality of groundwater in the Beijing area is generally acceptable, but almost all available groundwater resources are already developed. Beijing has suffered from over-exploitation of this source. In the late 1970s and early 1980s, drought forced farmers to turn to groundwater, which had previously only been used
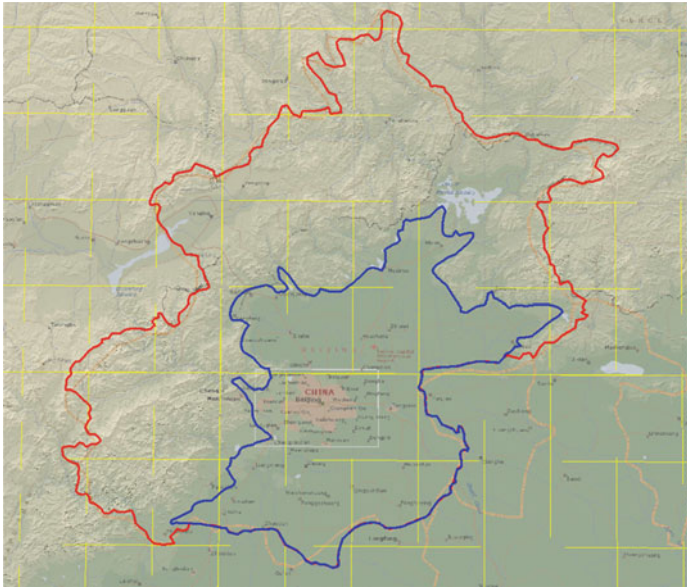
Fig. 6.10 Boundary of the Beijing municipal region (*blue*) and boundary of groundwater model area (*red*)

by industry and households. As a result of over-pumping, the water table fell throughout the 1980s with a citywide subsidence rate of 0.5 m/year with up to 1 m/year in some places. Groundwater levels in some areas have fallen by as much as 40 m since the late 1970s, with some spots pumped down to the bedrock. Surface water supply in the Beijing region depends mainly on upstream inflows. The major river systems affecting this region include the Chaobai, North Grand Canal, Yongding. Almost all of these river systems stem from the mountainous areas in neighboring provinces. Aside from problems such as excessive withdrawal and water quality deterioration of surface waters, the lack of regional coordination leads to issues such as uncoordinated withdrawals (e.g. upstream withdrawals affecting downstream cities negatively) and upstream water contamination.

More than 80 reservoirs have been constructed in the last century in the region to store surface water and provide flood protection, whereby the two largest reservoirs, Miyun and Guanting, account for 92 % of the total storage capacity of 9.31 bn. m^3. The surface water is transported to the water treatment plants of Beijing city using natural rivers as well as artificial surface or subsurface channels.

The decision support system developed for the Region is based on the framework in Chap. 5. The architecture includes basic functionalities for processing, filing and visualization of data. Furthermore the decision support system include a dynamic model of the essential elements of the Beijing water supply system based on the WaterLib Library and FeFlow® (see Chaps. 2–4). The DSS uses a state-of-art optimizer, which allows the derivation of optimal management strategies in depen-

dence of the decision horizon as well as assumptions for environmental conditions (drought, flood) and the future development of socio-economic conditions.

6.2.1 Simulation Model of the Beijing Water System

The structure of the system is shown in Fig. 6.11. All essential parts of the Beijing water supply system are considered in the model [50]. First, there are four reservoirs Miyun, Huairou, Baihebao and Guanting. The watershed models are integrated in this system in order to take into account the precipitation and the evapotranspiration. Further sources are groundwater storages. Secondly, there are the water transportation systems such as channels and rivers. Miyun and Huairou reservoirs are connected by the Beijing-Miyun water diversion. The arrows show the directions of water flows and describe the hydraulic behavior of water flow in the simulation model. Baihebao and Guanting reservoir are connected by tunnel and river Guishui. From Guanting, water runs into the Yongding river water diversion system to Beijing. Existing retention areas for flood control are also considered in the simulation model.

The water from channels and rivers, and groundwater is delivered to the customers (environment, industry, domestic and agriculture) in two ways, directly or through the waterworks.
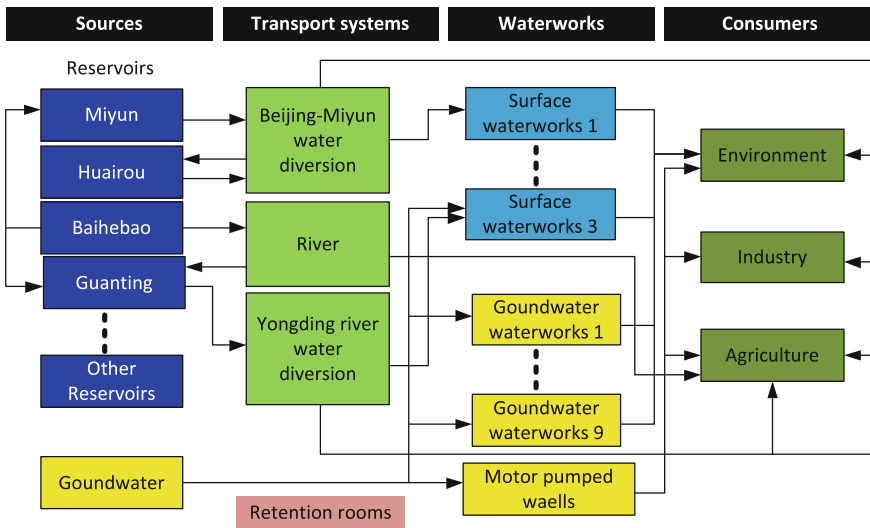
Fig. 6.11 Structure of the Beijing water supply system

6.2.1.1   Surface Water Modeling

The surface water model comprises all important elements for the storage and distribution of water within the considered region. The retention time along the different transport elements (river reaches, channel or pipelines) is less than the desired minimum time step for decision of one day. Therefore, a simple static approach for the flow processes is sufficient and the use of sophisticated models for the dynamics of wave propagation (e.g. Saint-Venant-Equations) with respect to control decisions is avoided. The surface water system is described as a Simulink® model using elements of the WaterLib described in Sect. 6.1 (see Fig. 6.12). The bus lines in the Simulink® model characterize the direction of the transport elements. The blocks represent reservoirs, lakes, points of water supply or extraction and simple junction points as well as transport elements, e.g. rivers, channels. As described in Chap. 2 every reservoir block constitutes a balance equation involving the edges linked with and possibly the storage volume. The sole nonlinearity results from Modeling the evaporation from the water surface of the storages (volume-area-curve), which is described by a piecewise polynomial approach. Channels with a very low slope are modelled as water storages.

6.2.1.2   Groundwater Modeling

The Beijing region includes one of the worlds largest groundwater aquifer systems [16]. But due to the permanent increase of population and the economical prosperous
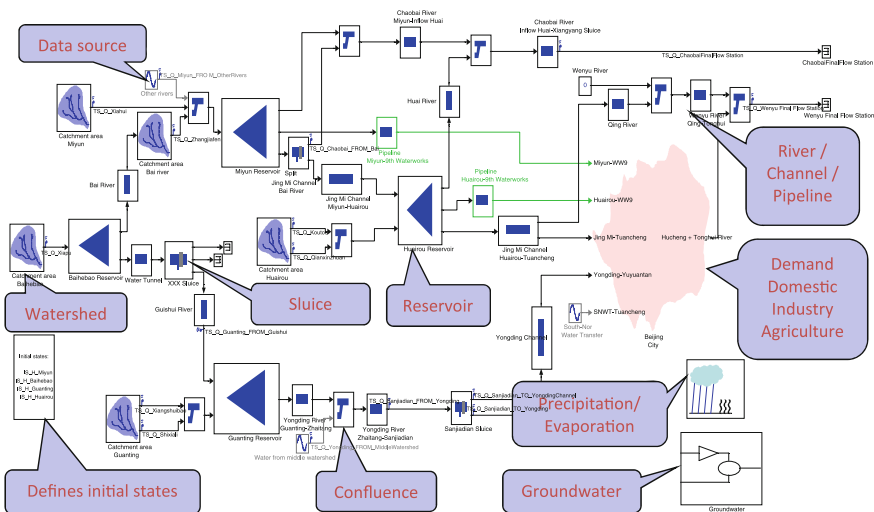
Fig. 6.12   Part of the Beijing water supply system as a Simulink® model

development of the last decades the water demand increased as well and caused a decline of the groundwater level of 1 (m/a) and more [107, 200, 346].

The groundwater model area, depicted in Fig. 6.10 is defined at the Northern part of the NCP, which is the largest alluvial plain of eastern Asia. The North China Plain is a basin with quaternary aged surficial deposits (loess, sand, gravel and boulder, silt and clay). According to the hydrogeological profiles of Beijing the quaternary system in this region is fairly complicated. A great variety of different sedimentary facies exists with different thicknesses ranging from several tens of meters around the Piedmont area to 150/350 m in the Northern central part of the NCP [57]. Groundwater is exploited in the layers of quaternary deposits, i.e. in the loose stratum/porous aquifers with high to very high water storage capacities. From the Taihang Mountains in the West to East there are two main geomorphological units in the model area: the Piedmont Plain below the mountain escarpments and the flood plain. In the Piedmont Plain the aquifers structure is coarse and becomes finer from West to East. In the flood plain the structure of aquifer is fine with silt sand, clay and silt interlay and in areas of ancient rivers and paleochannels the aquifer is composed mainly of gravels and coarse sands with good permeability. Therefore, the distribution of groundwater in the Beijing region is inhomogeneous. Regions of high abundance and high yielding porous groundwater aquifers are the Piedmont Plain and the Northeastern districts of Miyun, Huairou and Shunyi whereas less yielding aquifers are found in the Yangqing and Tong districts. In the transition zone from the Taihang Mountains to the NCP the quaternary sediments with low thickness of e.g. some tens of meters are lying on the older rock formations of the regions.

In the mountainous districts unstable groundwater distributions were assumed in dependence on the form of the rocks with geological discontinuities (fractures, joints, dissolution features) and the groundwater flow. In the transition area from the Taihang and Yanshan Mountains to the NCP stratigraphic sequences of various ages ranging from archaean metamorphic rocks to quaternary are documented in the geological and hydrogeological maps. The very old archaean rocks are distributed mainly in the Miyun and Huairou counties in the northeastern outskirts of Beijing municipality. It is composed of metamorphic and magma rocks e.g. gneiss, amphibolite and granite. In the mountain areas exist partly water yield fractured rock aquifers and karst aquifers e.g. the fractured and karstified ordovician limestones and generally fractured sandstones, granites and gneisses with a high variability with respect to discharge and a low to medium storage capacity [144]. On the other hand the claystones, shales and volcanic rocks represent very low yield aquifers or aquitards.

Following the procedures described in Sects. 2.3.5 and 2.3.6 and on the base of a conceptual hydrogeological model a horizontal and vertical structured 3D-groundwater model was developed. It describes the saturated zone till approx. 200 m depth below ground surface (bgs.) in the area of the quaternary sediments of the NCP. In addition, the borehole data from about 125 drillings homogeneously distributed within the model area, were incorporated into the groundwater model.

Eq. (2.115), which was derived in Sect. 2.3 is the governing equation for the subsequent description. The terms on the right hand side of (2.115) summarize all sources and sinks that coincide with the time dependent groundwater exploitation due to

industry, households and agriculture ($Q_{expl}[1/T]$) and recharge ($Q_{rech}[1/T]$ e.g. due to precipitation and irrigation) in the domain Ω. The partial differential Eq. (2.115) describes an initial-boundary value problem which has to be solved numerically for h in the 3 dimensional model domain Ω. As already mentioned in Sect. 2.3.2 the model, depicted in Fig. 6.13 was implemented in FeFlow®, which is a specialized Finite Element (FEM) software for subsurface flow [152]. The initial condition $h(\Omega, t_0)$(groundwater surface) at the initial time t_0 was given in the form of maps describing the groundwater surface of the complete model area of 6300 (km²). Boundary conditions were chosen of the Dirichlet type, i.e. $h(\partial\Omega)$ at the boundary $\partial\Omega$ and in of well boundary conditions. Since the inflow and outflow rates were derived from the water budget which contains volume rates only it was the simplest way to implement these boundary conditions in terms of well boundary conditions with negative signs ("pumping wells"). Nevertheless for mathematical reasons it is necessary that at least one Dirichlet boundary condition is implemented as well. Hence, in the particular model a mixture of both boundary condition types was implemented.

In addition to this there were also regular well boundary conditions implemented describing the exploitation rates of the well fields (see Fig. 6.17). The vertical resolution of the model consists of 25 layers and a automatized time stepping scheme was used. The resulting 3D finite element model consists of more than 150.000 nodes producing the corresponding huge computational costs. The simulation of 5 years needed ~15 min on a Intel Core 2 Duo CPU (2.5 GHz), which was the motivation for the model reduction (see next subsection).

One of the main tasks with respect to the groundwater model is the parameterization of the large-scaled model covering an area of 6300 km². On one hand the time independent soil parameters k_f, S_0 have to be estimated and generalized for the whole domain Ω by a (small) set of measured values. On the other hand the time dependent and spatially distributed source/sink terms Q_{expl} and Q_{rech} have to be calculated. In order to get these data the procedure was applied that is described in the Sects. 2.3.3 and 2.3.5 (Fig. 6.14). The results are time series of maps for Q_{rech} and Q_{expl} which

Fig. 6.13 Finite element model for the Northern Chinese Plain in the Beijing municipal region
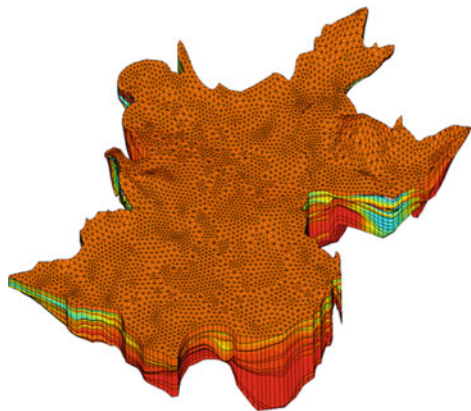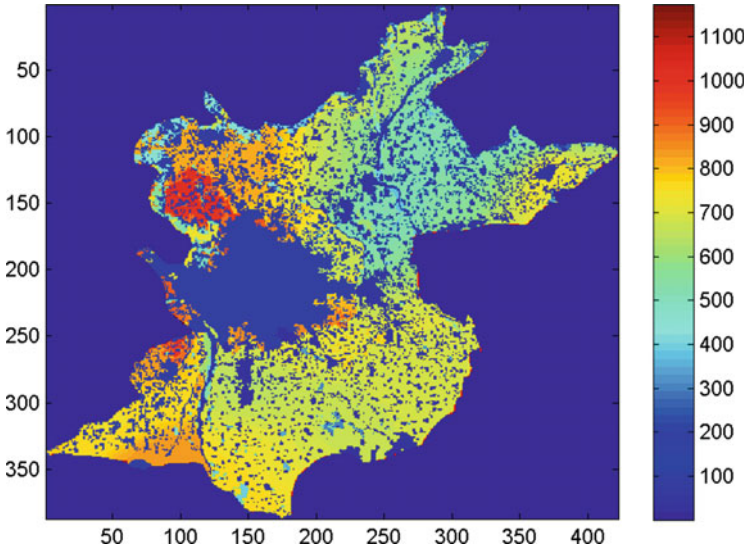
Fig. 6.14 Exemplary map for the estimated total yearly exploitation in the Beijing region

were derived from precipitation maps and maps for the agricultural water demand. The entire water demand consists of the three user groups: households, industry and agriculture (see [29] for details). The scenario wizard includes a parameterization issue supporting the budget based creation of time series of maps for the exploitation and groundwater recharge.

In the end the groundwater model calculates a time series of the hydraulic head for any finite element node which are interpolated such that a spatial distribution for the whole model areas is obtained. A sample for the groundwater surface map
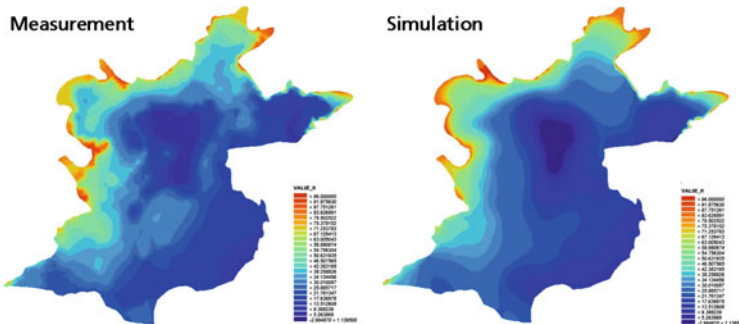
Fig. 6.15 Exemplary map for the estimated total yearly exploitation in the Beijing region

is depicted in Fig. 6.15 and the comparison with the measured groundwater surface map shows a quite good match. The calculated distribution of the hydraulics head results from a 4 year simulation run where the input data where adopted in a yearly manner. The match is sufficiently good and especially the depression zone is covered by the model quite well.

6.2.1.3 Groundwater Model Reduction

For the optimization of the water allocation system the full 3D Finite Element model (with $>100,000$ nodes) is not very suitable due to the mentioned large computational time. As for the optimization task a prediction of the hydraulic head (groundwater level) at a set of representative and fixed points is sufficient, an input-output model (e.g. a linear state space model) with considerably smaller order n (e.g. $n < 50$) than the original FEM model has to be derived.

As discussed in Chap. 2, methods for model reduction of those large scale systems have gained increasing importance in the last few years [9]. Most of these approaches have in common that they aim to approximate the state vector x with respect to a performance criterion, e.g. minimize the deviation between original system and reduced system for a given test input. As for our purpose, a black box input-output model would be sufficient there is no need to approximate the whole state vector x. Furthermore, the dimension n of a reduced model which approximates the whole state space vector x would be in most cases $n > 100$. With this dimension, for the given optimization problem the solution time would be unacceptably high ($\sim$hours). Last but not least the use of the commercial software FeFlow$^\circledR$ also prevents the application of e.g. a Krylov based method as no model representation (e.g. state space model) is provided by the software.

The basic idea of the proposed model reduction method is sketched in Fig. 6.16. We assume the existence of a reference scenario which means that the time dependent
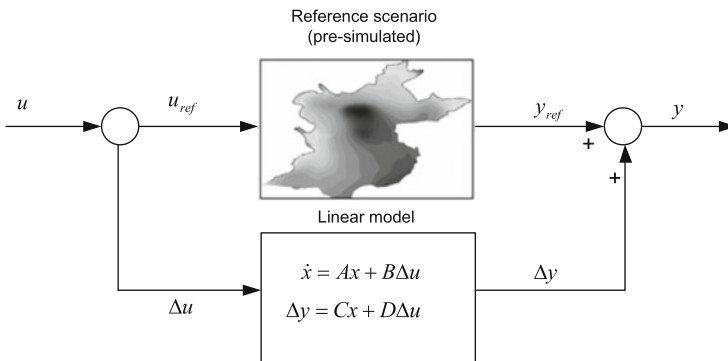
Fig. 6.16 Model reduction concept based on a reference scenario and an identified linear state space model

input parameters $u_{ref}(t)$ of the FEM groundwater model (especially groundwater exploitation Q_{expl} and recharge Q_{rech}) are determined for the whole optimization horizon. In practical cases these reference scenarios are mostly available or can be generated by plausible assumptions. Hence the task consists in the derivation of a model which approximates the behavior of the full FEM model in the case that the input parameters u differ from $u_{ref}(t)$. This model is gained by identification techniques: Test signals (e.g. steps) are added to the reference input $u_{ref}(t)$ (dimension p) and the corresponding deviations from the reference output $y_{ref}(t)$ (dimension q) are identified. Doing this separately for every component of the input-/output vectors u and y, we finally merge the $p * q$ single input-single output (SISO) models to a multi input-multi output (MIMO) model. For the groundwater model, the input parameters are e.g. cumulated (e.g. spatially integrated) exploitation of certain regions or cumulated exploitations of large well fields. The output parameters of the groundwater model are the hydraulic head at representative points ("observation wells"). In our application 13 input and 13 output parameters were defined by the users: The identified inputs consist of 9 counties and 4 wellfields, the 13 output parameters are 12 observation wells and the mean hydraulic head of the whole area of the water supply system (see Fig. 6.17). As the slow stream groundwater flow can be interpreted as diffusion process only nearby located input and output parameters (e.g. regions/wellfields and the corresponding observation wells) have some correlation and a SISO model with these input-/output combinations can be obtained. Due to this physical reason the number of relevant SISO models is relatively small and hence the resulting MIMO model of relatively low dimension ($n < 50$) which is appropriate for the optimization problem.
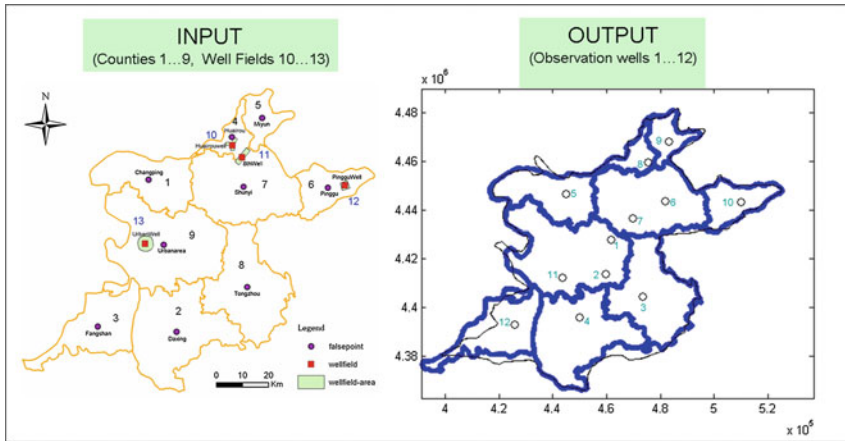
Fig. 6.17 In/outputs of the reduced model for the model area

6.2.2 Beijing Optimal Water Allocation System

To facilitate the optimization algorithm as described in Chap. 5, the Beijing water supply system is transformed in to a directed graph as shown in Fig. 6.18.

The nodes represent reservoirs, lakes, points of water supply or water extraction and simple junction points. The water distribution process is described by the edges (e.g. river reaches, channels), whereas the flow dynamics is neglected according to the specified time step for decision support. The surface water model consists of 53 nodes and 57 edges.

The dynamic optimization problem is formulated as required (refer to Sect. 5.3). In Eq. (5.1) The state variables x are the volume content of the reservoirs and channels with small slope and the states of the reduced groundwater model. Control variables u are the discharge of the transport elements as well as the water demand of the customers. The uncontrollable inputs z are the direct precipitation and the potential evaporation for the reservoirs and the flow of rivers entering the considered region, which is derived by means of rainfall-runoff-models.

The process Eq. (5.1) consist of the balance equations of the storage nodes and the reduced groundwater model. The balance equations of the non-storage nodes are formulated as general equality constraints (5.3)–(5.7). The objective function (5.2)
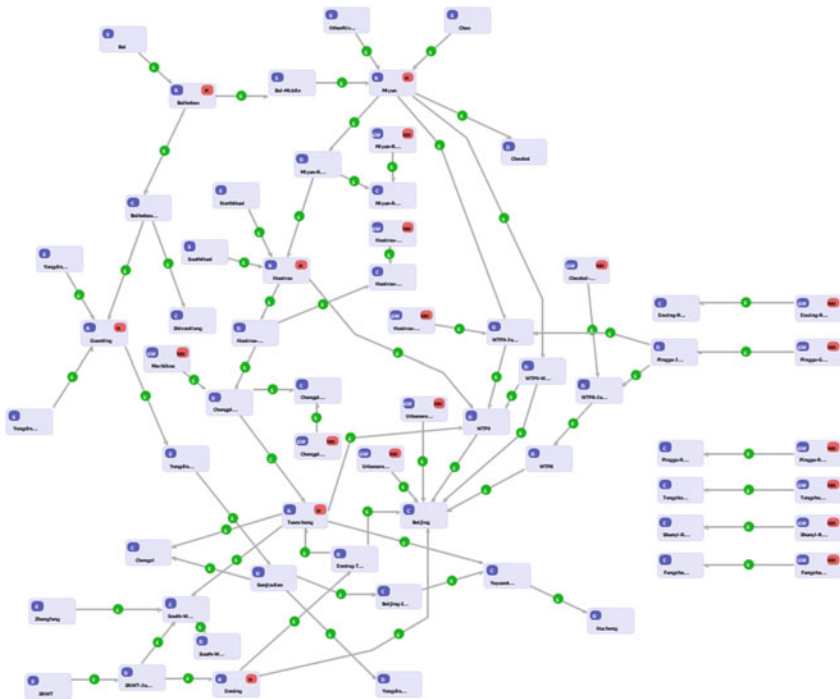
Fig. 6.18 Beijing Node-Link-Network

contains the goals of the water management, which are primarily the fulfillment of the customer demand, the compliance with targets for the reservoir and groundwater storage volume and the delivery of water with respect to environmental purposes. Therefore, quadratic terms are formulated, which penalize the deviations from desired values, like e.g. for the demand deficit of the demand node j:

$$f_0^k \left(u_j^k \right) = \rho_j^k \, \Delta t^k \frac{\left(u_j^k - q_{dem,ref,j}^k \right)^2}{(q_{dem,ref,j}^k)^2}, \tag{6.1}$$

where $q_{dem,ref,j}$ is the demand of and u_j is the discharge delivered to the customer. While this term applies for every time step within the optimization horizon, other terms are formulated only for the final point of the horizon, e.g. for the desired volume content of the reservoirs.

The inequality constraints Eqs. (5.3) and (5.7) are governed by the technical capabilities of the water distribution system and rules to guarantee safe operation, which are simple bounds for the control variables:

$$u_{\min}^k \leq u^k \leq u_{\max}^k,$$

as well as constraints for the reservoir volume x_v:

$$x_{v,\min}^k \leq x_v^k \leq x_{v,\max}^k$$

and the hydraulic head h_{hydr} of the observation wells:

$$h_{hydr,\min}^k \leq g^k \left(x_{gw}^k \right) \leq h_{hydr,\max}^k.$$

With respect to the practical applicability selected parts of the inequality constraints Eqs. (5.3) and (5.7) can be relaxed in order to avoid infeasible optimization problem with respect to unrealistic management demands.

The following objective functions were formulated in consultation with stakeholders, mainly the Beijing Water Authority:

Maximize supply to customers

$$\max \sum_{i=1}^{T} \sum_{j=1}^{n} WS_{ij}$$

Minimize demand deficit

$$\min \sum_{i=1}^{T} \sum_{j=1}^{n} \frac{WD_{i,j} - WS_{i,j}}{WD_{i,j}}; \; WD_{i,j} \geq WS_{i,j}$$

Maximize Water level of Miyun at final time

$$\max \ H_{T,Miyun}$$

Maximize average groundwater head at final time

$$\max \ H_{T,GW}$$

This formulated optimization problem is solved by the methods described in Chap. 5 using large scale non-linear programming solver (e.g. IPOPT and HQP). In this application the objective function of Eq. (5.1) is expanded by adding barrier terms for the inequality constraints:

$$\min_{y} \ \left\{ J(y) + \mu \sum_{j=1}^{n_g} \ln\left(-g_j(y)\right) \ | \ h(y) = 0 \right\}. \tag{6.2}$$

The solution of the original NLP results from the subsequent solution of Eq. (6.2) with a decaying sequence of $\mu \to 0$. The identification of right active set with its combinatorial complexity is avoided. The state of the art non-linear interior point solver IPOPT is used for the application at hand [339]. The interface for multistage optimal control problems of the optimization solver HQP [282], which provides an efficient way for problem formulation along with routines for the derivation of the ∇J, ∇h, ∇g by means of automatic differentiation [3], is used and coupled to IPOPT.

A typical water management problem for Beijing (horizon of 5 years, discretization of one month) has about 8000 optimization variables, 5500 equality constraints and 7200 inequality constraints. The numerical solution takes approximately 60 iterations and a calculation time of 10 s on a Intel Core 2 Duo CPU (2.5 GHz).

6.2.3 Sample Results of the Decision Support System

To illustrate the performance of the system, several example results of the simulation model (Catchment model, River system model, Groundwater and reduced ground water model) and the management tool will be presented below.

Figures 6.19, 6.20, 6.21 shows the results of Modeling a selected catchment area as an example. The model was calibrated with data from 1981 to 1990 and validated with future data. The y-axis in the Nash-Sutcliffe-Bias-Diagram shows the Bias value of the simulated to the measured data and the x-axis shows the Nash–Sutcliffe value. A perfect model would have the Bias value of 0 and the Nash–Suttcliffe value of 1. In Figs. 6.20 and 6.21, the model shows good training and validation Nash-Sutcliffe values of 0.73135 and 0.67845, respectively.

Figures 6.22 and 6.23 show the simulated/measured water inflow into the Guanting reservoir and the corresponding water level for a period of a year, respectively. The

Fig. 6.19 Outflow from
Miyun watershed (Training
performance)
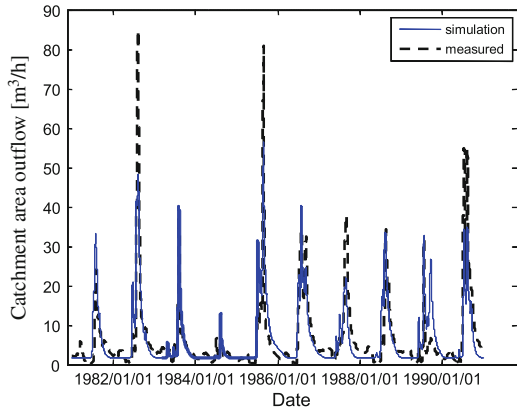
Fig. 6.20 Outflow from
Miyun watershed (Cost
function)
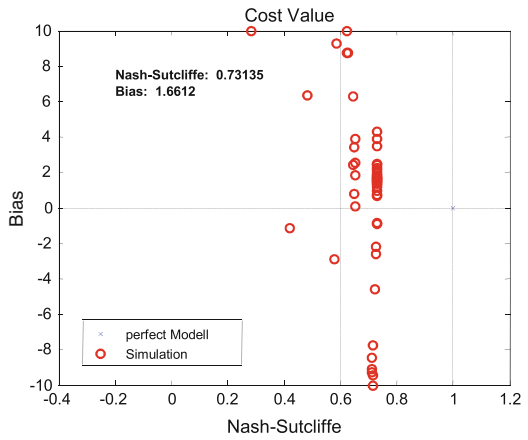
Fig. 6.21 Outflow from
Miyun watershed (Validation
performance)
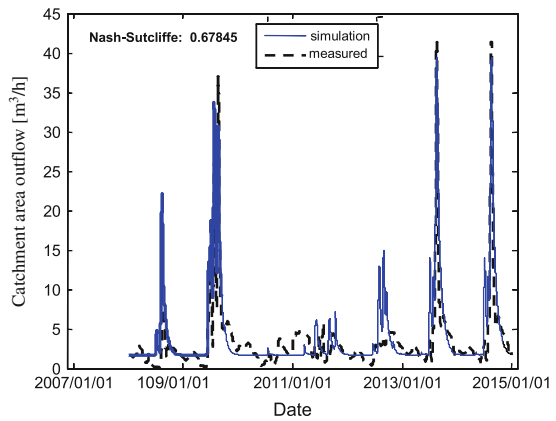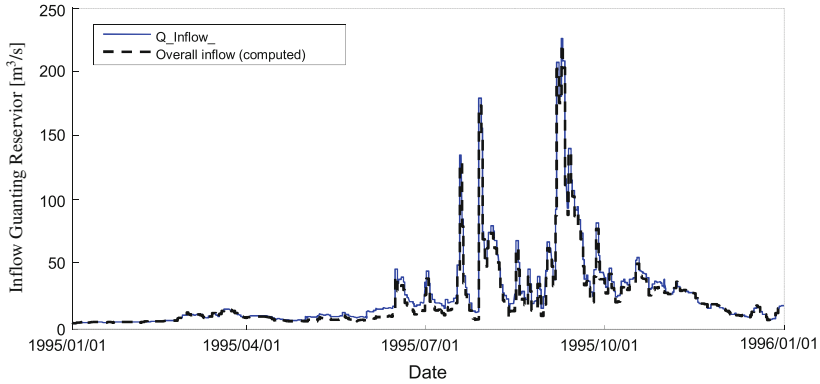
Fig. 6.22   Overall inflow to Guanting reservoir
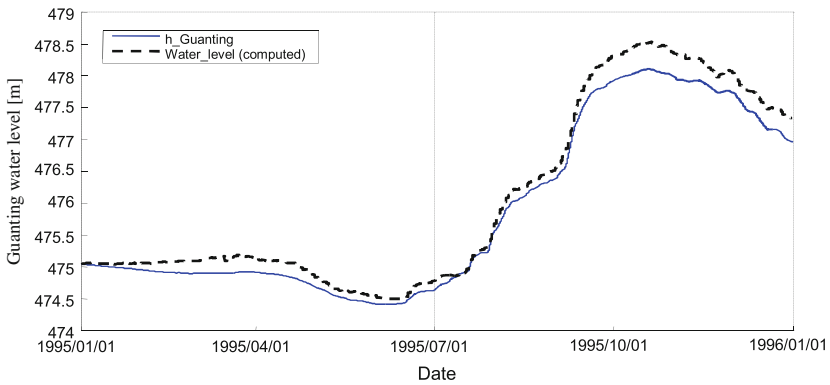
Fig. 6.23   Water level in the Guanting reservoir

peaks of the inflow can get up to practically $240\,\mathrm{m}^3/\mathrm{s}$. The water level at the beginning of the year is 475 m and at the end of the year the net reservoir water level has increased to 477.5 m. The downward slope in the graph from January to July is to be attributed to the effect of evaporation, or other water diversions. The little additional inflow fails to compensate for these outflows. The start of the rainy season becomes apparently in July. The inflows are then greater than the outflows. The water level rises until about mid October. After that, the outflow again dominates and the level at the end of the year is 477.5 m. Conclusively, if the outflow regime selected is continued, the water supply from Guanting Reservoir can be sustainably maintained.

Figures 6.24 and 6.25 show the water inflow into the Miyun reservoir and the corresponding water level. The value of the water level taken at the beginning of the year was 153.4 m. At the end of the year the reservoir does still have a level of 152.0 m. The downward slope in the graph between January and July is to be attributed to the effect of evaporation, of water diversion into the Beijing-Miyun channel, into the river Chaobai, and of the demand from the No. 9 waterworks. The
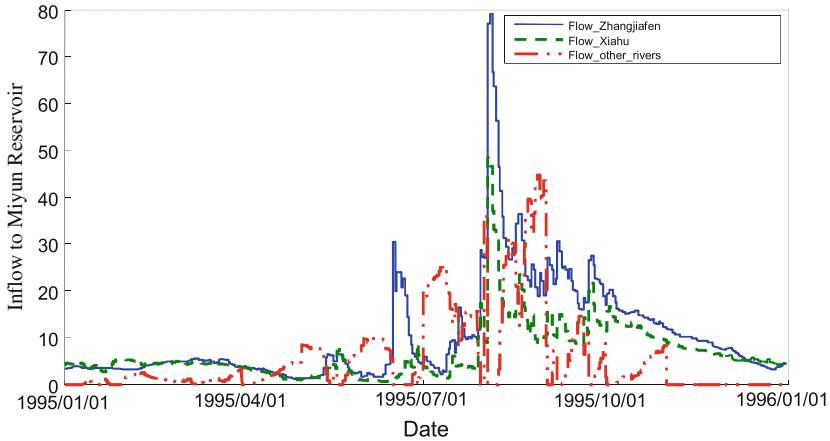
Fig. 6.24 Miyun inflow
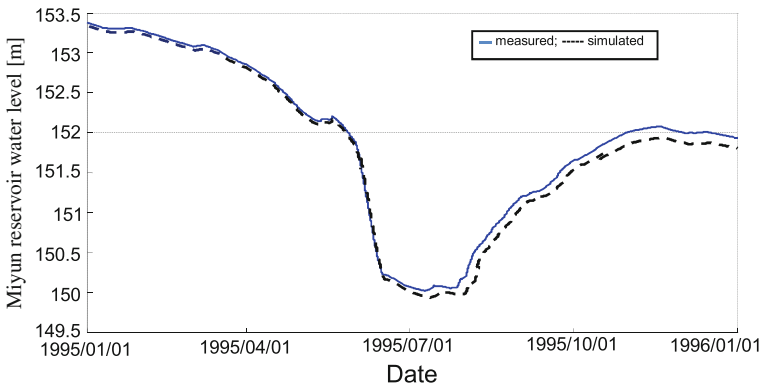
Fig. 6.25 Miyun water level

little additional groundwater coming from the catchment areas fails to compensate for these outflows. The start of the rainy season becomes apparent in July. The inflows are then greater than the outflows. The water level rises until about October. After that, the outflow again dominates and the level at the end of the year is 152.0 m. If the outflow regime selected is continued, a similar inflow figure over 5 years would mean that considerable restrictions must be set on consumption (the outflow) to assure sustainability.

The proposed concept for optimal water management is evaluated for two sets of experiments. The first set of experiments compares two scenarios. In scenario 1 of this experiment, we want to minimize demand deficit and keep demand constant for the next 10 years and in scenario 2 we want to minimize demand deficit and increase demand 5 % yearly for the next 10 years. The results of the two scenarios are illustrated in the Figs. 6.26, 6.27 and 6.28. Scenario 1 shows that the demand

can be fulfilled for the ten years, but without considering sustainability, the Miyun-Reservior and the groundwater are overexploited (see Fig. 6.28). By increasing the demand yearly, then we can see in scenario 2 that the demand won't be fulfilled anymore and within 1.5 years Miyun has already reached its minimum and at the end of the 10 years, the systems groundwater level has sunk rapidly.

In the second set of experiments, three scenarios based on the same set of input data (historical rainfall measurements and customer demands reflecting the predicted development of population size and economic growth) were studied. The objective function contains four quadratic terms in order to penalize deviations from the desired final water level of largest reservoir in the system (Miyun reservoir), from the desired final average hydraulic head of the groundwater storage as well as the deficit of the customer demand separated into two groups for household/industry and agriculture. The deficit of the delivered water must be less than 5 % for domestic/industrial
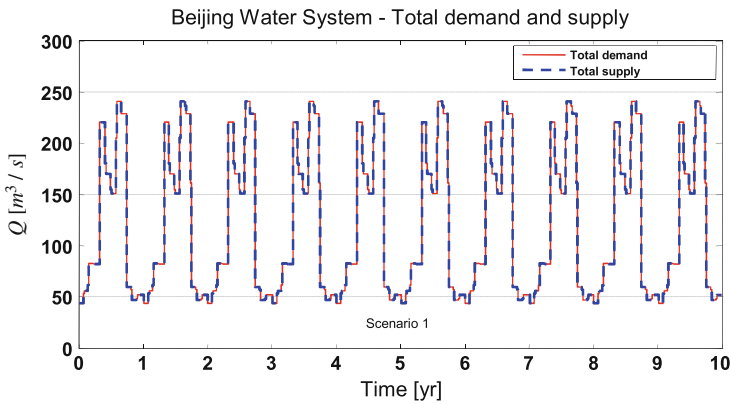
Fig. 6.26 Demand versus supply—scenario 1
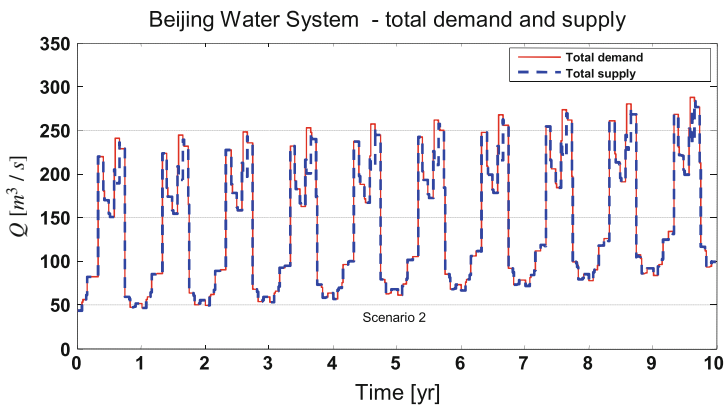
Fig. 6.27 Demand versus supply—scenario 2
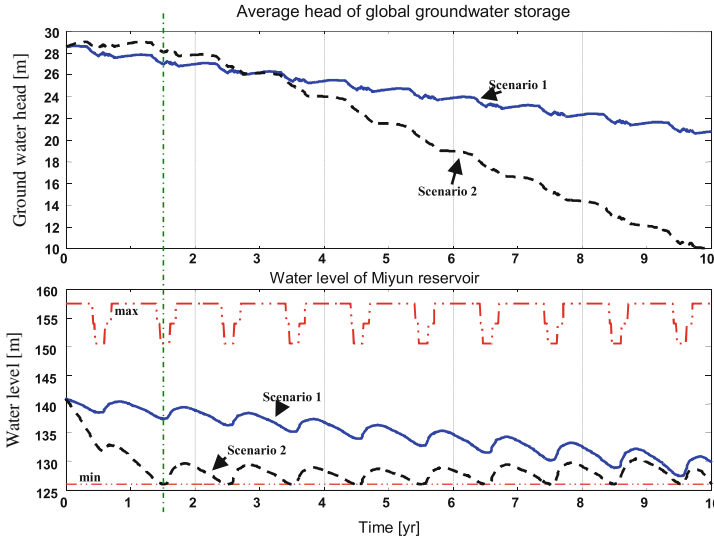
Fig. 6.28   Mean groundwater head and Miyun Reservoir

clients and less than 25 % for agricultural clients. For the third scenario it is assumed
that water can be transferred to the considered region up to an annual amount of
300 Mio. m³ starting from the third year within the optimization horizon.

The overall water requirement exceeds noticeably the natural sources. The
reduced groundwater model has been derived under the assumption that this over-
consumption was covered by the groundwater storage. This leads to a strong reduction
of the average hydraulic head of the groundwater storage of about 9 m during the
5 years (scenario 1, see Fig. 6.5). Using the initial state of the Miyun reservoir and the
final value of the reference trajectory for the average groundwater head as target in
the objective function, for the base scenario (scenario 1) there are only small observ-
able deviations from these values in combination with a minor demand deficit. In the
second scenario the increase of the target value for the final groundwater hydraulic
head at 5 m and a corresponding shift of penalty coefficients in order to keep this
value lead to a better spreading of the overdraft over the different storages as well as
to the customers.

Figure 6.29 shows the course of the water level for the Miyun reservoir. Because
of its capacity of 4.1×10^9 m³ the Miyun reservoir plays an important role for the
long term management of the overall system.

As can be seen, the years with an above-average precipitation produce only a
medium rise of the water level. The second scenario, which attempts to reduce
the decline of the average hydraulic head of the groundwater storage, results
in an increased release of this reservoir compared to the base scenario, which
corresponds to a change of the final water level from 142 m above sea level to 137 m.
In the third scenario, a part of this release is replaced by water from outside of the
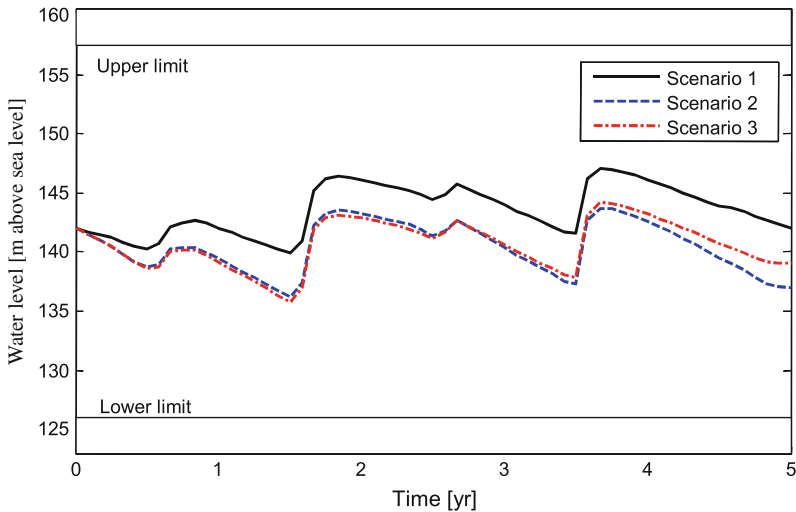
Fig. 6.29 Water level of Miyun-reservoir

considered region, which reduces the water level decrease at about 2 m. The second reservoir is situated at a channel from the Miyun-Reservoir to the city of Beijing and serves only as intermediate storage. The admissible range for water management is completely utilized by the optimal control approach. The shift in the management target causes a different operating strategy because water from the connected channel is taken to replace groundwater abstractions in the nearby regions. The change of the management target for the second and third scenario also induce an increase of the overall demand deficit from 0.1 % to 3.5 % (second scenario), which is nearly $6.8 \times 10^8 \mathrm{m}^3$ over the full horizon.

Figure 6.30 shows the time plot of the mean groundwater level of the optimization scenarios. It is obvious that in scenarios 2 and 3 that aim to increase the target value for the final groundwater hydraulic head at 5 m is nearly achieved.

In Fig. 6.31 the impact of the different strategies to the exemplary input 1 (exploitation in a certain region) and exemplary output 5 (groundwater level at a defined observation point) can be studied. The exploitation is clearly decreased in scenarios 2 and 3, which corresponds to an increase of the groundwater level at the observation point.

Finally, in Fig. 6.32 it can be seen that the performance of the drastically reduced groundwater model is good, regarding the fact that the original FEM model with more than 100.000 nodes has been reduced to a state space model with 36 states.

It has been proven that in spite of the large area which has to be managed and the corresponding complex surface and groundwater models the optimization problem could be solved in an appropriate computation time ($\sim$min). This could be achieved by a drastical reduction of the complex groundwater model to a state space model of relatively low dimension ($n < 50$). The user (i.e. water allocation decision maker)
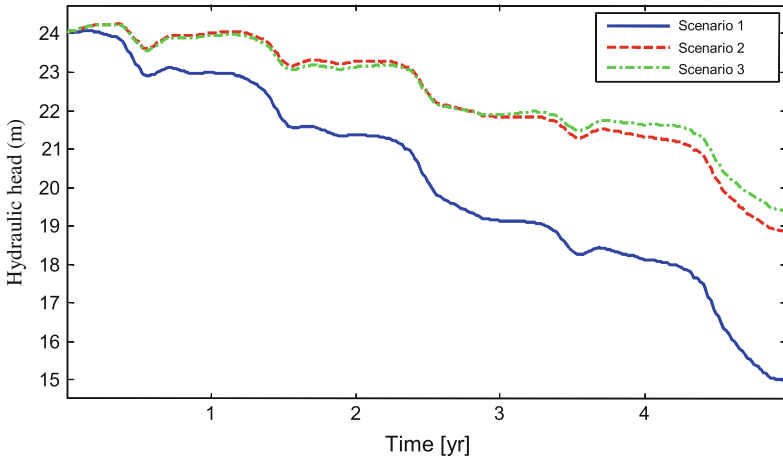
Fig. 6.30 Mean groundwater level from scenarios 1–3
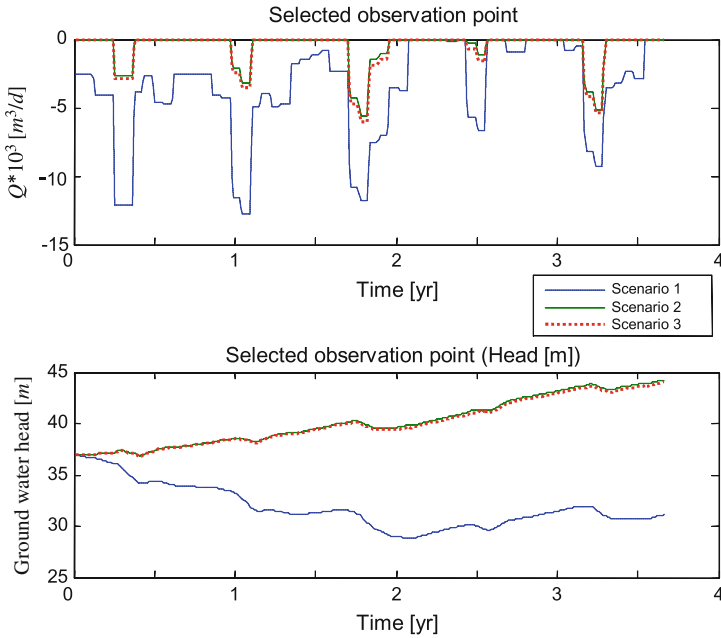
Fig. 6.31 Exploitation and groundwater head at a specific observation point
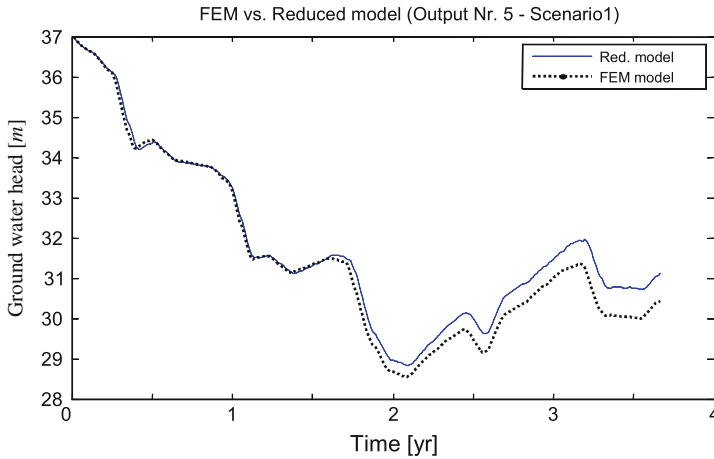
Fig. 6.32 FEM model compared with the reduced model using values from scenario 1

is enabled to select from a number of predefined performance criteria as well as to assign constraints to the elements of the water allocation system in order to specify the management targets according to his/her needs. The performance of the proposed concept is demonstrated by realistic optimization scenarios, whereby the benefit of a new strategic channel has been investigated with a planning horizon of 5 years. Actually the developed DSS is now being used by the decision makers.

6.3 Pipeline Network Simulation for Public Services

Thomas Westerhoff and Buren Scharaw

6.3.1 Introduction

As described in Sect. 3.2, water supply networks are one of the largest and most important infrastructures for public live. The safe supply with drinking water is one of the most important challenges for engineers. Because of the complexity of water distribution systems (WDS) and the used hydraulic models engineers need computer programs to simulate or optimize such systems. In the past decade a lot of programs for that where developed. Because of their experience for many years in water distribution engineering, also a universal simulation tool called *HydroDyn* was developed at Fraunhofer's Application Center for Systems Engineering in Ilmenau (Germany).

This chapter will describe the main features of *HydroDyn* and will demonstrate its capabilities with some example projects.

6.3.2 System Architecture of HydroDyn

HydroDyn was developed in cooperation with different water distribution companies and public services in Germany over the last years. The main goal was the development of an easy usable tool for engineers with the following features:

1. modeling and simulation of pressurized water supply networks,
2. modeling and simulation of sewer systems,
3. modeling and simulation of gas networks,
4. optimizing the operation of that systems,
5. combining spatial information with asset data,
6. advanced analysis and query support,
7. data access for SCADA systems.

HydroDyn is based on a client-server structure. The tool contains of four main system components

1. Oracle Database,
2. *HydroDyn* Calculation Server,
3. *HydroDyn* Clients,
4. *HydroDyn* Plugins.

The whole structure of the *HydroDyn system* is shown in Fig. 6.33 with the use of this distributed structure and the use of TCP/IP protocol for communication it is possible to place the systems component all over the world. The communication between the components will be done via Internet.
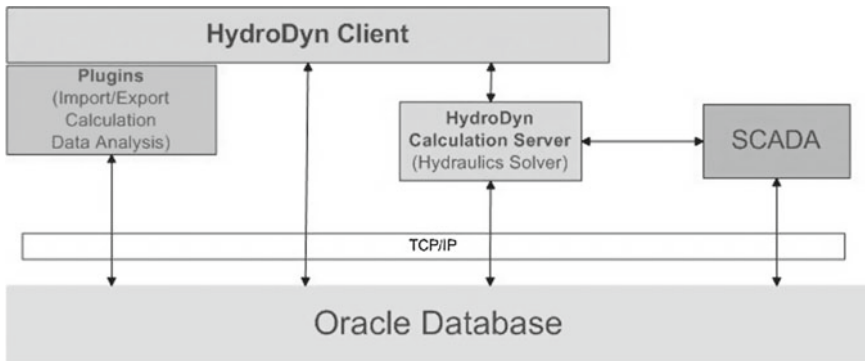
Fig. 6.33 System structure of *HydroDyn*

The first part of *HydroDyn* and the main data storage is the Oracle RDBS. All the model data for several networks, the calculation results, the spatial informations and the imported SCADA data are stored within this database. This gives the user the possibility to use all the advantages of Oracle database for storing a large amount of information like redundancy, partitioning, clustering etc. Therefore the system is scalable. For small models one can use a cheap Oracle license (e.g. Oracle Standard Edition One). If one wants to handle very large systems like mega cities it is also possible by the use of a larger Oracle license (e.g. Oracle Enterprise Edition). Oracle gives the user also the possibility to access all the data with a large amount of powerful tools for SQL-based data access and data exchange tools on the market.

The second part of the system is the *HydroDyn Calculation Server* (HDCS). It is designed as a MS Windows service that should be run on the Oracle Database Server. The HDCS does all the simulation and optimization tasks of the system. It has a direct connection to the oracle database. Each calculation that have to be executed is triggered from signals from the connected clients. There is also the possibility to trigger simulations and optimization tasks from a SCADA system. So the SCADA system can run daily tasks like pump scheduling optimization or leakage detection without the manual access of an engineer via *HydroDyn* client. SCADA can store actual measured values (e.g. tank levels, pump status, valve openings, metered demands …) into the Oracle database and run a simulation or optimization with that
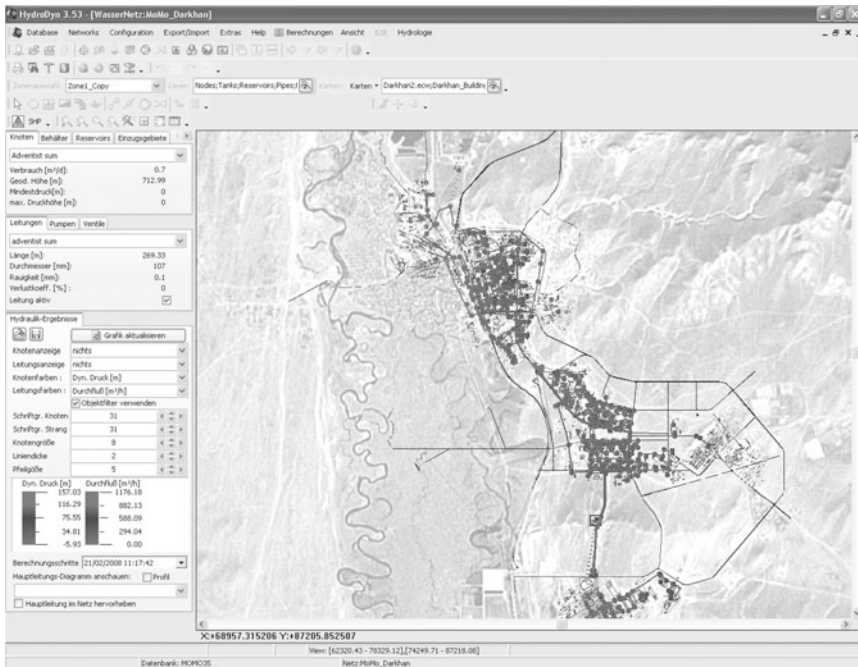
Fig. 6.34 *HydroDyn* client

values. Each Oracle Database has at least one *HydroDyn* calculation service. If one needs redundancy and availability for the system then more than one HDCS can be installed. The additional services starts in "wait-mode" and resume the calculation tasks if the main service fails or crashes (Fig. 6.34).

The third party of *Hydrodyn* is the *Hydrodyn Client* (HDC). The client is the main user interface to the engineer. With the HDC one can build up the system models, run calculations, analyze data, building reports and so on. *HydroDyn* has a very powerful support for geographical map formats like DXF, ESRI Shape File, ECW, GeoTiff, JPG, BMP etc. All map types can be referenced and aligned to match each other. Multiple clients can access one database and so all work can be done by several editors in parallel. At the moment there is only a Client version for MS Windows available.

The fourth and one of the most flexible parts of *HydroDyn* is its integrated plugin system. With the plugin interface it is possible to extend the functional range of the system step by step according to the customers requirements. There are a lot of plugins available for several purposes like
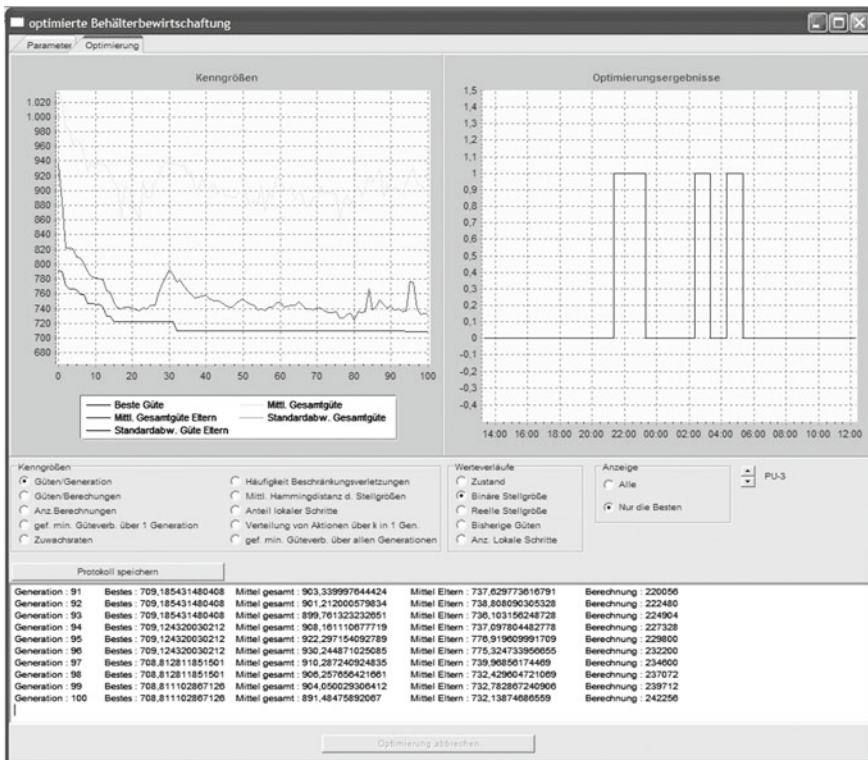
Fig. 6.35 Optimal pump scheduling plugin

1. Optimization plugins (Optimal pump scheduling plugin,…)
2. Database import and export plugins (pumps, valves, spatial data, elevation profils,…)
3. Data report plugin (customers demands, leakage reports, pump schedules,…)
4. SCADA connection plugins (OPC, SAT-RSI,…)
5. and a lot more…

As an example Fig. 6.35 shows the screen of the plugin for optimized pump scheduling.

6.4 Water Quality Modeling for the Lower Havel River

Albrecht Gnauck

6.4.1 Introduction

Today's environmental research is confronted with increasing inquiries for management re-commendations. The public expects fast and reliable statements on critical changes of environmental conditions and its effects on living conditions. Decision makers have to take management measures in time for safeguarding the living quality of people. The water cycle is one of the global problems with regional and local consequences. Especially, increasing nutrient inputs to water bodies lead to an increase of symptoms of freshwater eutrophication. Eutrophication is characterised by an increase of dissolved nutrients in water bodies, mainly phosphorus, carbon and nitrogen, by excessive growth of plants, mainly algae, and by restricted water uses due to anoxic water conditions as well as by odour problems [127, 327].

Eutrophication processes of freshwater ecosystems are supported by intensive man-made activities in river basins. Sediments have been accumulated nutrients over several decades [80]. They act as internal nutrient sources. Polluted water due to eutrophication affects not only the functioning of freshwater ecosystems, but also endangers human health [334]. Thereby, not only the various kinds of freshwater uses will be restricted, but also the availability of a landscape for culture, recreation and tourism [162]. Then, high financial budgets are required for water treatment and for restoration of damaged freshwater ecosystems [229, 232]. Mostly, eutrophication will be more indicated by their effects but less by actual changes of matter concentrations. In the past, enhanced input of phosphorus into water bodies due to intensive use of mineral fertilizers on agricultural areas, or orthophosphate in laundry detergents, as well as intensive inputs of sewage effluents has led to exceptionally high loads of phosphorus into rivers and lakes [230]. These man-made impacts caused a shift from oligotrophic to eutrophic and sometimes to hypertrophic freshwater ecosystems.

Freshwater ecosystems are highly complex, with plenty of functions and a great number of biotic structural elements. The biological structure, state, function, and evolution of a freshwater ecosystem depend on exchange of matter and energy with the environment as well as on the relationship between entropy-generating and entropy-reducing processes in the interior of the water body under consideration and in the sediment layer in exchange with it. Contributory to local entropy generation are not only thermal flow, friction, diffusion, light extinction, and chemical transformation of matter but also biological processes, such as primary production, respiration, grazing, ingestion, and excretion, with the process rates being non-linear functions of chemical affinities [212]. The entropy generated within the ecosystem is compensated by an inflow of negentropy, so that stationary non-equilibrium states are maintained [171]. Therefore, a thermodynamic description of a freshwater ecosystem is based on mass balances of state variables, pulse and energy balances as well as on the generalised Gibbs' fundamental equation for the entire system.

Freshwater ecosystems in northern Germany are characterised by low-flow conditions and by an increase of easily degradable substances mostly. The nutrient content of treated wastewater, the re-suspension of clay particles and the remobilisation of nutrients from sediment lead to a secondary load of the water body. Despite of reduction of external sources since the late 1980s the intended water quality goal of reduced nutrient levels in the water body has not been achieved. Now it has become clear, that the sediments have been accumulated nutrients, especially phosphorus, over several decades so that they now act as an internal nutrient source. Compared with the amount of phosphorus in the pelagic zone of eutrophic lakes, the phosphorus content of sediments of shallow water bodies is considerably higher [328, 329]. Therefore, eutrophication is now more sustained by internal than by external pollution sources.

Generally, a water quality Modeling and simulation framework is a fixed part of control schemes and decision support tools for water management. For the shallow river-lake system of the Lower Havel River such a framework (called *CEUS*— Cottbus EUtrophication Simulator) was developed to control the water quality. Firstly, modern time series analysis methods are used for process identification [113]. By means of wavelet analysis interrelations between water quality indicators and sediment characteristics could be identified. Reference [124] as well as [151] developed a 1D-process model describing the phosphorus remobilisation from sediment. Later on, changing water quality levels are simulated by the eutrophication simulator *CEUS* [118] carried out within the *MATLAB* development environment. To get a software tool for water quality management of river basins the *CEUS* simulator was coupled with the optimisation tool *ISSOP* [123, 187].

6.4.2 The Hydrological System of Lower Havel River

The Lower Havel River (LHR) belongs to the Federal Waterways of Germany. Hydraulic works as sluices and weirs and banked-up water levels influence the water flow as well as the intensity and kinetics of nutrient dynamics along the course
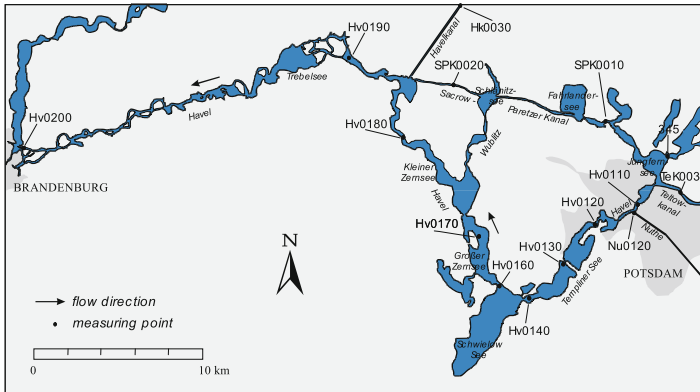
Fig. 6.36 Experimental area of the Lower Havel River

of the river. The catchment ranges from the junction of rivers Havel and Spree at Berlin-Spandau over the cities of Potsdam, Brandenburg/Havel and Rathenow up to the mouth of the Havel River into the River Elbe close to the City of Havelberg. Figure 6.36 shows a cut-off from the catchment up to the City of Brandenburg.

Especially, the experimental area under consideration is penetrated by the hydraulic work of the City of Brandenburg. Within this area the water flow is divided into two approximately equal parts of 25 (m/s). One part runs through the so called Sacrow–Paretz channel, and the other part through the River Havel. The Sacrow-Paretz channel, which was constructed between Lake Jungfernsee and Lake Gttinsee, by-passes the big loop of the course of the river between the City of Potsdam and the City of Brandenburg. Compared with sea level the average water level of LHR is given by 29.4 m above sea level. In opposite to the very strong urbanised area of Berlin/Potsdam with a lot of channel-like enlargements of the waterway and small harbours for industry as well as marinas for recreational purposes, the landscape is characterised by natural banks, shallow lakes with low-flow conditions, wetlands and marshy country, as well as by high evaporation rates. For low-flow situations, a slope of the water level of 2 (cm/km) was observed. The active sediment layer is given by 2–15 (cm). Table 6.1 contains some selected averages of hydro-morphological characteristics of the hydrological system of LHR.

Until 1990, the water quality of the River Havel was characterised by high eutrophication rates. Since 1990, the nutrient concentrations of effluents of sewage water treatment plants are diminished according to German environmental laws. A reduced usage of fertilisers as well as changes in the land use of agricultural areas has diminished the amount of nutrients from external diffuse sources. But, this management options have not led to a better water quality. Because of high retention times within the shallow lakes and large sediment surfaces, algal blooms, mainly diatoms and cyanobacteria, are supported by internal or secondary pollution of the water body due to nutrient remobilisation from sediment.

Table 6.1 Averages of hydro-morphological characteristics of LHR (cf. Fig. 6.36)

River/ Lake/ Channel	River km	Aver. Length (m)	Aver. Width (m)	Aver. depth (m)	Aver. Area (ha)	Aver. Volume (m)
Spandauer Havel	0.58–4.50	3920	1112	3.5	435.90	15256640
L. Kladow See	4.50–11.00	6500	1050	3	682.50	20475000
L. Kladow See	11.00–16.31	5310	1072	5	569.23	28461600
L. Jungfernsee	16.31–20.80	4490	500	4	224.50	8980000
L. weisser See	20.80–22.00	1200	389	2	46.68	933600
Sacrow Paretz-Channel	22.00–23.50	1500	130	3	19.50	585000
Sacrow Paretz-Channel	23.50–27.00	3500	60	3	21.00	630000
L. Schlaenitzsee	27.00–28.00	1000	1000	1.5	100.00	1500000
Sacrow Paretz-Channel	28.00–31.40	3400	60	4	20.40	816000
Potsdamer Havel	0.00–4.70	4700	268	3	125.96	3778800
Potsdamer Havel	4.70–10.20	5500	862	3	474.10	14223000
Potsdamer Havel	10.20–14.70	4500	785	4	353.25	14130000
Potsdamer Havel	14.70–17.00	2300	1800	3	414.00	12420000
Potsdamer Havel	17.00–25.10	7100	893	4	634.03	25361200
Potsdamer Havel	25.10–26.20	1100	50	2.5	5.50	137500
Potsdamer Havel/L. Goetiinsee	26.20–28.60	2400	513	2.3	123.12	2831760
Havel Channel	0.00–34.90	34900	200	2	698.00	13960000
LHR	28.60–32.56	3960	1300	2.3	514.80	11840400
LHR	32.56–38.00	5440	416	1.5	226.30	3394560
LHR/L. Trebelsee	38.00–41.50	3500	753	1.5	263.55	3953250
LHR	41.50–46.50	5000	585	2	292.50	5850000
LHR	46.50–56.17	9670	281	2	271.73	5434540
LHR	56.17–68.00	11830	304	2.5	359.63	8990800
LHR	68.00–79.00	11000	328	3	360.80	10824000
LHR	79.00–81.78	2780	150	4	41.70	1668000

6.4.3   Data Material

For water quality Modeling of LHR daily data are used which were available from the Environmental Authority of the State of Brandenburg at Potsdam. Long-term data sets of dissolved oxygen (DO), chlorophyll-a (CHA), ammonia (NH_4-N), nitrate (NO_3-N), orthophosphate phosphorus (o-PO_4-P), water temperature (WT) and water flow (Q) are used to simulate the water quality of LHR. For simulation the course of LHR were divided into segments of different length (Fig. 6.37). The river segments are characterised by their input and output observation points.

Because of irregular sampling all time series were processed by advanced static and dynamic statistical methods to get equidistant data. For the river-lake system under consideration in the linear interpolation method has been proved delivering the smallest standard error in comparison to the nearest neighbour method, cubic splines or cubic Hermite polynomials (Table 6.2).

6.4.4   Process Identification

Within freshwater ecosystems the eutrophication process is stimulated by external nutrient inputs but also by internal nutrient sources. The latter one is supported under certain meteorological, hydro-chemical and hydro-physical conditions by remobilisation of nutrients from sediments where water temperature is one of the most important control variables [195]. In consequence, a nutrient enrichment of the pelagic water column takes. Wind fetch on shallow water bodies causes uniform mixing of water, and leads to an uniform distribution of algal nutrients within the water body. To identify the phosphorus remobilisation process of LHR time series of water
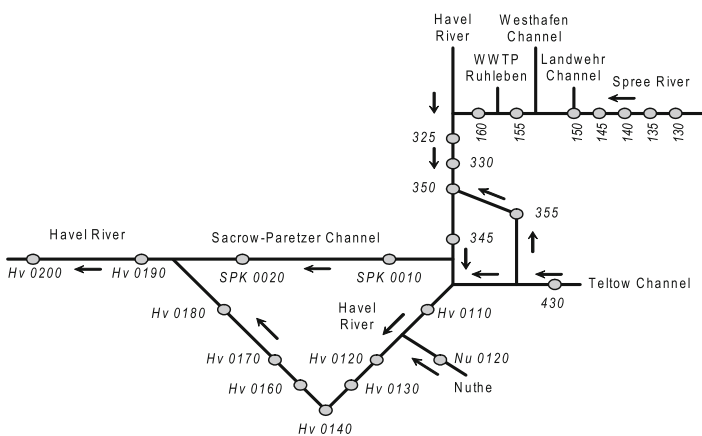
Fig. 6.37 Segmentation of rivers Spree and Havel

Table 6.2 Interpolation methods used for data sets of LHR

Indicator	River Spree	Teltow Channel	River Havel
Chlorophyll-a	Linear	Linear, spline	Linear
Conductivity	Linear, spline	Linear, spline	Linear, spline, polynomial
NH4-N	Linear	Linear, spline	Linear
NO2-N	Linear	Linear	Linear
NO3-N	Linear	Linear	Linear
o-PO4-P	Linear, spline, polynomial	Linear, spline	Linear
Turbidity	Linear	Linear, spline	Linear
UV absorption	Linear, spline	Linear, spline	Linear, spline, polynomial

temperature and phosphate phosphorus of two different sampling points of the river-lake system have been investigated. Figure 6.38 shows a comparison of phosphate phosphorus concentrations of the River Havel at Potsdam (input) and at Ketzin (output) of the shallow lake area under consideration. The amplitudes at Ketzin are much higher than at Potsdam which is explained by a higher secondary load caused by remobilisation of phosphate from sediments.

The underlying phenomenon was described by different authors for shallow lakes. Reference [26] as well as [195] reported on temperature dependencies of phosphate remobilisation in shallow water bodies connected with changing dissolved oxygen conditions where decreasing water temperature causes increasing phosphate remobilisation from sediment. Changes of the intensity of biochemical processes follow changes of water temperature which depend on changes of heat quantity added to the water body. Dead organic matter (mainly dead algal biomass) will be mineralised by micro-organisms. This process needs electron acceptors which are supplied from the water column where nitrate and dissolved oxygen are the major electron
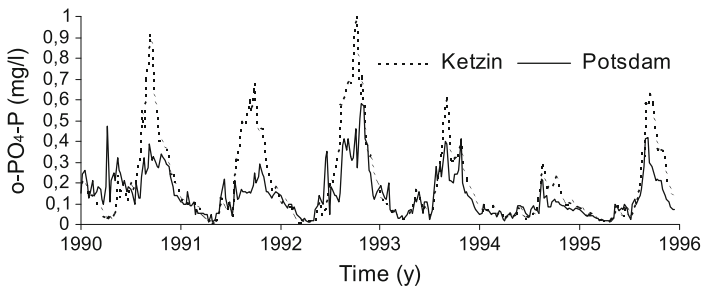
Fig. 6.38 Phosphate concentrations of input (Potsdam) and output (Ketzin) of a sub-watershed of the LHR

acceptors before iron is consumed. The order of consumption is determined by Gibbs free energy gained in the reaction. Methane formation due to decay of organic material in sediments leads to an increase of nitrogen and phosphorus within the pore water. Nutrients enter the sediment by molecular diffusion, convection, or bioturbation. In the case of aerobic conditions at the mud-water interface, phosphate will be stored and fixed in the sediment. For anaerobic conditions formation of hydrogen sulphide takes place and causes a destruction of stable iron (III) phosphate and iron (III) hydroxide layers of the mud-water interface which prevent phosphorus remobilisation under aerobic conditions. Due to diffusion processes phosphorus and also other nutrients come up from pore water to the water column.

From a wavelet analysis (Daubechies 3) of respective water quality time series with daily data [112, 124] resulted that the control of phosphate storage into sediment and phosphate remobilisation from sediment depend not only on the actual water temperature WT but on its gradient dWT/dt (positive or negative) and on the change of heat quantity d^2WT/dt^2 transferred to the water body. A visualisation of these effects is presented in Fig. 6.39.

The process observed is valid in all shallow lakes of the course of LHR. In the beginning at time d = 110 water temperature is increasing and forces bacterial decay of organic matter. The gradients of water temperature are f'(WT) > 0 and f''(WT) > 0 (Phase 0). If dissolved oxygen concentration is sufficient, then phosphorus will be stored into the sediment. Intensive bacterial activity leads to a higher demand of dissolved oxygen and at least to a deficit of DO at the mud-water interface. At this point phosphorus remobilisation is started. In parallel, a diminished increase of water temperature reduces the bacterial activity, and, in consequence, the demand of dissolved oxygen. If the gradient of WT reaches its maximum, then the amount of heat quantity transferred to the water body f''(WT) tends to negative values (Phase 1). A decrease of water temperature leads to negative values of the gradient of water temperature (dWT/dt) and its derivation which is connected with an increase of phosphorus remobilisation (Phase 2). A further, but diminished decrease of water temperature, that means smaller negative gradients, leads to positive values
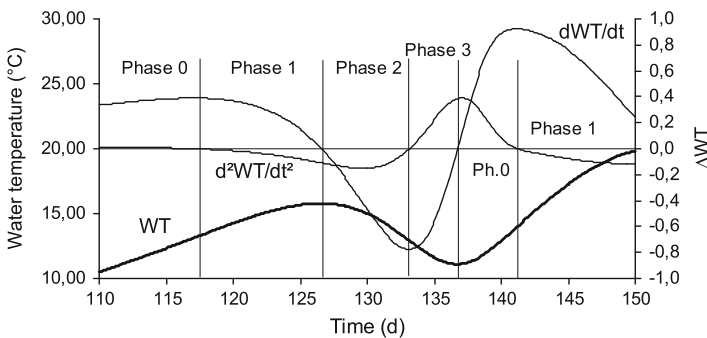
Fig. 6.39 Temperature control of phosphate remobilisation

Table 6.3 Phases of temperature control of phosphate remobilisation in shallow lakes

Phase	Change of heat quantity	Temperature gradients	P dynamics
0	Increase of WT	f'(WT) > 0, f''(WT) > 0	Storage of phosphate in sediment
1	Diminished increase of WT	f'(WT) > 0, f''(WT) < 0	Start of phosphorus remobilisation
2	Decrease of WT	f'(WT) < 0, f''(WT) < 0	Increase of phosphorus remobilisation
3	Diminished decrease of WT	f'(WT) < 0, f''(WT) > 0	Stop of phosphorus remobilisation
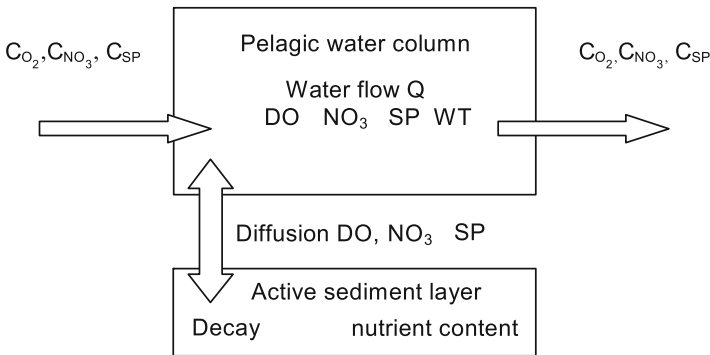
Fig. 6.40 Model concept of P-remobilisation (SP—soluble phosphorus, DO—dissolved oxygen, NO_3—nitrate nitrogen, WT—water temperature) (after [151], adapted from [118])

of the heat transfer to the water body. The phosphorus remobilisation from sediment will be smaller and will be stopped at least (Phase 3). Import of dissolved oxygen causes aging oxic conditions at the mud-water interface. Then, increasing water temperature starts again an intensive bacterial decay of organic matter characterised by phase 0. The process of storage or remobilisation of phosphorus will go on.

Corresponding with Fig. 6.39 four phases of soluble phosphorus dynamics in shallow lakes can be distinguished in dependence of water temperature (Table 6.3).

To compute this dynamic behavior [151] developed and validated a process model. The model concept is shown in Fig. 6.40.

The input to each river-lake segment is given by the input boundary conditions for dissolved oxygen, nitrate and soluble phosphorus bio-available for phytoplankton. The processes which take place in the mud-water interface are stimulated by the active sediment layer. The respective model equation for P-remobilisation from sediment (PSED) is given by:

$$\frac{dPSED}{dt} = (-1)^{\Theta} \cdot phi \cdot hs \left(-\frac{\frac{\left(1-\ln\left(phi^2\right)\right)\left(SP-\left(\frac{PSED}{hs \cdot phi}\right)\right)}{hs}}{2} \right.$$

$$\left. + \Theta \left(cpcrit - \frac{cpEA}{cpcrit} \right) \cdot (KFe\ cpFe\ +\ qp) \right)$$

$$(6.3)$$

where $\Theta = 1$, if $cpEA \leq cpcrit$, and $\Theta = 0$, if $cpEA > cpcrit$. The meaning of parameters is listed in Table 6.4. For Modeling of this process the *AQUASIM* software [269] was used.

Table 6.4 Model parameters for the P-remobilisation sub-model

Parameter/Variable	Explanation
cpcrit	Critical value of cpEA
$cpDO = DO/31{,}998$	Dissolved oxygen concentration in pore water
$cpEA = 2cpDO + 5cpNO_3$	Electron acceptor concentration in pore water
cpFe	Iron concentration in pore water
$cpNO_3 = NO_3/14.007$	Nitrate concentration in pore water
DSP	Diffusion coefficient of dissolved phosphorus
hs	Thickness of active sediment layer (m)
$K_1(20)$	Decay rate of organic material in pore water at $20\,^\circ$C
$KFe = K_1(WT)/36$	Iron concentration in pore water
$K_1(WT) = K_1$ $20^{(0.1 \cdot lg2/lgK1(20)(TEMP-20)+1)}$	Temperature dependent decay rate of organic material in pore water
phi	Sediment porosity
PSED	P-concentration remobilsed from sediment
qp	Ratio P/Fe of reducible iron
SP	Soluble phosphorus

For Modeling Modeling the P-remobilisation process of different parts of the river-lake system under consideration an average diffusion coefficient of 7.9×10^{-10} m/s for soluble phosphorus and a value of 0.9 for sediment porosity was assumed [151].

6.4.5 The CEUS Eutrophication Simulator

To simulate the eutrophication process in shallow water bodies a stationary 1D-model was developed. The model is an extension of the model *AQUAMOD* 1 [304] adapted to shallow eutrophic water bodies. The model concept is given in Fig. 6.41. It was realised with the *MATLAB* software development environment.

Model state variables are given by the water quality indicators phytoplankton (A), zooplankton (Z), dissolved orthophosphate phosphorus (PO_4-P), ammonia nitrogen (NH_4-N), and nitrate nitrogen (NO_3-N). The variables phytoplankton and orthophosphate phosphorus are connected with the sub-model for phosphorus remobilisation from sediment characterised by the active sediment layer. To cover the phosphorus remobilisation process from sediment the sub-model (PSED) given above was included in the phosphorus balance equation assuming that a quarter of soluble phosphorus is originated by P-remobilisation from sediment. Q_{IN} and Q_{OUT} describe the average discharges into and out of a river segment or lake under consideration. External driving forces like photoperiod (FOTOP), solar radiation (I) and water temperature (WT) influence the biological activity within the water body.

The mathematical model consists of five differential equations, site-specific functions, water-specific disturbance variables and environmental constants as well as model-specific parameters. A description of model equations and parameters, site constants and ecosystem specific parameters is given by [112, 118]. The time
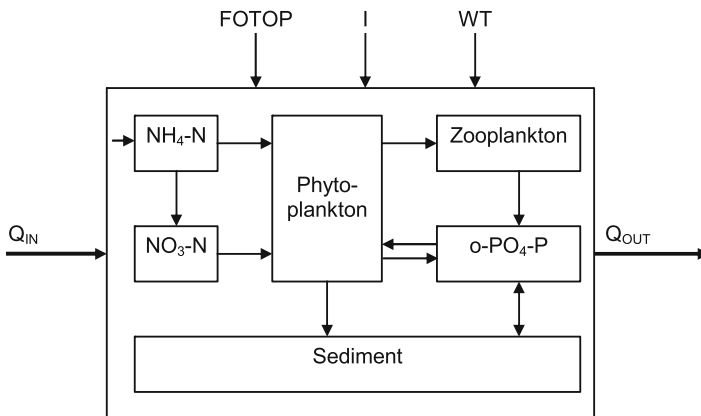
Fig. 6.41 Conceptual model of the eutrophication simulator

behavior of physical variables is modelled by trigonometric functions as well as by polynomials. The following equations are used:

Phytoplankton biomass A (mg CHA/l)

$$\frac{dA}{dt} = \frac{Q}{V\,(A_{IN} - A_{OUT})} + GROW - UA\,f\,(t)\,A - FRZ \cdot CR \cdot Z \cdot A$$
$$+ RESP \cdot WT \cdot A \tag{6.4}$$

Phosphate phosphorus P (mg P/l)

$$\frac{dP}{dt} = \frac{Q}{V\,(P_{IN} - P_{OUT})} + FRZ \cdot CR \cdot Z \cdot A \cdot C((1 - AZP)(KSA/(KSA + A)))$$
$$+ RESP \cdot WT \cdot A - GROW + 1/4 \cdot PSED \tag{6.5}$$

Ammonia nitrogen NH4-N (mg N/l)

$$\frac{dNH4}{dt} = \frac{Q}{V\,(NH4_{IN} - NH4_{OUT})} + B3 \cdot NORG$$
$$- B1 \cdot NH4 - FA1 \cdot FUP \cdot GROW \tag{6.6}$$

Nitrate nitrogen NO3-N (mg N/l)

$$\frac{dNO3}{dt} = \frac{Q}{V\,(NO3_{IN} - NO3_{OUT})}$$
$$- FA1\,(1 - FUP) \cdot GROW + B1 \cdot NH4 \tag{6.7}$$

Filtrating zooplankton Z (mg C/l)

$$\frac{dZ}{dt} = \frac{Q}{V\,(Z_{IN} - Z_{OUT})} + FRZ \cdot CR \cdot Z \cdot C \cdot AZP$$
$$\cdot \left(\frac{KSA}{KSA + A}\right) - MORT \cdot Z \tag{6.8}$$

Site-specific disturbance functions

Global radiation (J/cm$^2 \times$d)

$$I = 280 + 210 \cdot \sin\left(\frac{2\pi}{365} \cdot (t + 240)\right)$$

Foto period (h)

$$FOTOP = 12 - 4 \cdot \cos\left(\frac{2\pi}{365}t\right)$$

Water-specific disturbance variables

Water temperature (°C)

$$WT = 13.55 + 9.68 \cdot \sin\left(\frac{2\pi}{357} \cdot (t - 114)\right)$$

Sinking function of phytoplankton

$$f(t) = 0.8 + 0.25 \cdot \cos\left(\frac{2\pi}{365} \cdot t\right) - 0.12 \cdot \cos\left(\frac{2\pi}{\frac{365}{2}} \cdot t\right)$$

$$DO = 10.70 + 1.52 \cdot \sin\left(\frac{2\pi}{500} \cdot (t + 98)\right) + 1.53 \cdot \sin\left(\frac{2\pi}{122}(t + 60)\right)$$

Water-specific environmental constants

$$EP = 0.2; z_{mix} = 2$$

Model-specific parameter values

AZP = 0.6; IK = 1.25; KSA = 60; MORT = 0.075; FRZ = 0.9×10^{-3}; KSSP = 100; UA = 0.05; RESP = 0.005.

Explanations of functions and parameters used in the model *CEUS* are given in Table 6.5.

The simulator *CEUS* was calibrated and validated by comparisons of measured and simulated time series of water quality indicators. Time series of water quality data from 1998 to 2004 from different observation points along the course of LHR were used for modeling and parameterisation. As recommended by the Federal Institute of Hydrology of Germany time series of water quality indicators from 1997 are taken as reference data [351]. For this reason time series at observation point 325 (cf. Fig. 6.37) are compared with simulated water quality indicators for different river segments of LHR. The water body is well mixed and nutrient rich with an equal water temperature distribution. In the case of Sacrow–Paretz Channel (SPK0010) the water quality is mainly influenced by the anthropogenic activities of the urbanised area of the capitals Berlin and Potsdam.

The bioproduction follows the same yearly dynamics but with higher variations at monitoring station 325 caused by intensive man-made activities within the sub-catchment (Fig. 6.42). At the other stations concentration lines are more smoothed. Phytoplankton variations show local maxima in spring caused by diatoms and higher ones in late summer and early fall by cyanobacteria. With decreasing water temperature and decreasing natural light intensity the algal bloom collapses. The phytoplankton biomass drops down to the initial level. Because of differences in water mass movement the phytoplankton maxima of observation points 345 and SPK0100 are shifted approximately by one week.

Table 6.5 Functions and parameters of model CEUS

Function/parameters	Explanation
AZP	Part of nutrients utilised by zooplankton
B1	Rate of oxidation of ammonia
B3	Rate of ammonification
C	Ratio of carbon to chlorophyll of the algal biomass (mg C/mg CHA)
CR	Part of filtered algal biomass
EP	Coefficient of light extinction
FA1	Nitrogen part of algal biomass (mg N/mg CHA)
FRZ	Filtration rate of zooplankton
$FUP = PFNH4/(NH4PF + (1-PF)NO3)$	Chemical transfer rate of ammonia nitrogen to nitrate nitrogen
$GROW = UPTAKE(\arctan(RATE) - \arctan(RATEe^{(-EPSzmix)}))$ $SP/(SP + KSSP)NO3/(NO3 + KSNO3)$	Phytoplankton growth
GROWMAX	Maximum growth rate of phytoplankton biomass
I	Solar radiation
IK	Light dependency of phytoplankton growth
KSA	Half saturation constant of zooplankton
$KSNO_3$	Half saturation constant of nitrate nitrogen
KSSP	Half saturation constant of soluble phosphorus
MORT	Mortality rate of zooplankton
NORG	Organic nitrogen
PF	Preference factor for nitrogen
$PMAX = 0.0193e^{0.09WT}$	Temperature dependency of phytoplankton growth
Q	Flow of water mass
$RATE = I/(2IKFOTOP)$	Light dependency of phytoplankton growth
RESP	Respiration rate of phytoplankton
UA	Sinking rate of phytoplankton
$UPTAKE = 2$ $GROWMAXFOTOPPMAX/(EPzmix)A$	Nutrient dependency of phytoplankton growth
V	Volume of river/lake segment
z_{mix}	Mixing depth (m) of river/lake segment under consideration (cf. average depth in Table 6.1)

In accordance with this behavior soluble phosphate phosphorus is decreased in spring by nutrient uptake due to diatoms. The strong increase in late summer is caused by phosphorus remobilisation from sediment. Of course the soluble phosphorus concentrations are higher at observation point 325 compared with observation point 345. But it is remarkable that at observation point SPK0100 the same concentration
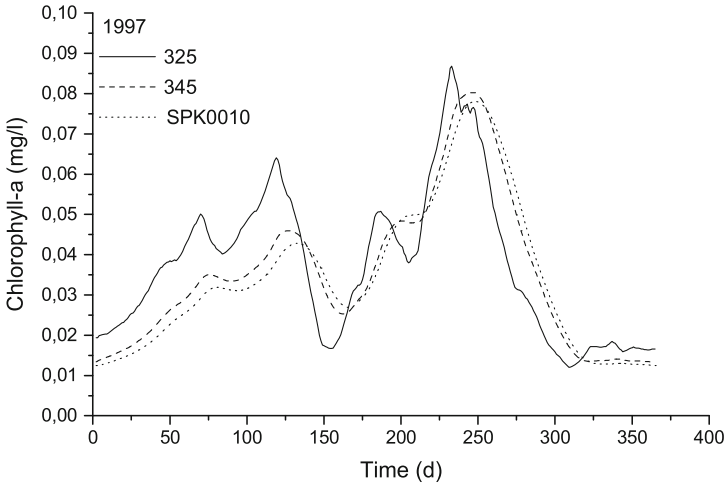
Fig. 6.42 Validation of *CEUS* for phytoplankton biomass
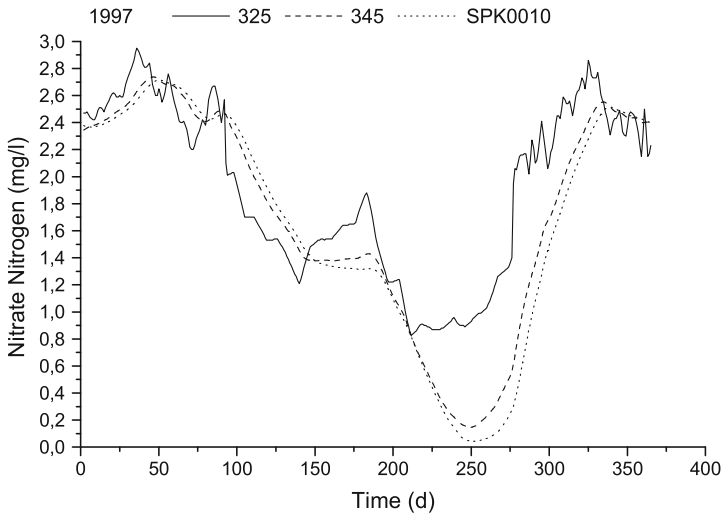
Fig. 6.43 Validation of *CEUS* for nitrate nitrogen

value soluble phosphorus is reached as at observation point 325 after the conjunction of River Spree and River Havel.

The nitrogen compounds ammonia and nitrate show an opposite dynamic compared with this of orthophosphate phosphorus. Ammonia nitrogen and nitrate nitrogen are directly coupled. Figure 6.43 shows the nitrate nitrogen dynamic with higher values in spring but lower values in late summer and fall. This overall behavior is based on two different processes. The first process is known as nitrification (bacterial

oxidation of ammonia to nitrate in two steps). The other one is referred to nitrate uptake by cyanobacteria. Increase of nitrogen content at the end of the year is caused by import processes from other river segments.

6.4.6 The Optimisation Tool ISSOP

For parameter optimisation the software tool *ISSOP* (**I**ntegrated **S**ystem for **S**imulation and **Op**timisation) was used [187]. Originally it was developed to support manufacturing, organisational and logistic processes based on discrete parameter optimisation methods. In Fig. 6.10 an overview of the inner architecture of *ISSOP* and the optimisation methods included is presented. Before starting an optimisation run each real problem will be automatically transformed into the standard optimisation problem. The following optimisation procedures are included: CENUM—Component wise enumeration, DISOPT—a quasi-gradient method, EVOL—an evolutionary optimisation strategy, SIMCARLO—optimisation by MCM, SIMGEN—optimisation by a genetic algorithm, THRESHACC—optimisation by a threshold algorithm, QUADLS—optimisation by a cube method as a mixture of local search and exhaustive enumeration. For analysis of parameter sensitivity the method SENSIT can be used. Further optimisation procedures can be added to *ISSOP* (Fig. 6.44).

ISSOP contains an open interface for *MATLAB* models. Therefore, the *MATLAB* based eutrophication model *CEUS* was coupled with *ISSOP* to get optimised parameter sets for simulation. Figure 6.45 shows the general structure of coupling [123].
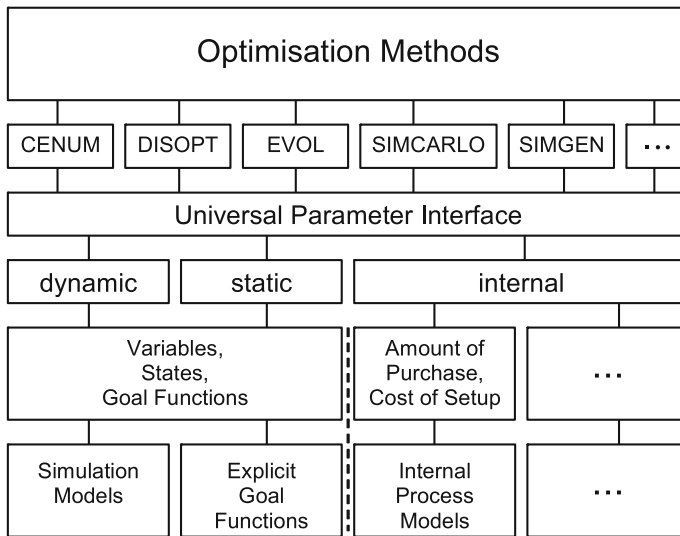
Fig. 6.44 Optimisation methods contained in ISSOP
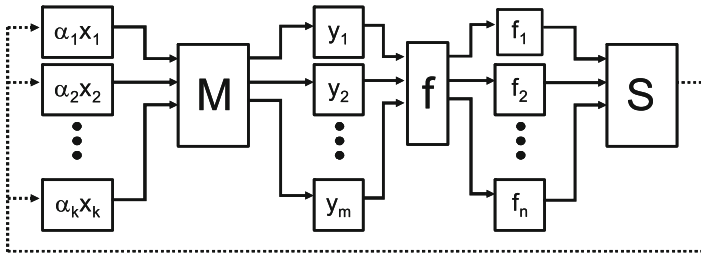
Fig. 6.45 Structure of coupling between simulation model *M* and optimisation tool *S*
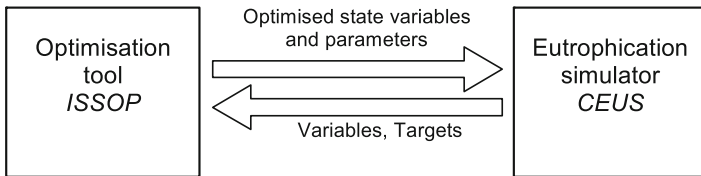
Fig. 6.46 Information exchange between *ISSOP* and *CEUS* (adapted from Gnauck et al. 2003a)

The input variables of the simulation model **M** are denoted by $\alpha_1 x_1, \ldots, \alpha_k x_k$, while the outputs of *M* are symbolised by $y_1, \ldots, y_m$. They will be valuated by goal functions $f = \{f_1, \ldots, f_n\}$ with $f_i(M(\alpha_1 x_1, \ldots, \alpha_k x_k)) = f_i(y_1, \ldots, y_m)$ for $i = 1, \ldots n$. Arbitrary continuous functions f_i can be used as goal functions. There are no restrictions for goal functions (e.g. convexity). If $n > 1$, then goal functions $f_1, \ldots, f_n$ are aggregated to a weighted sum $S = \Sigma w_i f_i$. For weighting factors w_i the condition $\Sigma |w_i| = 1$ is valid. The model results will be optimised simultaneously.

The data transfer between optimisation and simulation system is given in Fig. 6.46. The tool *ISSOP* uses the model variables and target values of *CEUS* as input data and gives optimised state variables and parameters back to the eutrophication simulator *CEUS*.

6.4.7 Simulation Results and Discussion

After calibration and validation the simulator *CEUS* was used to generate simulation results of phytoplankton and nutrient dynamics of LHR at different locations (Fig. 6.47, cf. Fig. 6.36). Because of nutrient rich water within each river segment the bioproduction is relatively high in spring but in summer and fall as well. During the first four months an increase of phytoplankton biomass is observed. The growth of phytoplankton is dominated by diatoms. Their ecophysiological preference is stimulated by low water temperature and high concentration of soluble phosphorus within the water body. The speed of phytoplankton growth is high. By the middle of April (d 110) the growth of phytoplankton drops down because of increasing water tem-
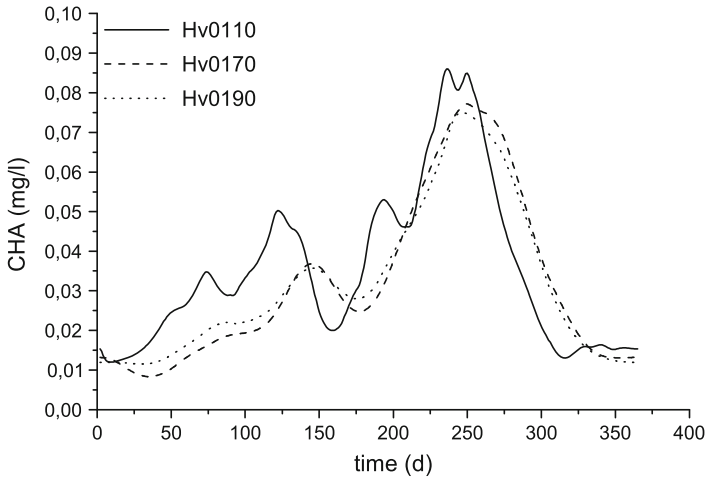
Fig. 6.47 Simulated yearly dynamics of algal biomass of LHR

perature. Another very high increase of phytoplankton biomass can be seen in the second half of the year. In opposite of spring biomass, cyanobacteria are the dominant algal species now. Cyanobacteria prefer nitrogen as nutrient source instead of phosphorus starting in June (cf. Figs. 6.49 and 6.50). In the interval between diatom and cyanobacteria growth green algae species grow up.

In late summer resp. early fall algal blooms collapse. As a result, high concentrations of dead organic matter settle down to the bottom in each of the river segments. This leads to high decay rates of dead organic matter with high rates of oxygen consumption by bacteria. In consequence, anoxic conditions exist at the sediment-water interface and change its chemical behavior. The nutrients stored in the pore water of
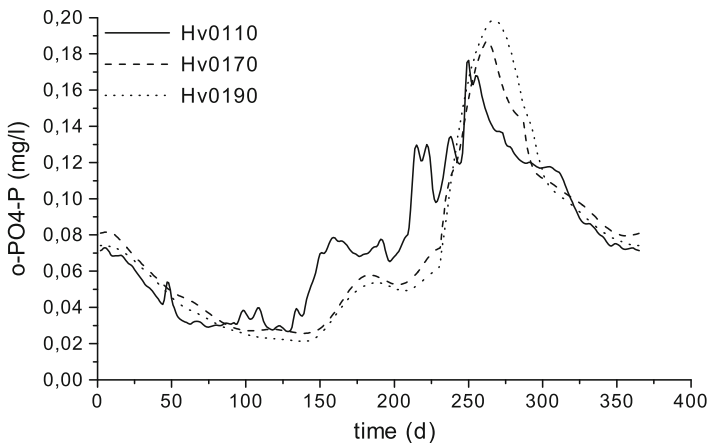
Fig. 6.48 Simulated yearly dynamics of soluble phosphorus of LHR
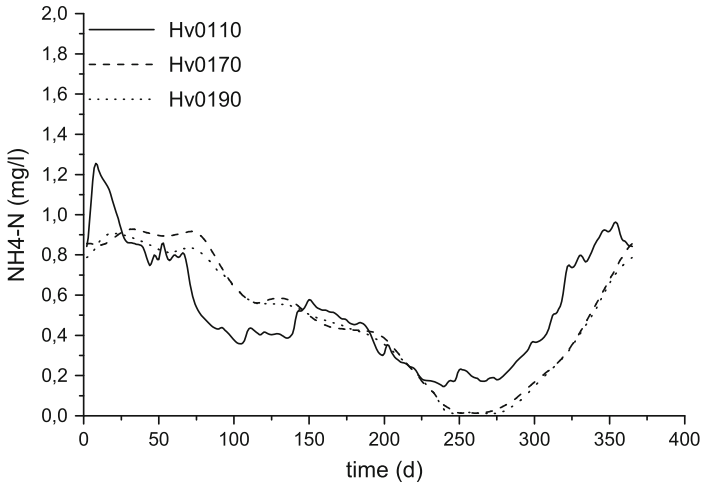
Fig. 6.49 Simulated yearly dynamics of ammonia nitrogen of LHR

the sediment will now be remobilised from it by diffusion processes and distributed over the whole water column due to wind fetch.

This effect can be seen from Fig. 6.48 which shows the yearly dynamics of soluble phosphorus.

The decreasing behavior in the first half of a year will be alternated by a strong increase of phosphate phosphorus concentration starting at end of May (d = 150). The time shift between diatom biomass maximum and orthophosphate phosphorus minimum is approximately three weeks. This means, than the losses of soluble phosphorus will be partly equalised by phosphorus remobilisation from sediment. The extremly increase of phosphorus in the second half of the year can take place because the species composition of algal biomass has been changed.

In opposition to that, the inorganic nitrogen components ammonia and nitrate show another dynamic behavior. Both components are imported by the river flow from underlying river segments. They show increasing concentrations up to the end of February and beginning of March. The processes behind this dynamics are snow melting and anthropogenic inputs by wastewater (Fig. 6.49). With increasing water temperature the chemical transfer processes of nitrification go on faster. But the increase of nitrate nitrogen will be compensated by algal growth, mainly green algae.

Because of nutrient rich water body and high water temperatures the growth of cyanobacteria causes an extremly decrease of nitrogen concentrations. Ammonia nitrogen is now totally converted to nitrate nitrogen. All nitrate is utilised by cyanobacteria (Fig. 6.50). The nitrate concentration level tends to zero between August and September. Both the import of ammonia due to water inflow and the nitrification process are too small to fill up the nitrate nitrogen pool. After the collapse of the algal bloom both the nitrogen components reach their initial values by external pollution from the watershed and internal matter transfer processes.
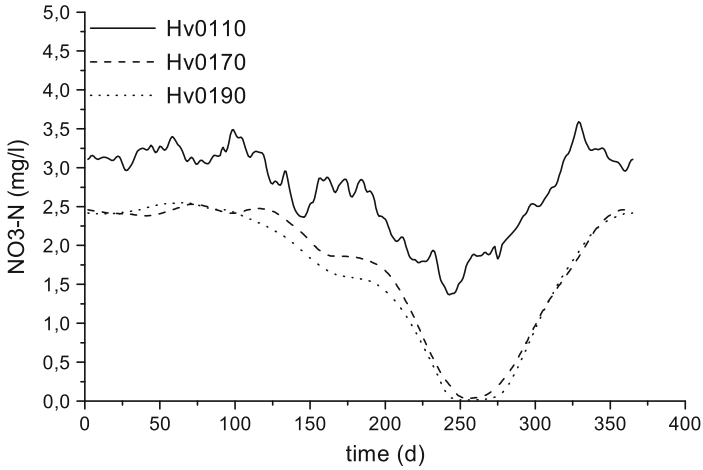
Fig. 6.50 Simulated yearly dynamics of nitrate nitrogen of LHR
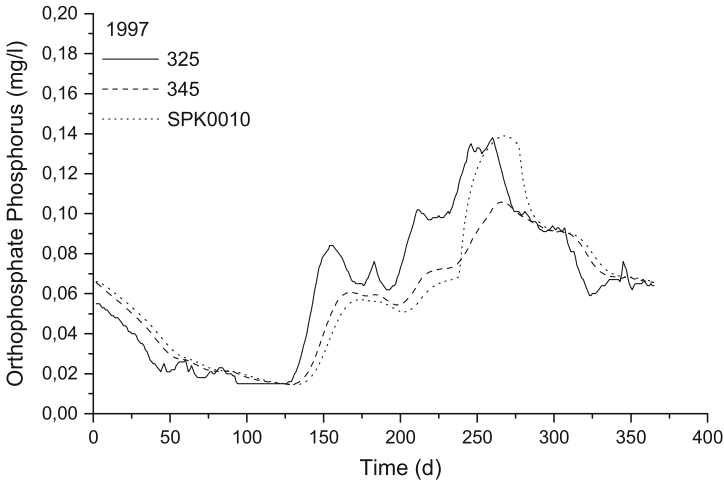
Fig. 6.51 Validation of *CEUS* for soluble phosphorus

Additionally, the simulator *CEUS* was also applied to generate statements on nutrient dynamics of Lower Havel River. Simulations of nutrient dynamics were carried out between measuring points Hv0170 and Hv0190. As can be derived from Fig. 6.51 two different processes influence the phosphorus dynamics: Decrease of phosphorus concentration due to phytoplankton uptake by diatoms in spring, and an extremely increase of soluble phosphorus concentration due to phosphorus remobilisation from sediment in late summer and early fall (Fig. 6.52). Some time before the phytoplankton increase will drop down because of nitrogen deficiency (cf. Fig. 6.53). The prerequisites for P-remobilisation are fulfilled (relatively high water tempera-
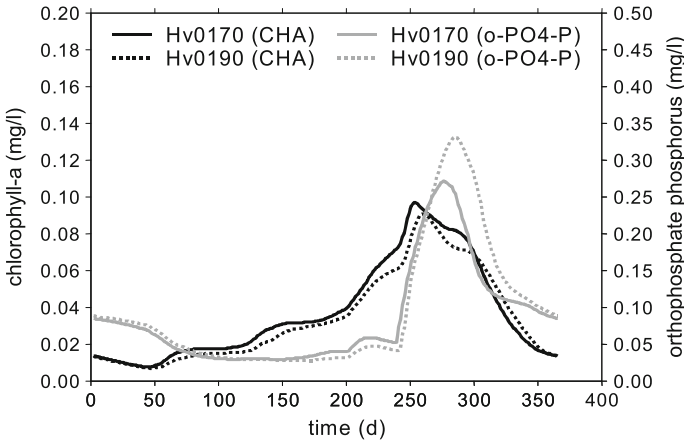
Fig. 6.52 Simulation of orthophosphate phosphorus dynamics

ture, high decay rate of dead organic matter) and chemical processes can start. It can be seen from Fig. 6.52 that phosphorus concentration at Hv0190 is higher and reaches its maximum later than at Hv0170 due to export of soluble phosphorus from foregoing river segments and run time effect within the water body.

According to Fig. 6.43 the nitrogen compounds ammonia and nitrate show higher values in spring but lower values in late summer and fall. Increase of biomass by cyanobacteria causes a drastic decrease of nitrogen concentrations close to zero due to biomass uptake. Because of nitrogen deficiency over a longer time (approximately 30–40 days) the bloom of cyanobacteria is stopped. At the end of the year the nitrate concentration reaches the initial value. This effect can be explained by import of ammonia–nitrogen due to waste water input and bacterial oxidation of ammonia to nitrate as well as by diffuse pollution from the watershed.

After confirmation of validated simulation runs the simulator *CEUS* was applied to generate optimal forecasts of algal and nutrient dynamics of the Lower Havel River for water management purposes. For this reason the simulator was combined with the optimisation tool *ISSOP* (cf. Sect. 6.4.6). The structure of scenarios can be seen from Fig. 6.54 where **M** denotes model run. Data of control gauge 345 are used now as input time series. Simulation runs of algal and nutrient dynamics were carried out between control gauges Hv0110 and Hv0190. After the first model run optimal forecasts of concentration levels at control gauge Hv0110 will be get. With these results the simulation starts again to get results for the next control gauge and so on up to control gauge Hv0190.

The vector of goal functions $f = \{f_1, \ldots, f_3\}$ is defined as follows:

1. Phytoplankton biomass $f_1(t) = \Sigma_x \Sigma_t y_1(x, t) \to$ min.
2. Orthophosphate phosphorus $f_2(t) = \Sigma_x \Sigma_t y_2(x, t) \to$ max.
3. Nitrate nitrogen $f_3(t) = \Sigma_x \Sigma_t y_3(x, t) \to$ max.
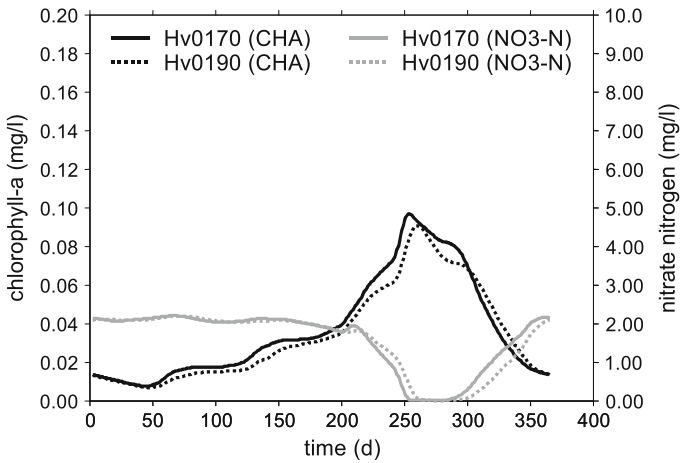
Fig. 6.53 Simulation of orthophosphate phosphorus dynamics

The model transfer structure reads $M(\alpha_1 x_1(t), \alpha_2 x_2(t), \alpha_3 x_3(t)) = (y_1(\mathbf{p},t), y_2(\mathbf{p},t), y_3(\mathbf{p},t))$ with $x_1(t)$: CHA, $x_2(t)$: o-PO_4-P, $x_3(t)$: NO_3-N as input variables and $y_1(\mathbf{p},t)$: CHA, $y_2(\mathbf{p},t)$: o-PO_4-P and $y_3(\mathbf{p},t)$: NO_3-N as output variables. The vector $\mathbf{p}$ denotes the model parameter sets for each of the river segments. Corresponding to the input variables following restrictions are valid for the control parameters $\alpha_1 = 1$: CHA is not directly controllable, $\alpha_2 \in [0.01,1]$: o-PO_4-P varies between 1 and 100 %, and $\alpha_3 \in [0.01,1]$: NO_3-N varies between 1 and 100 %. The optimisation problem was solved by using gradient search method combined with Monte Carlo Simulation for normalised weights. The weighting factors w_1, w_2 and w_3 of goal functions with $|w_1| + |w_2| + |w_3| = 1$ are considered for two management strategies. The first one is based on the limiting nutrient concept (LNC) of algal biomass (cf. [327]). The second one is derived on the recommendations of the German Administrative Working Group on Water (cf. [192]).

1. Water quality management based on LNC concept

The concept is based on the average elementary composition of phytoplankton biomass in aquatic ecosystems given by $C_{106}H_{180}O_{45}N_{16}P_1$ (so-called Redfield Ratio; [308, 309]. For simplicity the C:N:P-ratio is used. Reductions of P- and N- concentrations in freshwater ecosystems lead to a diminished phytoplankton growth. The values of normalised weights of goal functions are presented in Table 6.6. The optimisation problem was solved for control parameters $\alpha_2 = 0.01$ and $\alpha_3 = 0.90$.

The computed results are presented in Fig. 6.55. The management strategy according LNC leads to a decrease of phytoplankton growth in spring and in late summer due to optimised lower nutrient concentrations. This can be done by reduction of nutrient inputs into the water body due to point sources (e.g. input from wastewater treatment plants, industrial wastewater input) [47] and reduced nutrient input from non-point sources (e.g. buffer strips along the river, reduced input of fertilisers) [38, 229]. For the shallow lake area of LHR optimal averages of goal functions are

Fig. 6.54 Scheme of
simulation runs for water
quality management of LHR
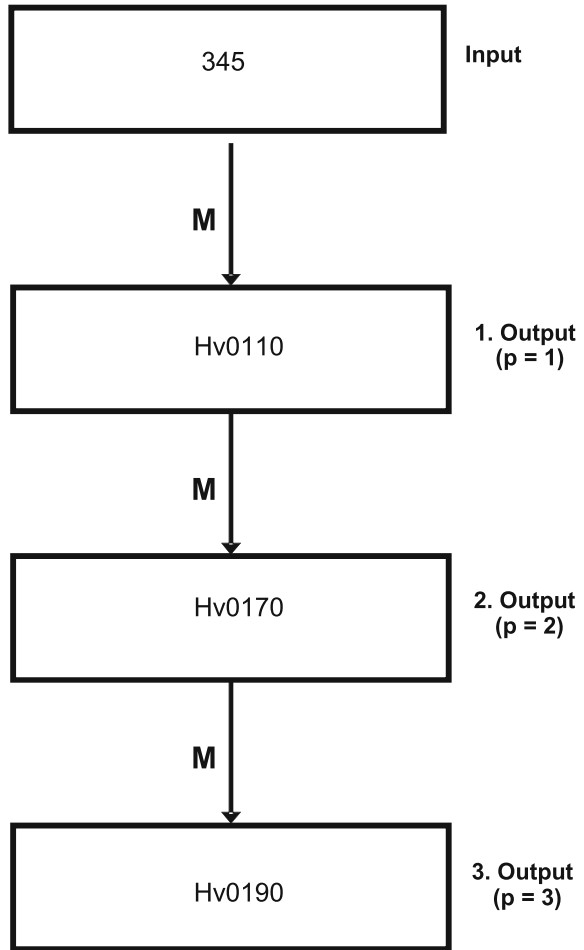
determined as follows: CHA: $f_1 = 44.991\,\mu\mathrm{g/l}$, soluble phosphorus $f_2 = 1.472\,\mu\mathrm{g/l}$,
nitrate nitrogen $f_3 = 1.54\,\mathrm{mg/l}$,

Diatoms are the dominant algal species of LHR in spring. The increase of phy-
toplankton biomass corresponds with the high utilisation rate of soluble phosphorus

Table 6.6 Normalised weights $|w_i|$ of goal functions according LNC concept

Variable	Quota CHA (%)	Normalised weight w_i	Normalised weight $|w_i|$ (%)
CHA (mg/l)	90.5	0.905	90.5
o-PO4-P (mg/l)	1.1	−0.011	1.1
NO3-N (mg/l)	8.4	−0.084	8.4
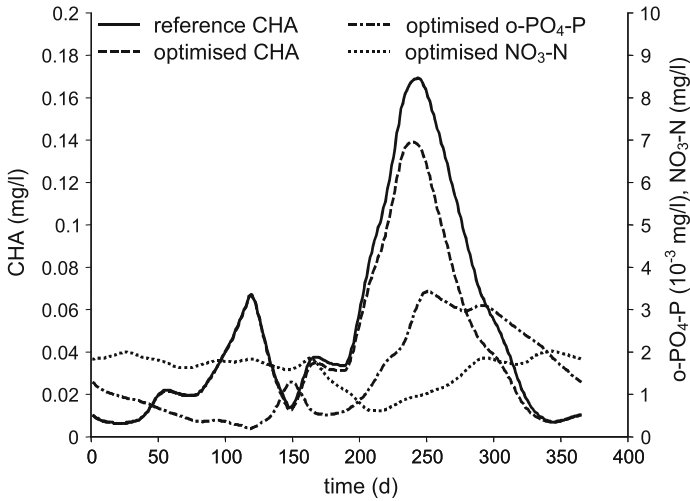
Fig. 6.55 Optimised results for water quality management according LNC strategy

concentration. It comes to a minimum at the end of this season and causes a breakdown of algal bloom. The bacterial decay of dead algal biomass on the sediment surface leads to anoxic chemical conditions within the active sediment layer and therefore to phosphorus remobilisation from sediment. The orthophosphate phosphorus concentration reaches a local maximum. With increasing water temperature the algal species composition will be change to green algae which are now the dominant species for a short time. This effect is shown by a second local maximum of chlorophyll-a concentration accompanied by decreasing soluble phosphorus concentration. In summer the algal composition turns to cyanobacteria species which will be dominating until fall. Instead of phosphorus the nitrogen pool will be utilised now while the phosphorus concentration increases due to high remobilisation rates because of the high amount of dead phytoplankton biomass. In late fall/early winter the whole nutrient pool is filled up again by import due to external pollution. At the end of the year, the phosphorus and nitrate pools reach their initial values in correspondence with water flow.

Soluble phosphorus and nitrogen compounds are the most important drivers of phytoplankton growth which can be influenced by operations in the watershed. Changing the weights of goal functions different scenarios can be computed to support decision making processes for water quality management. The weights are $w_1 = 0.917$, $w_2 = -0.028$ and $w_3 = -0.055$. A stronger weighting of f_2 and a smaller weighting of f_3 lead to a diminished phytoplankton maximum in late summer but higher phosphorus content at the end of the year (Fig. 6.55).

Then, a weighting of goal functions by $w_1 = 0.910$, $w_2 = -0.040$ and $w_3 = -0.050$ that means a stronger weighting of f_2 lead to a non acceptable high soluble phosphorus concentration over the year (Fig. 6.57). The nitrogen pool is not affected (Fig. 6.56).
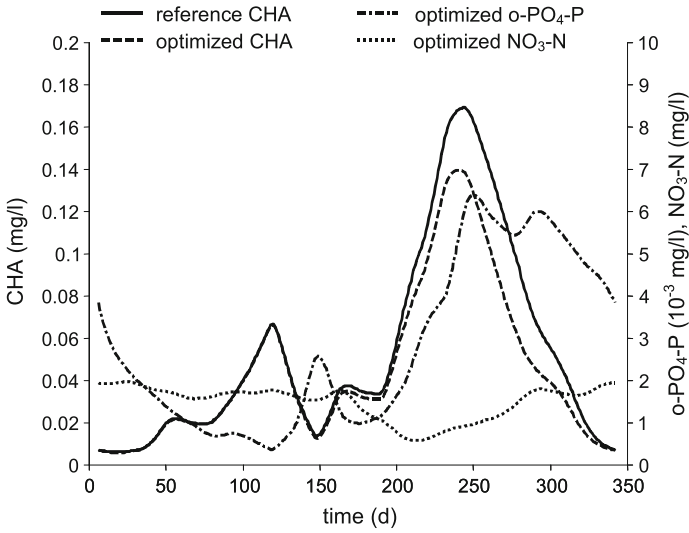
Fig. 6.56 Changing the weighting of goal functions according to LNC strategy
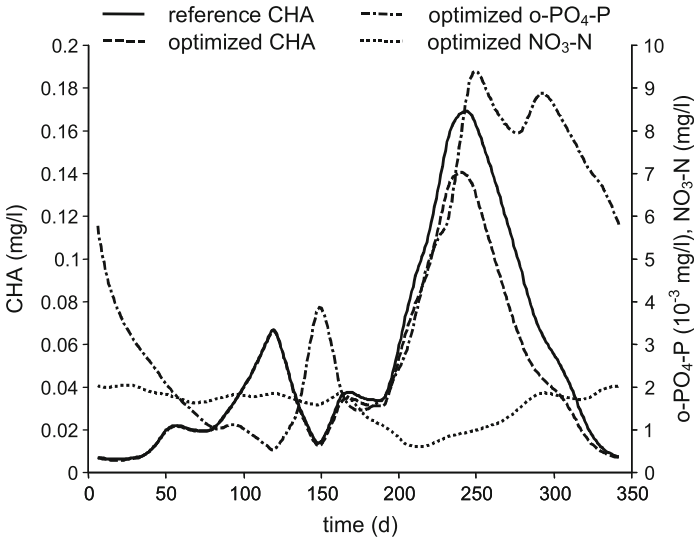
Fig. 6.57 Water quality management proposal according to LNC with changed weight of goal function f_2

Table 6.7 Normalised weights $|w_i|$ of goal functions according LAWA strategy

Variable	Target value (mg/l)	Reciprocal value (l/mg)	Normalised weight w_i	Normalised weight $|w_i|$ (%)
CHA (mg/l)	0.08	12.5	0.42	42
o-PO4-P (mg/l)	0.06	16.7	−0.57	57
NO3-N (mg/l)	3.7	0.27	−0.01	1

2. Water quality management based on LAWA recommendations

A second management strategy for the LHR refers to the target values recommended by German LAWA Group. The external driving forces and the water-related internal algal succession are the same as for the LNC strategy. The goal of this concept is to get a sufficient good water quality according to the European Water Framework Directive. In the case of LAWA strategy the optimisation problem was solved for control parameters $\alpha_2 = 0.03$ and $\alpha_3 = 0.91$. The values of normalised weights of goal functions are presented in Table 6.7.

For the shallow lake area of LHR optimal averages of goal functions are determined as follows: CHA: $f_1 = 48.762$ µg/l, soluble phosphorus $f_2 = 0.166$µg/l, nitrate nitrogen $f_3 = 0.08$ mg/l. Optimised simulation results are presented in Fig. 6.58.

From this simulation study results that water quality management of LHR according to LAWA target values leads to nearly the same phytoplankton biomass content of the water body in spring but to smaller differences of phytoplankton maxima in late summer. The nutrient concentration levels are low over the course of the year. In consequence the LAWA strategy leads to lower nutrient concentrations but to a slight increase of phytoplankton biomass. In opposite of that, eutrophication control by means of limiting nutrient concept results in lower phytoplankton concentrations but higher admissible nutrient inputs. It depends from the administrative engineer-
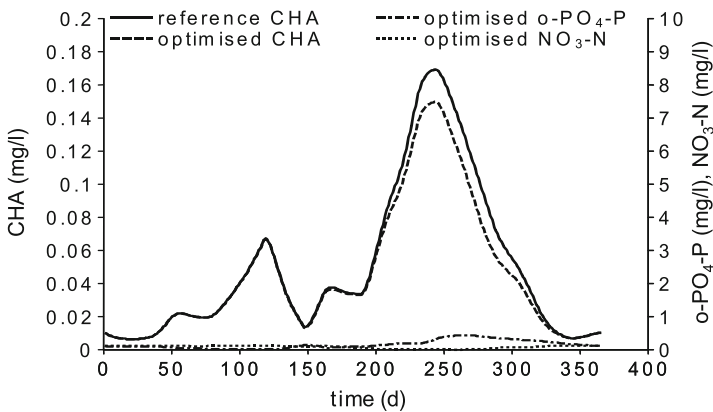
Fig. 6.58 Control of algal biomass according to target values of LAWA

ing and economic goals which strategy should preferred. But, political goals and economical constraints as well as socio-economic aspects are not included in the model. Therefore, the simulation results have to be discussed within the context of environmental goals and budgetary constraints where the weighting of goal functions is one of the crucial points.

From optimised simulation runs alone a decision which is the best water quality management strategy cannot be made. What can be done with such water quality simulation models like *CEUS*? The simulation model used considers only a few internal and external driving forces. Because of the complexity of freshwater ecosystems it is not possible to formulate predictions for future water quality developments by interpretation of simulation results. But by means of the model output it is possible to derive quantified estimations on essential freshwater ecosystem variables like phytoplankton content and nutrient levels in a water body as realistic base for decision making. In this sense, the simulation runs carried out for LHR by means of *CEUS* are important mathematical and engineering approaches to water quality management and model-based decision making.

6.5 Optimal Control of Run-off-River Hydroelectric Power Plants

Thomas Rauschenbach

6.5.1 The Classical Multi-criteria Problem Setting

The control of run-off-river hydroelectric power plants represents a typical case of application of the poly-optimisation problem. It is based on the assumption that several target functions $I_i(t)$ must be taken into account at one and the same time. If it is possible to set objectified weights for the n partial target functions, then

$$I(t) = \sum_{i=1}^{n} \alpha_i I_i(t) \tag{6.9}$$

can be established as compromise target function. For all further considerations, it is also assumed that the following relation holds true:

$$\sum_{i=1}^{n} \alpha_i = 1 \tag{6.10}$$

The schema of the classical multi-criteria optimisation is shown in Fig. 6.59. Here, $\underline{u}_{NS}(t)$ is the non-controllable system input vector, $\underline{u}_S(t)$ is the controllable system input vector, and $\underline{y}(t)$ is the system output vector. However, the case in which the
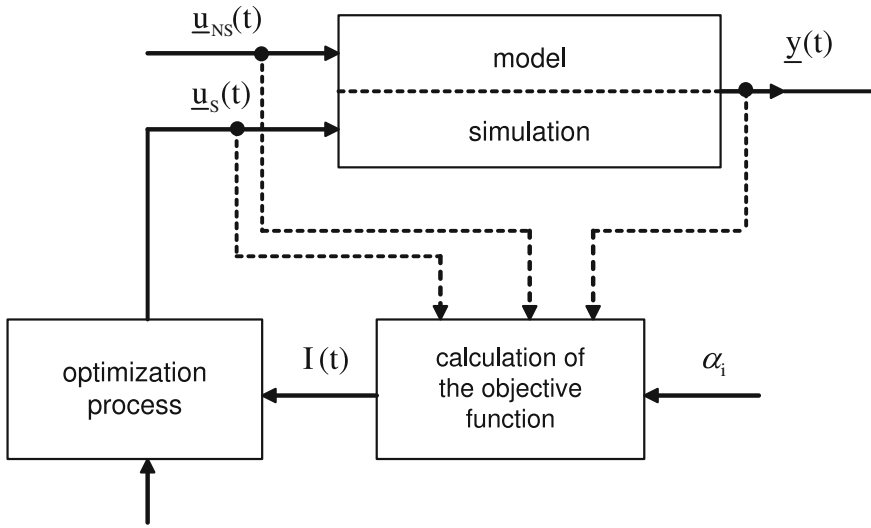
Fig. 6.59 Scheme of the classical multi-criteria optimisation

weights cannot be fixed, leading to the target function vector

$$\underline{I}(t) = [I_1(t), I_2(t), \ldots I_n(t)]^T \tag{6.11}$$

is left out of consideration. The result obtained by applying the known solution procedures [245, 255] is the optimal compromise set, also called Pareto set. Out of this set of possible efficient points, the decision maker must fix one point as compromise by taking some further criteria into account.

6.5.2 The Multi-criteria Problem Setting with the Adaption of the Weighting Factors

For the case of a time-variant behavior of systems and signals, however, the classical multi-criteria problem setting is not suitable. If it is possible to vary the weighting factors α_i in the compromise target function as a function of the time-variant behavior of the signals and/or the system, the known efficient solution strategies of poly-optimisation can be applied again. Thus, from Eq. (6.9), the following relations result:

$$I(t) = \sum_{i=1}^{u} \alpha_i(t)I_i(t) \quad mit \quad \sum_{i=1}^{u} \alpha_i = 1. \tag{6.12}$$

The weighting factors valid at time t are determined via a fuzzy system according to Fig. 6.60.
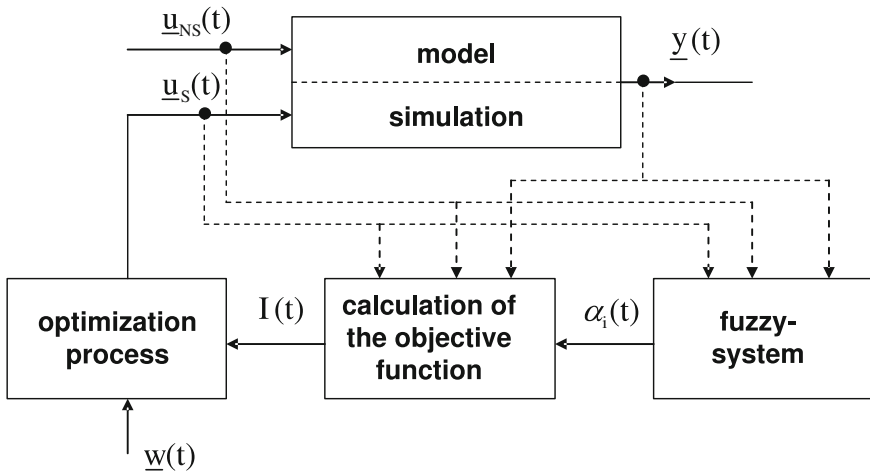
Fig. 6.60 Diagram of the multi-criteria optimisation with adaptive weighting factors

The input of the fuzzy system is a feature vector $\underline{m}(t)$ which describes the time-variant behavior of signals and systems sufficiently well. It can be formed from the signals and states $\underline{x}$ in the following form:

$$\underline{m}^T = f\left(\underline{u}_S, \underline{u}_{NS}, \underline{y}, \underline{x}\right) \tag{6.13}$$

The fuzzy system is designed on the basis of the known strategies. The following items have been chosen for:

1. the fuzzification of the features m_i

   - three to five linguistic variables,
   - trapezoidal description with a maximum of 4 supporting points,

2. the weighting factors α_i

   - three to five linguistic variables,
   - singletons,

3. the interferences

   - max-min or max-prod,

4. the defuzzification

   - the centre of gravity method.

The set of rules of the fuzzy system consists of n rules of the form:

if *premise* then *conclusion*.

6.5.3 The Control System of the Barrage Cascade of the Austrian Danube

In the framework of a long-term cooperation between the Austrian Hydropower AG, Vienna, the scientific regional academy for Lower Austria Krems, and the Ilmenau University of Technology, a system for the model-based multi-criteria control of single barrages and of barrage cascades has been developed and tested [262]. The system has already been put into practice for the barrage cascade Abwinden-Wallsee-Ybbs-Melk. With the setting up of a new central control room, the strategy designed will be extended to all nine barrages.

The functions of the barrages are mainly:

1. energy generation,
2. shipping,
3. flood protection.

In normal operation (flow about 3000 m^3/s), the power generated by the four barrages mentioned above amounts to approximately 760 MW. The following relation has been set up as objective function:

$$I(t) = \underbrace{\alpha_1(t) \cdot I_1(t) + \alpha_2(t) \cdot I_2(t)}_{floodprotection} \tag{6.14}$$

$$+ \underbrace{\alpha_3(t) \cdot I_3(t)}_{shipping} + \underbrace{\alpha_4(t) \cdot I_4(t)}_{energy}$$

For the partial criteria I_i and the constraints G_i, it holds:

$$I_1(t) = q_{KWab,max} \tag{6.15}$$

$$I_2(t) = \left(\frac{dq_{KWab}(t)}{dt} \right)^2 \tag{6.16}$$

$$I_3(t) = \int (h_{KW}(t) - h_{soll}) \, dt \tag{6.17}$$

$$I_4(t) = - \int P(t) dt \tag{6.18}$$

$$G_1 = (h(t) - h_{max}) \leq 0 \tag{6.19}$$

$$G_2 = \left(\frac{dh(t)}{dt} - v_{h,max} \right) \leq 0 \tag{6.20}$$

with $q_{KWab,max}$ being the maximum power plant run-off, q_{KWab} the power plant run-off, h_{KW} the water level at the upstream, h_{soll} the nominal value of the water level at the upstream, P the electrical power, h the water level, h_{max} the maximum permissible water level, and $v_{h,max}$ the maximum permissible rate of change of the water level.
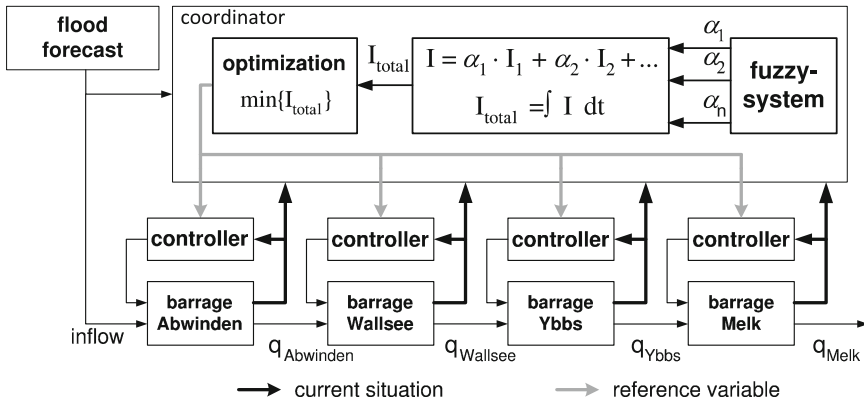
Fig. 6.61 Principle of the coordinated barrage control

On the basis of models for the barrages (including turbines, weirs, locks), the retention areas and the inflows [260], the hierarchical concept—shown in Fig. 6.61—of the coordinated multi-criteria control of the barrage cascade has been designed, subjected to simulative tests, and also implemented.

The design of the fuzzy system for the situational determination of the weighting factors $\alpha_i(t)$ has been realised for each of the l barrages. A preliminary analysis revealed that the weighting factors $\alpha_{ij}(t)$ of the single jth barrage strongly depend on the flow $q_j(t)$, on the change of flow $\Delta q_j(t)$ and on the forecast flow maximum $q_{j,max}$. Thus, the following relation holds:

$$\alpha_{ij} = f\left(q_j(t), q_{j,max}, \Delta q_j(t)\right) \quad mit \ \ i \in [1, 2, 3, 4]. \tag{6.21}$$

Figure 6.62 shows the basic set-up of the system for determining the weighting factors.

Optimisation studies revealed that the energy-optimal reversal is best taken into account if the weighting factor α_{4j} for the partial criterion I_{4j} is kept constant, thus supporting an energy-optimum control in all reversal ranges, also when returning to the 'normal state' (state of normal watercourses). In the range of flow peaks when a maximum flood protection is extremely important, this partial criterion will no longer be automatically effective as the generated electrical power becomes zero due to the
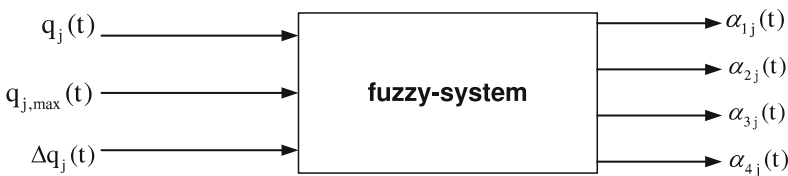
Fig. 6.62 Fuzzy system for determining the weighting factors $\alpha_{ij}(t)$

fact that the minimum fall height is not reached. The factor α_{4j} was fixed to be 0.1. Therefore, α_{4j} is not calculated in the fuzzy system. The term 'reversal' relates to the situation of a normal watercourse (normal situation) going over to a flood situation and back to the normal situation.

For the input quantities, the following attributes are used:

- q_j [LOW, HIGH]
- $q_{j,max}$ [LOW, HIGH] and
- Δq_j [NEG_G, NEG_K, NULL, POS_K, POS_G].

The attributes given below are assigned to the output quantities of the fuzzy system, that is, to the weighting factors of the partial criteria. They are identical for all outputs:

- α_{ij} [LOW, MEDIUM, HIGH]

Figure 6.63 shows the principle runs thus resulting for the membership function of the inputs and the outputs. For establishing the set of rules, all situations which are relevant to the choice of the weighting factors must be taken into account. These are:

- Situation 1: normal situation,
- Situation 2: transition from normal to flood situation,
- Situation 3: flood situation,
- Situation 4: transition from flood to normal situation.

As an example of the construction of the set of rules of the single situations, Table 6.8 gives an extract from the set of rules for the transition of a barrage from the normal to the flood situation (situation 2). The complete set of rules for situation 2 consists of 15 rules. The rules shown in Table 6.8 apply to a situation which is characterized as follows:

Fig. 6.63 Example of the membership functions of an input (Δq_j) of the fuzzy system
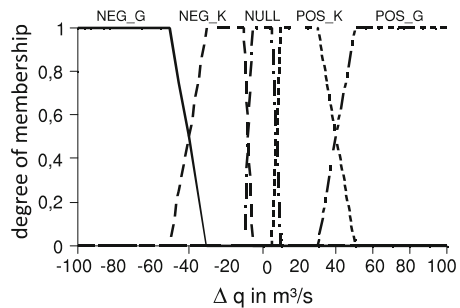
Table 6.8 Extract from the set of rules for situation 2

if $\left(q_j(k) = LOW\right)$ and $\left(q_{j,max}(k) = HIGH\right)$ and $\left(\Delta q_j(k) = POS\_K\right)$ then $\alpha_{3j} := LOW$
if $\left(q_j(k) = LOW\right)$ and $\left(q_{j,max}(k) = HIGH\right)$ and $\left(\Delta q_j(k) = POS\_K\right)$ then $\alpha_{2j} := MEDIUM$
if $\left(q_j(k) = LOW\right)$ and $\left(q_{j,max}(k) = HIGH\right)$ and $\left(\Delta q_j(k) = POS\_K\right)$ then $\alpha_{1j} := MEDIUM$
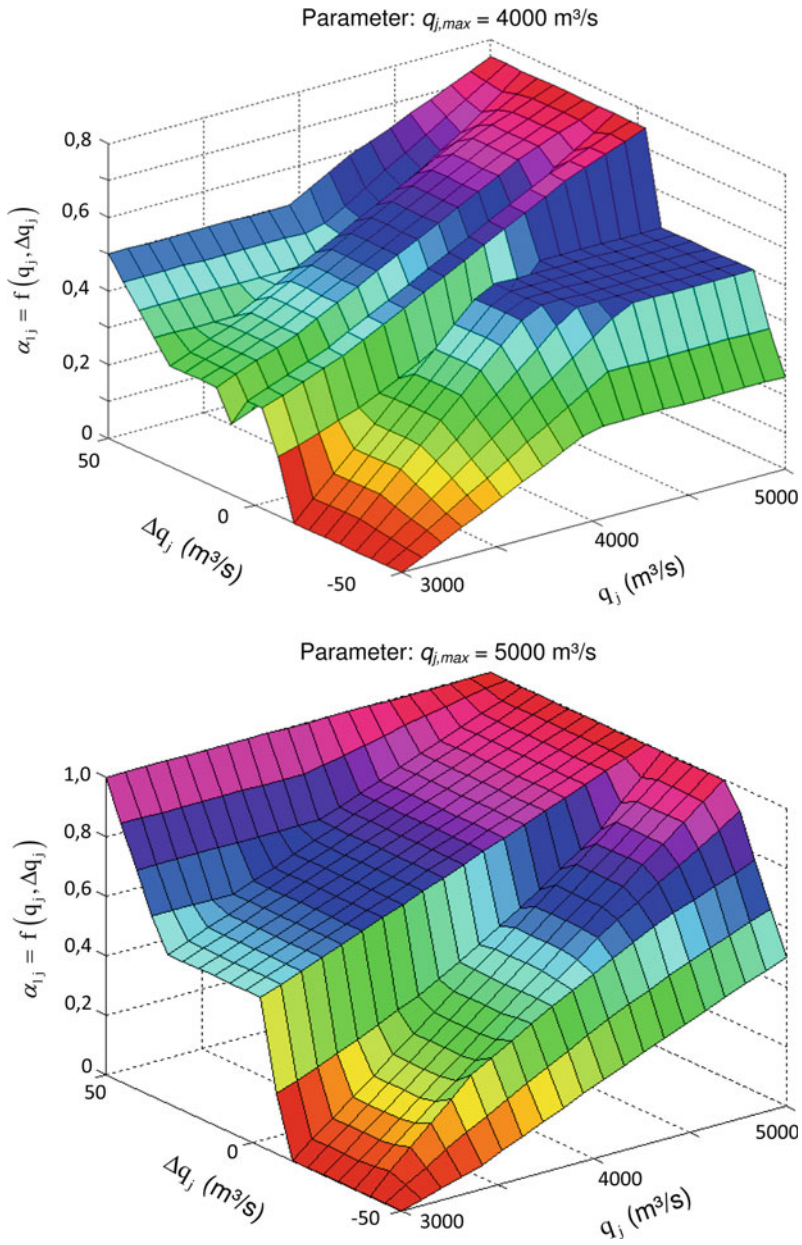
Fig. 6.64 Weighting factor α_{1j} as a function of q_j and Δq_j (parameter $q_{j,max}$)
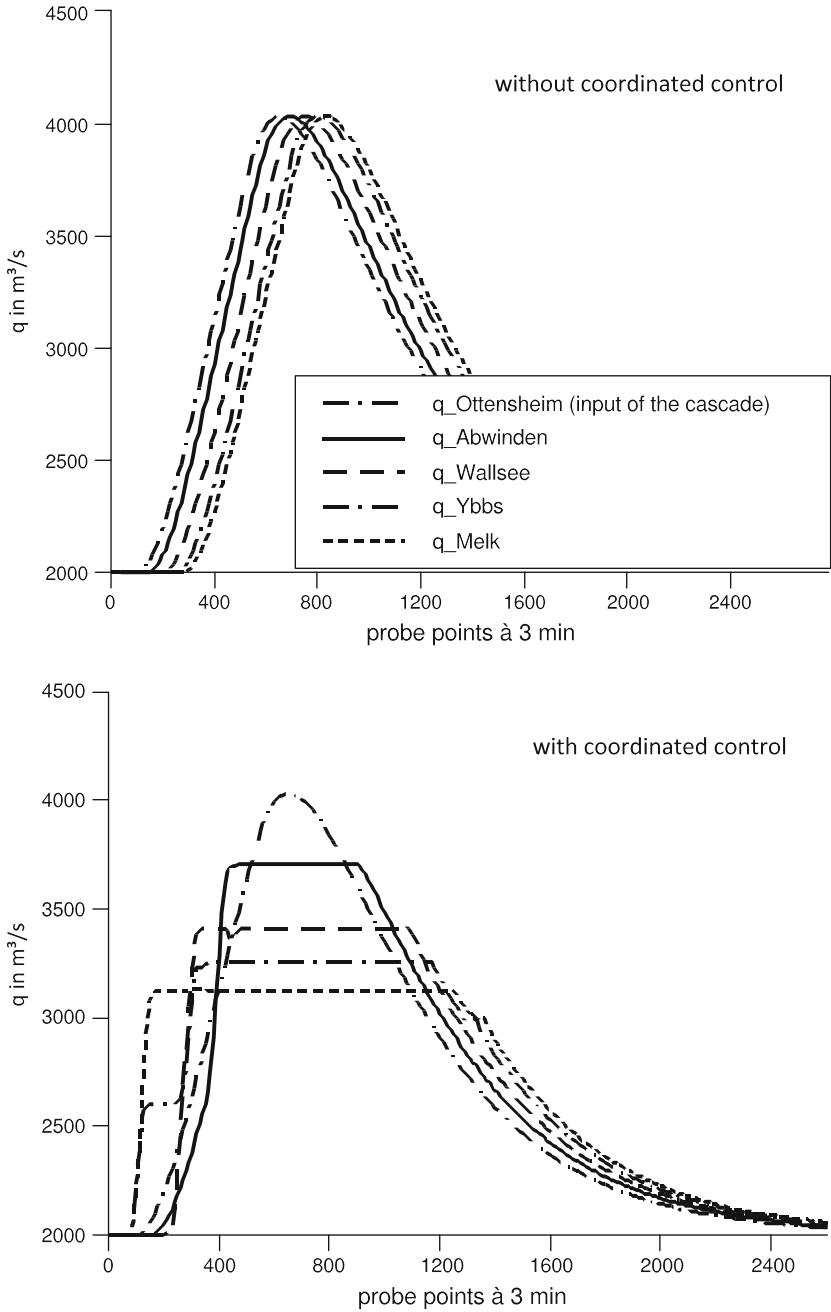
Fig. 6.65 Results of coordinated control (medium flood)

- At the current time k the flow in the barrage j is low ($q_j(k) = LOW$),
- The flow maximum forecast for barrage j at the time k is high ($q_{j,max}(k) = HIGH$), and
- the change in flow forecast for barrage j at the time k is positive with small value ($\Delta q_j(k) = POS\_K$).

Thus, the rules describe a slowly rising flood with a high predicted peak. For this reason, the weighing factor for navigation α_{3j} is assigned the attribute *LOW*. For the two weighting factors α_{1j} and α_{2j}, which are relevant to the flood protection measures, the attribute *MEDIUM* is chosen.

A fuzzy system can be illustrated particularly well by representing the dependence of the output quantities on the input quantities in a 3D-diagram. Figure 6.64 shows the diagrams for the weighting factor α_{1j} as a function of the flow q_j in the barrage and of the predicted flow gradient Δq_j. The forecast maximum flow $q_{j,max}$ was used as parameter. In the case of medium flood events, the application of the multi-criteria optimal barrage control by using adaptive weighting factors entails a noticeable decrease in the maximum flow, with the energy output increasing at the same time, thus ensuring the safety in navigation.

Figure 6.65 shows—as an example—the improved flood protection, achieved through the coordinated control, compared with the decentralized control applied so far. Without any coordination, the flood wave is passed on from barrage to barrage in an almost undisturbed way. In contrast to this, the coordinated control allows the flow maximum to be diminished in each of the four barrages. In the case of extreme flood events, however, the utilisation of the storage capacities of the barrages makes little sense. In these cases, retention areas must be opened in a controlled way.

References

1. Alcamo, J., Döll, P., Henrichs, T., Kaspar, F., Lehner, B., Rösch, T., Siebert, S.: Development and testing of the WaterGAP 2 global model of water use and availability. Hydrol. Sci. J. **48**(3), 317–337 (2003). doi:10.1623/hysj.48.3.317.45290

2. Allen, R., et al.: Crop evapotranspiration–guidelines for computing crop water requirements. FAO Irrigation and Drainage, vol. 56 (1998)

3. Allen, R.G., Pereira, L.S., Raes, D., Smith, M.: FAO Irrigation and Drainage Paper. FAO, Rome (1977)

4. Ambrose, R.B., Wool, T.A., Connolly, J.P., Schanz, R.W.: WASP4 A hydro-dynamic and water quality model: model theory, userś manual, and programmers guide. Report EPA-600/3-87/039, US EPA, Athens (1988)

5. Ambrose, R.B., Wool, T.A., Martin, J.L.: The water quality simulation program WASP5: model theory, userś manual, and programmerś guide. In: Environment Research Laboratory, US EPA, Athens (1993)

6. Anderson, D., Sweeney, D., Williams, T., Martin, K.: An introduction to management science, 12th edn. Thompson southwestern (2003)

7. Antoulas, A., Sorensen, D.: Approximtion of large-scale dynamical systems: an overview. Int. J. Appl. Math. Comput. Sci **11**, 1093–1121 (2001)

8. Antoulas, A.C.: Approximation of Large-Scale Dynamical Systems. SIAM Press, Philadelphia (2005)

9. Armstrong, N.E.: Development and Documentation of Mathematical Model for the Paraiba River Basin Study, Simulation of Water Quality in Streams and Estuaries, vol. 2 (1977)

10. Arnold, E., Tatjewski, P., Wolochowicz, P.: Two methods for large-scale nonlinear optimization and their comparison on a case study of hydropower optimization. J. Optim. Theory Appl. **81**(2), 221–248 (1994)

11. ATV: A General Available Water Quality Model. Report 02WA9104/4 ATV, Hennef. (in German) (1996)

12. Ayvaz, M., Karahana, H.: A simulation/optimization model for the identification of unknown groundwater well locations and pumping rates. J. Hydrol. **357**(1–2), 76–92 (2008)

13. Bachhiesl, M.: Entwicklung eines Hochwasservorhersagemodells für das Einzugsgebiet der Salzach(development of a flood forecasting model for the river basin of the river salzach). In: XVIII. Konferenz der Donauländer über hydrologische Vorhersagen und hydrologisch-wasserwirtschaftliche Grundlagen, vol. 19/1, pp. B-13-B-18. Graz (1996)

14. Baran, B., Lücken, C., Sotelo, A.: Multi-objective pump scheduling optimisation using evolutionary strategies. Adv. Eng. Softw. **36**, 39–47 (2005)

15. Bates, B., Kundzewics, Z., Wu, S., Palutikof, P.: Climate change and water. Technical report, Technical Paper of the Intergovernmental Panel on Climate Change, IPCC Secretary (2008)

16. Bauch, W.: Die Hochwasserwelle im ungestauten und gestauten Fluss(the flood wave in undammed and dammed river) (In German). Tech. Rep. 16, Versuchsanstalt für Wasserbau der Technischen Universität München - Oskar v. Miller Institut, München (1967)

17. Bauch, W.: Untersuchungen über Wasserstandsvorhersagen an einem 600 m langen Modell der Donaustrecke Regensburg-Straubing(studies on water level predictions on a 600 m long model of the section of the danube regensburg - straubing)(In German). Tech. Rep. 10, Versuchsanstalt für Wasserbau der Technischen Universität München - Oskar v. Miller Institut, München (1967)

18. Baumann, D.D., Boland, J.J., Hanemann, W.M.: Urban Water Demand-Management and Planning. McGraw Hill Inc. (1998)

19. Baumert, H., Kummer, V.: Optimierung der Manning-Beiwerte in den St.-Venant-Gleichungen für instationären Durchfluss in einem Experimentalgerinne(optimizing the manning coefficients in the st. venant equations for unsteady flow in an experimental river) (In German). Gerlands Beiträge zur Geophysik 88(6), 463–466 (1979)

20. Beck, M.B.: Water Quality Management: A Review of the Development and Application of Mathematical Models. Springer, Berlin (1985)

21. Beck, M.B., Schilling, W.: Uncertainty Risk and Transient Pollution Events. IWA Publishing, London (1996)

22. Beck, M.B., Van Straten, G.: Uncertainly and Forecasting of Water Quality. Springer, Berlin (1983)

23. Becker, A., Sosnowski, P.: Eine Impulsantwort für Flussabschnitte zur Durchflussvorherbestimmung(an impulse response of river sections for flow determination) (In German). Wasserwirtschaft-Wassertechnik (12), 410–418 (1969)

24. Bellman, R.: Dynamic Programming. Princeton University Press, Princeton (1962)

25. Bendoricchio, G.: Integrated Management of Water Quality: The Role of Agricultural Diffuse Pollution Sources. IWA Publishing, London (1999)

26. Bendoricchio, G., Malagoli, M.: Overview on non-point pollution models: experiences and applications. In: Environmental Models: Emissions and Consequences, pp. 345–357 (1990)

27. Benndorf, J., Recknagel, F.: Problems of application of the ecological model SALMO to lakes and reservoirs having various trophic states. Ecol. Model. **17**, 139–145 (1982)

28. Bernard, T., Linke, H., K.: A concept for the long term optimization of the regional water supply systems using a reduced finite element groundwater model. VDI/VDE GMA-Kogress, VDI-Berichte 1980, pp. 751–752. Baden-Baden, Germany (2007)

29. Beven, K.J.: Rainfall-Runoff Modelling: The Primer Models for Water Quality. Wiley, New York (2001)

30. Biswas, A.K.: Models for Water Quality Management. McGraw-Hill, New York (1981)

31. Blaney, H., Criddle, W.: Determining water requirements in irrigated areas from climatological and irrigation data. Technical report, U.S. department of agriculture, soil conservation service. Technical paper 96, p. 48 (1950)

32. Bohne, K.: An Introdcution into Applied Soil Hydrology. Catena Verlag GmbH (2005)

33. Bollrich, G., Preißler, G.: Technische Hydromechanik (Technical hydromechanics) (In German), vol. 1 and 2. Verlag für Bauwesen, Berlin, München (1992)

34. Borchardt, D., Reichert, P.: River water quality model no 1: Case study I. Compartmentalisationapproach applied to oxygen balances in the River Lahn (Germany). WaterSci. Technology **43**(5), 41–49 (2001)

35. Boulos, P.F., Wu, Z., Orr, C.H., Moore, M., HSsiung, P., Thomas, D.: Optimal Pump Operation of Water Distribuion Systems Using Genetic Algorithm, H2ONET Users Guide. MW Software Inc (2000)

36. Boumans, R., Costanza, R., Farley, J., Wilson, M.A., Portela, R., Rotmans, J., Villa, F., Grasso, M.: Modeling the dynamics of the integrated earth system and the value of global ecosystem services using the GUMBO model. Ecol. Econ. **41**, 529–560 (2002)

37. Brebbia, C.A., Cheng, A.H.D., Anagostopoulos, P., Katsifarakis, K.E.: Water Resources Management. WIT Press, Southampton (2001)

38. Bretschneider, H.: Hydraulische Berechnung von Fließgewässern (hydraulic calculation of water courses) (In German). DVWK-Merkblatt (Entwurf) (1990)

39. Brooke, A., Kendrick, D., Meeraus: A. GAMS, A USER'S Guide. The Scientific Press, 507 Seaport Court, Redwood City, CA 94063–2731 (1988)

40. Brouwer, C., Heibloem, M.: Irrigation Water Management: Irrigation Water Needs. FAO (1986)

41. Brouwer, C., Heibloem, M.: Irrigation Water Needs. FAO (1986). http://www.fao.org/docrep/S2022E/S2022E00.htm

42. Brouwer, C.J., Heibloem, M.: Irrigation Water Needs. FAO (1986). http://www.fao.org/docrep/S2022E/S2022E00.htm

43. Brown, L.C., Barnwell, T.O.J.: The Enhanced Stream Water Quality Models QUAL2E and QUAL2E-UNCAS: Documentation and User Manual. US EPA Report EPA/600/3-87/007, Athens (1987)

44. Builder, C.H., Bankes, S.C., Nordin, R.: Command Concepts–A Theory Derived from the Practice of Command and Control. Rand Corporation, Santa Monica (1999)

45. Burgschweiger, J., Gnadig, B., Steinbach, M.C.: Optimization Models for Operative Planning in Drinking Water Network. 04–48. Konrad-Zuse-Zentrum für Informationstechnik Berlin, ZIB-Report (2004)

46. Burke, G.W., Singh, B.R., Theodore, L.: Handbook of Environmental Management and Technology. Wiley, Chichester (2000)

47. Burn, D.H., McBean, E.A.: Application of nonlinear optimization to water quality. Applied Mathematical Modelling **11**, 438–446 (1987)

48. Burn, H.: Generating robust solutions: a water quality management example. Civ. Eng. Environ. Syst. **12**(4), 273–286 (1995)

49. BWA: The introduction of water resources in beijing and the demand analysis. Technical report, Beijing water authority, Beijing, People's Republic of China (2003)

50. Calow, P., Petts, G.E.: The Rivers Handbook, vol. 2. Blackwell, Oxford (1997)

51. Camp, T.R.: Water and Its Impurities. Chapman and Hall, London (1963)

52. Carroll, R.W.H., Warwick, J.J.: Uncertainty analysis of the Carson River mercury transport model. Ecol. Model. **137**, 211–224 (2001)

53. Cerco, C.F., Cole, T.M.: CE-QUAL-RIV1: A Dynamic One-Dimensional (Longitudinal) Water Quality Model for Streams: User's manual. US ACE, Waterways Experiments Station, Vicksburg (1995)

54. Chapra, S.C.: Surface Water Quality Modeling. McGraw-Hill, New York (2004)

55. Chen, C.W., Orlob, G.T.: 1975: Ecological simulation for aquatic environment. In: Patten, B.C. (ed.) Systems Analysis and Simulation in Ecology, vol. III, pp. 476–588 (1975)

56. Chen, J., Tang, C., Shen, Y., Sakura, Y., Kondon, A., Shimada, J.: Use of water balance calculation and tritium to examine the dropdown of groundwater table in the piedmont of the north China plain (NCP). Environ. Geol. **44**, 564–571 (2003)

57. Chen, Q.: Cellular Automata and Artificial Intelligence in Ecohydraulics Modelling. Balkema Publishers, Delft (2004)

58. Chow, V.T.: Open-Channel Hydraulics. McGraw-Hill, London (1959)

59. Chow, V.T.: Stochastic modeling of watershed systems. Adv. Hydrosci. **11**, 1–93 (1978)

60. Churchill, M.A., Elmore, H.L., Buckingham, R.A.: The prediction of stream re-aeration rates. Int. J. Air, Water Pollut. 6, 467–504 (1962)

61. Ciriani, T.A., Maione, U., Wallis, J.R.: 1977: Mathematical Models for Surface Water Hydrology. Wiley, Chichester (1977)

62. Cole, T., Buchak, E.: 1995: CE-qual-w2: A two-dimensional, laterally averaged, hydrodynamic and water quality model. US ACE, Technical Report EL-95, Waterways Experiments Station, Vicksburg. 2.0 (1995)

63. Cole, T.M., Wells, S.A.: Ce-qual-w2: A Two-dimensional, Laterally Averaged, Hydrodynamic and Water Quality Model, Version 3. Instruction Report EL-2000 (2000)

64. Conn, A.R., Gould, N., Toint, P.L.: LANCELOT, a FOTRAN package for large scale nonlinear optimization. In: 17th in Springer Series in Computational Mathematics. Springer, Heidelberg (1992)

65. Cook, Z.: Domestic, Commercial, Municipal and Industrial Water Demand Assessment and Forecast in Ada and Canyon Counties. Idaho. IDWR, Boise Idaho (2001)
66. Cook, Z., Urban, S., Maupin, M., Pratt, R., Church, J.: Domestic, Commercial, Municipal and Industrial Water Demand; Assessment and Forecast in Ada and Canyon Counties. Idaho, Idaho Department of Water Resources IDWR (2001)
67. Costanza, R.: Ecosystem services and ecological indicators. In: Handbook of Ecological Indicators for Assessment of Ecosystem Health, 2nd edn. pp. 189–198 (2010)
68. Costanza, R., d'Arge, R., de Groot, R., Farber, S., Grasso, M., Hannon, M.B., Limburg, R., Naeem, S., O'Neill, R.V., Paruelo, J., Raskin, R.G., Sutton, P., van den Belt, M.: The value of the world's ecosystem services and natural capital. Nature pp. 253–260 (1997)
69. Crockett, P.: Water quality modelling. Rivers Handb. **2**, 213–226 (1994)
70. Deb. K., Agarwal, A.: A fast elitist nondominated sorting genetic algorithm for multi-objective optimisation: Nsga-ii. In: Parallel Problem Solving from Nature VI Conference, pp. 849–858. Springer, Berlin (2000)
71. Deb, K., Goel, T.: Controlled elitist non-dominated sorting genetic algorithms for better convergence. In: First International Conference on Evolutionary Multi-criterion Optimisation, pp. 67–81. Zurich (2001)
72. Delft Hydraulics.: Ribasim: River Basin Simulation Model (2006)
73. DHI: MIKE 11 User Manual. Danish Hydraulic Institute, Horsholm (1992)
74. Diaz, G., Fontane, D.: Hydropower optimization via sequential quadratic programming. J. Water Resour. Plan. Manag. **115**(6), 715–734 (1989)
75. Diersch, H.J.: Chemical reactions. Feflow White Pap. **1**, 197–217 (2005)
76. Diersch, H.J.: Feflow Reference Manual. Wasy GmbH Institute for Water Resources Planning and Systems Research (2005)
77. Diersch, H.J.: On the primary variable switching technique for simulating unsaturated-saturated flows. Feflow White Pap. **1**, 9–66 (2005)
78. DiToro, D.M.: Sediment Flux Modelling. Wiley, Chichester (2000)
79. DiToro, D.M.: Sediment Flux Modelling. Wiley, Chichester (2002)
80. Dobbins, W.E.: Bod and oxygen relationships in streams. Proc. ASCE, J. San. Eng. Div. 90SA 3, 53–78 (1964)
81. Döll, P.: Global modeling of irrigation water requirements. Water Resour. Res. 38(4) (2002). doi:10.1029/2001WR000355
82. Döll, P., Fiedler, K.: Global-scale modeling of groundwater recharge. Hydrol. Earth Syst. Sci. **12**(3), 863–885 (2008). doi:10.5194/hess-12-863-2008
83. Döll, P., Kaspar, F., Lehner, B.: A global hydrological model for deriving water availability indicators: model tuning and validation. J. Hydrol. **270**(1–2), 105–134 (2003). doi:10.1016/S0022-1694(02)00283-4
84. Draper, A., Munevar, A., Reyes, E., Parker, N., Chung, F., Peterson, L.: Calsim: generalized model for reservoir system analysis. J. Water Res. Plan. Manag. **130**(6), 480–489 (2004)
85. Dubois, D.M.: Progress in Ecological Engineering and Management by Mathe-matical Modelling. Cebedoc, Liege (1981)
86. Duke, J.H.J.: Provision of a Steady-State Version of the Stream Model QUAL. US EPA, Washington (1973)
87. Dunlop, E.: Local government computer services board. In: WADI Users Manual, Equation (5)-(14). Dublin, Ireland (1991)
88. Dyck, S.: Angewandte Hydrologie (Applied hydrology) (In German), vol. 2. Verlag für Bauwesen, Berlin (1978)
89. Dyck, S., Peschke, G.: Grundlagen der Hydrologie (Basics of hydrology) (In German). Verlag für Bauwesen, Berlin (1983)
90. Einax, J.W., Zwanziger, H.W., Gei, S.: Chemometrics in Environmental Analysis. VCH, Weinheim (1997)
91. Eykhoff, P.: System Identification: Parameter and State Estimation. Wiley, Chichester (1974)
92. Faber, B., Harou, J.J.: Multiobjective optimization with HEC Res-PRM application to the upper mississippi reservoir system. In: World Environmental and Water Resources Congress (ASCE), pp. 215–224 (2007)

93. Fair, G.M.: The dissolved oxygen sag an analysis. Sew. Works J. **11**(3), 445–449 (1939)

94. Fan, L.T., Nadkarni, R.S., Erickson, L.E.: 1971: Dispersion model for a stream with several waste inputs and water intakes. Water Res. Bull. **7**, 1210–1220 (1971)

95. Fedra, K.: Environmental Modelling Under Uncertainty: Monte Carlo Simulation. IIASA, RR-83-28, Laxenburg (1983)

96. Fedra, K.: Models, GIS, and Expert Systems: Integrated Water Resources Models. Maidment, D.R. In: Application of Geographic Information Systems in Hydrology and Water Resources Management, IAHS Press, Wallingford (1993)

97. Fedra, K.: Gis and simulation models for water resources management: a case study of the kelantan river, malaysia. GIS Dev. **6**(8), 39–43 (2002)

98. Fehse, K.U.: Zur Sorption von Zink-Ionen an natürliche und technische Sorbentien unter Berücksichtigung des Feststoff: Lösung-Verhältnisses. Ph.D. thesis, Landwirtschaftlichen Fakultät der Martin-Luther-Universität Halle-Wittenberg (2004)

99. Fischer, H.B.: Dispersion predictions in natural streams. Proc. ASCE, J. San. Eng. Div. 94(SA5): pp. 927–943 (1968)

100. Fischer, H.B.: The effects of bends on dispersion in streams. Water Resour. Res. **5**, 496–506 (1969)

101. Fischer, H.B., Imberger, J., List, E.J., Koh, R.C., Brooks, N.H.: Mixing in Inland and Coastal Waters. Academic Press, New York (1979)

102. Fletcher, R.: Practical Methods of Optimization, 2nd edn. Wiley, New York (1981)

103. Fongwa, E., Gnauck, A., Müller, F.: Petri net modelling of ecosystem services: methodological development. In: Gnauck, A., Modelling and Simulation of Eco-systems, Workshop Koelpinsee 2011. Shaker, Aachen (2012)

104. Fongwa, E., Petschick, M., Gnauck, A., Müller, F.: 2010: decision support system for balancing ecosystem services at the landscape scale: petri nets modelling application. J. Probl. Landsc. Ecol. **28**, 241–252 (2010)

105. Fonseca, C.M., Fleming, P.J: Genetic algorithms for multi-objective optimisation: formulation, discussion and generalisation. In: Fifth International Conference on Genetic Algorithms, pp. 416–423. California (1993)

106. Foster, S., Garduno, H., Evans, R., Olson, D., Tian, Y., Zhang, W., Han, Z.: Quarternary aquifer of the north China plain. Hydrogeol. J. **12**, 81–93 (2004)

107. Franke, R., Arnold, E.: A Solver for Sparse Nonlinear Optimization. http://hqp.sourceforge.net/index.html

108. Franke, R., Arnold, E.: The Solver Omuses/HQP for Structured Large-scale Constrained Optimization: Algorithm, Implementation and Example Application. http://hqp.sourceforge.net/index.html (1999)

109. Furrer, G., Wehrli, B.: Biogeochemical processes at the sediment-water interface: measurements and modelling. In: Applied Geochemistry: Environmental Geochemistry, pp. 117–119. Uppsala (1993)

110. Gaylord, R.J., Nishidate, K.: 1996: Modeling Nature?. Cellular Automata Simulations with Mathematica. Springer/Telos, New York (1996)

111. Gnauck, A.: Simulation of shallow lake eutrophication. In: Marx Gmez, J., Sonnenschein, M., Müller, M., Welsch, H., Rautenstrauch, C. (eds.) Information Technologies in Environmental Engineering, pp. 483–495 (2007)

112. Gnauck, A.: Time series analysis of water quality data. In: Scholz-Reiter, B., Stahlmann, H.-D., Nethe, A. (eds.) In: Process Modelling. Springer, Berlin (1999)

113. Gnauck, A.: On the use of real-time estimation methods for mathematical modeling of limnic ecosystems. Proc. IV. IFAC-Symp **2**, 124–133 (1976)

114. Gnauck, A.: Fundamentals of ecosystem theory from general systems analysis. In: Jørgensen S. E. and Mueller, F., Handbook of Ecosystem Theories and Management. Lewis, Boca Raton (2000)

115. Gnauck, A.: Interpolation and approximation of water quality time series and process identification. Anal. Bioanal. Chem. 380(3) (2004)

116. Gnauck, A.: Modelling environmental information processes: a meta-model approach for water management. In: Schade, W., Smits, P., Innovations in Sharing Environmental Observations and Information. Part 1. pp. 130–136 (2010)

117. Gnauck, A., Heinrich, R., Luther, B.: Simulation of eutrophication of shallow lakes of the lower havel river. In: Gnauck, A., Heinrich, R. (eds.) The Information Society and Enlargement of the European Union. Part 2, pp. 963–966. Metropolis, Marburg (2003)

118. Gnauck, A.: Jørgensen, S.E., Luther, B.: The role of ecosystem modelling for long-term ecological research. In: Müller, F., Baessler, C., Schubert, H., Klotz, S. (eds.) Long-term Ecological Research. Springer, Berlin (2010)

119. Gnauck, A., Luther, B.: An eutrophication model for a lowland river-lake system. Ecosystems and Sustainable Development VI (2007)

120. Gnauck, A., Luther, B., Krug, W.: 2011: Using a commercial optimisation tool for finer tuning of parameters of an eutrophication model. ISESS 2011. IFIP AICT 359, 618–624 (2011)

121. Gnauck, A., Luther, B., Heinrich, R.: 2002: Modelling and simulation of internal pollution of shallow lakes. In: Pillmann, W., Tochtermann, K. (eds.) Environmental Communication in the Information Society. ISEP, Vienna (2002)

122. Gnauck, A., Luther, B., Wiedemann, T., Krug, W.: Coupling of simulators for optimal control of water quality. In: Gnauck, A., Heinrich, R. (eds.) The Information Society and Enlargement of the European Union. Part 1, Metropolis, Marburg, pp. 373–380 (2003)

123. Gnauck, A., Tesche, T.: Modelling the sediment-water interaction for riverine lakes. Int. Rev. Hydrobiol, Spec. Issue pp. 207–214 (1998)

124. Gnauck, A., Winkler, W.: Do-process models for shallow systems part 1: Ponds and lakes. Acta Hydrochim. Hydrobiol. **11**(1), 109–124 (1983)

125. Gnauck, A.L.: Larry Li, B-L., Feugo, J.D.A., Luther, B.: The Role of Statistics for Long-Term Ecological Research. In: Müller, F., Baessler, C., Schubert, H., Klotz, S. (eds.) Long-term Ecological Research. Springer, Berlin (2010)

126. Goltermann, H.L.: The Chemistry of Phosphate and Nitrogen Compounds in Sedi-ments. Kluwer, Dordrecht (2004)

127. Goodman, A.S., Tucker, R.J.: Time varying mathematical model for water quality. Water Res. **5**, 227–241 (1971)

128. Gordu, F., Yurtal, R., Motz, L.H.: Optimization of groundwater use in the goksu delta at silifke, turkey. First International Conference on Saltwater Intrusion and Coastal Aquifers Monitoring, Modeling, and Management. Essaouira, Morocco, 43(1) (2001)

129. Gould, N., Orban, D., Toint, P.: LANCELOT_simple, a simple interface to lancelot b. Technical report, TR07/12, Departement of Mathematics, University of Namur–FUNDP, Namur, Belgium (2007)

130. Grant, W.E., Pedersen, E.K.: Marín, S.L.: Ecology and Natural Resource Management. Wiley, New York (1997)

131. Gromiec, M.J.: Biochemical Oxygen Demand-Dissolved Oxygen: River Models. In: Jørgensen, S.E. (ed.), Elsevier, Amsterdam (1983)

132. Gromiec, M.J., Loucks, D.P., Orlob, G.T.: Stream quality modeling. In: Streams, Lakes, and Reservoirs, Mathematical Modeling of Water Quality, Wiley, Chichester (1983)

133. de Groot, R.S.: Functions of Nature: Evaluation of Nature in Environmental Planning Management, and Decision Making. Wolters-Noordhoff, Groningen (1992)

134. de Groot, R.S., Alkemade, J.R.M., Braat, L., Hein, L.G., Willemen, L.L.J.M.: Challenges in integrating the concept of ecosystem services and values in landscape planning, management and decision making. Ecol. Complex. **7**(3), 260–272 (2010)

135. de Groot, R.S., Ketner, P., Ovaa, H.: Selection and use of bio-indicators to assess the possible effects of climate change in Europe. J. Biogeogr. **22**, 935–943 (1995)

136. Günther, M.: Zeitdiskrete Steuerungssysteme (Time discrete control systems) (In German). Verlag Technik, Berlin (1986)

137. Gutknecht, D., Sengschmitt, D.: Mathematische Modelle offener Gerinne–Wehrbetrieb–Staulegung (mathematical models of open flumes–weir operation–damming up water) (In German). In: Seminar Konstruktiver Landschaftswasserbau, vol. 17, pp. 135–153. Wien (1995)

138. Haefner, J.W.: Modeling Biological Systems. Springer, New York (2005)
139. Hahn, H.H.: Model of the neckar river, federal republic of germany. In: Models for Water Quality Management, pp. 158–221 (1981)
140. Hajda, P., Novotny, V.: 1996: Modelling impact of urban and upstream nonpoint sources on eutrophication of the Milwaukee River. Water Sci. Technol. 33(4–5) (1996)
141. Hamam, Y., Brameller, A.: Hybrid method for the solution of piping networks. Proceeding of the IEE. 113(11), pp. 1607–1612. Leicester Polytechnic, Leicester, UK (1971)
142. Hameed, T., O'Neill, R.: River management decision modelling in IQQM. In: Proceedings of International Congress on Modelling and Simulation, pp. 170–176 (2005)
143. Han, Z.: Groundwater resources protection and aquifer recovery in China. Environm. Geol. 44, 106–111 (2003)
144. HEC: HEC-5 simulation of flood control and conservation systems, appendix on water quality analysis. In: Hydrologic Engineering Center Report, CPD-5Q, US ACE, Davis (1986)
145. Van der Heijden, K.: Scenarios: The Art of Strategic Conversation, 2nd edn. Wiley, New York (2005)
146. Heim, K.J., Warwick, J.J.: Simulating sediment transport in the carson river and lahontan reservoir, nevada. USA. J. AWRA 33(1), 177–191 (1997)
147. Henderson-Sellers, B.: Decision Support Techniques for Lakes and Reservoirs. CRC Press, Boca Raton (1992)
148. Henze, M., Gujer, W., Mino, T., van Loosdrecht, M.: 2000: Activated Sludge Models ASM1, ASM2, ASM2d and ASM3. IWA Publishing, London (200)
149. Hinkelmann, W.: Manuskript zur vorlesung hydrologie und wasserwirtschaft (manuscript for the lecture hydrology and water resources) (In German). Technical report, Technische Universität Berlin, Berlin (2005)
150. Hoffmann, A.: Mathematical modelling of phosphorus dynamics in rivers with special regard to phosphate remobilization from sediment. Diploma Thesis. BTU Cottbus (1999)
151. Hölting, B., Coldewey, W.: Hydrogeologie-Einführung in die Allgemeine und Angewandte Hydrogeologie, 6 edn. Spektrum Akademischer Verlag Elsevier GmbH München (2005)
152. Horn, H., Zielke, W.: Das dynamische Verhalten von Flussstauhaltungen(the dynamic behavior of river impoundments) (In German). Technical report 29, Versuchsanstalt für Wasserbau der Technischen Universität München-Oskar v. Miller Institut, München (1973)
153. Horn, J., Nafpliotis, N., Goldberg, D.E.: A niched pareto genetic algorithm for multi-objective optimisation. In: First IEEE Conference on Evolutionary Computation, vol. 1, pp. 82–87. New Jersey (1994)
154. Hua, W., Pang, Y.P.: Water quantity operation to achieve multi-environmental goals for a waterfront body. Water Resour. Manag. 23(10) (2009)
155. Huang, W.: Distributed Tank Model and Game Reanalysis Data Applied to the Simulation of Runoff within the Chao Phraya River Basin. Thailand. Wiley, Japan (2006)
156. Hughes, T.J.R.: The Finite Element Method. Dover Publications (Reprinted in 2000)
157. Hunger, M., Döll, P.: Value of river discharge data for global-scale hydrological modeling. Hydrol. Earth Syst. Sci. 12(3), 841–861 (2008). doi:10.5194/hess-12-841-2008
158. HydroLogics: Oasis User Manual version 4. (2010)
159. Imberger, J., Patterson, J.C.: A dynamic reservoir simulation model DYRESM5. Transp. Models Inland Coast. Waters. pp. 310–361 (1981)
160. Isaacs, W.P., Gaudy, A.F.: Atmospheric oxidation in a simulated stream. Proc. ASCE, J. San. Eng. Div. 94 (SA3): 319–344 (1968)
161. Islam, S.N.: Sustainable Eco-Tourism as a Practical Site Management Policy?. AH Development Publishing House, Dhaka (2003)
162. Ivanov, P., Masliev, I., Kularathna, M., Kuzmin, A., Somlyody, L.: Desert–Decision Support System for Evaluating River Basin strategies. IIASA, WP-95-23, Laxenburg (1995)
163. Jacobi, M., Karimanzira, D., Heß, M., Rauschenbach, T., Ament, C.: Water demand models for Beijing. In: Proceedings of the Second IASTED International Conference on Environmental Modelling and Simulation, pp. 1–6 (2006)

164. James, R.T., Martin, J., Wool, T., Wang, P.F.: A sediment resuspension and water quality model of lake okeechobee. J. AWRA 33(3) (1997)
165. Jolma, A., de Marchi, C., Smithc, M., Pererad, B.J.C., Somlyódye, L.: Streamplan: a support system for water quality management on a river basin scale. Environm. Model. Softw. **12**(4), 275–284 (1997)
166. Jørgensen, S.E.: A eutrophication model for a lake. Ecol. Model. **2**, 147–165 (1976)
167. Jørgensen, S.E.: Fundamentals of Ecological Modelling. Elsevier, Amsterdam (1986)
168. Jørgensen, S.E.: Integration of Ecosystem Theories: A Pattern. Kluwer, Dordrecht (1992)
169. Jørgensen, S.E.: Fundamentals of Ecological Modelling, 2nd edn. Elsevier, Amsterdam (1994)
170. Jørgensen, S.E.: A general outline of thermodynamic approaches to ecosystem theory. In: Jørgensen, S.E., Müller, F. (eds.) Handbook of Ecosystem Theories and Management (2000)
171. Jørgensen, S.E., Gromiec, M.: 1989: Mathematical Submodels of Water Quality Systems. Elsevier, Amsterdam (1989)
172. Jørgensen, S.E., Halling-Sørensen, B., Nielsen, S.N.: Handbook of Environmental and Ecological Modeling. Lewis, Boca Raton (1996)
173. Jørgensen, S.E., Müller, F.: Handbook of Ecosystem Theories and Management. Lewis, Boca Raton (2000)
174. Jørgensen, S.E., Xu, F.L.: Handbook of Ecological Indicators for Assessment of Ecosystem Health and 2nd. CRC Press, Boca Raton (2010)
175. Kaden, S., Becker, A., Gnauck, A.: 1989: Decision-support systems for water management. IAHS Publ. **180**, 11–21 (1989)
176. Kanzow, D.: Ein finites Element Modell zur Berechnung instationärer Abflüsse in Gerinnen und seine numerischen Eigenschaften(a finite element model for calculating unsteady runoff in channels and its numerical characteristics) (In German). Technical report 38, Versuchsanstalt für Wasserbau der Technischen Universität München-Oskar v. Miller Institut, München (1978)
177. Kao, J.J., Lin, W.L., Tsai, C.H.: 1998: Dynamic spatial modelling approach for etsimation of internal phosphorus load. Water Res. **32**(1), 47–56 (1998)
178. Karimanzira, D., Jacobi, M., Ament, C.: Determinants of domestic water demand for the Beijing region. In: C.A. Brebbia, A.G. Kungolos (eds.) Water Resources Management IV, pp. 101–110 (21–23 May 2007). doi:10.2495/WRM070111
179. Katsifarakis, K., Tselepidou, K.: Pumping cost minimization in aquifers with regional flow and two zones of different transmissivities. J. Hydrol. **377**(1–2), 106–111 (2009)
180. Kaule, G.: Ecologically Orientated Planning. Peter Lang, Frankfurt am Main (2000)
181. Kelly, M.G., Hornberger, G.M., Cosby, B.J.: Continuous automated measurement of rates of photosynthesis and respiration in an undisturbed river community. Limnol. Oceanogr. **19**, 305–312 (1974)
182. Koivo, A.J., Phillips, G.R.: Optimal estimation of DO, BOD, and stream parameters using a dynamic discrete time model. Water Resour. Res. **12**, 705–711 (1976)
183. Kothandaraman, V., Ewing, B.B.: A probabilistic analysis of dissolved oxygen, biochemical oxygen demand relationships in streams. J. WPCF 41 (1969)
184. Krawczak, M., Mizukami, K.: River pollution control as a conflict. Ser. Syst. Anal. **6**, 211–239 (1985)
185. Krenkel, P.A., Novotny, V.: 1980: Water Quality Management. Academic Press, New York (1980)
186. Krug, W.: Modelling, simulation and optimisation for manufacturing, Organisational and Logistical Processes, SCS Europe Publishing House, Delft (2002)
187. Kularathna, M., Somlyody, L.: River Basin Water Quality Management Models: A State-of-the-Art Review. IIASA, WP-94-3, Laxenburg (1994)
188. Kutas, T., Herodek, S.: A complex model for simulating the lake balaton ecosystem. In: Modeling and Managing Shallow Lake Eutrophication, Springer, Berlin (1986)
189. Labadie, J.: MASCE: Optimal operation of multireservoir systems: state-of-the-art review. J. Water Resour. Plan. Manag. **130**(2), 93–111 (2004)
190. Labadie, J.W., M.L.Baldo: MODSIM: Decision Support System for River Basin Management (Documentation and User Manual). Department of Civil Engineering, Colorado State University (2000), http://modsim.engr.colostate.edu/download.html

191. LAWA: Evaluation of Water Quality of Rivers in the German Federal Republic-Chemical Water Quality Classification. Kulturbuchverlag, Berlin (in German) (1998)
192. Lee, Y.H., Singh, V.P.: Tank model for sediment yield. In: Water Resources Management. Springer, Gyeongsan, Korea (2005)
193. Lees, M.J., Camach, L., Whitehead, P.G.: Extension of the quasar river water quality model to incorporate dead-zone mixing. Hydrol. Earth Syst. Sci. 2(2–3) (1998)
194. Lijklema, L.: Considerations in modeling the sediment-water exchange phosphorus. Hydrobiologia, pp. 219–231 (1993)
195. Lindenschmidt, K.E., Ollesch, G., Rode, M.: Implementing more physically-based hydrological modelling to improve the simulation of non-point dissolved phosphorus transport in small and medium-sized river basins. Hydrol. Sci. J. **45**(3), 495–510 (2004)
196. Lindenschmidt, K.E., Rauberg, J., Hesser, F.B.: 2005: Extending uncertainty analysis of a hydrodynamic-water quality modelling system using high level architecture (HLA). Water Qual. Res. J. Canada 40(1) (2005)
197. Lindenschmidt, K.E., Rode, M.: Linking hydrology to erosion modelling in a river catchment decision support and management system. IAHS Publ. **272**, 243–248 (2001)
198. Litrico, X., Pomet, J.B., Guinot, V.: Simplified nonlinear modeling of river flow routing. Ad. Water Res. **9**, 1015–1023 (2010)
199. Liu, J., Zheng, C., Zheng, L., Lei, Y.: Ground water sustainability: methodololgy and application to the North China plain. Ground Water **46**, 897–909 (2008)
200. Ljung, L.: The plenary on perspectives on system identification at the IFAC world congress in seoul in July 2008. In: IFAC World Congress in Seoul. Seoul (2008)
201. Lorent, B., Gevers, M.: Identification of a rainfall-runoff process. In: IFAC Symposium on Identification and System Parameter Estimation. Tbilisi (1976)
202. Los, F.J.: An algal bloom model as a tool to simulate management measures. In: Hypertrophic Ecosystems. Junk, The Hague (1980)
203. Loucks, D.P.: Water quality models for river systems. In: Biswas, A.K. (ed.) Models for Water Quality Management. McGraw-Hill, New York (1981)
204. Lumbroso, D. (ed.): Handbook for the Assesment of Catchment Water Demand and Use. HR Wallingford (2003)
205. Lung, W.: Water Quality Modeling for Wasteload Allocations and TMDLs. Wiley, New York (2001)
206. Mahendrarajah, S., Jakeman, A.J., McAleer, M.: Modelling Change in Integrated Economic and Environmental Systems. Wiley, Chichester (1999)
207. Manning, R.: On the flow of water in open channels and pipes. Trans. Inst. Civ. Eng. Irel. **20**, 161–209 (1895)
208. Marchi, D.C., Jolma, A., Masliev, I., Perera, B.J.C., Smith, M.G., Somlyody, L.: STREAM-PLAN user's manual. IIASA, Laxenburg (1996)
209. Mario, T.L., Barros, T., Tsai, C., li Yang, S., Lopes, J.E.G., William, W., Yeh, G.: Optimization of large-scale hydropower system operations. J. Water Resour. Plng. Mgmt. 129(3), 178–188 (2003)
210. Marr, G.: Vergleich zweier Differenzenverfahren in einem mathematischem Modell zur Berechnung von instationären Abflussvorgängen in Flüssen(comparison of two differences methods in a mathematical model for calculating unsteady runoff processes in rivers) (In German). Technical report 17, Versuchsanstalt für Wasserbau der Technischen Universität München-Oskar v. Miller Institut, München (1970)
211. Mauersberger, P.: General principles in deterministic water quality modeling. In: Orlob, G.T. (ed.) Mathematical Modeling of Water Quality: Streams, Lakes and Reservoirs. pp. 42–115 (1983)
212. Mays, L.: Water Distribution Systems Handbook. McGraw-Hill, New York (2000)
213. McKinney, D.: International survey of decision support systems for integrated water management. Technical report, Bucharest, Romania (2004)
214. Megiddo, N.: Linear programming in linear time when the dimension is fixed. J. Assoc. Comput. Mach. 31(1) (1984)

215. Merkel, B.J., Planer-Friedrich, B.: Groundwater Geochemistry–A Practical Guide to Modeling of Natural and Contaminated Aquatic Systems. Springer, Heidelberg (2005)
216. Mohrlok, U.: Simple Approach for Balancing Transient Unsaturated Soil Processes in Urban Areas by the Analytical Model Ulflow. IWA Publishing, London (2006)
217. Moriasi, D.N., Van Liew, M.W., Bingnert, R.L., Harmel, R.D., Veith, T.L.: Model evaluation guidelines for systematic quantification of accuracy in watershed simulations. Trans. Am. Soc. Agric. Biol. Eng. **3**, 885–900 (2007)
218. Müller, F., Baessler, C., Schubert, H., Klotz, S.: Long-Term Ecological Research. Springer, Berlin (2010)
219. Müller, F., Leupelt, M.: 1998: Eco Targets, Goal Functions, and Orientors. Springer, Berlin (1998)
220. Müller, S.: ATV Water Quality Model: Description of Model Compartments. ATV, München (2001)
221. Murtagh, B., Saunders, M.A., Murray, W., Gill, P.E., Raman, R., Kalvelagen, E.: Gams/minos: A Solver for Large-scale Nonlinear Optimization Problems (2002)
222. Muzik, I.: Lumped Modeling and GIS in Flood prediction. In: Singh, V.P., Fiorentino, M. (eds.) Geographical Information Systems in Hydrology. Kluwer, Dordrecht (1996)
223. Nandalal, K., Bogardi, J.: Dynamic Programming Based Operation of Reservoirs: Applicability and Limits, 2nd edn. Cambridge University Press (2007)
224. Nejedly, A.: The effect of longitudinal dispersion on the rate of the deoxygenation process in polluted streams. J. WPCF **45**, 1601–1605 (1973)
225. Ngo, L., Madsen, H., Rosbjerg, D., Pedersen, C.: Implementation and comparison of reservoir operation strategies for the hoa binh reservoir, vietnam using the mike 11 model. Water Resour. Manag. 22(4) (2008)
226. Ngo, T., Dyck, S.: Digitale Simulation von instationären Durchflüssen in einem Elbeabschnitt (digital simulation of unsteady flows in an)
227. Nielsen, S.N.: Ecosystems as Information Systems. In: Jørgensen, S.E., Müller, F. (eds.) Handbook of Ecosystem Theories and Management. Lewis, Boca Raton (2000)
228. Novotny, V.: Water Quality? Diffuse Pollution and Watershed Management, 2nd edn. Wiley, New York (2003)
229. Novotny, V., Chesters, G.: Handbook of Nonpoint Pollution. Van Nostrand-Reinhold, New York (1981)
230. Novotny, V., Olem, H.: Water Quality: Identification Prevention and Management of Diffuse Pollution. Reinhold-Van Nostrand, New York (1994)
231. Novotny, V., Somlyody, L.E.: Remediation and Management of Degraded River Basins. Springer, Berlin (1995)
232. O'Connor, D.J.: The temporal and spatial distribution of dissolved oxygen in streams. Water Resour. Res. **3**, 65–79 (1967)
233. O'Connor, D.J., DiToro, D.M.: Photosynthesis and oxygen balance in streams. Proc. ASCE, J. San. Eng. Div. 96(SA2): 96, 547–571 (1970)
234. O'Connor, D.J., Dobbins, W.E.: Mechanism of re-aeration in natural streams. Trans. ASCE **123**, 641–659 (1958)
235. Odum, H.T.: Systems Ecology. Wiley-Interscience, New York (1983)
236. OECD: Extended Producer Responsibility (2006)
237. Orlob, G.T.e.: Mathematical Modelling of Water Quality: Streams, Lakes and Reservoirs. Wiley, Chichester (1983)
238. Osiadacz, A.: Simulation and Analysis of Gas Networks. Gulf Publishing Co (Juli 1987) (1987)
239. Ostfeld, A., Shamir, U.: Optimal operation of multi-quality networks. J. Water Resour. Plan. Manag. I: Steady Cond. 119(6), 645–662 (1993)
240. Owens, M., Edwards, R.W., Gibbs, J.W.: 1964: Some reaeration studies in streams. Int. J. Air Water Poll. **8**, 469–486 (1964)
241. Pahl-Wostl, C.: The Dynamic Nature of Ecosystems. Wiley, Chichester (1995)

242. Pahl-Wostl, C.: Transition towards adaptive management of water facing climate and global change. Water Resour. Manag. **21**, 49–62 (2007)

243. Pahl-Wostl C., P.K., Moeltgen, J. (eds.) Adaptive and Integrated Water Management, Coping with Complexity and Uncertainty. Springer, Berlin (2008)

244. Papageorgion, M.: Optimierung–statische, dynamische, stochastische Verfahren fuer die Anwendung (Optimization–static, dynamic, stochastic methods for the application) (In German). R. Oldenburg Verlag, Müunchen (1991)

245. Parinet, B., Lhote, A., Legube, B.: 2004: Principal component analysis: an appropriate tool for water quality evaluation and management? application to a tropical lake. Ecol. Model. **178**, 295–311 (2004)

246. Park, R.A., Collins, C.D., Leung, D.K., Boylen, C.W., Albanese, G., de Caprariiis, P., Forstner, M.: The aquatic ecosystem model MS CLEANER. In: Jørgensen, S.E. (ed.) State-of-the-Art of Ecological Modelling. ISEM, Copenhagen (1979)

247. Park, R.A., Scavia, D., Clesceri, L.S.: CLEANER, the Lake George Model. Ecological Modeling in a Management Context. Resources for the Future, Washington (1975)

248. Patten, B.C.: System Analysis and Simulation in Ecology, vol. III (1974)

249. Patten, B.C.e.: System Analysis and Simulation in Ecology, vol. I (1971)

250. Patten, B.C.e.: System Analysis and Simulation in Ecology, vol. II (1972)

251. Patten, B.C.e.: System Analysis and Simulation in Ecology, vol. IV (1976)

252. van der Perk, M.: Soil and Water Contamination from Molecular to Catchment Scale. Taylor and Francis (2006)

253. Perterson, S., Richmond, B.: STELLA II: Technical Documentation. High Performance Systems, Hanover (1994)

254. Peschel, M., Riedel, C.: Polyoptimierung (Multi-criteria optimization)(In German). Verlag Technik, Berlin (1976)

255. Pezeshk, S., Helweg, O., Oliver, K.: Optimal operation of ground water supply distribution systems. J. Water Resour. Plan. Manag. **120**(5), 573–582 (1994)

256. Pickett, P.J.: Pollutant loading capacity for the Black River-Chehalis River system. Washington. J. AWRA 33(2) (1997)

257. Rabinowitz, G., Mehrez, A., Oron, G.: A nonlinear optimization model of water allocation for hydroelectric energy production and irrigation. Manag. Sci. **34**(8), 973–990 (1988)

258. Rappaz, M., Bellet, M., Deville, M.: Numerical Modelling in Material Science and Engineering. Springer Series in Computational Mathematics. Springer, Heidelberg (2003)

259. Rauschenbach, T.: Eine allgemeingültige Methode zur Modellierung und mehrkriteriellen Führung von Staustufen und Staustufenkaskaden (A general method for modeling and mzlti-criteria control of reservoirs and cascades of reservoirs) (In German). VDI Verlag, Düsseldorf (1999)

260. Rauschenbach, T.: Simulation and optimal control of rivers and hydropower plants. In: Hamaza, M.H. (ed.) IASTED–International Conference on Intelligent Systems and Control, IASTED (The International Association of Science and Technology for Development), Clearwater (Florida), pp. 85–89 (2001)

261. Rauschenbach, T.: Optimal co-ordinated control of hydropower plants. In: 16th IFAC–World Congress. Prague (2005)

262. Rauschenbach, T., et al.: Untersuchung an österreichischen donaustaustufen zur steuerung bei hochwasser: Die modellbildung und das steuerkonzept (Study at austrian danube runoff hydropower plants to control during flood: The modeling and the control concept) (In German). In: XVIII. Konferenz der Donauländer über Hydrologische Vorhersagen und Hydrologisch-wasserwirtschaftliche Grundlagen, vol. 19/1, pp. A31–A36. Graz (1996)

263. Reckhow, K.H.: The use of a simple model and uncertainty analysis in lake management. Water Resour. Bull. 15(3) (1979)

264. Reckhow, K.H., Chapra, S.C.: Engineering approaches for lake management. Ecol. Inform. 1 (1983)

265. Recknagel, F.: Ecological Informatics. Springer, Berlin (2003)

266. Recknagel, F., Benndorf, J.: Validation of the ecological simulation model SALMO. Int. Rev. ges. Hydrobiol. **67**, 113–125 (1982)
267. Reddy, J.N.: An Introduction to Finite Element Method, 2. edn. McGraw-Hill (1993)
268. Reichert, P.: Aquasim: A tool for simulation and data analysis of aquatic systems. Water Sci. Technol. 30(2), 21–30 (1994)
269. Reichert, P., Borchardt, D., Henze, M., Rauch, W., Shanahan, P., Somlyady, L., Vanrol-leghem, P.A.: River Water Quality Model No. 1. IWA Publishing, London (2001)
270. Reynolds, C.S.: Planktic community assembly in flowing water and the ecosystem health of rivers. Ecol. Model. **160**, 191–203 (2003)
271. Rinaldi, S., Soncini-Sessa, R., Stehfest, H., Tamura, H.: Modeling and Control of River Quality. McGraw-Hill, New York (1979)
272. Ritter, W.F.: Reducing impacts of non-point source pollution from agriculture: a review. J. Environ. Qual. **23**, 645 (1988)
273. Roesner, L.A., Giguere, P.R., Evenson, D.E.: User's Manual for the Stream Water Quality Model QUAL-II. US EPA, Athens (1981)
274. Romanowicz, R., Petersen, W.: Statistical modelling of algae concentrations in the Elbe River in the years 1985–2001 using observations of daily oxygen concentrations, temperature and pH. Acta Hydrochim. Hydrobiol **31**, 319–333 (2003)
275. Rosegrant, M.W., Ringler, C., Msangi, S., Cline, S.A., Sulser, T.B.: International Model for Policy Analysis of Agricultural Commodities and Trade (IMPACT-Water): Model description. Washington D.C, International Food Policy Research Institute (2005)
276. Rosegrant, M.W., Ringler, C., Msangi, S., Sulser, T.B., Zhu, T., Cline, S.A.: International Model for Policy Analysis of Agricultural Commodities and Trade. IMPACT), Model Description (2008)
277. Rutherford, J.C.: River Mixing. Wiley, Chichester (1994)
278. Sandoval, M.G., Verhoff, F., Cahill, T.: Mathematical modeling of nutrient cycling in rivers. in: Canale, r.p. (ed.) (1976)
279. Scavia, D.: An ecological model of lake Ontario. Ecol. Model. **8**, 49–78 (1980)
280. Scavia, D., Powers, W.F., Canale, R.P., Moody, J.L.: Comparison of first-order error analysis and Monte Carlo simulation in time-dependent lake eutrophication models. Water Resour. Res. 17(4) (1981)
281. Schanze, J.: Flood risk management? a basic framework. In: Schanze, J., Zeman, E., Marsalek, J. (eds.) Flood Risk Management Hazards. Vulnerability and Mitigation Measures. Springer, Berlin (2006)
282. Scheffer, F., Schachtschnabel, P. (eds.): Lehrbuch der Bodenkunde, 16. edn. Spektrum Akademischer Verlag (2010)
283. Schnoor, J.L.: Environmental Modeling. Wiley, Chichster (1996)
284. Schoel, A., Kirchesch, V., Bergfeld, T., Müller, D.: Model-based analysis of oxygen budget and biological processes in the regulated rivers Modelle and Saal: Modelling the influence of benthic filter feeders on phytoplankton. Hydrobiologia **410**, 167–176 (1999)
285. Seuront, L.: Fractals and Multifractals in Ecology and Aquatic Science. CRC Press, Boca Raton (2010)
286. Shastry, J.S., Fan, L.T., Erickson, L.E.: Nonlinear parameter estimation in water quality modelling. Proc. ASCE, J. Environm. Eng. Div 99(3) (1973)
287. Simonsen, J.F., Harremoes, P.: Oxygen and PH fluctuations in rivers. Water Res. **12**, 477–489 (1978)
288. Sincock, A.M., Wheater, H.S., Whitehead, P.G.: Calibration and sensitivity analysis under unsteady flow conditions. J. Hydrol. 277(3–4) (2003)
289. Singh, V.: Computer Models of Watershed Hydrology. Water Resources Publications, Louisiana (1995)
290. Sivapalan, M., Grayson, R., Woods, R.: Scale and scaling in hydrology. Hydrol. Process. 18(6) (2004)
291. Somlyody, L.: Challenges of water management in Central and Eastern Europe. World Meteorol. Organ. Bull. **45**(4), 342–346 (1996)

292. Somlyody, L., Varis, O.: 1992: Water Quality Modeling of Rivers and Lakes. IIASA, WP-92-041, Laxenburg (1992)
293. Somlyody, L., van Straten, G.: Modeling and Managing Shallow Lake Eutrophication. Springer, Berlin (1986)
294. Sposito, G.: Scale Dependence and Scale Invariance in Hydrology. Cambridge University Press, Cambridge (1998)
295. Srinivas, N.D.K.: Multi-objective optimisation using non-dominated sorting genetic algorithm. In: Evolutionary Computation 1994, vol. 2, pp. 221–248 (1994)
296. Stevenson, R.J., Sabater, S.: Global Change and River Ecosystems: Implication for Structure Function and Ecosystem Services. Springer, Dordrecht (2011)
297. Straškraba, M.: Natural control mechanisms in models of aquatic ecosystems. Ecol. Model. **6**, 305–321 (1979)
298. Straškraba, M.: The effects of physical variables on freshwater production: analyses based on models. In: Le Cren, E.D., Lowe-McConnel, R.H. (eds.) The Functioning of Freshwater Ecosystems. Cambridge University Press, Cambridge (1980)
299. Straškraba, M.: The application of predictive mathematical models of reservoir ecology and water quality. Can. Water Resour. J **7**, 283–318 (1982)
300. Straškraba, M.: Ecotechnological measures against eutrophication. Limnologica **17**, 239 (1986)
301. Straškraba, M.: Ecotechnology as a new means for environmental management. Ecol. Eng. **2**, 311 (1993)
302. Straškraba, M.: Ecotechnological models for reservoir water quality management. Ecol. Model. **74**, 1–34 (1994)
303. Straškraba, M., Gnauck, A.: Freshwater Ecosystems: Modelling and Simulation. Elsevier, Amsterdam (1985)
304. Straškraba, M., Tundisi, J.G.: Reservoir water quality management. In: Guidelines of Lake Management, vol. 9 (1999)
305. Streeter, H.W., Phelps, B.: A study of the pollution and natural purification of the Ohio River. Publ. Health Bull. **146**, 1–25 (1925)
306. Stüben K., C.T.: Algebraic multigrid methods (amg) for the efficient solution of fully implicit formulations in reservoir simulation. In: SPE 105832 presented at the 2007 SPE Reservoir Simulation Symposium. Houston, TX (2007)
307. Stumm, W.: Formal discussion, paper g.a. rohlich. In: Advances in Water Pollution Research, pp. 216–230 (1964)
308. Stumm, W., Morgan, J.J.: Aquatic Chemistry. Wiley-Interscience, New York (1970)
309. Sun, Y., Yang, S.L., Y., W.G., Louie, P.: Modeling reservoir evaporation losses by generalized networks. J. Water Resour. Plan. Manag. (1996)
310. Svirezhev, Y.: Stability Concepts in Ecology. pp. 361–383 (2000)
311. Tan, D.: Optimal allocation of water resources in large river basins: Ii. application to yellow river basin water resources management. Water Resour. Manag. 9(1), 53–66 (1995)
312. Thomann, R.V.: Systems Analysis and Water Quality Management. McGraw-Hill, New York (1972)
313. Texas Water Development Board.: Simulation of Water Quality in Streams and Canals. Program Documentation and User's Manual, Austin (1970)
314. The Math Works.: MATLAB On-line Manuals. Natick (2004)
315. Thomann, R.V.: Effect of longitudinal dispersion on dynamic water quality response of streams and rivers. Water Resour. Res. **9**, 355–366 (1973)
316. Thomann, R.V., DiToro, D.M., O'Connor, D.J.: 1974: Preliminary model of Potomac estuary phytoplankton. Proc. ASCE, J. Env. Eng. Div. 100(EE6), 699–715 (1974)
317. Thomann, R.V., DiToro, D.M., Winfield, R.P., O'Connor, D.J.: Mathematical modelling of phytoplankton in lake ontario i. model development and verification. US EPA, Report 660/3-75-005 (1975)
318. Thomann, R.V., Mueller, J.A.: Principles of Surface Water Quality Modeling and Control. Harper and Row, New York (1987)

319. Thomas, A.H.J.: Pollution load capacity of streams. Water Sew. Works **95**, 405–409 (1948)
320. Timmerman, J.G., Langaas, S.: Environmental Information in European Transboundary Water Management. IWA Publishing, London (2004)
321. Tkach, R.J., Simonovic, S.P.: A new approach to multicriteria decision making in water resources. J. Geograph. Inf. Decis. Anal. **1**, 25–44 (1997)
322. Todini, E., Pilati, S.: A gradient method for the analysis of pipe networks. In: International Conference on Computer Applications for Water Supply and Distribution. Leicester Polytechnic, UK (1987)
323. Trott, W., Yeh, W.: Use of stochastic dynamic programming for reservior management. Water Resour. Res. **23**(6), 983–996 (1987)
324. Tsivoglou, E.C., Wallace, J.R.: Characterization of Stream Reaeration Capacity. EPA Report, EPA-R3-72-012, Washington (1972)
325. Tufford, D.L., McKellar, H.N.: Spatial and temporal hydrodynamic and water quality modelling analysis of a large reservoir on the South Carolina (USA) coastal plain. Ecol. Model. **3**, 137–173 (1999)
326. Uhlmann, D.: Hydrobiology. Wiley-Interscience, New York (1975)
327. Uhlmann, D.: Anthropogenic perturbation of ecological systems: A need for a transfer from principles to applications. In: Ravera, O. (ed.) Terrestrial and Aquatic Ecosystems-Perturbation and Recovery, pp. 47–61 (1991)
328. Uhlmann, D., Guderitz, T.: The significance of the internal nutrient load to hypertrophic shallow waters. Int. Rev. Ges. Hydrobiol. **73**, 275–295 (1988)
329. Uhlmann, D., Paul, L.: Causes and effects of "nitrate saturation" in phosphorus deficient water bodies. Water Sci. Technol. **30**, 281–288 (1994)
330. Umgiesser, G., Zampato, L.: Hydrodynamic and salinity modeling of the venice channel network with coupling 1d–2d mathematical models. Ecol. Model. **138**, 75–85 (2001)
331. Uslaender, T.: Trends of environmental information systems in the context of the European water framework directive. J. Environ. Model. Softw. **20**, 1532–1542 (2005)
332. Uslaender, T.: Service-oriented Design of Environmental Information Systems. Ph.D. Thesis, Karlsruhe Institute of Technology (KIT), Karlsruhe (2010)
333. Vitousek, P.M., Mooney, H.A., Lubchenco, J., Melillo, J.M.: Human domination of earth's ecosystems. Science **5325**, 494–499 (1997)
334. Vollenweider, R.A.: The scientific basis of lake and stream eutrophication, with particular reference to phosphorus and nitrogen as factors in eutrophication. OECD Technical report DAS/CSI/68.27 (1968)
335. Vollenweider, R.A.: Input-output models. with special reference to the phosphorus loading concept in limnology. Schweiz. Z. Hydrol. **37**, 53–84 (1975)
336. Vollenweider, R.A.: Advances in defining critical loading levels for phosphorus in lake eutrophication. Mem. Ist. Ital. Idrobiol. **33**, 53–83 (1976)
337. Wächter, A.: An interior point algorithm for large-scale nonlinear optimization with applications in process engineering, Ph.D. thesis, Carnegie Mellon University, Pittsburgh (2002)
338. Wächter, A., Biegler, L.T.: On the implementation of a primal-dual interior point filter line search algorithm for large-scale nonlinear programming. Math. Progr. **106**(1), 25–57 (2006)
339. Wade, A.J., Neal, C., Soulsby, C., Smart, R.P., Langan, S.J., Cresser, M.S.: Modelling stream water quality under varying hydrological conditions at different spatial scales. J. Hydrol. **217**, 266–283 (1999)
340. Walker, W.W.: Simplified Procedures for Eutrophication Assessment and Prediction: User Manual US ACE, Instruction Report W-96-2. Waterways Experiment Station, Vicksburg (1996)
341. Walski, T.M., Chase, D.V., Savic, D.A., Grayman, W., Beckwith, S., Koelle, E.: Advanced Water Distribution Modeling and Management. Heasted Press, Waterbury (2003)
342. Wang, P.F., Martin, J., Morrison, G.: Water quality and eutrophication in tampa bay, state Florida. Estuar. Coast. Shelf Sci. **49**, 1–20 (1999)
343. Wang, L.Z., Fang, L., Hipel, K.W.: Water resources allocation: a cooperative game theoretic approach. J. Environ. Inf. **2**(2), 11–22 (2003)

344. Wang, S., Song, X., Wang, Q., Xiao, G., Liu, C., Liu, J.: Shallow groundwater dynamics in North China plain. J. Geograph. Sci. **19**, 175–188 (2009)
345. Warwick, J.J., Cockrum, D., Horvath, M.: Estimating non-point source loads and associated water quality impacts. J. Water Resourc. Plann. Manage. **123**, 302–310 (1997)
346. Warwick, J.J., Cockrum, D., McKay, A.: Modeling The Impact of Subsurface Nutrient Flux on Water Quality in the Lower Truckee River, vol. 35. Nevada. J, AWRA (1999)
347. Water Resources Engineers.: Computer Program Documentation for the Stream Quality Model QUAL-II. US EPA, Washington (1973)
348. Wei, S.K., Gnauck, A.: Simulating water conflicts using game theoretical models for water resources management. In: Tiezzi, E., Marques, J.C., Brebbia, C.A., Jørgensen, S.E. (eds.) Ecosystems and Sustainable Development, vol. VI, 3–12 (2007)
349. Wei, S.K., Gnauck, A.: Water supply and water demand of Beijing–a game theoretic approach for modeling. In: Marx Gmez, J., Sonnenschein, M., Müller, M., Welsch, H., Rautenstrauch, C. (eds.) Information Technologies in Environmental Engineering, pp. 525–536 (2007)
350. Wenzel, V., Eidner, R., Finke, W., Oppermann, R., Rachimow, C.: Integrated water resources management in terms of quantity and quality in the berlin region under the conditions of global change. In: Schmitz, G.H. (ed.) Proceedings of Third International Conference on Water Resources and Environment Research, TU Dresden, vol. 1, 413–416 (2002)
351. Whitehead, P.G.: Modelling and operational control of water quality in river systems. Water Res. **12**, 377–384 (1978)
352. Whitehead, P.G.: An instrumental variable method of estimating differential equation models of dispersion and water quality in non-tidal rivers. Ecol. Model. **9**, 1–14 (1980)
353. Whitehead, P.G., Beck, M.B., ÓConnell, P.E.: A systems model of stream flow and water quality in the bedford ouse river system – ii. Water quality modelling. Water Res. **15**, 1157–1171 (1981)
354. Whitehead, P.G., Williams, R.J., Lewis, D.R.: Quality simulation along river systems (quasar): model theory and development. Sci. Total Environ. **194**(195), 447–456 (1997)
355. Whitehead, P.G., Young, P.C.: A dynamic-stochastic model for water quality in part of the bedford-ouse river system. In: Vansteenkiste, G.C. (ed.) Computer Simulation of Water Resources Systems, pp. 417–438. North-Holland, Amsterdam (1975)
356. Whitehead, P.G., Young, P.C., Hornberger, G.M.: A systems model of stream flow and water quality in the bedford ouse river system–i stream flow modelling. Water Res. **13**, 1155–1169 (1979)
357. Wierzbicki, A.P., Makowski, M., (eds.), J.W.: Model-Based Decision Support Methodology with Environmental Applications, Kluwer, Dordrecht (2000)
358. Willis, R., Anderson, D.R., Dracup, J.A.: Steady-state water quality modelling in streams. Proc. ASCE, J. Environm. Eng. Div. 101(EE2) pp. 245–258 (1975)
359. Wu, R.S., Sue, W.R., Chen, C.H., Liaw, S.L.: Simulation model for investigating effect of reservoir operation on water quality. Environ. Softw. **3**, 143–150 (1996)
360. Wurbs, R.: Comparative Evaluation of Generalized River/Reservoir System Models (2005). http://twri.tamu.edu/reports/2005/tr282.pdf
361. Xu, F.L.: Application of ecological and thermodynamic indicators for the assessment of ecosystem health of lakes. In: Jrgensen, S.E., Xu, F.L., Costanza, R. (eds.) Handbook of Ecological Indicators for Assessment of Ecosystem Health, 2, 63–300 (2010)
362. Xu, F.L., Tao, S., Dawson, R.W., Li, B.G.: A GIS-based method of lake eutrophication assessment. Ecol. Model. **144**, 231–244 (2001)
363. Yates, D., Purkey, D., Sieber, J., Huber-Lee, A., Galbraith, H.: Weap21a demand-, priority-, and preference-driven water planning model: Part 1: model characteristics. International Water Resources Association **30**(4), 487–500 (2005)
364. Young, P.C.: Non-stationary time series analysis and forecasting. Progr. Environ. Sci. **2**, 3–48 (1999)
365. Young, P.C., Whitehead, P.G.: A recursive approach to time series analyses for multivariable systems. Int. J. Control **25**, 457–482 (1977)

366. Zagona, E., Magee, T., Goranflo, G., Fulp, T., Frevert, D., Cotter, J.: Riverware, Chapter 21 in Watershed Models (2005)
367. Zemansky, M.W.: Heat and Thermodynamics. McGraw-Hill (1968)
368. Zitzler, E., Thiele, L.: Multi-objective evolutionary algorithms: a comparative case study and the strength pareto approach. IEEE Transactions on Evolutionary Computation **3**, 257–271 (1994)
369. Zotter, K.: End-of-pipe versus process-integrated water conservation solutions: a comparison of planning, implementation and operating phases. J. Clean. Prod. **12**(7), 685–695 (2004)

Index